SLAC-144
UC-34
(TH), (EXP), (EXPI)

PROCEEDINGS OF THE JOINT JAPANESE - U. S. SEMINAR ON ELEMENTARY-PARTICLE PHYSICS WITH BUBBLE CHAMBER DETECTORS

Held at
Stanford Linear Accelerator Center
February 24 - 26, 1971

Edited by
GEORGE CHADWICK AND I. O. SKILLICORN
STANFORD LINEAR ACCELERATOR CENTER
STANFORD UNIVERSITY
Stanford, California 94305

Sponsored by the U. S. National Science Foundation and the Japan Society for the Promotion of Science as a part of the United States-Japan Cooperative Science Program. Also supported by the U. S. Atomic Energy Commission under Contract AT(04-3)-515.

March 1972

Printed in the United States of America. Available from National Technical Information Service, U. S. Department of Commerce, 5285 Port Royal Road, Springfield, Virginia 22151.
Price: Printed Copy $3.00; Microfiche $0.95.

FOREWORD

The joint Japanese-U.S. Seminar on Elementary Particle Physics with Bubble Chamber Detectors was organized with a threefold purpose. First, as a review and introduction for Japanese physicists who wished to enter intensively into this field, especially in view of the construction of their new proton accelerator; second, to provide a group of U. S. experimental physicists who have amassed considerable experience in the field to engage in a thoroughgoing and critical review, especially timely in view of the rapidly growing competitive technique of wire chamber spectrometers; and third, to participate in a discussion which included theoretical ideas of the present status of elementary particle physics.

The number of participants was kept small, namely, twenty-two, of which eight were from Japan and one from Australia. In order to broaden the base of the Seminar some of the sessions were held as public lectures, and local physicists from Stanford University and the University of California at Berkeley attended some of the seminars.

I believe the Seminar achieved its purposes, and I wish to thank all the participants for their hard work, patience and excellent contributions to its ultimate success. Professor Kitagaki was untiring in his efforts to bring this Seminar to reality from the Japanese side, for which I wish to express my warm appreciation. I would also like to thank the numerous people at the Stanford Linear Accelerator Center for their cooperation and help, and especially to thank Mr. William T. Kirk and Mrs. Helen Morrison for their devotion to making the Seminar run quite smoothly.

J. Ballam
Stanford Linear Accelerator Center

PREFACE

Background. The Joint Japanese-U.S. Seminar on Elementary Particle Physics with Bubble Chamber Detectors was held at the Stanford Linear Accelerator Center on February 24-26, 1971. The Seminar was organized as a part of the United States-Japan Cooperative Science Program, an activity which is carried out under the joint auspices of the U. S. National Science Foundation and the Japan Society for the Promotion of Science.

Participants. The following individuals took part in the Seminar:

Y. Hara	Tokyo University of Education
G. Takeda	Tohoku University, Sendai
T. Kitagaki	Tohoku University, Sendai
K. Takahashi	Tohoku University, Sendai
M. Teranaka	Osaka City University
T. Yamagata	Tokyo University
T. Hirose	Tokyo University
S. Yamamoto	Tokyo University
D. C. Peaslee	Australian National University, Canberra
J. Ballam	SLAC, Stanford University
M. Peters	University of Hawaii, Honolulu
S. Flatte	LRL, University of California, Berkeley
C. Baltay	Columbia University, New York
T. Ferbel	University of Rochester
J. J. Sakarai	University of California, Los Angeles
M. Derrick	Argonne National Laboratory
I. A. Pless	Massachusetts Institute of of Technology, Cambridge
R. Plano	Rutgers University, New Brunswick
H. Harari	SLAC and Weizmann Institute, Rehovat
H. Yuta	Argonne National Laboratory
G. Chadwick	SLAC, Stanford University
J. Loos	SLAC, Stanford University

In addition, R. Ries attended the Seminar as a representative of the U. S. National Science Foundation.

Purpose. The intent of the Seminar was summarized by J. Ballam in his introductory remarks:

> The idea was to get a number of people together who have been active in the field of bubble chamber physics in recent years, and to try to take stock of where we stand in the field right now. What we want to discuss here is the present status, and the prospects for the near future, of the technique of doing physics with bubble chambers. I specified "near future" because it is very difficult to look ahead more than a few years in this field. In my opinion it is quite important to take a hard look at the physics that has been done to see whether there are responses we should make dictated mainly by the physics. Please don't hesitate to be acidic, critical, reasonably friendly — whatever — and we will try to work into each other activities as much as possible to try to understand the problems.

Editors' Notes. The papers presented at the Seminar reported on recent experimental results and theoretical studies, with a general emphasis on the characteristic kinds of problems that arise in bubble chamber experimentation and on attempts to predict future trends in this field. The discussions after each paper were quite informal; we have tried to preserve some of the flavor of the exchanges in these Proceedings.

Both the presentation of papers and the succeeding discussions were tape recorded. In addition, most of the speakers provided us with written copies of their papers. In editing the discussions, we have cut out anything that appeared to be well covered in the written papers. One regretable incident occurred when H. Harari's talk on two-body reactions at high energy was lost through faulty recording technique; only an abstract of this talk is included here.

We hope that these Proceedings will be useful to those who are interested in formulating plans for future bubble chamber experimentation and to the many workers who follow the activities in this field.

G. Chadwick
I. O. Skillicorn
Editors

TABLE OF CONTENTS

[Note: The pages in this volume are numbered 1-1, 1-2, . . ., 2-1, 2-2, . . ., and so on, where the first number refers to the enumeration shown in the following list.]

QUARKS, DUALITY AND STRUCTURE OF HADRONS

Yasuo Hara

Department of Physics
Tokyo University of Education
Tokyo, Japan

Abstract

The hadron is suggested to be composed of qqq or $q\bar{q}$, and a core consisting of an infinite number of $q\bar{q}$ pairs. The hadronic levels in the model are discussed. The s-channel helicity conservation is also discussed.

1. Quark Model

Through investigation of the quark model, Regge pole model, duality, dual resonance model and other models we now have a considerable understanding of the structure of hadrons.[1]

The quark model picture of hadrons (the qqq structure of baryons and $q\bar{q}$ structure of mesons) is supported by the nonexistence of exotic particles and that of abnormal mesons. Most of the observed particles except for the possible double peaks of A_2 meson may be explained by the quark model with radial excitation.

The quark model is also supported by the additivity of scattering amplitudes.[2] This additivity is well satisfied by diffraction scattering, or Pomeron-exchange scattering, of baryon-baryon and meson-baryon scattering (for example, $\sigma_{BB}/\sigma_{MB} = 3/2$). The additivity of diffraction-scattering amplitudes is very convenient in explaining the s-channel helicity conservation recently discovered in the reaction $\gamma p \to \rho^0 p$ in the diffractive region[3] (above 2 GeV). There are also indications that this conservation "law" is true for πN scattering[4] (P and P' exchange).

If s-channel helicity is always conserved by diffraction scattering or Pomeron-exchange scattering, we have to find the physical origin of the conservation. It is rather easy to make a plausible argument for the conservation of s-channel helicity for fermions, but it is difficult to explain the conservation of s-channel helicity for mesons without assuming that mesons are

composed of fermions. About four years ago I reported the following facts.[5] If the interaction is chiral SU(2) × SU(2) symmetric, if nucleons transform linearly under the transformation, and if the high energy scattering is dominated by the exchange of Regge trajectories with natural parity, then the NN scattering amplitude is given by

$$(\bar{\psi}\gamma_\mu\psi)\ (\bar{\psi}\gamma_\mu\psi) \tag{1}$$

at high energies, where the nucleon mass may be negligible; i.e., isovector exchange (ρ and A_2 exchange) is negligible compared with isoscalar exchange (P, P' and ω exchange), and the s-channel helicity is conserved. Thus, in this model, the s-channel helicity of the nucleon is always conserved at high energies because of the factorization of the Regge pole residues. It is also easy to make a model in which the s-channel helicities of quark-quark and quark-antiquark diffraction scattering are conserved.

If we assume s-channel helicity conservation in qq and $q\bar{q}$ diffraction scattering, if we assume the additivity of diffraction scattering amplitudes, and if we assume that the octet of baryons (B_8) and the nonet of vector mesons (V_9) are S-wave bound states of qqq and $q\bar{q}$, respectively, then we obtain s-channel helicity conservation in the sense that helicity-flip ± 1 ($|\Delta h| = 1$) amplitudes are suppressed in the diffraction scattering (for small θ),

$$f_{|\Delta h|=1}/f_{|\Delta h|=0} = \frac{\theta^3}{3} \qquad \text{for } B_8$$

and (2)

$$f_{|\Delta h|=1} = 0 \qquad \text{for } V_9 .$$

For the nonet of vector mesons and the decuplet of baryons, $|\Delta h| = 2$ transitions are allowed, but they are not important in diffraction scattering at high energies because of the kinematic factor $\sin^2\frac{\theta}{2}$.

In our model, s-channel helicity is not conserved in general in the reactions $\gamma p \to gp$, Bp, $\pi p \to A_1 \cdot p$, $A_2 \cdot p$, $KN \to QN$, $\pi N \to \pi N^*(I=1/2)$, $NN \to NN^*$, $KN \to KN^*$, etc., even though Pomerons can be exchanged in these reactions. If s-channel helicities are found not to be conserved in these reactions, this nonconservation will support our model.

A trouble with the quark model may be the fact that we have not yet discovered quarks. Quarks may be particles with spin 1/2, with unitary spin,

and with heavy mass, say about 10 GeV. However, if such heavy quarks were really observed, our present quark model may be meaningless. Another trouble is the statistics of quarks. Bose and parafermi statistics have been suggested for quarks in order to explain the success of the SU(6) symmetry model of the ground-state octet of baryons and the decuplet of baryons which belong to the totally symmetric [56] dimensional representation. If we assume bose quarks, the $|\Delta I| = 1/2$ rule of nonleptonic decays is obtained for the charged current interaction,[6] but we have difficulty with the charge conjugation property of currents and mesons. For parafermi quarks there is no trouble if quarks appear only as bound states. However, for free parafermi quarks we cannot construct wave functions with the cluster property.[7] Thus, two free parafermi quarks cannot be independent even though they are widely separated. Therefore, if quarks obey bose or parafermi statistics, they may be mathematical rather than physical objects.

2. Duality

Next let me briefly discuss duality.[8] Duality means that high energy scattering or Regge poles in the t-channel are related to low energy scattering in the s-channel through analyticity, or dispersion relations. It has been shown that the Regge t-channel description can produce circles in the s-channel Argand plot.[9] If we assume that low energy scattering amplitudes (minus Pomeron exchange or background[10,11] can be approximated by contributions from resonances, and if we further assume the nonexistence of exotic resonances, then we obtain exchange degeneracies among the leading vector and tensor Regge trajectories,[10]

$$\alpha_\rho = \alpha_\omega = \alpha_{A_2} = \alpha_f, \quad \alpha_{K^*} = \alpha_{K^{**}}, \quad \text{and} \quad \alpha_\phi = \alpha_{f'} \tag{3}$$

and relations among their residues. Thus, nonets of vector and tensor mesons are required to be ideal nonets.

If we apply the method used in deriving the exchange degeneracies among the leading Regge trajectories to $P_8B_8 \to V_9B_8$ and $V_9B_8 \to P_8B_8$ reactions, we obtain exchange degeneracies among the pseudoscalar (ps) and abnormal axial vector trajectories shown in Fig. 1 as well as the exchange degeneracies among the vector and tensor trajectories of Eq. (3).

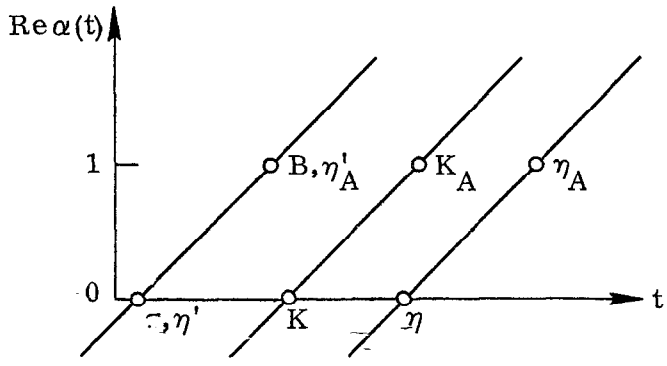

FIG. 1--Exchange degeneracies among pseudoscalar and abnormal axial vector trajectories.

That is, we obtain the relations,

$$\alpha_{\eta'} = \alpha_{\pi} = \alpha_{B} = \alpha_{\eta'_A} , \quad \alpha_{K} = \alpha_{K_A} , \quad \text{and} \quad \alpha_{\eta} = \alpha_{\eta_A} . \tag{4}$$

If we assume $m(B) = M(\eta'_A)$ and $\Gamma(B \to \pi\omega) = 100$ MeV, we find[12] $\Gamma\left[\eta'_A(I=0,\ C=-1) \to \pi\rho\right] = 300$ MeV. There does not seem to exist an isoscalar ps meson with $m_{\eta'} \approx m_{\pi}$. Therefore, an isoscalar ps Regge trajectory $\alpha_{\eta'}$ without an associated ps meson $\left[\beta_{\eta'}(t_0) = 0 \text{ for } \alpha_{\eta'}(t_0) = 0\right]$ and with $\alpha_{\eta'}(0) \approx 0$ has to exist. Then duality requires that

$$\beta_{\pi}(t_0) = 0 \quad \text{for} \quad \alpha_{\eta'}(t_0) = 0 . \tag{5}$$

These results (4) and (5) for secondary trajectories, i.e., for ps and abnormal axial vector trajectories, are less reliable than the relations (3) for the leading trajectories since unitarity is neglected in deriving these results and since unitarity corrections are expected to be more important to the relations among secondary trajectories. At any rate, it is extremely difficult to extract the contribution of isoscalar ps Regge poles from experiments. However, zeroes of the pion Regge pole residues have been found at $t \approx -0.03$ GeV^2 in the analysis of the $\gamma p \to \pi^+ n$ process[13] and the $np \to pn$ reaction[14] assuming conspiracy (Fig. 2). This zero of $\beta_{\pi}(t)$ may indicate the existence of $\alpha_{\ ,}(t)$ with $1 \gg \alpha_{\ ,}(0) > 0$.

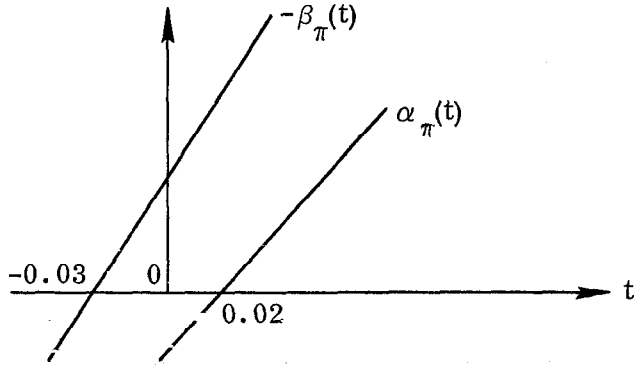

FIG. 2--$\alpha_\pi(t)$ and $\beta_\pi(t)$.

Secondary vector and tensor trajectories ρ', P'' and ω' have been introduced in the Regge pole model analysis of πN scattering,[15] and also in an attempt to avoid the trouble with the factorization of ω Regge pole residues.[16] These trajectories have been found to have

$$\alpha_{\rho'}(0) \approx \alpha_{P''}(0) \approx \alpha_{\omega'}(0) \approx 0 \ . \tag{6}$$

Duality requires the existence of $\alpha_{A_2'}$ with $\alpha_{A_2'}(0) \approx 0$.

Though the exchange degeneracy of α_π with $\alpha_{V'}$ and $\alpha_{T'}$ cannot be derived from duality, the fact that $\alpha_{V'}(0) \approx \alpha_{T'}(0) \approx \alpha_\pi(0)$ and the possibility that $\alpha_{V'}$ and $\alpha_{T'}$ may stand for Regge cuts suggests that α_π is exchange degenerate not with α and $\alpha_{\eta'_A}$ but rather with Regge cuts due to the exchange of Pomeron and α_V and/or α_T.

One of the puzzles of particle physics is why vector and tensor mesons form ideal nonets and why ps mesons form an octet. Since the zero of $\beta_\pi(t)$ is considered to be related to the Adler zero,[13] the origin of the difference may be attributed to the role of the ps mesons as the Goldstone bosons.

3. Structure of Hadrons

The quark model picture of hadrons (the qqq structure of baryons and the $q\bar{q}$ structure of mesons) has succeeded in the classification of low lying resonances. However, it is inconceivable that hadrons consist only of 3q or $q\bar{q}$. The 3q or $q\bar{q}$ may be surrounded by many (probably by an infinite number of) $q\bar{q}$ pairs. We name these $q\bar{q}$ pairs the core of the hadron.

The existence of the core is required by duality. If we assume the validity of duality, the sum of Regge poles (except for Pomeron) in the t-channel

is equal to the sum of resonances in the s-channel (Fig. 3). Thus if we look at Fig. 3, we immediately find that a resonance consists of an infinite number of particles ($q\bar{q}$ pairs).

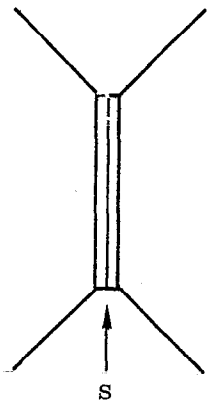

FIG. 3a--Resonances in the s-channel.

resonances ≈

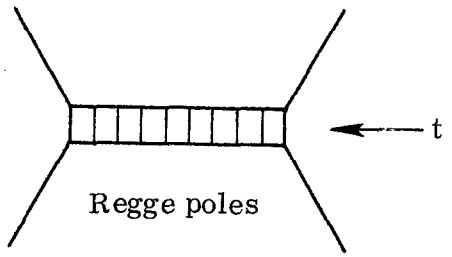

FIG. 3b--Regge poles in the t-channel.

We can now understand this situation if we study the dual resonance model.[17] The energy levels in this model correspond to the eigenstates of the operator

$$\sum n \, a_{\mu}^{(n)+} \, a_{\mu}^{(n)} \, . \tag{7}$$

Since the system consists of an infinite number of oscillators, hadrons must be composed of an infinite number of constituents in the model. The energy levels in the model are shown in Fig. 4.

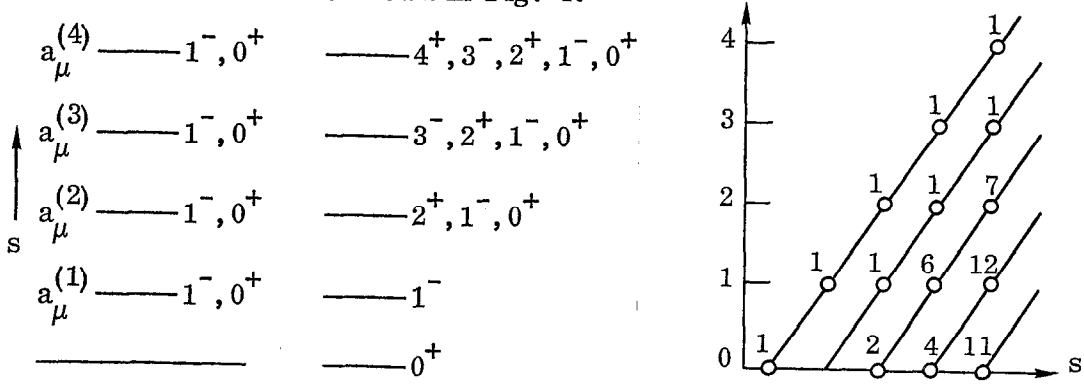

(a) Oscillators (b) Energy levels (c) Chew-Frautschi plot

FIG. 4--Dual resonance model.

For comparison we show the energy levels of the nuclear liquid drop in A. Bohr's surface vibration model in Fig. 5.

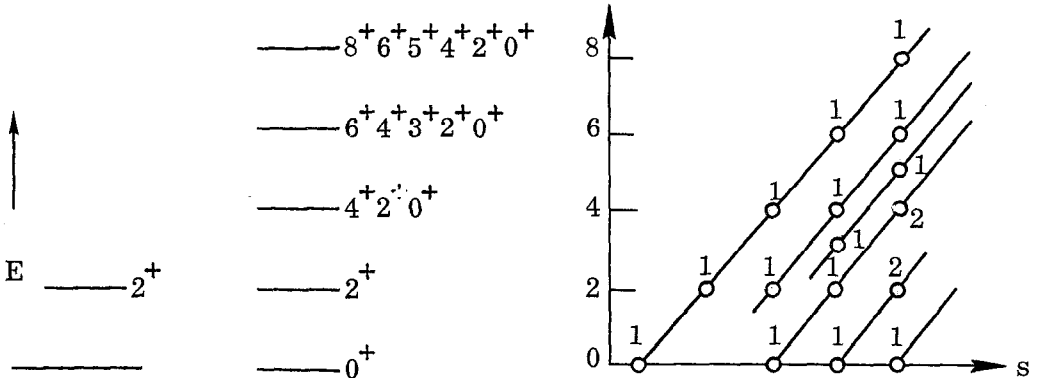

(a) Oscillator (b) Energy levels (c) Chew-Frautschi plot

FIG. 5--Surface vibration.

For large energy, n, the level density in the dual resonance model is given by $\exp(4\pi\sqrt{n/6})$. This level density and the linearity of the trajectories in $(\text{mass})^2$ cannot be expected from the simple quark model. The expected Chew-Frautschi plot of the mesons in the quark model is shown in Fig. 6.

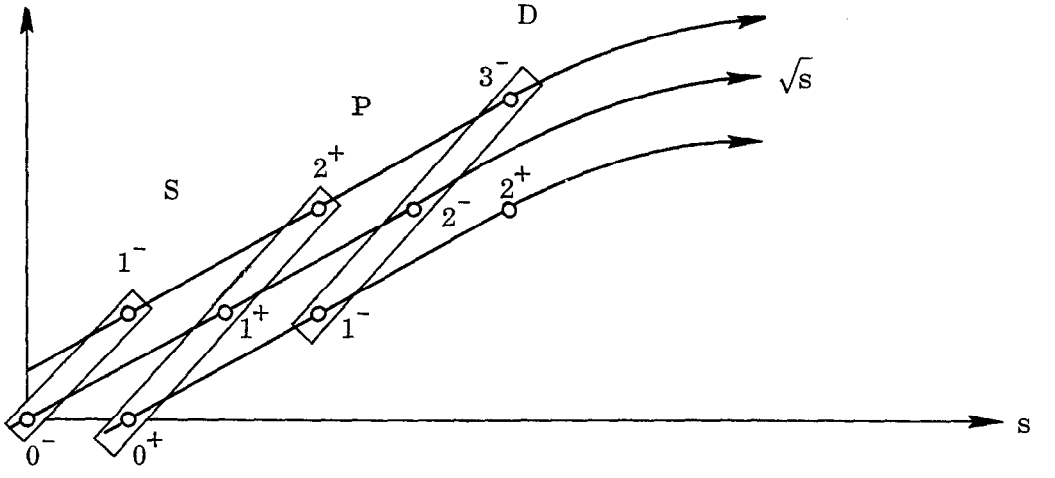

FIG. 6--Chew-Frautschi plot in the quark model.

Of course we have to add states with radial nodes to these states. In the quark model we expect $\alpha(s) \xrightarrow[s\to\infty]{} 0(\sqrt{s})$ if we assume the interaction with a finite range. The linearity of the trajectory may be regarded as support for the existence of the core consisting of an infinite number of $q\bar{q}$ pairs. As is

well known, the idea that hadrons consist of an infinite number of constituents, or partons, has been proposed in the parton model.[18]

The idea of surface oscillation of the hadronic matter has been proposed by Tati.[19] Nagasaki and Taketani proposed the excitation of hadronic matter due to its density oscillation.[20] However, we think it is too early to assume a specific model of the collective motion of the core. Instead we consider that at first we should make a model of the core which can explain the experimentally observed hadronic resonances and Regge trajectories.

Let us assume that a hadron is composed of qqq or $q\bar{q}$ pairs. Unlike the core in the nuclear shell model, which is a closed shell nucleus, the core of the hadron cannot exist without qqq or $q\bar{q}$, and it is therefore possible that the coupling of the core with qqq or $q\bar{q}$ is very strong. However, we assume that the coupling is rather weak. We consider that the weak coupling of $q\bar{q}$ with the core is suggested by the $\pi^+\pi^+$ scattering amplitude in the Veneziano model,[21]

$$\beta \frac{\Gamma(1-\alpha(t))\,\Gamma(1-\alpha(u))}{\Gamma(1-\alpha(t)-\alpha(u))} = \beta(1-\alpha(t)-\alpha(u))\ B(1-\alpha(t),\ 1-\alpha(u)) \quad . \tag{8}$$

Equation (8) suggests that the scattering amplitudes may be factorized into the $q\bar{q}$ factor and the core factor. The core is isoscalar, and the isospin of a resonance is determined by $q\bar{q}$ (or qqq). The $q\bar{q}$ factor $1-\alpha(t)-\alpha(u)$ may be taken to represent ρ and σ. The amplitude (8) contains many unobserved low lying resonances.

In the following we consider several possibilities. For simplicity we consider[22] only mesons with S=0.

Case (A)

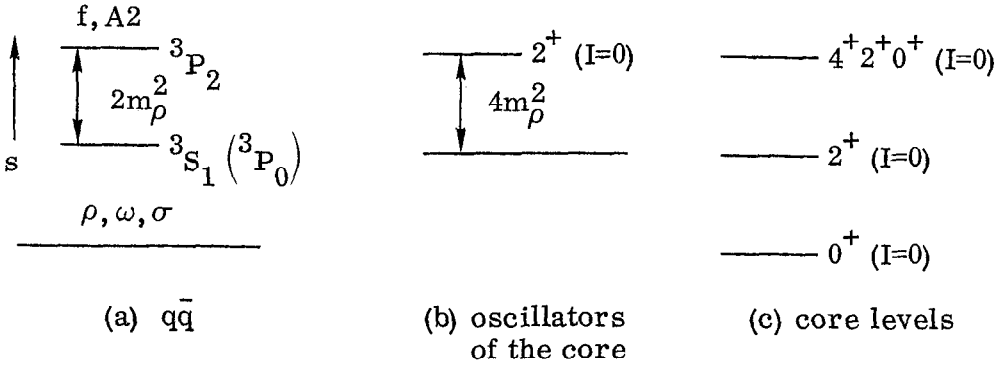

(a) $q\bar{q}$ (b) oscillators of the core (c) core levels

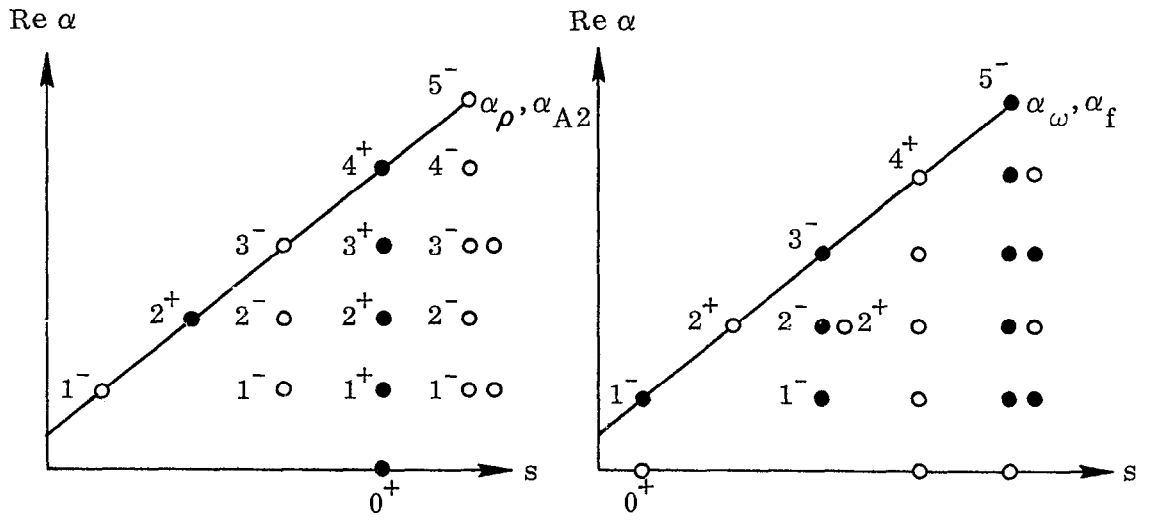

(d) I=1 mesons
G=+1, G=-1

(e) I=0 mesons
G=+1, G=-1

FIG. 7--Case (A)

Case (B) If Fig. 7a in the case (A) is replaced by Fig. 8a, we find the levels shown in Fig. 8b and 8c.

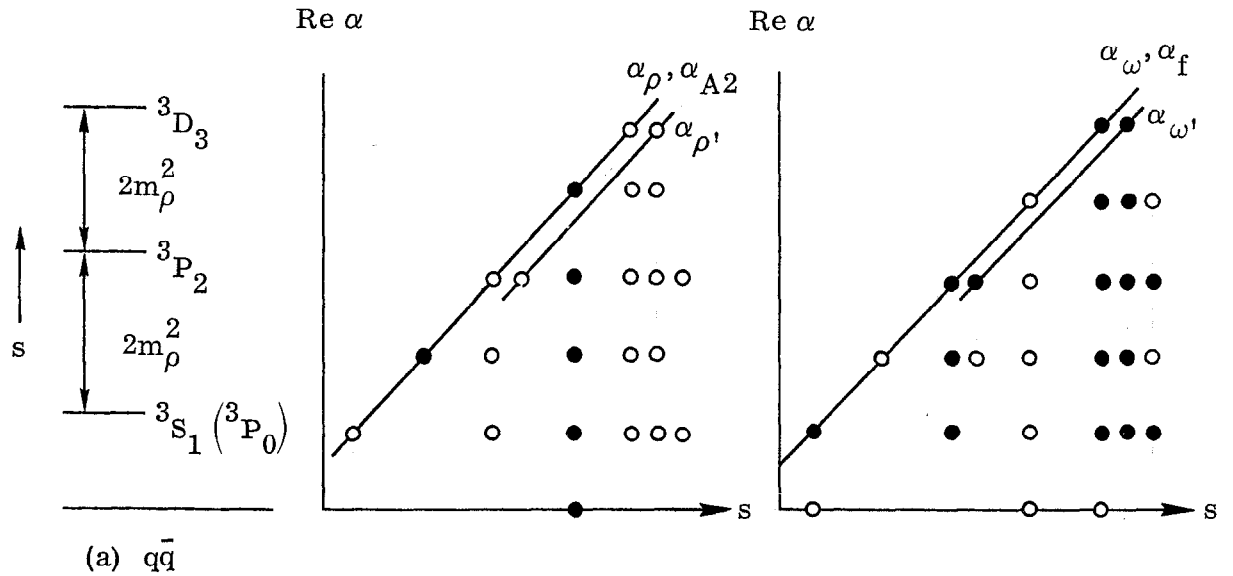

(a) $q\bar{q}$

FIG. 8--Case (B).

In this case the leading vector trajectories are degenerate. They may correspond to α_ρ, α_ω, $\alpha_{\rho'}$, and $\alpha_{\omega'}$.

Case (C) If we assume that $\alpha_{\rho'}$ and $\alpha_{\omega'}$ are exchange degenerate, the leading tensor trajectories have to be degenerate in case (B). The degenerate leading vector and tensor trajectories can be obtained either by replacing Fig. 7a by Fig. 9a or by replacing Fig. 7b by Fig. 9b.

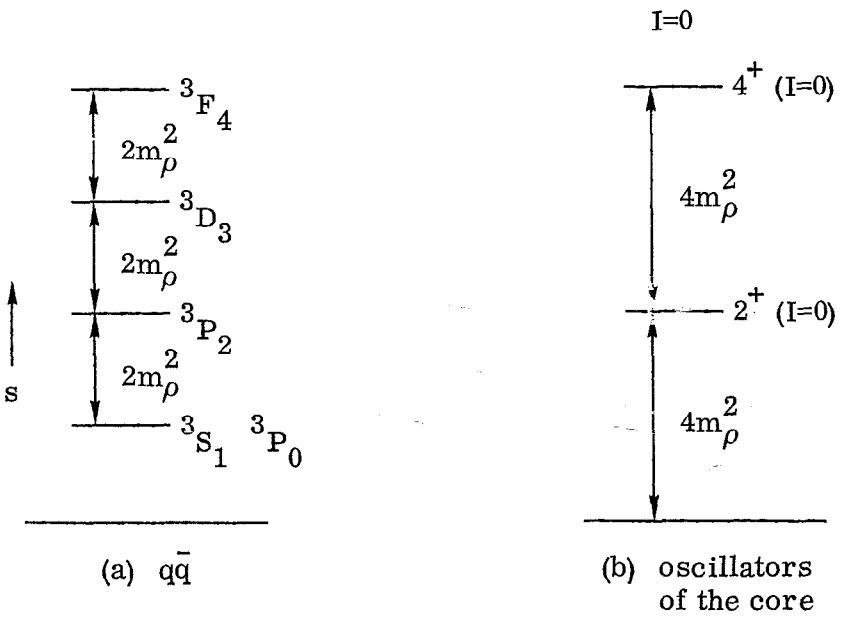

(a) $q\bar{q}$

(b) oscillators of the core

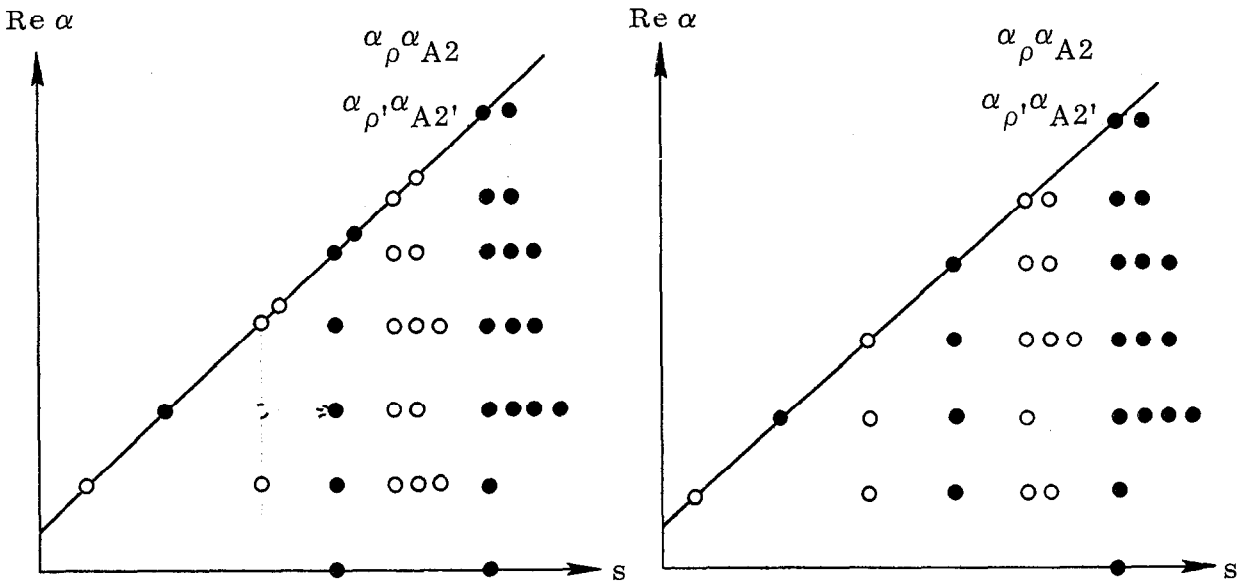

(c) I=1 mesons for (a)

(d) I=1 mesons for (b)

FIG. 9--Case (C).

Case (D) If the normal vibration of the core is isoscalar and vector (Fig. 10b), we obtain the hadronic levels shown in Figs. 10d and e.

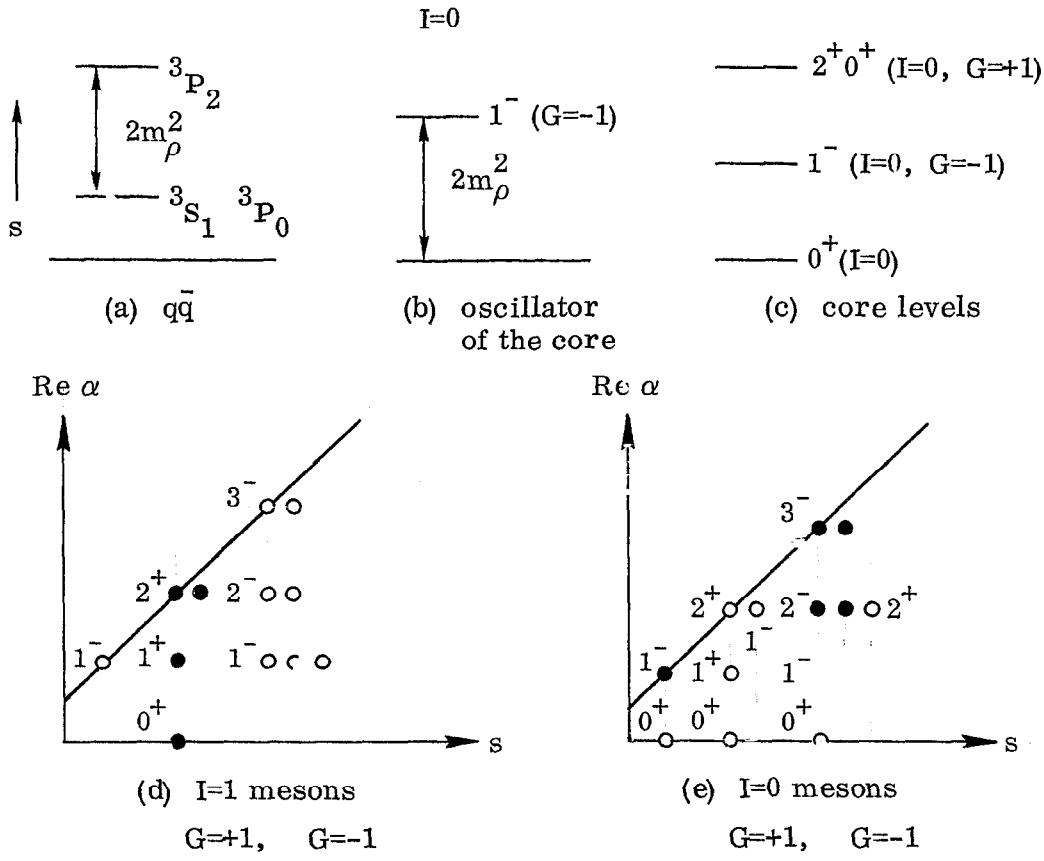

FIG. 10--Case (D).

In this case all tensor mesons are degenerate. However, this model will not be able to explain the A_2 splitting since two tensor peaks in our model will be incoherent.

So far we have discussed only nonstrange mesons. We can discuss mesons belonging to π and η families, strange mesons and baryons in a similar way. In general the core of a baryon and that of a meson can be different.

It is difficult to discuss the reactions of hadrons in our model. What we can say is the following. The interaction between the cores of colliding particles is rather weak in diffraction scattering. On the other hand many particles (or $q\bar{q}$ pairs) have to be exchanged between the cores of colliding particles in nondiffraction scattering. This is required by duality.

References

1. See, for example, review talks by J. D. Jackson, H. J. Lipkin and M. Jacob, Proceedings of the Lund International Conference on Elementary Particles, Lund, Sweden, June 25 - July 1, 1969.
2. E. M. Levin and L. L. Frankfurt, JETP Letters 2, 65 (1965); H. J. Lipkin and F. Scheck, Phys. Rev. Letters 16, 71 (1965).
3. J. Ballam et al., Phys. Rev. Letters 24, 960 (1970).
4. F. J. Gilman, J. Pumplin, A. Schwimmer and L. Stodolsky, Phys. Letters 31B, 387 (1970).
5. Y. Hara, Prog. Theor. Phys. 39, 1020 (1968).
6. R. P. Feynman, preprint (1970).
7. See, for example, the lecture by S. Kamefuchi at III Symposio Brasileiro de Fisica Theorica (1970).
8. R. Dolen, D. Horn and C. Schmid, Phys. Rev. 166, 1768 (1968).
9. C. Schmid, Phys. Rev. Letters 20, 689 (1968).
10. H. Harari, Phys. Rev. Letters 20, 1395 (1968).
11. P.G.O. Freund, Phys. Rev. Letters 20, 235 (1968).
12. Y. Hara, Nucl. Phys. B, to be published.
13. J. S. Ball, W. R. Frazer and M. Jacob, Phys. Rev. Letters 20, 518 (1968); P. DiVecchia et al., Phys. Letters 27B, 296 (1968).
14. R.J.N. Phillips, Nucl. Phys. B2, 394 (1967).
15. V. Barger and R.J.N. Phillips, Phys. Rev. 187, 2210 (1969).
16. V. Barger and L. Durand III, Phys. Rev. Letters 19, 1295 (1967).
17. See, for example, S. Fubini, D. Gordon and G. Veneziano, Phys. Letters 29B, 679 (1969).
18. J. D. Bjorken and E. A. Paschos, Phys. Rev. 185, 1975 (1969).
19. T. Tati, Prog. Theor. Phys. 43, 1596 (1970).
20. M. Nagasaki and M. Taketani, Prog. Theor. Phys. 44, 1112 (1970).
21. C. Lovelace, Phys. Letters 28B, 264 (1968).
22. For simplicity we do not consider particles belonging to π and η families.

Discussion

Harari: I have two questions. First of all, you discussed helicity conservation at the beginning, and you described the model in terms of helicity conservation on the quark level. Then you said that you predict that in elastic scattering you will have helicity conservation, but in something like π-nucleon goes to A_1-nucleon you should not have helicity conservation. This is actually nice because it seems to be the case experimentally, but now let me ask you a specific question concerning the spin. What would you predict for something like nucleon-nucleon goes to nucleon-N*, where the N* is also a spin-1/2 state, like the Roper resonance?

Hara: In order to predict the helicities of final particles, we have to assume the wave function of the excited particle.

Harari: Suppose the Roper resonance is a radial excitation of the nucleon in the quark model — what would happen then?

Hara: I think the honest answer is that the cross section is small, or something like that.

Ferbel: Do you expect to measure the polarization of the N*?

Unknown Speaker: Isn't that an empty question?

Harari: No it isn't empty, because it is the same story with π-nucleon scattering. It depends on what kind of decay you have. If you have only the decay of the nucleon and one pion, then of course you're all right. But when you have the decay of a nucleon with two pions, then with some correlations you might be able to see something. You will not be able to pin down all the amplitudes, but you may learn something. I think this question is very important — not because of this particular process, which may not be important — but if you compare elastic scattering events with π-nucleon goes to A_1-nucleon, then there are two differences. First of all, one is elastic and the other is inelastic. Secondly, in one case the spin of the initial and final particle is the same, while in the other case it isn't. The question is, is the experimental difference between the two cases caused by the fact that one is elastic and the other inelastic, or by the different spins. And the way to resolve this is to study nucleon-nucleon goes to nucleon plus Roper resonance in which the spin is the same but the reaction is inelastic.

Hara: I haven't considered this particular problem, but in general I expect helicity flip. The initial state is a totally asymmetric 3-quark wave function. After Pomeron exchange, the final state is mostly still a totally asymmetric state. We don't know the wave function of the Roper resonance, because the overlap between the nucleon state and the Roper state is small. We expect that the prediction of the quark model is not 3/2, and that is the reason we expect a large helicity flip ... What is your next question?

Harari: The other thing is this. You said at the end that you expect interaction between the cores of the colliding particles to be weak in diffraction scattering. So you consider diffraction scattering as mainly the interaction between ...

Hara: Between 3 quarks and 3 quarks. Otherwise I cannot explain the helicity conservation in the s-channel. Diffraction scattering consists partly of interactions of internal $q\bar{q}$ pairs with 3 quarks. The Pomeron interacts strongly only with the 3 quarks. That is the reason why helicity is conserved at high energy.

Ferbel: I think it is implied in what you say, but I would like to know if you eliminate the usual 4 quark system for mesons, or you say that the two sets of two are so completely decoupled — you assume only a weak interaction between all couples — so there is no possibility for exotic things?

Hara: Well, there is a possibility. I assumed an infinite number of $q\bar{q}$ pairs which can be excited into various states with some overall selection rules.

Sakurai: The ground state is a unitary singlet.

Ferbel: What are the other levels?

Hara: My philosophy is that the oscillator is chosen according to experimental results.

Ballam: I have a general sort of question. This is a complicated model, quite detailed in some sense even though it is a general model. So I would think that the model could make some relatively specific predictions. Do you have some "pet" predictions? You know, it is almost the same as in spectroscopy — someone would predict no line, and then it would turn out there was an intense line. Something of that sort.

Hara: I'm sorry, I don't have any specific predictions of that kind at present.

HIGH-ENERGY PHYSICS IN THE SEVENTIES*

J. J. Sakurai

Department of Physics
University of California
Los Angeles, California USA

Presumably theorists are invited to speak in a conference of this kind because the organizing committee feels that they may bring some urgent messages to the experimental community. I hope you won't be disappointed too much if I say, "I have no Nobel Prize experiments to suggest to you. Go ahead and do whatever you think to be important." If I were an experimentalist, most certainly I would not listen to theorists. First of all, by nature I don't like to be told what to do. More importantly, theorists are not very smart. Just to give an example, it took them more than seven years since the introduction of strangeness to formulate a simple symmetry scheme like the Eightfold Way.

Having said all this, allow me to present a highly personal view on some of the important problems in high-energy physics today.

If we go through the experimental proposals to NAL and CERN-ISR, we may get some ideas on how the frontier of high-energy physics may look a few years from now - quark search, W boson search, wide-angle proton-proton scattering, $K_L - K_S$ regeneration, inelastic μp and νp interactions, etc. But these are the same "old" experiments carried out at much higher energies. Sometime in the seventies I would like to see qualitatively new experiments performed.

Let me be specific and give an example of what I mean by qualitatively new experiments. Almost every year I start a new course in elementary particle physics by saying that there are three types of elementary particle interactions - strong, electromagnetic and weak - and that there is an immensely wide gap in strength between the electromagnetic and the weak, something like ten orders of magnitude in the squared dimensionless coupling

*Supported in part by the National Science Foundation.

constants. But then I pause and think; are we really so sure that there are no "intermediate" interactions characterized by strength halfway between the electromagnetic and the weak? By an intermediate interaction I mean a genuinely new interaction of intermediate strength, not just the square root of the usual weak interaction as in the W boson theory. If only hadrons participate in the conjectured interaction, and if this interaction conserves strangeness and parity, all its manifestations will be completely overshadowed by the usual strong interaction effects. Interactions of this kind, even if they existed, would not be discovered in my lifetime, not even in my sons' lifetime.

The whole situation is a little bit more favorable if there are particles that participate in the intermediate interactions but not in the strong interactions, just as the leptons participate in the weak interactions but not in the strong interactions. Let me call such particles "medions." Medions may be charged as well as neutral just as there are charged as well as neutral leptons. If medions are fermions, we can conceive of the conservation law of medion number. Charged medions can be produced in pairs in γ-nucleus and electron-positron collisions, but if the charged medions $m^{\pm}$ are much heavier than the neutral medions m^{o}, $\bar{m}^{o}$, we expect

$$m^{-} \rightarrow m^{o} + \text{hadrons}$$

with a lifetime shorter than 10^{-10} sec by several orders of magnitude. So we cannot hope to see bubble chamber tracks made by charged medions. In contrast, m^{o} could be absolutely stable just as the neutrino is absolutely stable. As a result, the penetrating component of neutral beams at SLAC may be made up, in part, of neutral medions, which can cause some striking events

$$\begin{array}{l} m^{o} + p \rightarrow m^{-} + \text{hadrons} \\ \qquad\qquad\quad \lfloor\!\rightarrow \text{hadrons} + m^{o} \end{array}$$

This may explain some rumored experimental result alleged to be obtained in this laboratory.

As a variant of this model, we may make the replacements

$$m^{\pm} \rightarrow h^{\pm}$$

$$m^{o}, \bar{m}^{o} \rightarrow \nu_h, \bar{\nu}_h$$

intermediate interaction $\rightarrow$ universal weak interaction,

where h is a charged heavy lepton analogous to the ordinary muon, ν_h its associated neutrino. In this case the predictions are much more specific because the relevant coupling constants are known exactly; in particular, the heavy lepton h is relatively long-lived. For instance, with $m_h = 600$ MeV, the lifetime of h^- can be computed to be 5×10^{-11} sec with $\pi^- + \nu_h$ as the most frequent decay mode. So we expect "kinks" due to $h^{\pm}$ decays which should be visible in a careful bubble-chamber experiment but probably not in a typical spark-chamber set-up.

In any case it is about time that somebody takes care of that funny lepton spectrum. Instead of asking, "Why are there muons?", it may be more appropriate to ask, "Are there heavy leptons?" The point I wish to emphasize is that there is essentially no experimental evidence for or against heavy leptons beyong the K meson mass. Perhaps there is an infinite sequence of heavy leptons!

Of course, it may turn out that explorations into higher energies uncover no glamorous particles - no medions, no heavy leptons, no quarks, no W bosons, no ghost photons, no dyons, no chimerons (whatever they may be!) . . . Yet there is plenty of work to be done with the ordinary hadron spectrum. In 1961, when Chew and Frautschi proposed a funny-looking plot with a lot of parallel straight lines, there were 19 trajectories and 21 hadronic states. Today nobody is laughing. There are straight-line trajectories with as many as five or possibly six hadronic states. Will these trajectories continue to be straight up to infinite energies? Do the "fine structures" seen in some boson spectrometer experiments really reflect the parallel daughter trajectories which play central roles in many theoretical models, e.g. the Veneziano model? Let us hope that A_2 splitting won't be the only hot subject in future meetings on boson resonances.

During the sixties a great amount of experimental data has been accumulated on two-body (including quasi-two-body) processes. What have we really learned? Regardless of whether or not you believe in the details of Regge pole models, we now know that the invariant amplitude of a typical two-body process in the forward direction can be characterized by a power law of the form

$$\mathcal{A} \sim \beta(t) s^{\alpha(t)}$$

or equivalently,

$$\frac{d\sigma}{dt} \sim F(t) s^{2\alpha(t)-2}$$

where the values of α depend on the quantum numbers of exchanged objects in the t channel, for example, $\langle\alpha\rangle \approx 1$ for difiractive processes with Pomeron exchange, $\langle\alpha\rangle \approx 0$ for $Y = \pm 1$, $T = \frac{1}{2}$ exchange, etc. A similar picture also holds in the backward direction where u channel exchange is relevant; for example, the absence of a conspicuous backward peak in $K^- p$ elastic scattering can be nicely explained by saying that exotic exchange with the quantum numbers of $Z^*(Y = 2)$ is characterized by a very low α. Beyond that most workers tend to agree on the following two points. (i) Even with all the sophistications like daughters, evaders and conspirators, pure Regge pole models are in trouble; cuts or absorption are needed. (ii) The duality idea of Dolen, Horn and Schmit, as well as the exchange degeneracy of Arnold, is on the right track. In addition, some theorists claim that there are simple rules for predicting dips and peaks; how good these are, I don't know. Perhaps Professor Harari knows.

Given the power law $s^{\alpha(t)}$, analyticity and crossing require that the phase of the amplitude be given by $I \pm e^{-i\pi\alpha(t)}$. So the concept of "signature factor" often discussed within the context of Regge pole models has a far greater generality. It is for this reason that a $K_L - K_S$ regeneration experiment of the type now being performed by Savin and collaborators at Serpukhov is almost as important as total cross section measurements.

As we go up with energies, the two-body reactions which stand up most prominently are expected to be diffraction-like processes dominated by Pomeron exchange. Yet the Pomeron is least well understood of all. For one thing, unlike other Reggions it does not appear to have a respectable dual partner. Some people say Pomeron exchange is just a manifestation of optical potentials. Bubble chamber experiments performed here at SLAC on ρ meson photoproduction have shown that the s channel helicity is conserved in this clearly diffractive process, but, according to Aachen et al., for diffractive production of A_1 and Q in πN and KN collisions it is in the Jackson frame, not in the helicity frame, that the spin component is preserved. Perhaps helicity conservation in a process like elastic pion-nucleon scattering has more to do with γ_5 invariance (chirality conservation).

Already at AGS energies the dominant fraction of two-body induced reactions involve multiparticle final states. We have here two striking features:

(i) The transverse momentum distribution of secondaries is independent of the incident energy and multiplicity and falls off sharply beyond $p_\perp \sim 400$ MeV/c.

(ii) The mean charged hadron multiplicity increases logarithmically with s.

The first feature has been well known for many years. The second feature, first conjectured on the basis of accelerator data covering a limited energy range, has recently received support from the beautiful Echo Lake experiment of Jones and coworkers up to $p_{lab} \approx 700$ GeV/c.

As for our theoretical understanding of multiparticle production, I feel that we are still in the Stone Age. But some theorists working in this field are optimistic. For instance, it has been claimed that many of the features of multiparticle production including those listed earlier actually follow from their calculations based on multi-Reggeism à la Chew-Pignotti, or on limiting fragmentation à la Yang, as the case may be.

When a 200 GeV/c proton strikes a target proton, on the average six charged hadrons come out. We cannot hope to study in detail the energy and

direction of each of the six particles. Inevitably one either relies on thermodynamical considerations à la Hagedorn or concentrates on what Feynman calls "inclusive experiments," in which only one of the hadrons is studied in detail. It is safe to predict that in the next few years there will be heated discussions on how the data should be plotted, which variables should be used to characterize a given reaction, etc. Let us hope that something positive will come out of all this.

What are the outstanding problems in the electromagnetic interactions? First, it is very important to check what Telegdi calls Ampère's law in high-energy physics: The current follows the charge. Specifically we should check whether the hadronic part of the electromagnetic current density has the same internal quantum numbers as the total charge, viz. $C = -1$, $I = 0, 1$. Possible consequences of an anomalous C component have been investigated extensively following suggestions of T. D. Lee and others. The existence of an isotensor component ($I = 2$) could be established by examining the ratio of

$$\gamma = N \rightleftarrows \Delta(1236) \rightleftarrows \pi + N$$

in various charge states, as recently emphasized by Sanda and Shaw. My colleagues at UCLA, Nefkens, Haddock and others, have tried to convince me that there is new experimental evidence for an isotensor component, but I prefer to wait.

Let us now turn to high-energy photoproduction. Setting aside your own theoretical prejudice for or against vector-meson dominance, it is fair to say that high-energy photoproduction reactions look like meson-induced reactions to a remarkable degree. The energy dependence and the angular distribution of ρ meson photoproduction resemble those of pion-nucleon elastic scattering; pseudoscalar-meson photproduction processes are characterized by the kind of peaks and dips observed in typical meson-induced reaction; the A dependence of γ-nucleus total cross sections is that characteristic of hadron-nucleus total cross sections. The more detailed question of whether we can really calculate the cross section and density matrix of $\pi^- + p \rightarrow \rho^0 + n$ from charged pion photo-production, etc. will be the central topic of my formal lecture tomorrow.

By this time even a child has heard of Bjorken's scale invariance, which is actually reminiscent of some speculation made by Kastrup several years earlier. When applied to inelastic electron-nucleon scattering, it implies that the dimensionless quantity $\nu W_2(q^2, \nu)$, which a priori could be a function of the two variables q^2 and ν, becomes a function of a single dimensionless variable

$$\omega = 2m_p \nu / q^2 = 1 + \left(s - m_p^2\right) / q^2$$

(ν = energy loss of the electron; $\sqrt{s}$ = final hadronic mass)

as both q^2 and s (or ν) become large with ω fixed. According to the famous SLAC-MIT collaboration, it seems to work well for $q^2 > 1$ GeV^2, $\omega \lesssim 8$ especially if the Bloom-Gilman variable $\omega' = 1 + (s/q^2)$ is used. In addition the data have revealed the following. (i) The ratio of the longitudinal to transverse cross section is small where good separation data are available ($\omega \lesssim 5$). (ii) If we assume that the deuteron correction is unimportant, there is a substantial difference between the electron-neutron and the electron-proton interaction for small values of ω ($1 \leq \omega \lesssim 5$), which indicates the presence of a sizable nondiffractive component. Some theorists say that this nondiffractive component is made up of s channel resonances which stay up even in the scaling limit; others prefer to argue that the electron is seeing point-like constituents inside the nucleon.

From proton-Compton scattering we know that the diffraction picture works for $q^2 = 0$ with $\nu \gtrsim 4$ GeV. It is conceivable that the idea of diffraction in inelastic electron-nucleon scattering works only when the final hadronic mass becomes much larger than the magnitude of the photon mass, i.e. $s >> q^2$ hence $\omega >> 1$, say $\omega \gtrsim 10$. Great as it is, the SLAC machine is a finite-energy accelerator. If we really want to test whether the diffraction picture works in high ω regions with moderately high values of q^2, s must be enormous; we therefore have to rely on muon beams at NAL or, better, raise the SLAC energy using the new technology of superconductivity. So an excellent argument can be advanced for improving this laboratory.

Most theoretical predictions on inelastic electron-nucleon scattering have been concerned with SLAC-MIT type experiments in which only the final electron is detected. This should not prevent experimentalists from looking at the final hadronic states in coincidence with the final electron. The transverse momentum distribution of final products, the q^2 dependence of hadron multiplicity at fixed s or fixed ω, and the electroproduction of specific final states such as $\rho^o p$ and $\pi^+ n$ are of vital importance.

One of the highlights of the Kiev Conference last summer was the large multiparticle cross section observed at Frascati (Adone) and also at Novosibirsk. It was reported that at $\sqrt{s} \sim 2$ GeV the total hadron cross section in electron-positron collisions is comparable to, or even larger than, the muon pair production. It is now popular to relate this to the large cross section obtained in inelastic electron-proton scattering. However, before I get convinced that they are really looking at single-photon processes

$$e^+ + e^- \rightarrow \gamma_{\text{virtual (time-like)}} \rightarrow \text{hadrons} \ ,$$

I would like to know whether backgrounds due to various higher-order electromagnetic processes are well understood. The apparent point-like cross section for multihadron states could, of course, be due to medion pair production or heavy-lepton pair production mentioned earlier. In any case whatever I say now about electron-positron colliding-beam experiments will become obsolete when DESY-DORIS and SLAC-SPEAR get going in a few years from now.

Turning now to the weak interactions, we notice that there are still many problems to be cleaned up in the low-energy domain - the possible existence of second-class (anomalous G) currents, more sensitive tests of the Cabibbo theory, better form factors in $K_{\mu 3}$ decay, more stringent limits on the $\Delta S = \Delta Q$ rule, etc. But the real frontier of the seventies is likely to lie in high-energy neutrino interactions. With the advent of "clean" neutrino experiments using hydrogen (or deuterium) bubble chambers, we are now at the threshold of accumulating a great deal of information on the axial vector form factor of the nucleon and the transition form factors of

low-lying nucleon resonances. In this seminar we expect to look at some pretty pictures of neutrino interactions in the large ANL chamber.

If we go to higher energies, the neutrino analog of deep-inelastic electron scattering is of paramount importance. The theoretical predictions based on current commutators are even cleaner here. For example, look at the famous Adler sum rule.

$$\int \left(W_2^{(\bar{\nu} p)}(q^2, \nu) - W_2^{(\nu p)}(q^2, \nu) \right) d\nu = 2 \left(\cos^2\theta_C = 2 \sin^2\theta_C \right)$$

where θ_C stands for the Cabibbo angle. This integral involving a structure function difference is predicted to be independent of q^2; so even if we go to very high q^2, the difference between νp and $\bar{\nu} p$ is supposed to stay up, which means, among other things, that there is a sizable nondiffractive component, just as in the electromagnetic case. Furthermore, the amount of the nondiffractive component is constrained to make the integral equal to a definite constant, numerically very close to 2. Despite this remarkable feature, many theorists now believe that the sum rule will work. On the other hand, a violation of the sum rule would provide a graveyard for a large class of theoretical papers based on current-density algebra and "reasonable" high-energy behavior.

There are other burning questions in high-energy neutrino physics theorists would like to know the answers to. Of particular interest is the question of whether the VA interference, commonly represented by the structure function W_3, stays up in the deep-inelastic limit. This can be tested by measuring the difference between $\sigma(\nu p)$ and $\sigma(\bar{\nu} n)$ [or between $\sigma(\nu n)$ and $\sigma(\bar{\nu} p)$].

What about CP violation? It is not inconceivable that the remarkable chapter opened up by Cronin, Fitch and collaborators nearly seven years ago is finally coming to a close. This is because the results of various recent experiments are slowly converging towards the predictions of the superweak theory, a model that says CP violation, for all practical purposes, is only in the off-diagonal element of the dispersive part of the $K^0 - \bar{K}^0$

mass matrix. Many experimentalists don't like the superweak theory because it is demoralizing. You, or your graduate students, may work like slaves for three years looking for some asymmetry effect only to get a result like $(0.05 \pm 0.07)\%$; then, some theorist, say Wolfenstein, says to you, "I told you so." But from a certain point of view the superweak theory is the prettiest model of CP violation. Given the overall strength of the CP violating $K^0 \longleftrightarrow \bar{K}^0$ virtual transition and the mass and lifetime difference of K_L and K_S, all the parameters of CP violating effects are predicted exactly:

$$n_{+-} = n_{00} = \epsilon \quad ,$$

$$\mathrm{Arg}(\epsilon) = \tan^{-1} \quad 2(m_L - m_S)/(\Gamma_S - \Gamma_L) \quad .$$

What more do you want?

There are, of course, other deeper questions in the weak interactions. Is the usual current-current interaction a phenomenological manifestation of a more fundamental W-boson-type coupling? What is the origin of the $\Delta I = \frac{1}{2}$ rule? Of the Cabibbo angle? Do the weak interactions ever become strong?; if yes, at what energies? Is the strength of self-interaction couplings, e.g. $(\bar{e}\nu)(\bar{\nu}e)$, given correctly by the naive current-current rule?

In this talk I have tried to indicate what we can look forward to learning in the near future. However, it is often the case that some of the more significant developments in high-energy physics are unpredictable. Unlike the discovery of the pion, the Yukawa particle, the discovery of strange particles in the late forties and early fifties was completely unexpected. Nobody, not even Dalitz or Lee and Yang, predicted in the early fifties that a careful examination of the disintegration products in τ decay would eventually lead to a revolution in our understanding of all weak interaction phenomena including nuclear beta decay. I honestly hope that the most important development in high-energy physics of this decade will lie outside the topics I covered in this talk. Thank you.

Discussion

Derrick: I have a couple of comments. I remember many years ago hearing a talk by Dennis Wilkinson on the BBC in which he talked about the fact that some particles have some interactions and other particles have other interactions, the point being that not all the interactions were shared by all the particles. Then he said that there might be another universe, co-existant with our universe, that had a completely different set of interactions, so that we would never know about it. But now if we happen to find a particle which has an interaction with our universe and also an interaction with the other universe, we would then be able to communicate between the two. That is a little like the medions you were mentioning. Perhaps the medions are coupled to mediums?

The other comment I have is a bit sociological. I think the way our science is set up these days -- with program committees and agencies who send your proposal out to be reviewed by your friends and enemies -- that it's really very difficult to do the kind of experiment you are suggesting. Of course one suspects that nearly all experiments of that kind will lead to a negative result, and when the time comes to renew the contract you don't have any publications to show -- except one that Physical Review Letters turned down. So you are out of a job. That's really a serious problem in the field today.

Sakurai: Another trouble is that all the detectors we have ultimately rely on electromagnetism. If you have a new particle which is completely divorced from electromagnetism, you will never find it.

Berman: You would see medion matter. If the particle were stable, it would eventually be seen. The fact that it hasn't been seen is an argument against its stability.

Ballam: There have been several experiments which searched for new particles. We had a search here at SLAC in the early days for any new particles that might be created through electromagnetic pair production. The difficulty is that any reasonable theory predicts that particles of high mass will have a very short lifetime. More recently M. Schwartz's experiment in a hole behind the beam dump is being done here -- although

I must admit that he had to appear before the committee five times before they agreed to let him go ahead with it.

Ferbel: Hara and Sakurai both seem to imply that Z* doesn't exist, but Amato, in a recent Physical Review Letters, says there is absolute eivdence for Z*.

Derrick: Theoretical evidence! The phase shift analysis of scattering shows no need for a Z*.

Ferbel: This is all theory. It's a case of seeing what you want to see.

Takahashi: Is there any possibility to have STP come again at high energy?

Sakurai: I haven't thought seriously about that.

Berman: You notice in Professor Sakurai's talk a very sharp difference in the type of questions that can be proposed for the strong interactions and the weak interactions. For example, you can propose testing a specific form of interaction like the diagonal interaction -- will unitarity be violated in the cross sections for neutrino processes? You can make very detailed and specific suggestions in the weak interactions, but in the strong interactions my prejudice is that the questions are not specific. That means that you can propose good weak interaction experiments, but it takes much more imagination to conceive of really qualitative kinds of strong interaction experiments. I want to appeal to experimentalists not to listen to theorists on the subject of the strong interactions. The experimentalists should use their imaginations to think up experiments that could test things like causality and the question of whether there is a quantum of distance, and other such fundamental things. What high energy physics really needs is another qualitative jump in its understanding of nature -- something like the invention of quantum mechanics, or in a lesser way the discovery of parity violation. And we are probably not going to see that in weak interactions but only in strong interactions, and I say again that there aren't any good suggestions by theorists for strong interaction experiments. Some real imagination is required in the 70's if we are going to have something to work with in the 80's at all.

Ballam: How do you feel about high multiplicity analysis in the strong interactions?

Berman: Well, it isn't a qualitative break of any sort. In fact the only thing that is interesting to me about that is in the area of electromagnetic interactions. For example, the really interesting question is, does scaling apply to all kinds of hadronic physics in connection with electromagnetic interactions? Does the scaling law apply to the multiplicity law? For example, is it going to scale like s/q^2? Those are specific questions, but again they are not in hadronic physics; they are in electromagnetic physics. I don't see anything qualitative in hadronic physics at all. The scaling is in electromagnetic physics where you can adjust the mass of the particle; you can't do that in hadronic physics. Some really substantial qualitative physics needs to be done, even if you have to do it by pounding on the scheduling committee. I think that someone who has the courage of his convictions or an interesting idea may see something profitable. I hope that some of my colleagues will not feel put down in spite of previous comments.

Kitagaki: I have a question. You (Sakurai) said that some theorists don't like the superweak theory very well. How about you?

Sakurai: I like it, because I haven't proposed an alternate theory. Unprejudiced theorists who haven't done any work on the subject, like myself, tend to like the superweak theory.

Takeda: You said that there might be an electric current with isospin 2 . . . Would this be about the same order of magnitude as the other components?

Sakurai: It could be.

Takeda: Is there any logic behind your assumption that medion number is conserved?

Sakurai: No.

Peters: On the subject of superweak, what are the possible consequences if this theory is right?

Sakurai: There is the possible decay $\Xi \rightarrow N\pi$, but the branching ratio would be many orders of magnitude down.

Berman: There is also a violation of the Boltzman H-theorem as a

result of that. I don't know if anyone has ever thought of how to test that with cosmological experiments, but it's a possibility.

Webber: I would like to make a comment, slightly disagreeing with what Berman said, about strong interactions. Something connected with high multiplicity. There is a very interesting preprint by Chan et al. which is called, I think, "A New Regge Phenomenology of Inclusive Reactions." It has something like 75 specific predictions about the properties of inclusive reactions, where you look at a final-state particle in conjunction with a high missing mass. And when you take this limit of high missing mass, you get a number of interesting results, based on Regge phenomenology. It seems likely that you can test some of these with existing data, and certainly there will be many more tests of that kind.

Ferbel: In fact, we just did test one of those crazy things. This was π^- production in K^+p and π^+p, looking in two exotic channels. They predicted that factorization holds and that the π^- distribution, scaled by the total cross section, should be identical at low longitudinal momentum transfers. We find that it seems to be true.

Pless: Hasn't Smith at Berkeley done something of this kind?

Flatte: There is a pp bubble chamber experiment also . . .

Berman: pp is a bad example. They looked at $pp \rightarrow p +$ anything. That's the experiment that shows the flat spectrum rather than the dx/x spectrum, so that's outside the realm of this explanation. This is the one experiment you shouldn't have mentioned!

Flatte: There are some studies of our K^+ film going on now which seem to satisfy some of the predictions quite well.

NEUTRINO PHYSICS IN A LARGE BUBBLE CHAMBER AT VERY HIGH ENERGIES

C. Baltay

Columbia University
New York, New York USA

1. Introduction

I would like to discuss briefly the features of using large cryogenic bubble chambers in the study of neutrino interactions at very high energies.

In the past, neutrino interactions have been studied using both bubble chambers and spark chambers at the proton accelerators at Brookhaven, CERN, and Argonne. The results of these investigations are available in the literature.[1] Future programs using large cryogenic bubble chambers in the 7- to 15-foot diameter range are underway or being planned at Brookhaven, CERN, Argonne, and at the large proton accelerator under construction at the National Accelerator Laboratory. For concreteness I will concentrate on the bubble chamber neutrino program at NAL. The accelerator is expected to produce protons up to 500 GeV, and thus an entirely new region of ν energies will be available for the first time. A neutrino facility is under construction, as is a 15-foot cryogenic bubble chamber with a total volume of 33 cubic meters. Most of the things I am about to discuss are contained in the 1968, 1969, and 1970 NAL Summer Study Reports, as well as a number of experimental proposals submitted to NAL.

Many of the interesting problems in neutrino interactions will be studied at NAL using instruments other than the bubble chamber. It is fair to say, however, that the bubble chamber is competitive with other techniques in all facets of neutrino interactions, and in many cases is the best or the only useful instrument presently available.

2. Some Physics Topics of Interest

Let me begin with a short summary of the physics topics which are of interest in the study of high energy ν interactions. Since these topics have been widely discussed in the literature, I will be very sketchy. The following list is not necessarily in order of importance, and is not meant to be exhaustive but is merely intended to provide some examples of what will be of interest.

1. Comparison of the total cross sections of ν on protons and neutrons and $\bar{\nu}$ on protons and neutrons. A variety of models of the fundamental structure of the elementary particles make predictions about the ratio of these cross sections. For example, a field-theoretical parton model predicts $\sigma(\nu$ on p or n) = $3\sigma(\bar{\nu}$ on p or n) for certain values of the kinematic variables; a diffraction model predicts $\sigma(\nu p) = \sigma(\nu n) = \sigma(\bar{\nu} p) = \sigma(\bar{\nu} n)$; and some quark models predict $\sigma(\nu n) = 2\sigma(\nu p)$ and $\sigma(\bar{\nu} p) = 2\sigma(\bar{\nu} n)$. Thus even crude measurements of the total cross sections could be very useful in distinguishing between these models.

2. Energy dependence of the total cross section. Assuming locality and scale invariance, the total cross section is expected to rise linearly with ν energy. A deviation of the total cross section from such a linear rise would thus be very interesting. In particular, the existence of an intermediate boson (W) would modify the total cross section by a factor $\left(1+q^2/m_W^2\right)^{-2}$. This measurement may thus be a sensitive search for the W up to a mass of 20 or 30 GeV.

3. Measurement of the differential cross section $d^2\sigma/dq^2 d\nu$ in the inelastic processes $\nu p - \mu^- +$ hadrons, where q^2 is the four momentum transferred from the ν to the μ^-, and $\nu = E_\nu - E_\mu$. This differential cross section depends on three form factors W_1, W_2, and W_3. A study of this differential cross section over a range of ν energies allows one to make some determination of these form factors, and their q^2 and ν dependence provide a test of scale invariance.

4. Measurements of the vector and axial vector form factors in quasi-elastic processes like $\nu n \rightarrow \mu^- p$, $\nu p \rightarrow \mu^- N^{*++}$, etc.

5. Study of the form factors in hyperon production processes like $\bar{\nu} p \rightarrow \mu^+ \Lambda^o$ and $\bar{\nu} n \rightarrow \mu^+ \Sigma^-$. These are the inverse of the hyperon beta-decay processes and provide a test of the Cabibbo theory at high momentum transfers.

6. Test of the various weak interaction selection rules like the $\Delta I = 1/2$, the $\Delta S < 2$, and the $\Delta S = \Delta Q$ rules, and tests of CVC and PCAC. Most of our present understanding of the weak interaction comes from the decay processes of various elementary particles, and is thus restricted to very low momentum transfers. High energy ν interactions allow us to extend this region by perhaps two orders of magnitude. It is of great interest to see to what extent these selection rules hold in this new region.

Some examples of the predictions of these various selection rules that can be tested are:

a. the $\Delta I = 1/2$ rule predicts

$$\sigma(\bar{\nu}n \to \mu^+ \Sigma^-)/\sigma(\bar{\nu}p \to \mu^+ \Sigma^0) = 2/1$$

and

$$\sigma(\bar{\nu}n \to \mu^+ \Lambda^0 \pi^-)/\sigma(\bar{\nu}p \to \mu^+ \Lambda^0 \pi^0) = 2/1$$

b. the $|\Delta I| = 1$ rule predicts

$$\sigma(\nu n \to \mu^- \Delta^+)/\sigma(\nu p \to \mu^- \Delta^{++}) = 1/3$$

and

$$\sigma(\bar{\nu}p \to \mu^+ \Delta^0)/\sigma(\bar{\nu}n \to \mu^+ \Delta^-) = 1/3$$

c. the processes $\nu n \to \mu^- \Sigma^+$ and $\nu n \to \mu^- \Lambda^c \pi^+$ are expected to be suppressed by the $\Delta S = \Delta Q$ rule compared to processes like $\bar{\nu}n \to \mu^+ \Sigma^-$ and $\bar{\nu}n \to \mu^+ \Lambda^0 \pi^-$.

d. the $\Delta S < 2$ rule predicts the reactions $\bar{\nu}n \to \mu^+ \Xi^-$, $\bar{\nu}p \to \mu^+ \Xi^0$, $\bar{\nu}n \to \mu^+ \Omega^-$, etc., to be absent.

7. Search for the direct production of the intermediate bosons W_1 and W_0, where W_1 and W_0 are the predicted vector and scalar[2] particles that mediate the weak interactions. The possible production and decay processes of interest are

$$\nu Z \to Z\mu^- W_1^+$$
$$\hookrightarrow \mu^+ \nu$$
$$\hookrightarrow e^+ \nu$$
$$\hookrightarrow W_0$$
$$\hookrightarrow \text{hadrons}$$

$$\nu Z \to Z\mu^- W_0^+$$
$$\hookrightarrow \text{hadrons} \quad .$$

Using neutrinos produced by a 500 GeV accelerator, one can search for these particles with masses up to 14 GeV or so. A large bubble chamber filled with neon is probably the only instrument that is sensitive to all of the decay modes listed above.

8. The purely leptonic four-fermion processes $\nu_\mu \rightarrow \mu^- e^+ \nu_e$ and $\nu_\mu \rightarrow \mu^- \mu^+ \nu_\mu$ are of great interest. In particular, the second one of these, often called the diagonal interaction has a different intrinsic strength from the nondiagonal one. These processes could occur in a bubble chamber in the Coulomb field of the target nucleus in the reactions $\nu Z \rightarrow Z\mu^- e^+ \nu$ and $\nu Z \rightarrow Z\mu^- \mu^+ \nu$. A measurement of these cross sections provides tests of locality and universality in the weak interactions.

3. Neutrino Beam Design and Fluxes

The main source of neutrinos and antineutrinos at a proton accelerator is the decay of pions and kaons produced by the primary protons in a target. Muon neutrinos come from the decays $\pi^+ \rightarrow \mu^+ \nu_\mu$ and $k^+ \rightarrow \mu^+ \nu_\mu$, and muon antineutrinos from $\pi^- \rightarrow \mu^- \bar{\nu}_\mu$ and $k^- \rightarrow \mu^+ \nu_\mu$. Electron neutrinos and antineutrinos, which come from decays like $k \rightarrow \pi e \nu_e$, are less abundant than the muon neutrinos by several orders of magnitude, so in the following I will consider ν_μ and $\bar{\nu}_\mu$ only.

The rough features of the neutrino beam at NAL are now fairly well defined, as shown in the schematic sketch of Fig. 1. The extracted primary proton beam strikes a target in which the pions and kaons are produced. The π and k decay tunnel is 1 meter in diameter and 400 meters long. The muon and hadron shield is 1000 meters of earth. Since the detector subtends a very small solid angle of the target, the ν flux can be increased considerably by placing some focusing device after the target to direct the pions and kaons toward the detector. These focusing devices may consist of quadrupole magnets or of specially designed conical current sheets, usually referred to as horns. The expected number of neutrinos per GeV and m^2 as a function of the ν energy is shown in Fig. 2 for 200, 350, and 500 GeV primary protons.[3] These curves were calculated assuming the Hagedorn-Rauft model for pion and kaon production by high energy protons. Horn focusing has been assumed, and the flux has been averaged over a detector radius of 1.35 meters. At 500 GeV, the integral of the spectrum shown corresponds to 3×10^{10} neutrinos per pulse for 10^{13} protons interacting in the target. For the same beam without any focusing device the flux is down by an order of magnitude at 20 GeV, and by a factor of four at 200 GeV. Antineutrino beams are produced by changing the polarity of the focusing elements so that negative particles are focused foward the detector. The resulting $\bar{\nu}$ fluxes are about a factor of 3 less than the ν fluxes of Fig. 2.

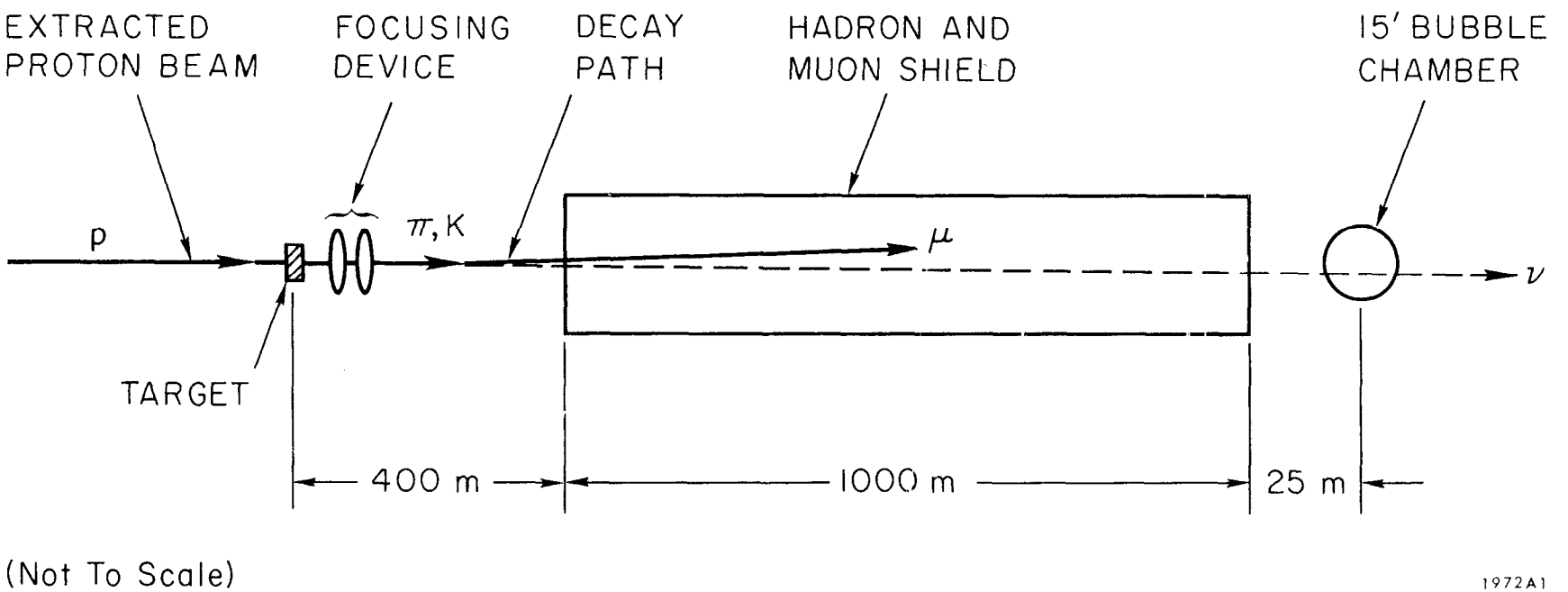

FIG. 1--Schematic drawing of the NAL neutrino beam.

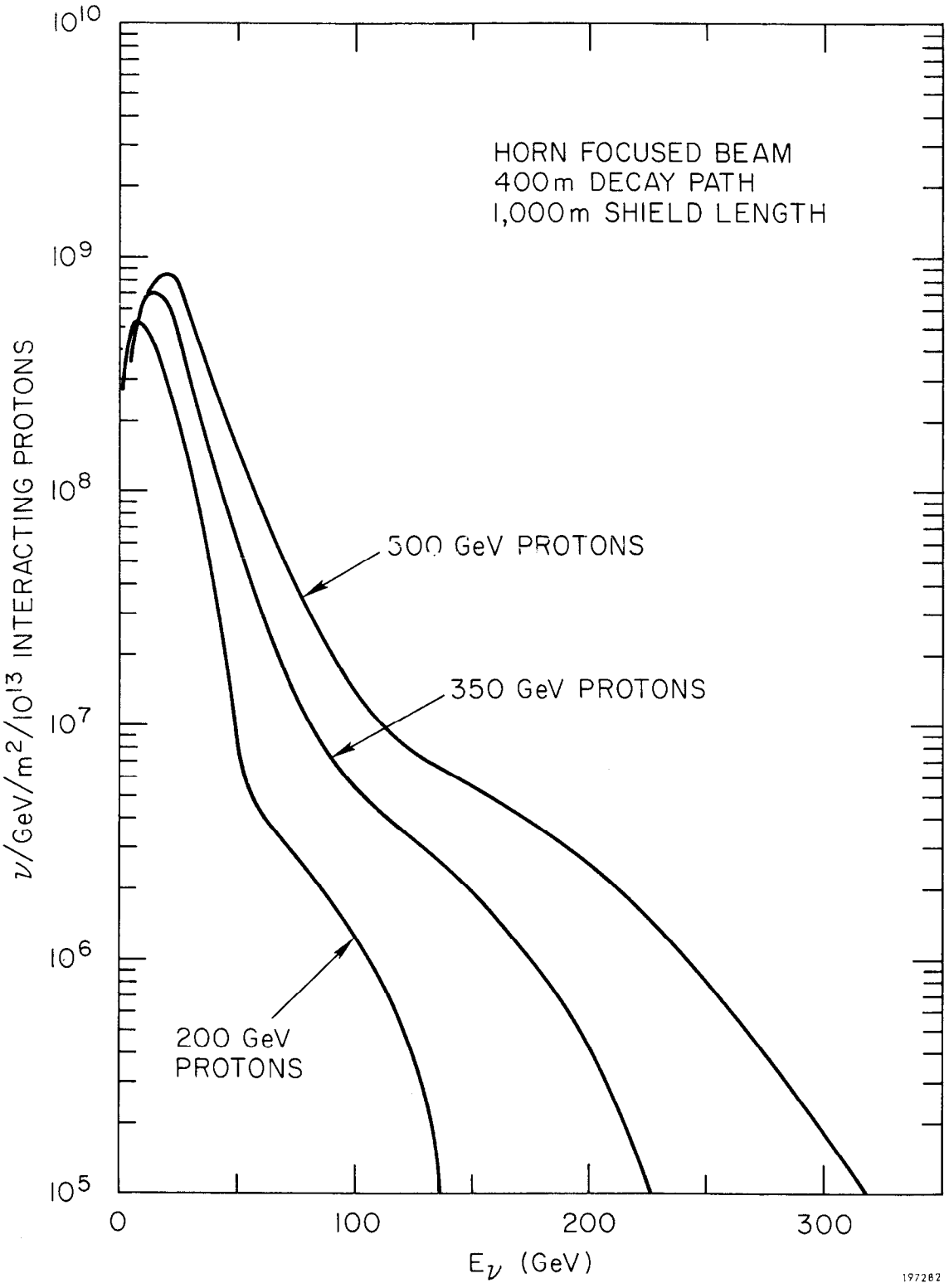

FIG. 2--ν spectra.

These beams are often called wideband beams because there is substantial flux over a wide range of ν energies. A narrowband beam can be constructed by making use of the kinematics of the two-body π and k decays. The focusing elements are replaced by a dipole magnet, a set of collimators, and several quadrupole magnets, such that a ±5% momentum-selected π and k beam is directed down the decay tunnel. Since in the two-body decays there is a correlation between the angle of the ν and its energy, the neutrinos that hit the detector, which is relatively small and far away, are confined to a narrow energy range. Due to the different kinematics of π and k decay, this type of beam produces two peaks — the neutrinos from k decay are near the energy of the momentum-selected π and k beam, and the neutrinos from π decay are near one-half of this energy. A rough calculation of the ν spectrum for such a beam[4] is shown in Fig. 3. In this calculation only the two-body decays were considered; three-body k decays and other effects will fill in the valley between the two peaks to a level of probably 10% of the peak intensities. Such a beam would be very well suited to certain measurements, like the energy dependence of the total cross section, where knowledge of the ν energy is important. For many other purposes, however, the narrowband beam is not very good due to the much reduced total ν flux.

4. Estimated Yield of Events

An estimate of the cross sections for some of the interesting reactions is shown in Table 1 and Figs. 4 and 5. The total and the "elastic" cross sections are extrapolations from the low-energy measurements of CERN.[1] The simple pion-production processes are from a calculation by Adler,[5] multiplied by a factor of two on account of the higher cross section measured at CERN[1] for the reaction $\nu p \rightarrow \mu^- p \pi^+$. The cross sections for the hyperon production reactions are from a calculation by Cabibbo and Chilton,[6] assuming some reasonable value for the axial vector form factor. The cross sections for the lepton pair production processes are from the theoretical calculations of Czys, Sheppy, and Walecka.[7] The intermediate vector boson production cross sections have most recently been calculated by Brown and Smith[8] for very high ν energies. And finally, the cross sections for the production of the recently proposed scalar boson, shown in Fig. 5 for various mass values, are from a recent theoretical calculation.[9]

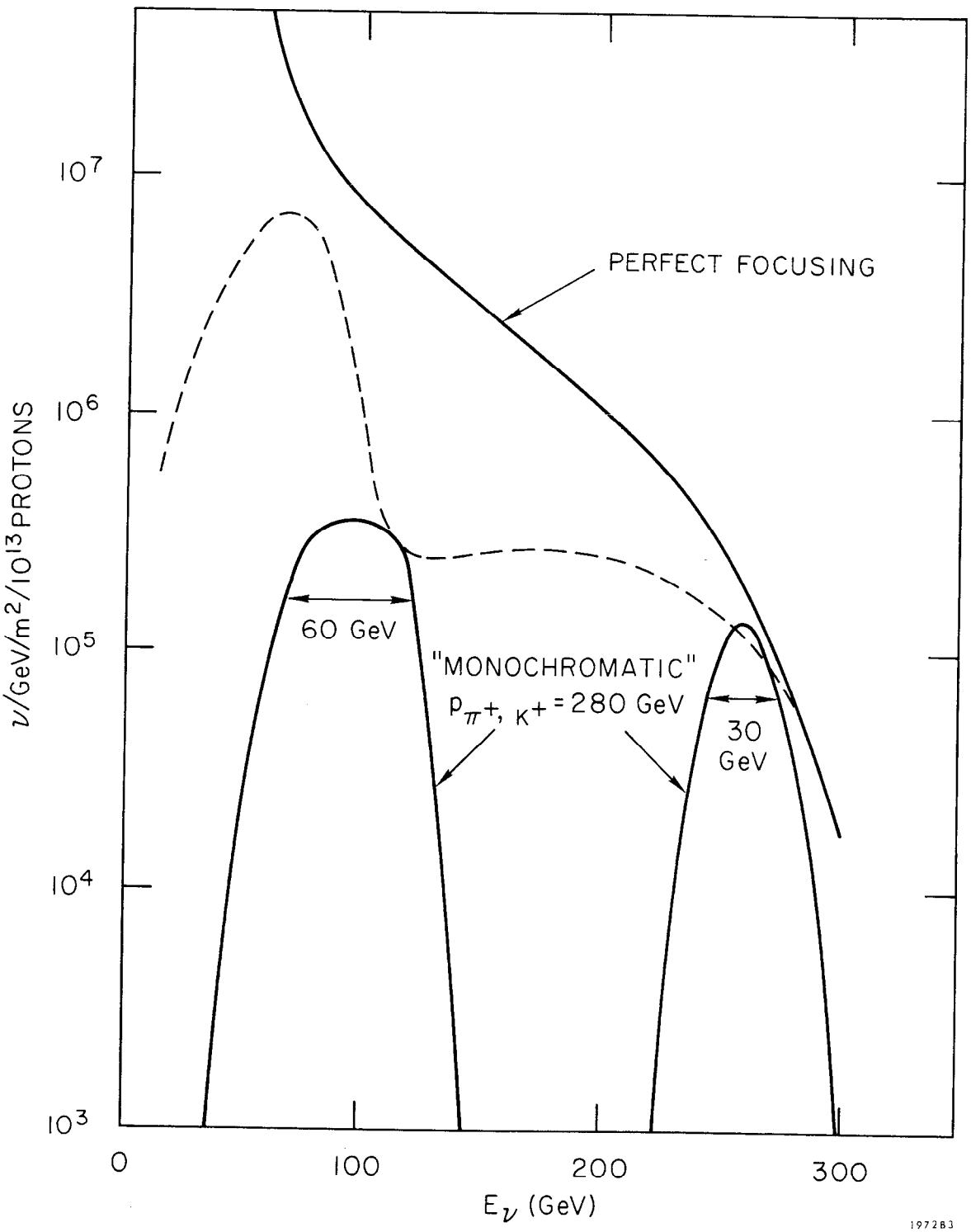
PERFECT FOCUSING
60 GeV
"MONOCHROMATIC"
$p_{\pi^+,\ K^+} = 280$ GeV
30 GeV
10^7
10^6
10^5
10^4
10^3
ν/GeV/m^2/10^{13}PROTONS
0
100
200
300
E_ν (GeV)
1972B3

FIG. 3

Table 1

Estimated Cross Sections

Reaction	σ in cm^2
Total	$0.8 \times E_\nu \times 10^{-38}$
$\nu n \rightarrow \mu^- p$	0.7×10^{-38}
$\nu n \rightarrow \mu^- p\pi^o$	0.24×10^{-38}
$\nu n \rightarrow \mu^- n\pi^+$	0.32×10^{-38}
$\nu p \rightarrow \mu^- p\pi^+$	0.88×10^{-38}
$\bar{\nu} p \rightarrow \mu^+ \Lambda^o$	3×10^{-40}
$\bar{\nu} p \rightarrow \mu^+ \Sigma^o$	1×10^{-40}
$\bar{\nu} n \rightarrow \mu^+ \Sigma^-$	2×10^{-40}
ν Ne $\rightarrow$ Ne $\mu^- e^+ \nu$	$10^{-42} - 10^{-40}$
ν Ne $\rightarrow$ Ne $\mu^- \mu^+ \nu$	$10^{-42} - 10^{-40}$
$\nu p \rightarrow \mu^- p W^+$	$10^{-42} - 10^{-36}$

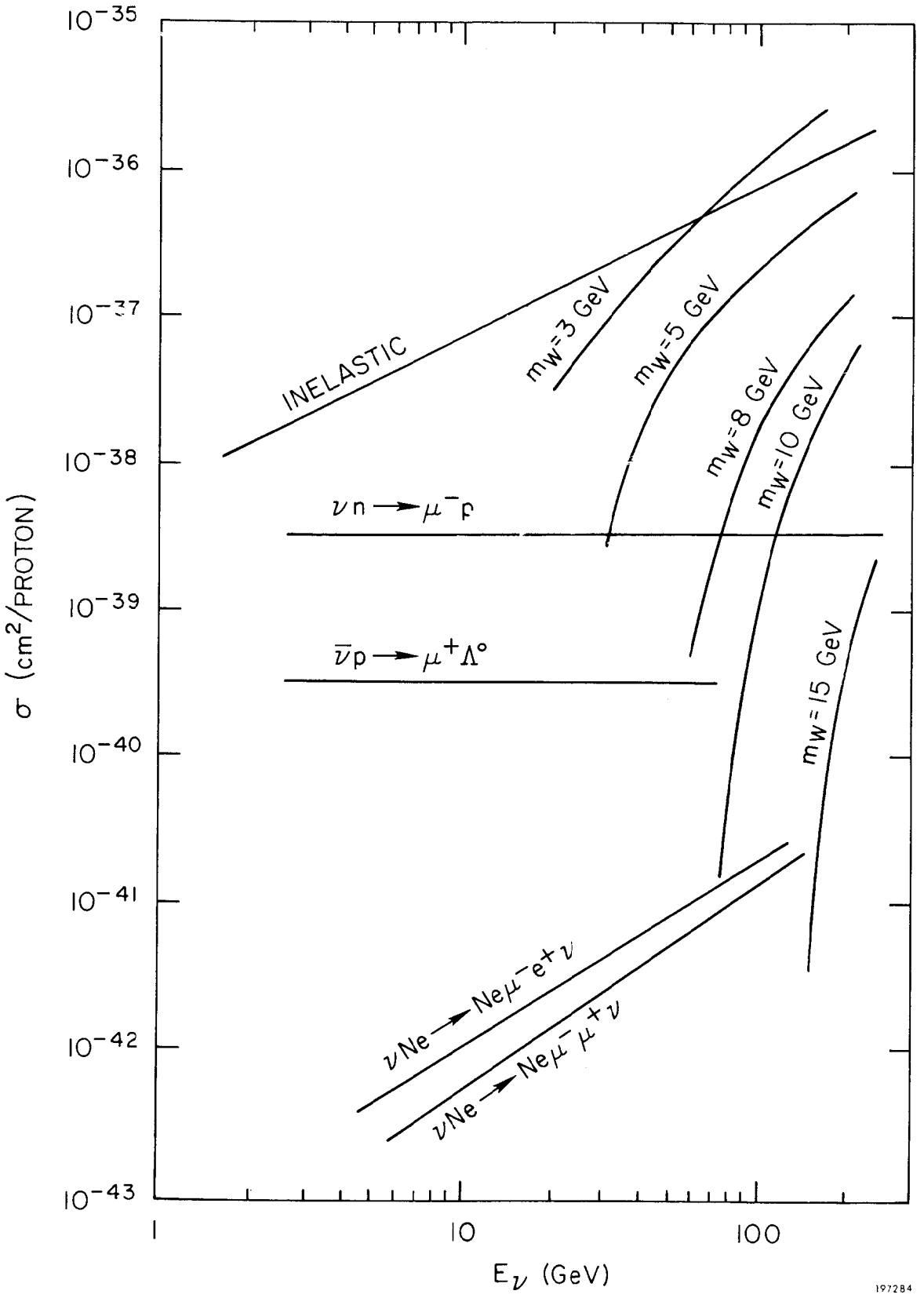

FIG. 4--Total cross sections in neon.

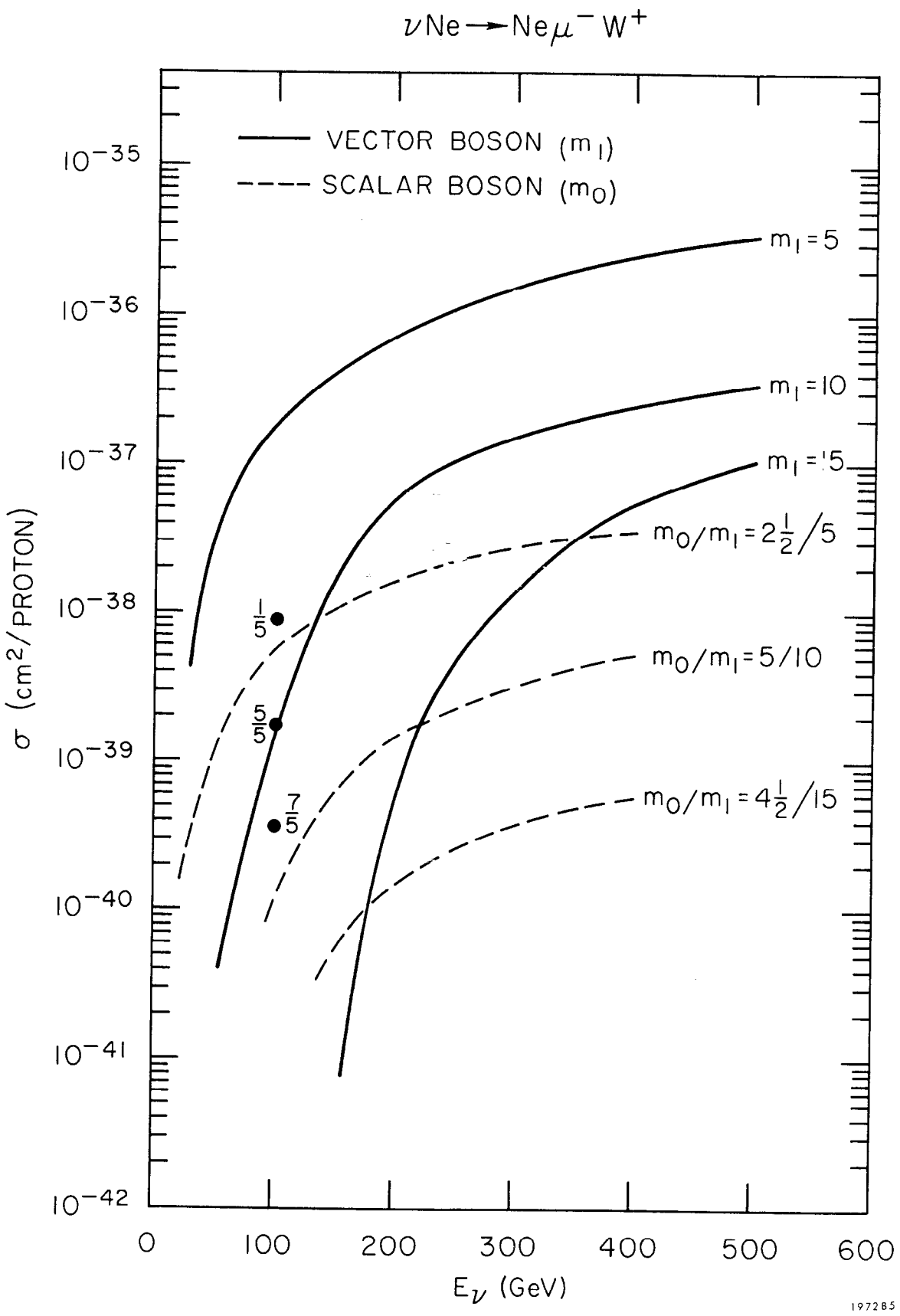

FIG. 5--Production cross sections.

Using these cross sections and the wideband neutrino fluxes of Fig. 2, the yield of events can be estimated. Some of these numbers are summarized in Tables 2 and 3 for a hypothetical experiment of 10^6 pictures in the 15-foot chamber, assuming 2×10^{13} protons per pulse and 500 GeV primary protons, for chamber fills of hydrogen, deuterium or neon, and using a restricted fiducial volume in the chamber. The number of intermediate bosons produced as a function of their masses is shown in Figs. 6 and 7. It is apparent from these numbers that the yields are sufficient to study most of the physics problems mentioned in Section 2 in a significant manner.

5. Detection Capabilities of the Bubble Chamber with Various Fills and Muon Detectors

The large cryogenic chamber under construction at NAL will be able to operate with fills of liquid hydrogen, deuterium, or neon. Some properties of these liquid are listed in Table 4. The main advantages of the bubble chamber (high multitrack efficiency, ability to identify complicated final states, and the measurement of angles and momenta of all charged particles in the 30 kG magnetic field of the chamber) of course apply to all of the fills, although errors due to multiple scattering are more severe in neon. Hydrogen and deuterium provide the simplest proton and neutron targets with a minimum of complication due to nuclear effects. This feature may be of crucial importance for some of the physics. Neon, with its short radiation length, is a very efficient γ, and therefore π^o, detector; it also unambiguously identifies electrons or positrons by their characteristic behavior; and the short collision length might be useful for detection of neutrons. One possible mode to keep the best of both, i.e., simple target liquid and efficient neutral detection, is to have a track-sensitive hydrogen or deuterium target in the chamber surrounded by several feet of neon for neutral detection. Such schemes are being actively pursued and seem very promising from tests in smaller chambers.

With either pure neon or a neon jacket arrangement it should be possible to estimate the total ν energy to 10% or better. On the average, half of the energy is taken by the muon, another third by charged hadrons, and the remaining one sixth goes into neutrals. Thus even a crude measurement of the total energy of the neutrals, together with the momentum measurement of the μ^- and the charged hadrons, suffices to measure the total ν energy to a good accuracy.

Table 2

Yield of Events in 10^6 Pictures

Assume: 2×10^{13} protons/pulse
500 GeV protons
Horn focusing

Reaction	15 m^3 H_2	15 m^3 D_2	10 m^3 Ne
Total	0.5×10^6	1.0×10^6	6×10^6
$\nu n \rightarrow \mu^- p$	---	1.4×10^4	1×10^5
$\nu p \rightarrow \mu^- p \pi^+$	1.8×10^4	1.8×10^4	1.2×10^5
$\nu n \rightarrow \mu^- n \pi^+$	---	4.8×10^3	3.2×10^4
$\bar{\nu} p \rightarrow \mu^+ \Lambda^o$	200	200	1300
$\bar{\nu} p \rightarrow \mu^+ \Sigma^o$	70	70	400
$\bar{\nu} n \rightarrow \mu^+ \Sigma^-$	---	130	800

Table 3

W and Four-Fermion Search in Neon

Assume: 10^6 pictures at 2×10^{13} protons/pulse
500 GeV protons
Horn Focusing

Reaction	Events in 10 m^3 Ne
$\nu_\mu Ne \rightarrow Ne\mu^- e^+ \nu_e$	100
$\nu_\mu Ne \rightarrow Ne\mu^- \mu^+ \nu_\mu$	50
$\nu\ Ne \rightarrow \mu^- W^+$	
$m_W =$ 5 GeV	2.5×10^5
8 GeV	2.5×10^4
10 GeV	5.5×10^3
12 GeV	1.2×10^3
14 GeV	250
16 GeV	50

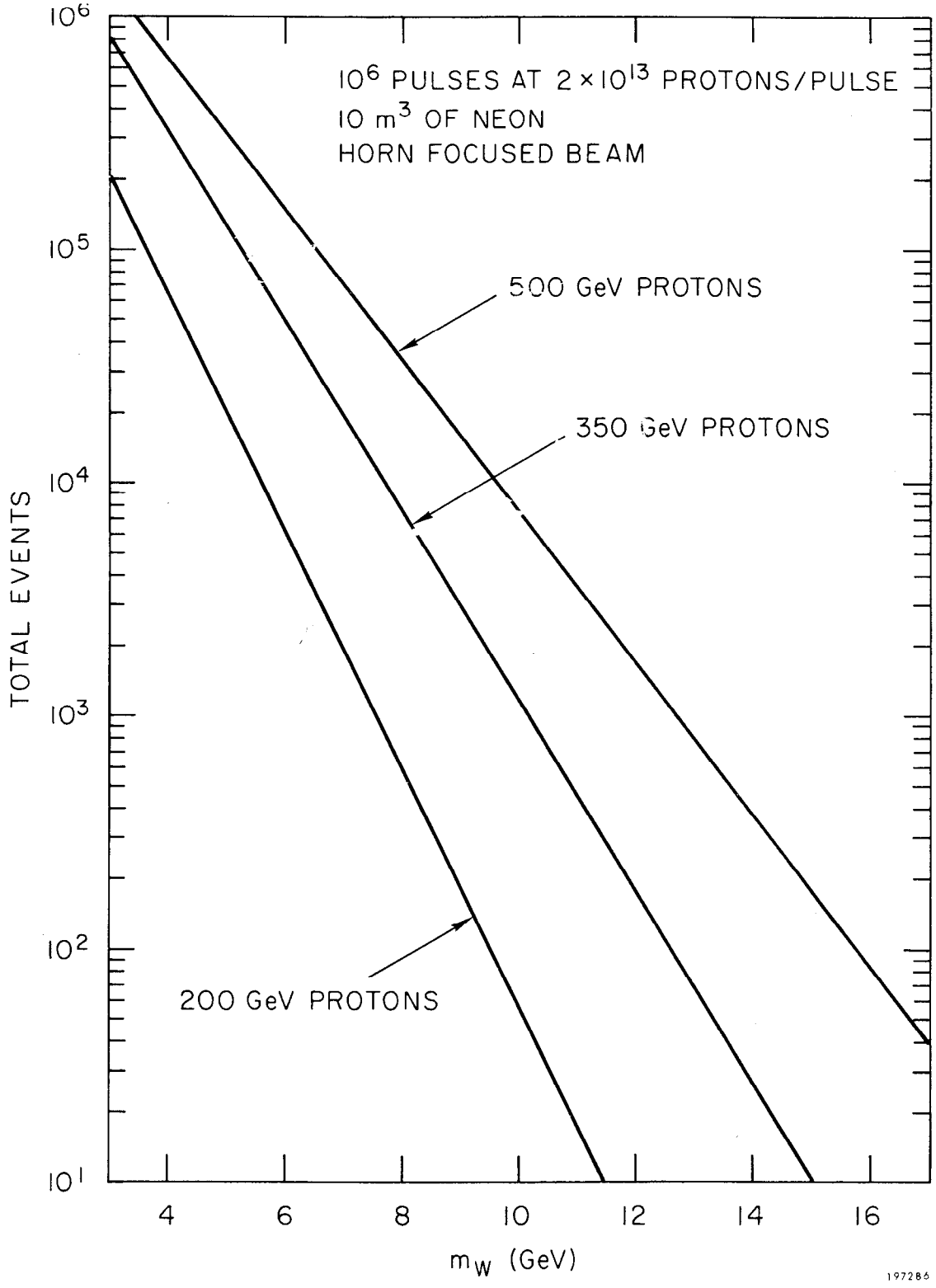

FIG. 6--Number of W_1's produced, all decay modes.

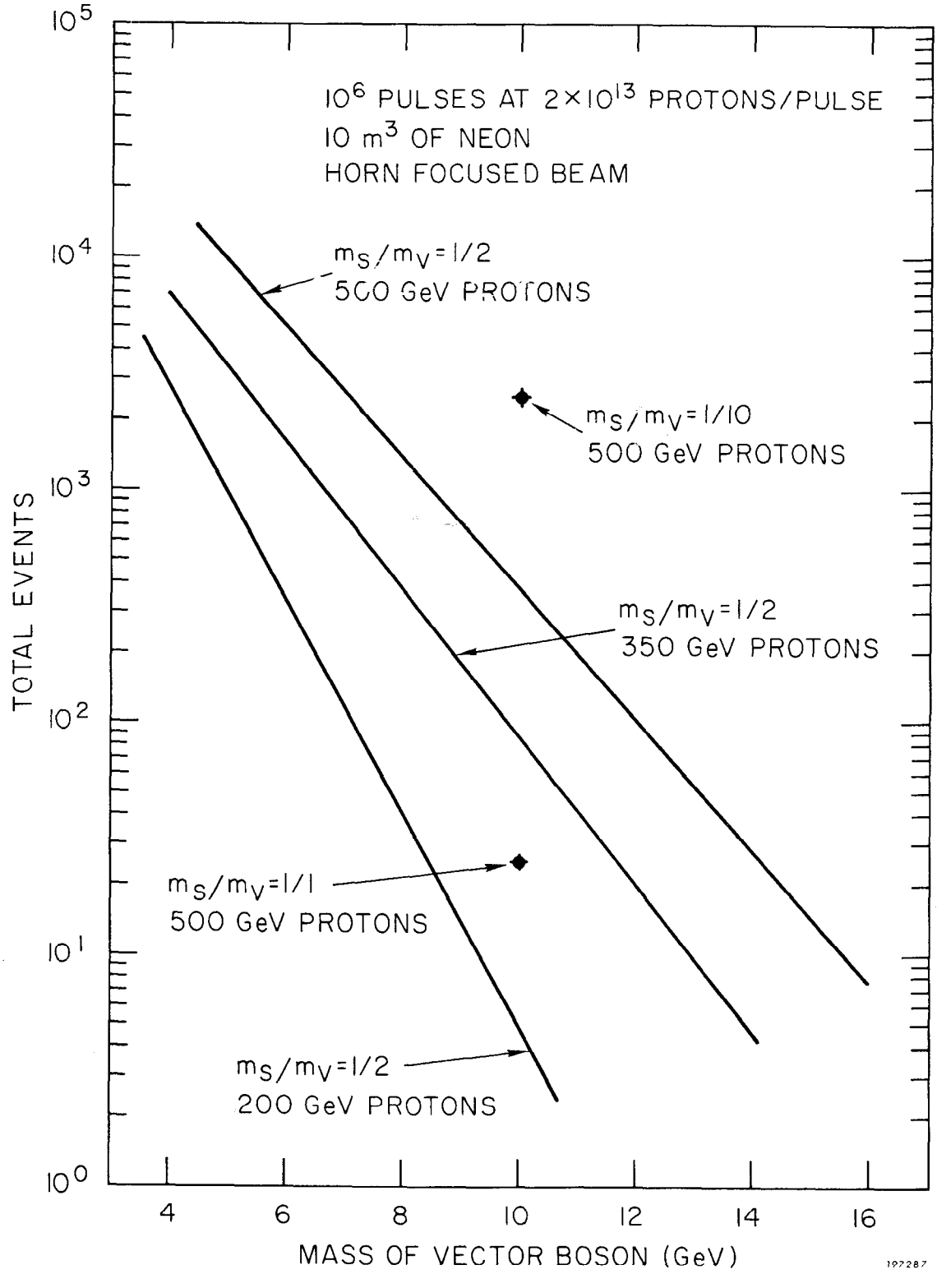

FIG. 7--Number of scalar bosons produced, all decay modes.

Table 4

Some Properties of Bubble Chamber Fills

Liquid	Density gr/cm^3	Mass of 30 m^3	Interaction Length	Radiation Length
H_2	0.06	1.8 tons	374 cm	1000 cm
D_2	0.12	3.6 tons	202 cm	1000 cm
Neon	1.20	36 tons	60 cm	24 cm

A positive identification of the muon will be very important for most of the ν interactions of interest. The basic idea used in all muon identifiers contemplated so far is to place a large amount of material in the path of the particle, which only a muon could traverse without a detectable interaction. The liquid in the chamber can be used for this purpose if the fill is neon; the probability of a hadron surviving the average path of 2 meters without interacting in less than 10%. Better discrimination can be obtained by using 5 or 6 interaction lengths of stainless steel. This can be in the form of a plate inserted in the chamber; with enough track-sensitive liquid visible behind the plate to photograph the track both before and after the plate, with some angle and momentum measurement possible on both sides of the plate. With such an arrangement the fraction of hadrons which simulate muons can be kept below 1%, with good geometric efficiency over the entire momentum range. The 6 interaction lengths of material can also be placed outside of the chamber, with counters on both sides of it to select tracks that traverse the material. Such an external muon identifier has to be quite large to subtend a useful solid angle at the center of the chamber, and therefore tends to be rather expensive. Also, one of the main sources of background of muon simulation are pions which decay into muons before reaching the muon detector. The path length in which the pions can decay is minimized by placing the muon detector inside the chamber, and thus this source of background is considerably reduced. However, with the external muon identifier the full fiducial volume of the chamber is useful for finding events, while with the inserted plate the useful volume is reduced by a factor of two.

Taken all together these capabilities make the large bubble chamber a uniquely powerful instrument for the study of neutrino interactions.

References

1. See for example the review by D. H. Perkins in the Proceedings of the 1969 CERN Weak Interactions Conference (CERN-69-7).
2. T. D. Lee, Phys. Rev. Letters 25, 1144 (1970).
3. D. Carey, Y. Kang, F. Nezrick, R. Stefanski, and J. Walker, NAL Report TM-265, and F. Nezrick and Y. Kang, private communication.
4. B. Barish and F. Sciulli, private communication.
5. S. Adler, Ann. Phys. 50, 189 (1968).
6. N. Cabibbo and F. Chilton, Phys. Rev. 137, B1628 (1965).
7. W. Czyz, G. D. Sheppy, and J. D. Walecka, Il Nuovo Cimento 34, 404 (1964).
8. R. W. Brown and J. Smith, Phys. Rev. D3, 207 (1971).
9. W. A. Cooper and T. D. Lee, private communication.

Discussion

Pless: Do you need all the beam?

Baltay: It depends on the flux. Half the beam (if the intensity is 5×10^{13}) would still be very handsome.

Harari: Most of the experiments will give mostly high multiplicity events. Why didn't you emphasize these more?

Baltay: Since the big chamber will convert most of the γ rays (especially if you use Ne - H_2 in part of the chamber), we can study the neutrals as well as the charged products in high-multiplicity events. I haven't discussed these much, mainly because of time limitations, and ignorance. There will be lots of other garbage in the chamber, however, which may make it hard to reconstruct the events (although scanners are very good at sorting things out after a bit of training).

Derrick: Doing neutrino physics at high energies could produce lots of new things, like a new family of heavy leptons.

Berman: Never. They probably need their own type of neutrino to make it. You might find baryon-lepton resonances.

Baltay: The new neutrino may be part of the original beam. They may be the Schwartz particles.

THOUGHTS ON THE LIMITATIONS OF PRESENT BUBBLE CHAMBER EXPERIMENTS

Stanley M. Flatté

Lawrence Radiation Laboratory
Berkeley, California USA

I believe my talk will be most useful if addressed directly to the Japanese experimentalists and their problem of choosing a future course for Japanese physics. This is difficult because I do not know them personally. However, from a brief study of the present Japanese program, including the planned 8 GeV proton synchrotron and the extensive bubble chamber program in progress, it appears that Japan is moving fast. I want to present the (not necessarily logical) thoughts of a working U. S. physicist in order to stimulate your thoughts, so I hope I won't be accused of being a dilletante philosopher for some of the things I say.

I restrict myself to discussion of the accomplishments of bubble chambers in the recent past, and the prospects for these same bubble chambers (mainly the hydrogen bubble chambers up to 2m in length) in the future. For specific examples I will draw on the work from the group to which I belong at LRL-Berkeley.*

The topics which bubble chamber experiments have been pursuing over the last three years include:

1. New Resonances
2. Properties of Resonances (J^P, branching ratios, etc.)
3. Exchange Mechanisms (Regge, absorption, pion, multiperipheral, Veneziano)
4. The Nature of Diffraction
5. $\pi\pi$ and $K\pi$ Scattering
6. Inclusive Reactions
7. Photoproduction

---

*The people who have worked on these experiments are the following: M. Alston-Garnjost, A. Barbaro-Galtieri, W. F. Buhl, P. J. Davis, S. E. Derenzo, L. D. Epperson, S. M. Flatté, J. H. Friedman, G. R. Lynch, M. J. Matison, R. L. Ott, S. D. Protopopescu, M. S. Rabin, F. T. Solmitz, N. M. Uyeda, V. Waluch, and Roland Windmolders.

One sees immediately that the overwhelming majority of the contributions are in strong interactions: the only exceptions are some decay modes of resonances, and the photoproduction results which derive almost entirely from one experiment with the backscattered laser beam in the SLAC 82" B.C. I believe this emphasis on strong interactions will continue to hold true.

Specific Examples

1. A_2 Structure

The A_2 structure seen in two CERN experiments has excited much interest in the physics world. Figure 1 shows our group's result[1] for three different decay modes of the A_2. Our bubble chamber result was the first significant work on A_2 structure after the CERN experiments, and we showed conclusively that the A_2 does not always look the same. (We saw no significant structure at all, our result being 6 standard deviations away from the structure seen at CERN.) Our experiment has 50 events/μb, and the resolution in mass we obtained was more than adequate for the A_2 structure analysis.

We also have looked at the mass distributions of two SU(3) companions of the A_2: the K*(1420) and the f^o (see Fig. 2 and 3). Again we saw no structure.[2,3]

A significant fact is that our A_2 and f^o studies have both been followed by counter experiments that have more than ten times the amount of data; and they also see no structure — so it is rather implausible that with ten times the data I would see a whole new world of fine structure.

2. Diffraction

For me the study of diffraction-like processes is of interest because it may lead to some global understanding of the interaction cross section without detailed understanding of every component (or particular reaction). An example of the stimulating results in this field lately is that of three reactions where helicity conservation has been studied:

Reaction	Helicity is Conserved in
$\gamma p \rightarrow \rho p$	s-channel
$K^- p \rightarrow Q^- p$	t-channel
$K^+ p \rightarrow Q^+ p$	neither

Our group has results on the apparently diffractive process[4]

$$K^+ p \rightarrow L^+ p \rightarrow K^+ \pi^+ \pi^- p \text{ at 12 GeV/c}$$

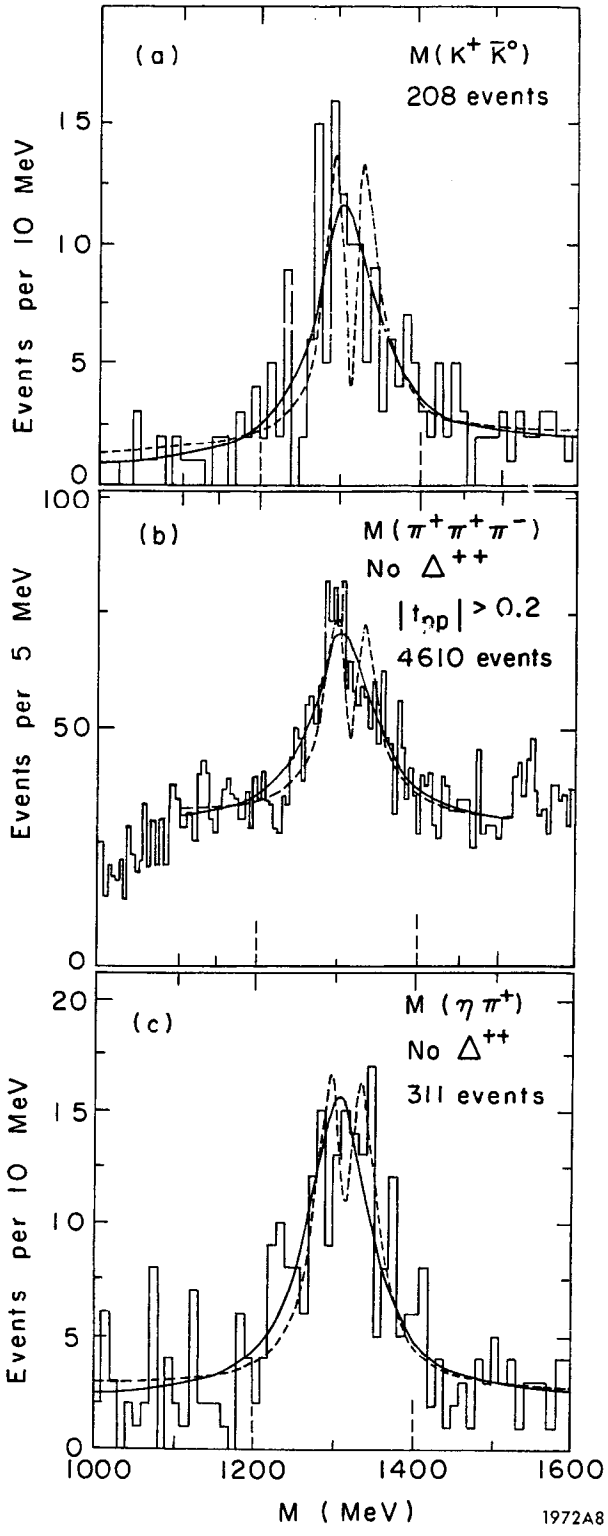

FIG. 1--Mass plots in the A_2 region. The curves are from the likelihood fit to the three decay modes simultaneously; BW (solid line) and DP (dashed line).

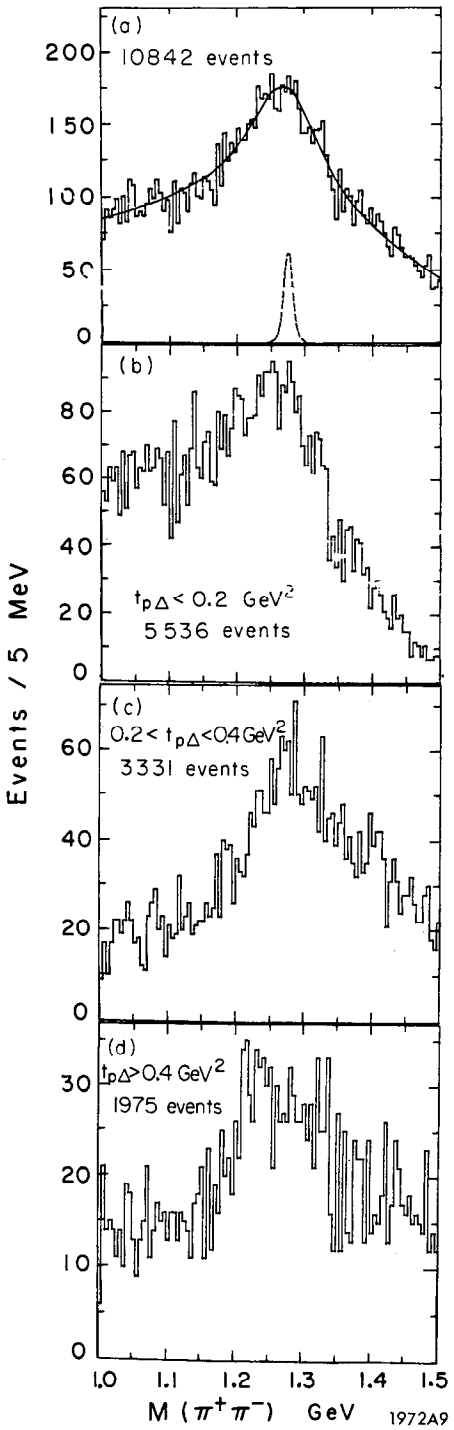

FIG. 2--Mass plots in the f^0 region. A Δ^{++} is always required. The solid curve is a fit with a Breit-Wigner s-wave resonance formula plus a linear background. The dashed curve is our resolution function normalized to 4% of the number of f^0 resonance events found in the fit.

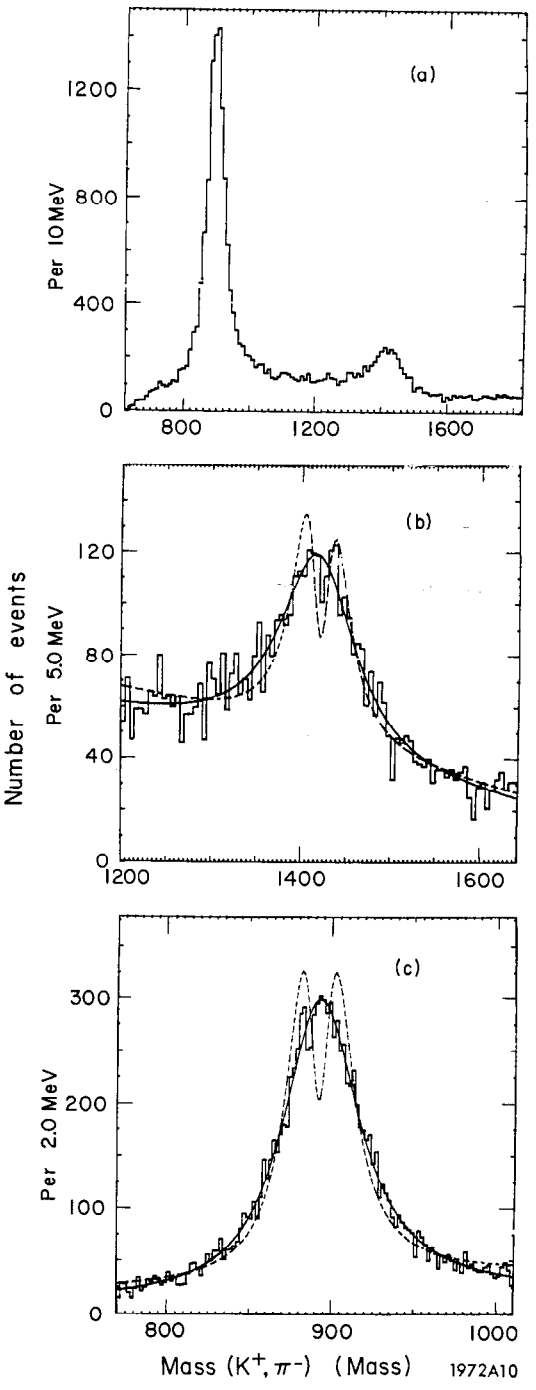

FIG. 3--$K^+\pi^-$ mass distributions in the reaction $K^+p \rightarrow K^+\pi^-\pi^+p$ at 12 GeV/c. No cuts have been made. (a) All events (27,000 events). (b) $K_N(1420)$ region. The solid curve is the best fit to a Breit-Wigner (CL = 47%), the dashed curve is the best fit to a double pole hypothesis (CL < 1%). Both curves have the experimental mass resolution function ($\Gamma/2 = 6.5$ MeV) folded in. (c) K*(890) region. The Breit-Wigner fit (solid curve) has a confidence level of 42%, the dipole fit (dashed curve) has a confidence level of $< 10^{-10}$. The resolution function has $\Gamma/2 = 5.1$ MeV.

Figure 4 shows the $K^+\pi^+\pi^-$ mass distribution where the shaded events are an estimate of the contribution of the $K_N(1420)$ to the graph. Thus it appears that the L enhancement is primarily a peak near threshold in the $K_N(1420)\ \pi$ system. In order to pursue this idea we plot the t distribution of the events in each $K\pi\pi$ mass region in Fig. 5. The peripherality of the reaction (and the consequent low mass peaking) is clearly evident except for the very highest mass regions where the end of kinematic phase space is being reached. The qualitative features of the data seem clear — lack of statistics does not appear to be a problem (this experiment is 35 events/μb). It is possible of course that with infinite statistics selections can be made which will concisely elucidate the interaction mechanism; however this possibility seems remote. What we do need is more manpower to think about the data in a detailed way to find some quantitative understanding.

General Remarks

1. The results I have presented from our group are based on ~ 50 event/μb exposures. Most bubble chamber exposures are still in the 5 event/μb category, and results are being published on resonances with 50 events. In most (but not all) cases this is inadequate for even a qualitative understanding of effects. In the future it seems to me that 50 events/μb is going to be required for most cases to do an adequate job.

2. Accuracy is not an overriding limitation — mass resolutions are adequate for most present results. Of course there may be a whole new world of fine structure at ten times better resolution, but present bubble chambers will not achieve that. In our experiments we are almost entirely limited by multiple scattering. Only an increase in magnetic field will help, and the attempt to gain here should await a reason, just as the first bubble chambers were built with the idea of investigating the world of K mesons.

3. The beauty of the B.C. is its universal coverage. It will continue to contribute to the refinement of our present regime but by itself it does not seem likely to blaze fantastic new trails (remember my restriction to present B.C.'s). If one is planning to attack the region of energy that has been covered over the last ten years, I think a very reasonable approach would be a comprehensive, very large statistics bubble chamber program, because the B.C. sees almost everything.

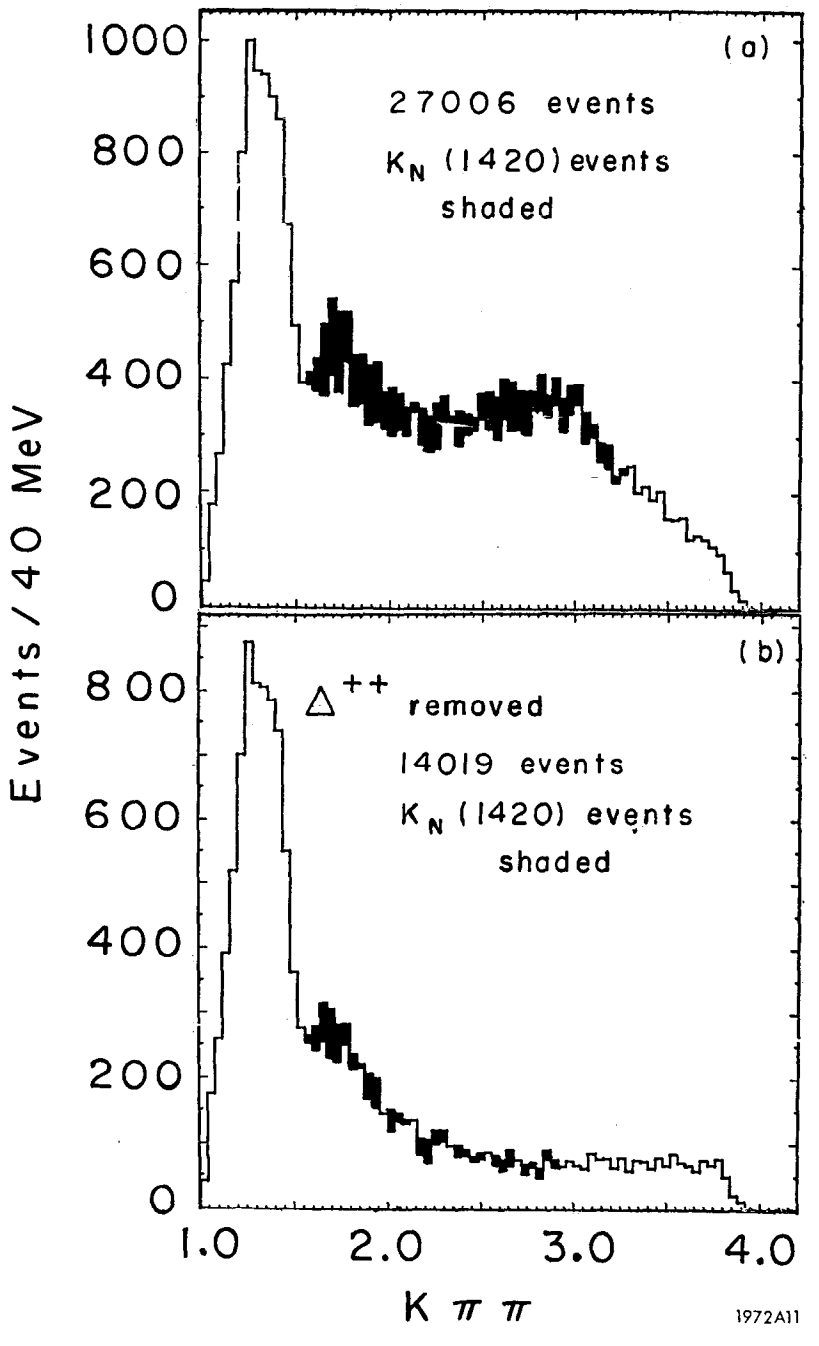

FIG. 4--$K^+\pi^+\pi^-$ mass distributions from $K^+p \rightarrow K^+\pi^-\pi^+p$ at 12 GeV/c. The shaded area is one possible estimate of the contribution from $K_N(1420)$ events.

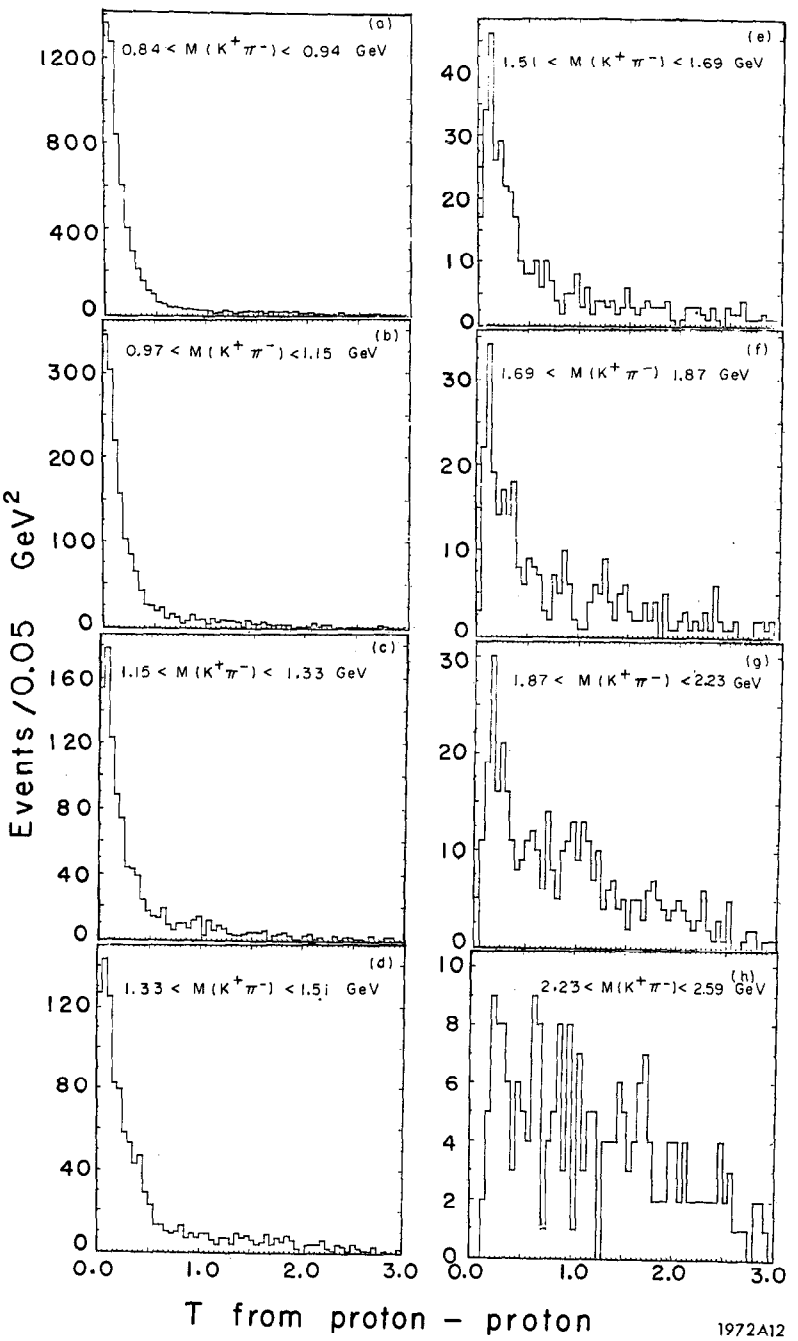

FIG. 5--Momentum transfer from incoming proton to outgoing proton for various $K^+\pi^-$ mass selections. Δ^{++} has been removed.

4. The possibilities of really new physics from bubble chambers appear to me to be in two areas:

a. Big bubble chambers for ν experiments and high energy hadron experiments at NAL and CERN II.

b. Triggered bubble chambers where the chamber is essentially demoted to one of the detectors in a counter experiment. One has to work hard here to fight the general rule that the more selective the trigger, the less useful the bubble chamber.

Finally, let us not forget what we are striving for. Some eminent people have suggested that we are at the point where the human mind is simply inadequate to rationally comprehend basic physics. I personally don't believe this, because the history of life, and physics in particular, is that people who foresee limits on the human mind have been proven wrong. And I feel that all avenues to possible understanding should be kept as open as possible.

References

1. M. Alston-Garnjost et al., Phys. Letters 34B, 156 (1971).
2. S. M. Flatté et al., Phys. Letters 34B, 551 (1971).
3. P. J. Davis et al., Phys. Rev. Letters 23, 1071 (1969).
4. A. Barbaro-Galtieri et al., Phys. Rev. Letters 22, 1207 (1969).

Discussion

Ferbel: What do you think of the Illinois analysis (partial waves analysis on all events including background) and would you do it on your data?

Flatté: That's an approach one can take, but perhaps our theoretical understanding is so low that we can never interpret the result. I think the problem with such reactions is a manpower limitation rather than in the bubble chamber limitations.

Derrick: The K*(890) I think was presented with around 10 events in it. Are you claiming that the resonances discovered now are not significant?

Flatté: There have been 10 new resonances claimed in Phys. Rev. Letters in the last year. I claim that almost all of them are wrong. The exceptions are ones with very low backgrounds. Also, if you think that a whole new world will open up with improved bubble chamber measurement resolution, e.g., very narrow resonances, you should do an experiment (with counters) to see one, then build your high field chambers.

Pless: I think it's bad advice. There may be cases where the chamber is the only way. Any time you turn over a fresh stone you find worms.

Ballam: In the desert?

Flatté: You really have to work hard to get a factor of 10 better resolution. The big bubble chamber at NAL is completely a new technique and is to me a better bet. Track-sensitive targets with triggers lose too much of the inherent advantages of the bubble chamber.

π - P INTERACTIONS AS MEASURED BY PEPR*

I. A. Pless

Massachusetts Institute of Technology
Cambridge, Massachusetts, U.S.A.

I would like to discuss four topics in this talk. The first is a progress report on PEPR; the second topic is a new technique useful in analyzing multi-body final states; the third is the application of this new technique to π^-p interactions at 3.9 and 5.8 GeV/c; and the fourth is possible practical applications of PEPR.

The development of PEPR is the work of many people, and I would like to mention some of them. The engineer in charge of the project, from the very beginning is Bernie Wadsworth. If anyone deserves special credit in the hardware development of PEPR it is he. He has been aided over the years by:

B. Brooks
J. Cormac
R. Kenyon
T. Lingjaerde
L. Monrad-Krohn
E. Sartori
J. Sokolowski and
J. Sharp

There are also many physicists who have aided the development of both the hardware, but especially the software of PEPR. At the head of the list are those grand old men of Data Analysis:

A. Rosenfeld
H. Taft and
F. Solmitz

---

*This paper was also presented at the 1971 New York Meeting of the American Physical Society.

We are still indebted to them for their contributions to the program. Over the years we were fortunate to have the aid of:

P. Bastien
C. Bordener
H. Crouch
F. Harris and
N. Nagle

In recent times the program has benefited from:

R. Hulsizer
T. Watts and
J. Snyder

In particular, we are indebted to J. Snyder for the summers he has spent with us.

And last, but by no means least, we have Richard Yamamoto, who has been with the Program from the very start and, if anyone deserves credit for making PEPR a success, it is he. We started physics production in 1967.

Three questions are always asked about a semi-automatic device:

1) How fast?
2) How accurate?
3) How successful?

Figure 1 answers the first two questions: We started out slowly and, in the calendar year 1970-71, we measured about 155,000 events. These are events on a DST ready for physics analysis. The limit here is our one shift of the scanning and pre-measuring. Our instantaneous rate, measured over an 8-hour period, is 140 events/hour. However, we hope to double the yearly rate without an increase in staff or a change of hardware. We hope to accomplish this with more efficient management. To produce 10^6 events/year will take a change in hardware; namely, three-view PEPR. But this should require no increase in scanning staff as the computer will do more of the work.

Figure 1a is the film plane RMS. This includes all optical constants and their errors. If done just on one view, this improves by factor 2. The third question is success rate. The answer to that depends on the definition of success. Any event where all the tracks reconstruct in TVGP with an acceptable RMS is called a success. By this definition over 85% of all events are successful.

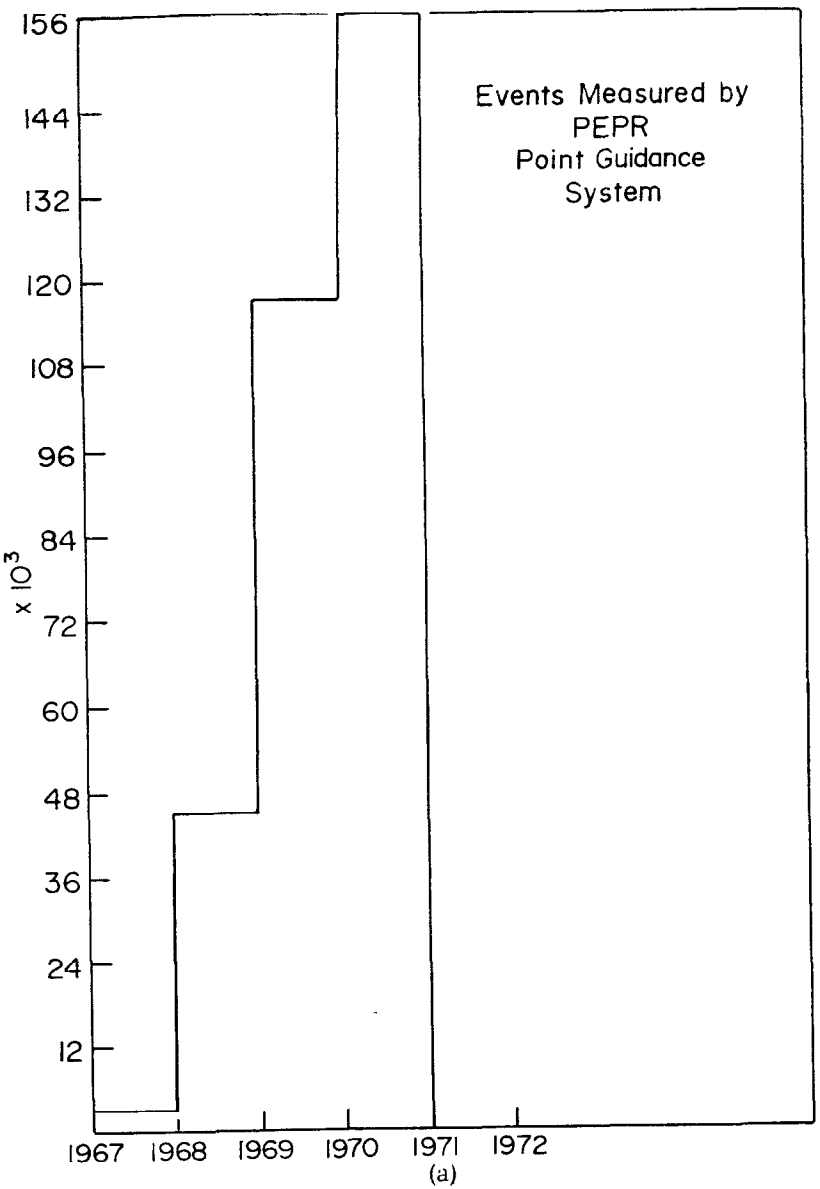
Events Measured by
PEPR
Point Guidance
System
156
144
132
120
108
96
84
72
60
48
36
24
12
x 10³
1967
1968
1969
1970
1971
1972
(a)

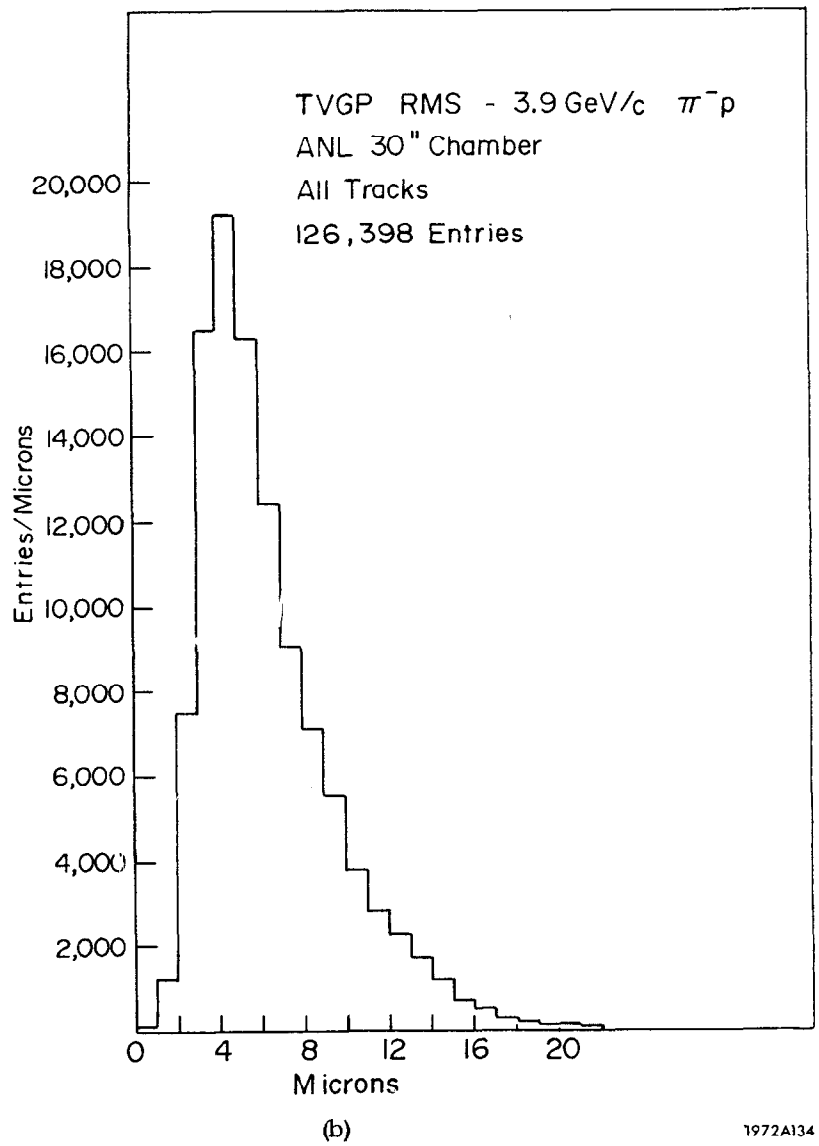
TVGP RMS - 3.9 GeV/c π⁻p
ANL 30" Chamber
All Tracks
126,398 Entries
Entries/Microns
20,000
18,000
16,000
14,000
12,000
10,000
8,000
6,000
4,000
2,000
0
4
8
12
16
20
Microns
(b)
1972A134

Fig. 1

The second part of my talk is devoted to a different way of analyzing multi-body final states. This is important to us as most of the work that we are interested in requires an understanding of these complicated events. We've called this analysis a "prism plot" analysis, and the reason for this name will be made clear. The work I'm discussing is again a cooperative effort of several people. They are:

J. Brau
F. T. Dao
M. Hodous
R. Singer

In particular, F. T. Dao has calculated some of the relationships in this analysis while M. Hodous has written the display programs that allow us to quickly utilize the power of the technique.

Since some of the mathematical details are tedious, I will not discuss them in this talk. If anyone wants the details, he can write me for:

PEPR Programming Note
Data Analysis System, Physics No. 101
"Definitions and Conventions of the N-Body Prism Plot."

As a specific example to work with, let us consider a three-body final state. The first question to consider is how many variables are required to specify this final state? If we assume the center-of-mass energy and final state masses are known, the three components of momentum of each particle certainly determine the final state. So, in principle, we need 9 variables. However, there are four energy-momentum constraints which reduce the required number of variables to 5. If the incident beam and target are unpolarized, the physics is invariant with respect to rotation about the incident beam, which reduces the required number of parameters to 4.

The object of this analysis is to choose four parameters which will help classify final state interactions. Figure 2 indicates the problem and the direction of our solution. The longitudinal momentum graphs shown have been used by many people, including Chan Hong-Mo and collaborators.

The basic idea is that each ordering describes the final state with respect to the longitudinal momentum of the particles. In the first ordering, the π^+ has

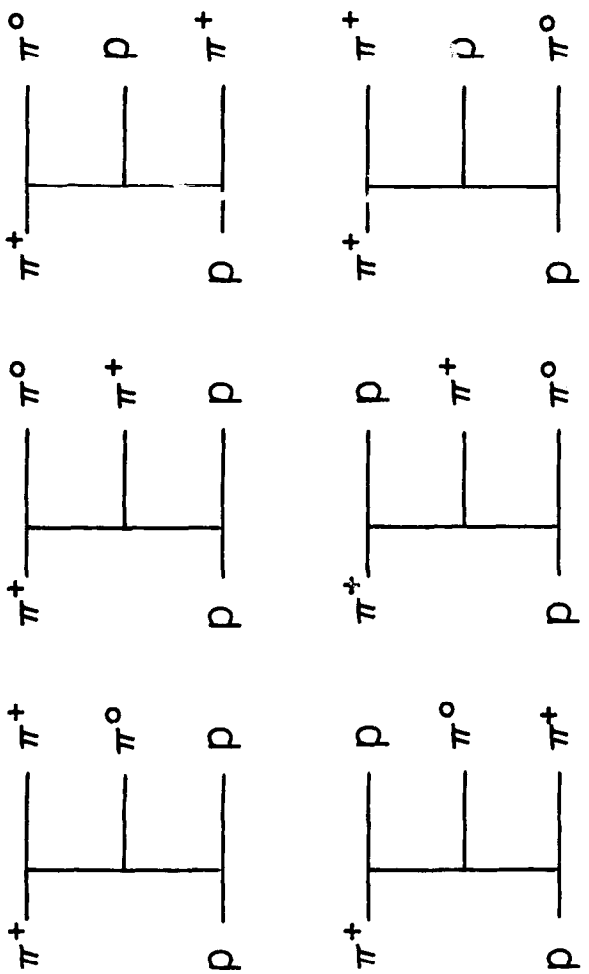

Fig. 2

the largest positive momentum, the proton has the largest negative momentum and the π^o has an intermediate momentum. The idea represented here is to assume that only adjacent particles resonate. The first ordering would contain events consisting of ρ^+, proton final states. Namely, the adjacent pions would resonate. In the first ordering the π^+ and proton would be unlikely to resonate as they are not adjacent, and one would expect no N* (1238) events to be contained in this ordering. On the other hand, Ordering No. 2 should contain many N* (1238), since the proton and π^+ are adjacent. Similarly, one should expect Ordering Number 5 to contain backward going N*(1238) as the proton and π^+ are adjacent, and the proton π^+ tends to go into the backward direction.

Hence, in some sense, these orderings allow us to determine which particles are likely to come from a particular final state resonance. The trouble with this representation is that it is quantized into six orderings, and there is no way to express the fact that one ordering blends into the next in a continuous fashion. This difficulty has been overcome by Van Hove and the introduction of his angular variables. Figure 3 explains and gives the definition of the Van Hove angle for the three-body final state.

If you choose three unit vectors 120 degrees apart to represent the longitudinal momentum of the proton, π^+ and π^o, a three-body final state event can be represented by vector on this plot. (See Fig. 3b.)

The components of this vector along any of the 3-particle axes is the corresponding longitudinal momentum of the particle. In this plot one has the kinematical hexagon, and a point can be represented by this Van Hove angle θ and a radius vector R. θ continuously sweeps past the LMO in the fashion shown in Fig. 3a. θ between 0^o and 180^o represents backward protons while θ between 180^o and 360^o represents forward going protons. Notice for a given angle θ there are an infinite number of possible final states, all represented by different values of R. However, for each angle θ there is a maximum R kinematically possible, labeled R/R_{max} (see Fig. 3d). For any event, R divided by R/R_{max} is the measure of how peripheral the event is or, another way of saying it, how much transverse momentum is involved in the event. If $R/R_{max} = 0$, the event lies in a plane perpendicular to the incident direction, and if $R/R_{max} = 1$ the event is colinear with the incident direction. We choose R/R_{max} and θ as two of our variables. Figure 3c defines all quantities explicitly.

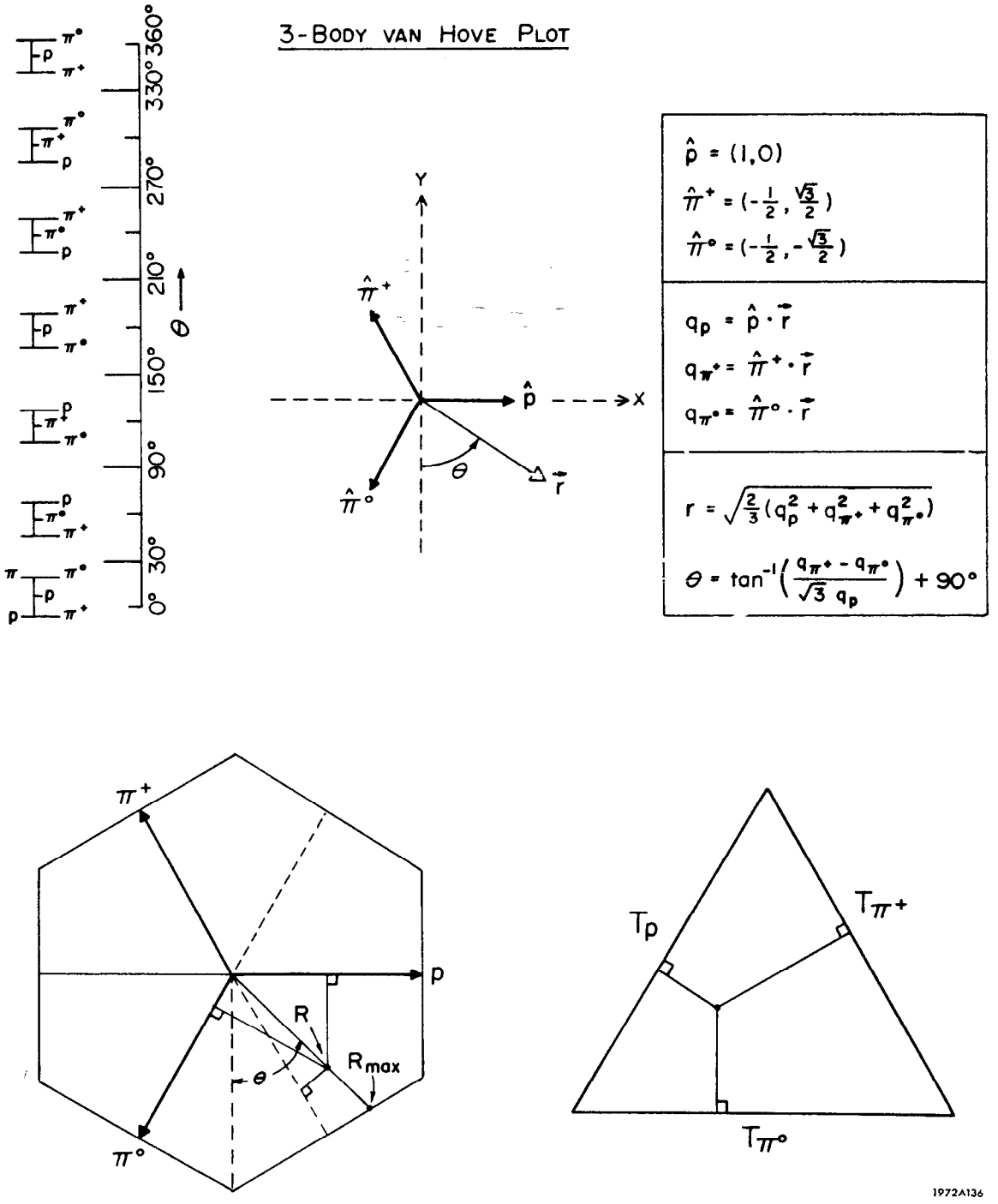
3-Body van Hove Plot
0° 30° 90° 150° 210° 270° 330° 360°
θ
Y
X
$\hat{p}$
$\hat{\pi}^+$
$\hat{\pi}^\circ$
$\vec{r}$
θ
$\hat{p} = (1,0)$
$\hat{\pi}^+ = (-\frac{1}{2}, \frac{\sqrt{3}}{2})$
$\hat{\pi}^\circ = (-\frac{1}{2}, -\frac{\sqrt{3}}{2})$
$q_p = \hat{p} \cdot \vec{r}$
$q_{\pi^+} = \hat{\pi}^+ \cdot \vec{r}$
$q_{\pi^\circ} = \hat{\pi}^\circ \cdot \vec{r}$
$r = \sqrt{\frac{2}{3}(q_p^2 + q_{\pi^+}^2 + q_{\pi^\circ}^2)}$
$\theta = \tan^{-1}\left(\frac{q_{\pi^+} - q_{\pi^\circ}}{\sqrt{3}\, q_p}\right) + 90°$
π^+
p
R
R_{max}
θ
π°
T_p
T_{π^+}
T_{π°
1972A136

Fig. 3

We take our other two variables from the Fabri-Dalitz plot. This is demonstrated by this equilateral triangle, where each side is the kinetic energy in the c.m. of the three particles. (See Fig. 3e). The $\perp$ distance to each side in the kinetic energy of each of the particles, and the sum of all three perpendiculars is equal to the altitude of the triangle or the total available energy in the c.m. We take as our other two variables the T_p and the T_{π^+}.

Figure 4 illustrates how we combine the equilateral triangle and the Van Hove angle into an equilateral rectangular prism. The triangle lies in the X-Y Plane, and θ is plotted along the z axis. What I am going to demonstrate is that if R/R_{max} is close to 1 and, if the available kinetic energy in the c.m. is equal to or larger than the mass of the resonance formed in the c.m., then the various resonant final states will occupy distinct regions in this prism plot.

Figure 5 shows some Monte Carlo events and real events plotted in the prism plot. Figures 5a and 5b [which are Monte Carlo data for Lorentz invariant phase space] have a diffuse set of points in the prism plot, and R/R_{max} is symmetric about 0.5 and has its maximum there. In contrast, Figs. 5b and 5c, which are our data at 3.92 GeV/c, show that the events cluster into three sharp tubes, and R/R_{max} peaks at around 0.9. One can immediately deduce that the Lorentz invariant phase plays almost no role in this final state. Another important point, which I will demonstrate, is that each of those tubes is associated with a particular final state resonance. I will show that the upper tube is all N*(1238) + π^0 production, that the long central tube is all $\rho^+ p$ production, and that the lower tube contains the singly charged N*(1238) and something I will call Diffraction Dissociation.

Figure 6a is the standard invariant mass plot of $p\pi^+$, and Fig. 6c is the invariant mass of the $p\pi^+$ in the upper tube. This data is an excellent fit to N*(1238). Figure 6b is the invariant mass of the $\pi^+\pi^0$, while Fig. 6d is the invariant mass of the events in the second tube. This is an excellent fit to a ρ^+.

Figure 7a shows the $p\pi^0$ invariant mass for all events. Fig. 7c shows these events in the lower tube which we classify as singly charged N*(1238). Fig. 7d shows those events in the lower tube which we classify as Diffraction Dissociation.

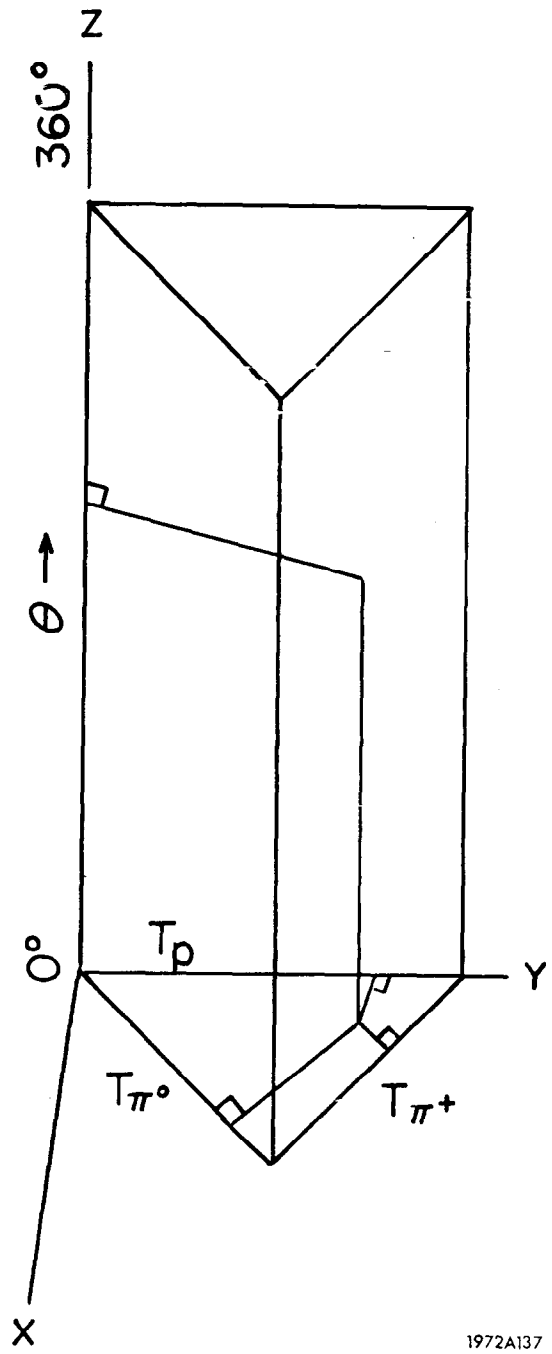

Fig. 4

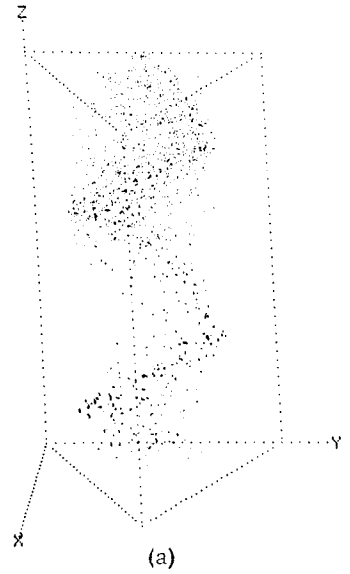

(a)

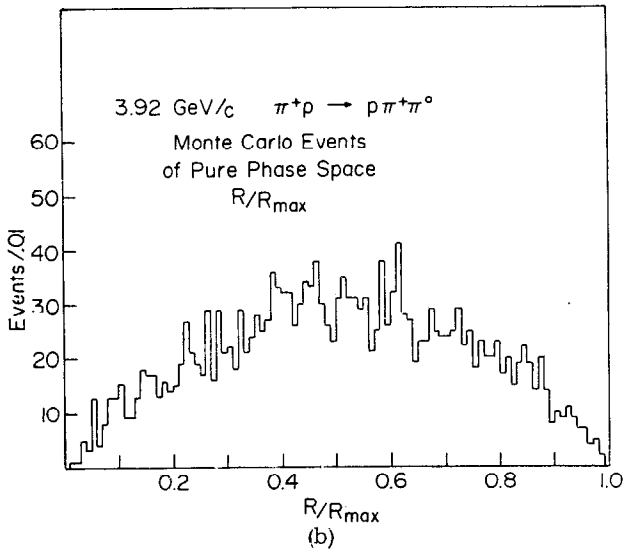

(b)

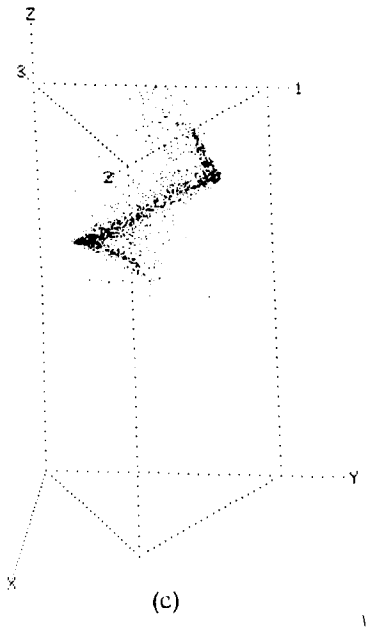

(c)

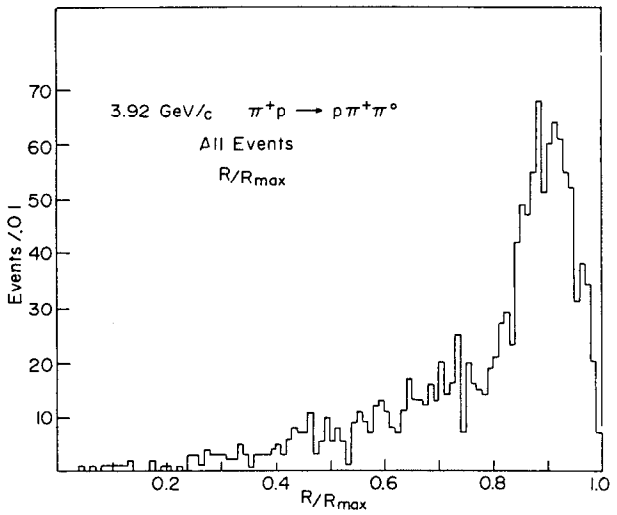

(d)

1972A138

Fig. 5

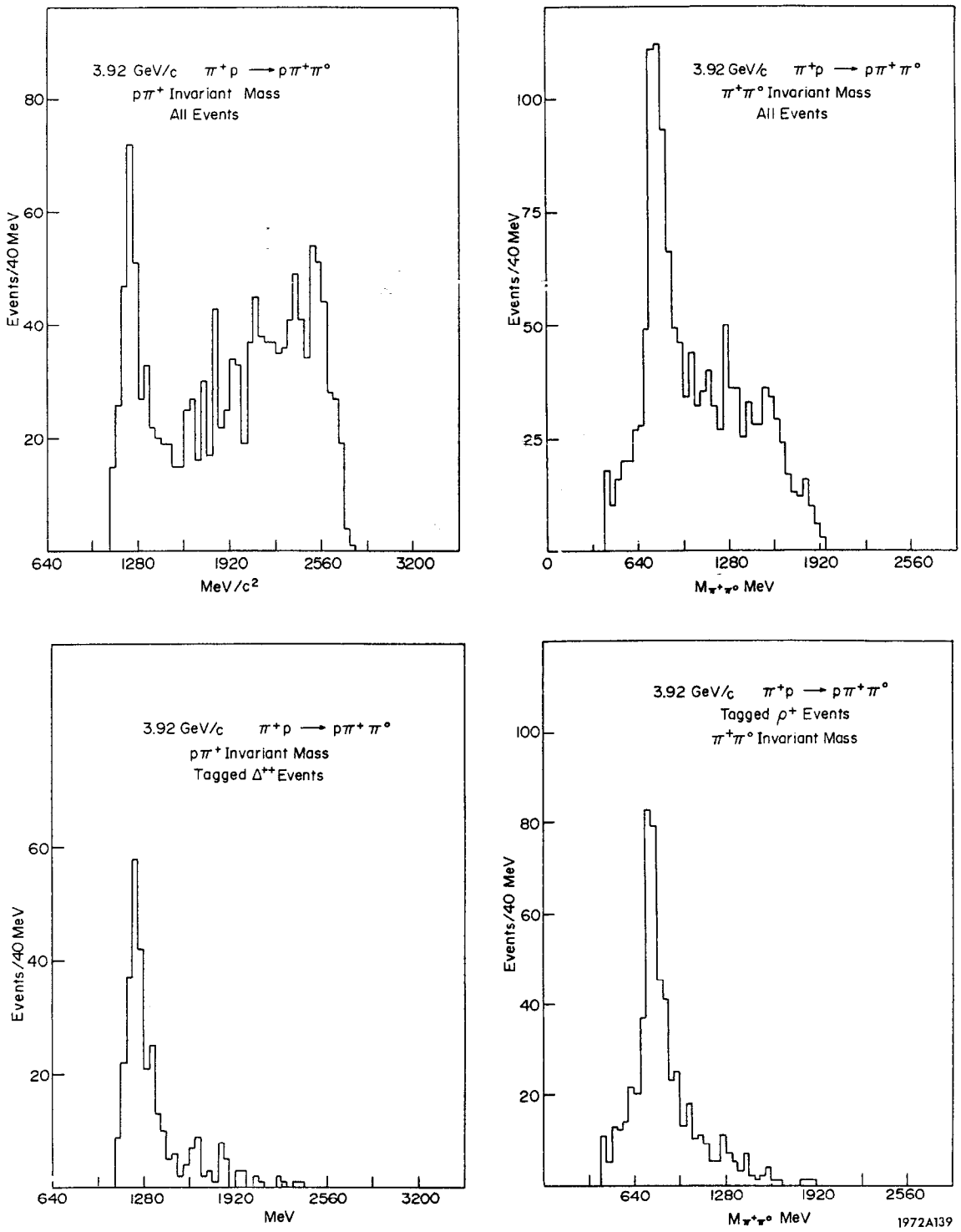
3.92 GeV/c $\pi^+p \rightarrow p\pi^+\pi^\circ$
$p\pi^+$ Invariant Mass
All Events
Events/40 MeV
MeV/c²
3.92 GeV/c $\pi^+p \rightarrow p\pi^+\pi^\circ$
$\pi^+\pi^\circ$ Invariant Mass
All Events
Events/40 MeV
$M_{\pi^+\pi^\circ}$ MeV
3.92 GeV/c $\pi^+p \rightarrow p\pi^+\pi^\circ$
$p\pi^+$ Invariant Mass
Tagged Δ^{++} Events
Events/40 MeV
MeV
3.92 GeV/c $\pi^+p \rightarrow p\pi^+\pi^\circ$
Tagged ρ^+ Events
$\pi^+\pi^\circ$ Invariant Mass
Events/40 MeV
$M_{\pi^+\pi^\circ}$ MeV
1972A139

Fig. 6

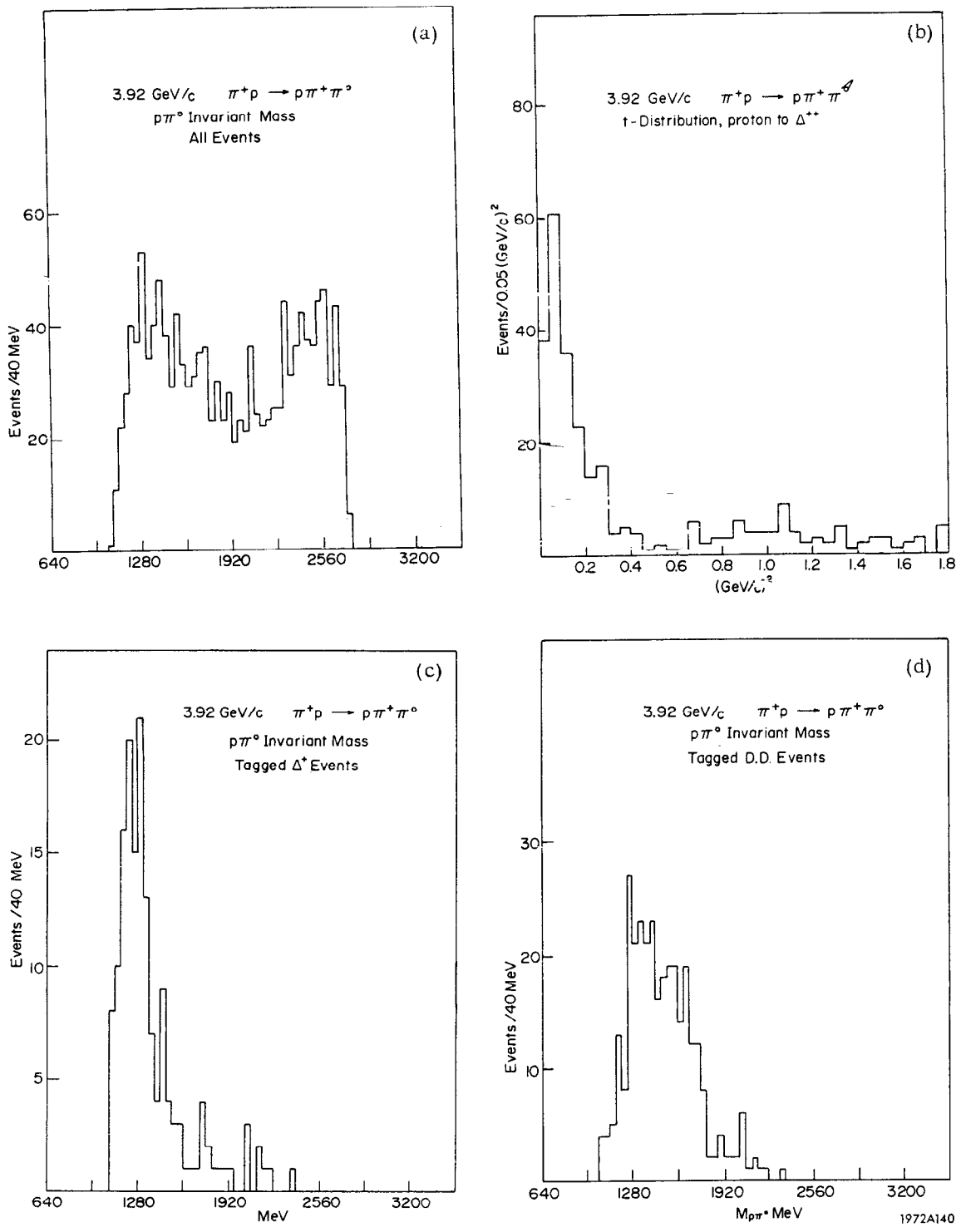
(a)
3.92 GeV/c $\pi^+p \rightarrow p\pi^+\pi^\circ$
$p\pi^\circ$ Invariant Mass
All Events
Events /40 MeV
60
40
20
640
1280
1920
2560
3200
(b)
3.92 GeV/c $\pi^+p \rightarrow p\pi^+\pi^-$
t-Distribution, proton to Δ^{++}
Events/0.05 (GeV/c)^2
80
60
40
20
0.2
0.4
0.6
0.8
1.0
1.2
1.4
1.6
1.8
(GeV/c)^2
(c)
3.92 GeV/c $\pi^+p \rightarrow p\pi^+\pi^\circ$
$p\pi^\circ$ Invariant Mass
Tagged Δ^+ Events
Events /40 MeV
20
15
10
5
640
1280
1920
2560
3200
MeV
(d)
3.92 GeV/c $\pi^+p \rightarrow p\pi^+\pi^\circ$
$p\pi^\circ$ Invariant Mass
Tagged D.D. Events
Events /40 MeV
30
20
10
640
1280
1920
2560
3200
$M_{p\pi^\circ}$ MeV
1972A140

Fig. 7

Figure 7b is the t-distribution of our N.(1238) events. Note that our technique is not equivalent to a t-cut. We have events at large t and clear evidence for a dip at t = 0.6 as would be expected from the Regge model.

Figure 8 is some of the new physical results we have obtained using this prism plot technique. The first point is that we have little, if any, phase space contribution to this final state. Two, we have explicitly measured the ratio of the doubly and singly charged N*(1238) production and show that this ratio is 9:4 in complete agreement with isospin invariance. In addition, we have isolated the phenomenon Diffraction Dissociation and measured cross section and angular distributions. We have also analyzed the $N\pi^+\pi^+$ final state and find a cross section for a similar reaction which is twice this, in agreement with the isospin 1/2 invariance. The nucleon-pion invariant mass and angular distributions are the same.

The prism plot generalizes directly to N-Dimensions, and I will quickly show you the 4-body extension.

Figure 9 shows the definition of the two Van Hove angles for the 4-body final state. In this case, the kinemential limits are a cube with the corners chopped off. We can again define an R/R_{max} that has the same meaning as for the 3-body case. We use, therefore, the two Van Hove angles θ_1 and θ_2, and R/R_{max}.

Figure 10 shows the longitudinal momentum orderings as a function of θ_1 and θ_2.

Figure 11 indicates the boundaries of the longitudinal momentum orderings shown in Fig. 10.

Figure 12 generalizes the Fabri-Dalitz plot. This is now a kinetic energy tetrahedron. Again, each event can be represented as a point inside this energy tetrahedron. The sum of the perpendiculars is equal to the altitude which is again the total energy in the c.m. We therefore use three of the kinetic energies as our variables.

Figure 13 indicates one of the interesting properties of the energy tetrahedron. The plane indicated here, under the conditions that $R/R_{max} = 1$ and that the total K.E. in the c.m. be equal to or greater than the mass of any resonance in the c.m., will contain the $\Delta^{++}\rho^0$ double resonance production. Since $\pi^+(1)$ and $\pi^+(2)$ are just labels given by our scanning personnel, there is an obvious symmetric plane that also contains these resonances.

$3.9\ \pi^+ p \rightarrow p\pi^+\pi^o$

	No.	%	σ (mb)
P.S.	34	3%	46 ± 40
ρ^+	536	41%	718 ± 55
Δ^{++}	307	23%	411 ± 30
Δ^+	123	9%	165 ± 40
D.D.	314	24%	423 ± 70

1972A141

Fig. 8

4-Body van Hove Plot

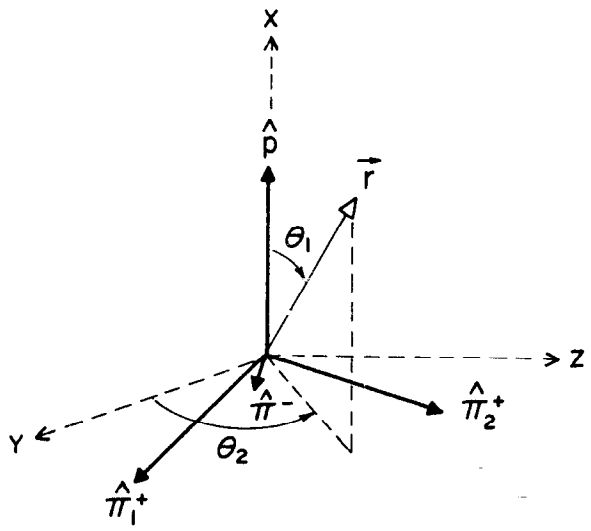

$\hat{p} = (1,0,0)$	$q_p = \hat{p} \cdot \vec{r}$	$r = \sqrt{\frac{3}{4}(q_p^2 + q_{\pi_1^+}^2 + q_{\pi_2^+}^2 + q_{\pi^-}^2)}$
$\hat{\pi}_1^+ = \left(-\frac{1}{3}, \frac{2\sqrt{2}}{3}, 0\right)$	$q_{\pi_1^+} = \hat{\pi}_1^+ \cdot \vec{r}$	$\theta_1 = \cos^{-1}\left(\frac{q_p}{r}\right)$
$\hat{\pi}_2^+ = \left(-\frac{1}{3}, \frac{-\sqrt{2}}{3}, \sqrt{\frac{2}{3}}\right)$	$q_{\pi_2^+} = \hat{\pi}_2^+ \cdot \vec{r}$	
$\hat{\pi}^- = \left(-\frac{1}{3}, \frac{-\sqrt{2}}{3}, -\sqrt{\frac{2}{3}}\right)$	$q_{\pi^-} = \hat{\pi}^- \cdot \vec{r}$	$\theta_2 = \tan^{-1}\left[\frac{3(q_{\pi_2^+} - q_{\pi^-})}{3\, q_{\pi_1^+} + q_p}\right]$

1972A142

Fig. 9

4-Body van Hove Plot

II Ordering

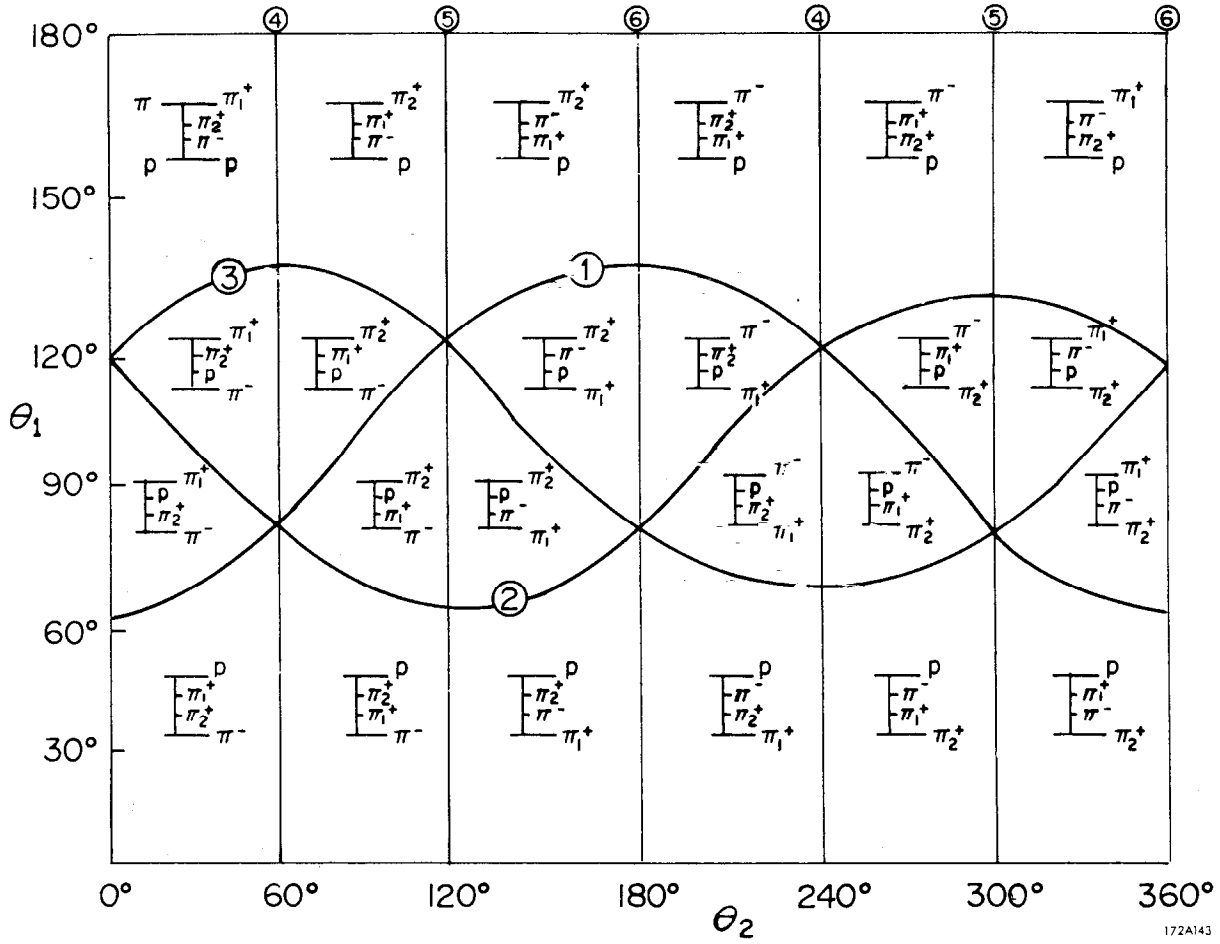

Fig. 10

① $q_p = q_{\pi_1^+}$: $\cot\theta_1 = \frac{1}{\sqrt{2}}\cos\theta_2$

② $q_p = q_{\pi_2^+}$: $\cot\theta_1 = -\sqrt{\frac{1}{8}}\cos\theta_2 + \sqrt{\frac{3}{8}}\sin\theta_2$

③ $q_p = q_{\pi^-}$: $\cot\theta_1 = -\sqrt{\frac{1}{8}}\cos\theta_2 - \sqrt{\frac{3}{8}}\sin\theta_2$

④ $q_{\pi_1^+} = q_{\pi_2^+}$: $\tan\theta_2 = \sqrt{3}$

⑤ $q_{\pi_1^+} = q_{\pi^-}$: $\tan\theta_2 = -\sqrt{3}$

⑥ $q_{\pi_2^+} = q_{\pi^-}$: $\tan\theta_2 = 0$

1972A144

Fig. 11

4-Body Prism Plot

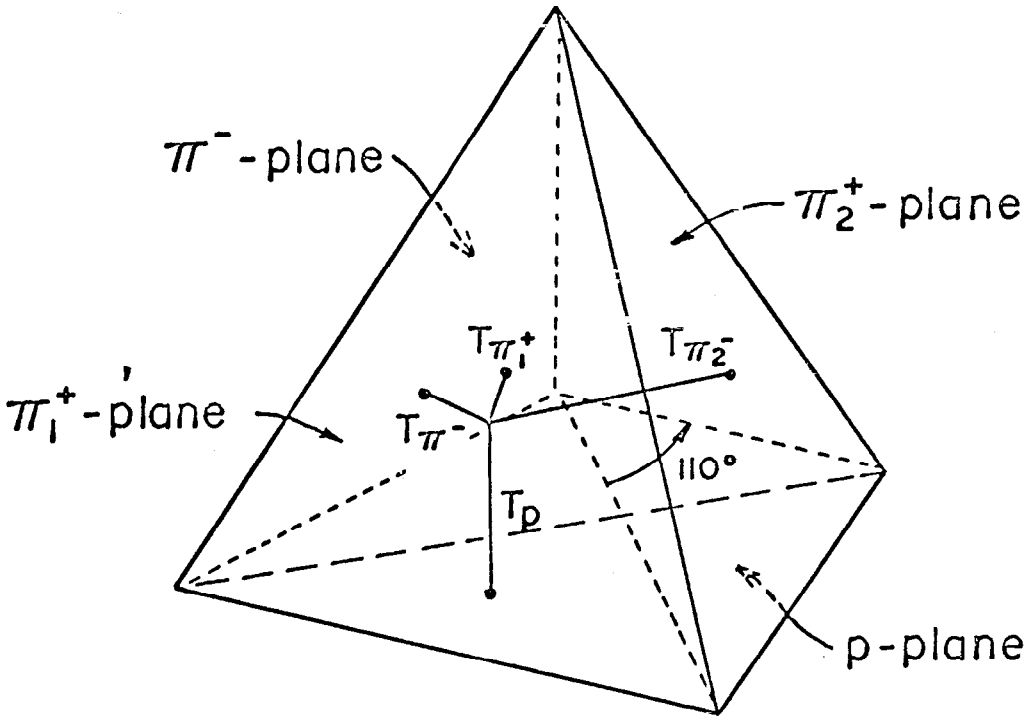

$$T_p + T_{\pi_1^+} + T_{\pi_2^+} + T_{\pi^-} = \text{constant}$$

1972A148

Fig. 12

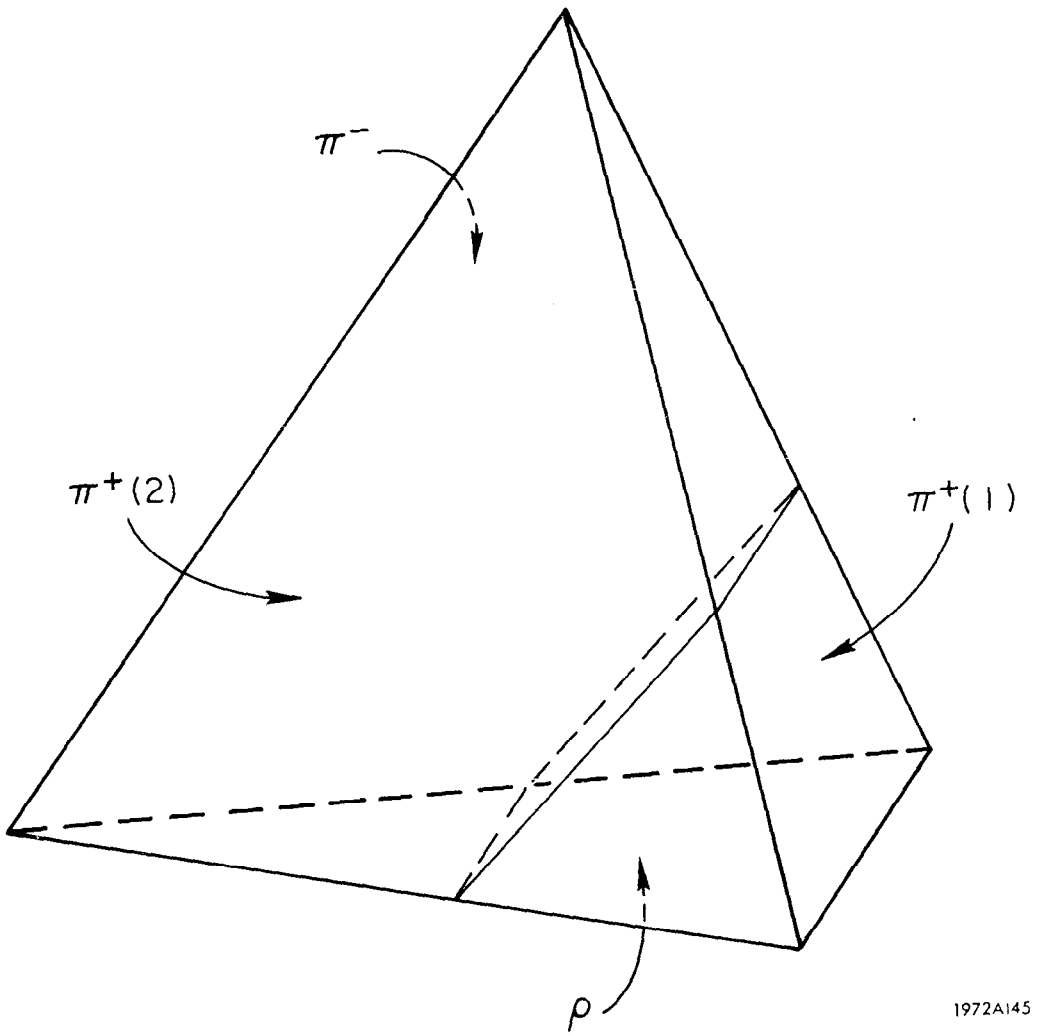

Fig. 13

Figure 14a is again R/R_{max} for Lorentz-invariant phase space. Again, the peak is at 0.5. Figure 14b shows R/R_{max} for our data at 5.72 BeV/c. For this data, the peak is at 0.9. This is evidence that Lorentz-invariant phase space plays only a small role, if any, in this reaction.

Figures 15a and 15b show Monte Carlo data of Lorentz-invariant phase space. The data is essentially uniform in both plots. However, the real data in Figs. 15c and 15d have striking structure. Figure 15c contains evidence for the plane which contains the N*(1238) - ρ^0 events. This plane plus the first prominent disc in Fig. 15d form a five dimensional tube in this five dimensional prism plot. Figure 16 shows what the events in this tube look like.

Figure 16a contains data showing the invariant mass of the $p\pi^+$, each event plotted twice, while Fig. 16c is the invariant mass of the $p\text{-}\pi^+(1)$ contained in the five dimensional tube. The curve speaks for itself. Figure 16b is the $\pi^+\pi^-$ invariant mass, each event plotted twice, while Fig. 16d is the same invariant mass for the events in the five dimensional tube. Again, the data speaks for itself. The generalization to N dimensions is straight forward. The energy tetrahedron becomes an N-dimensional simplex, and the Van Hove angles become the spherical angles in an N-dimensional sphere.

I would like to conclude this talk by discussing the possible applications to fields other than physics. Considering the present economical and social climate, I think it is important for people working in basic research to give more consideration to the possible applied physics applications of the gadgets they develop in their work. Several years ago, Art Rosenfeld and I concluded that, with minor modifications, a PEPR could be turned into a mass storage and retrieval system. One can write and read on a 70mm square piece of film some 1.6×10^7 bits. One can read this film area at a 10 megacycle rate. One also has random access to this area. We wrote a little patent disclosure on this and filed it away. Recently, the University of Oxford has taken this paper and has turned it into a proposal submitted both to industry and to the English Government. Their proposal is to develop the mass store capabilities of PEPR. In addition, they point out the usefulness of PEPR in producing intermediate masks for large scale integrated circuits. Finally, it has been proposed that PEPR can be used to recognize, classify and count cells which would be useful both medically and as a monitor on airborne and waterborne pollutions. We believe these potentials of PEPR should be explored not only in England but also here in the U.S.

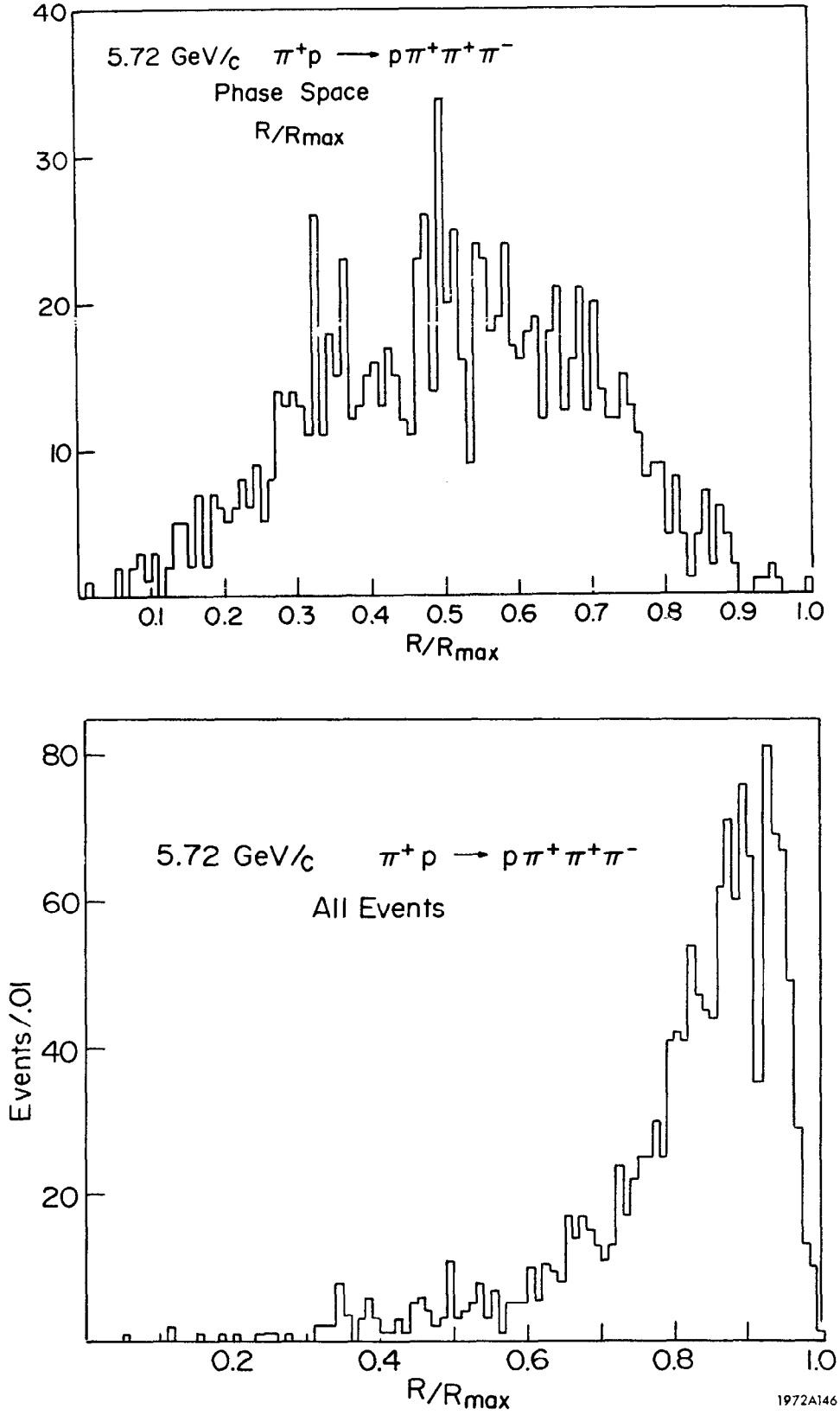
5.72 GeV/c $\pi^+p \longrightarrow p\pi^+\pi^+\pi^-$
Phase Space
R/Rmax
40
30
20
10
0.1
0.2
0.3
0.4
0.5
0.6
0.7
0.8
0.9
1.0
R/Rmax
5.72 GeV/c $\pi^+p \longrightarrow p\pi^+\pi^+\pi^-$
All Events
Events/.01
80
60
40
20
0.2
0.4
0.6
0.8
1.0
R/Rmax
1972A146

Fig. 14

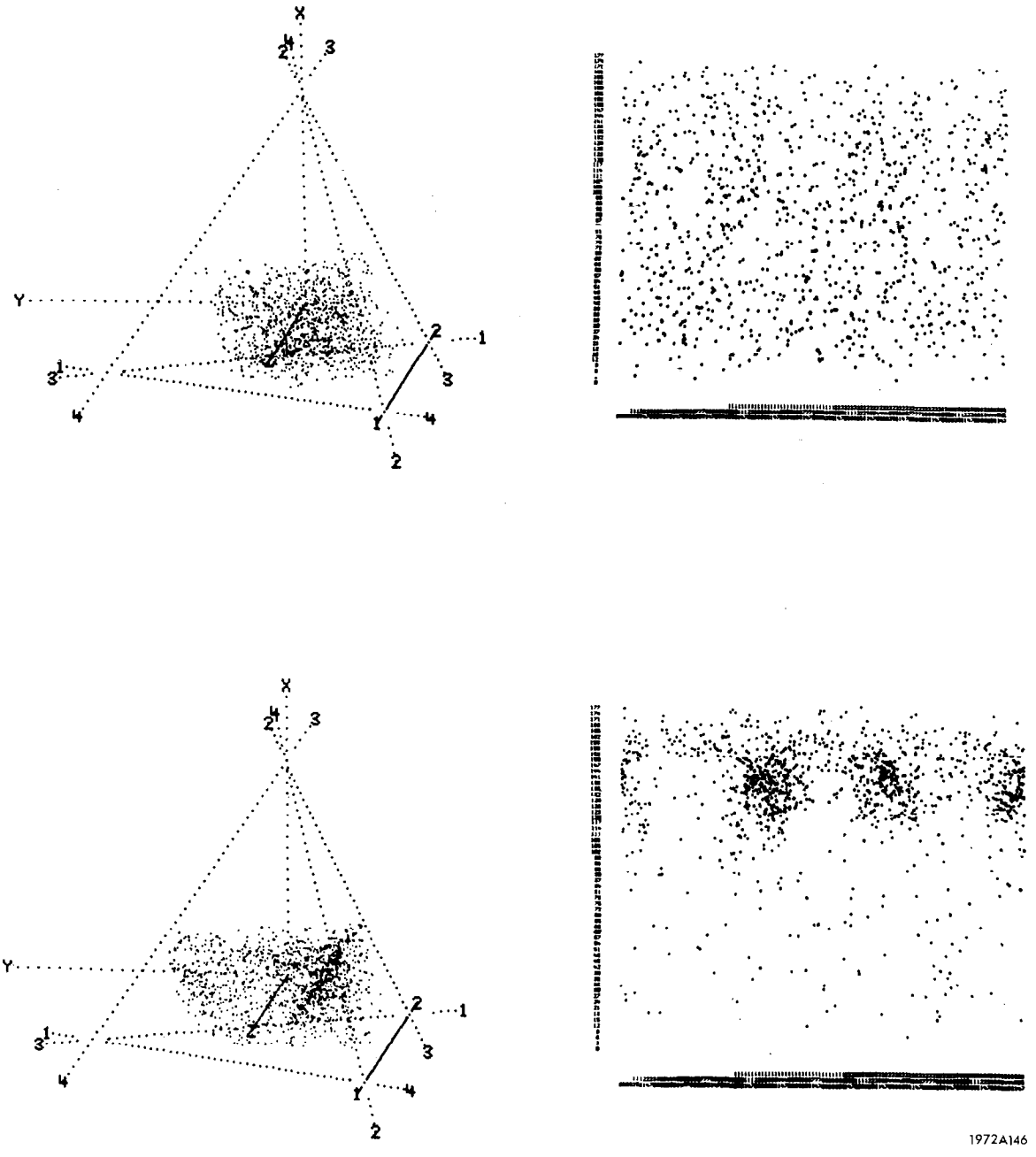

Fig. 15

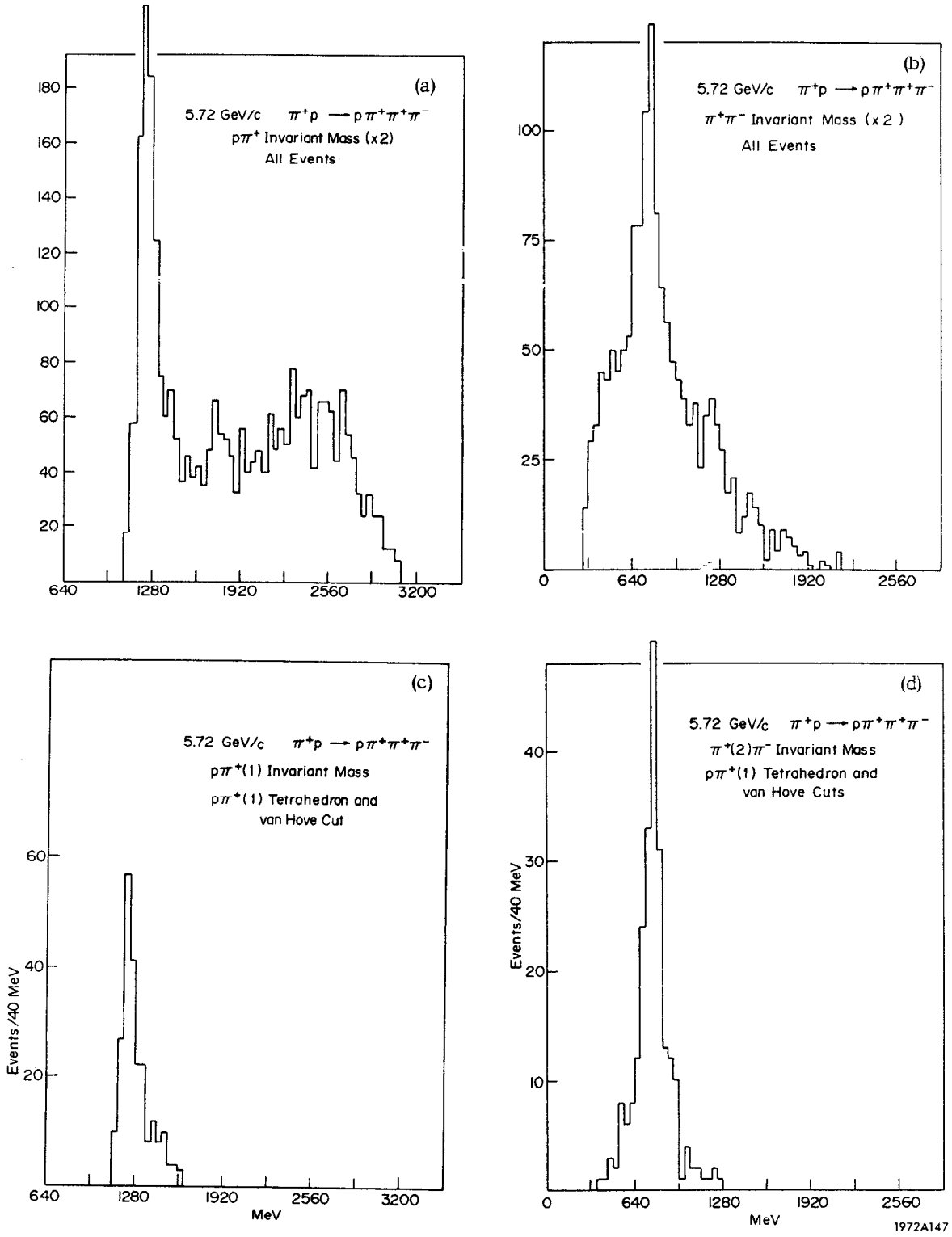
(a)
5.72 GeV/c $\pi^+p \rightarrow p\pi^+\pi^+\pi^-$
$p\pi^+$ Invariant Mass (x2)
All Events
(b)
5.72 GeV/c $\pi^+p \rightarrow p\pi^+\pi^+\pi^-$
$\pi^+\pi^-$ Invariant Mass (x 2)
All Events
(c)
5.72 GeV/c $\pi^+p \rightarrow p\pi^+\pi^+\pi^-$
$p\pi^+(1)$ Invariant Mass
$p\pi^+(1)$ Tetrahedron and van Hove Cut
(d)
5.72 GeV/c $\pi^+p \rightarrow p\pi^+\pi^+\pi^-$
$\pi^+(2)\pi^-$ Invariant Mass
$p\pi^+(1)$ Tetrahedron and van Hove Cuts
Events/40 MeV
MeV
1972A147

Fig. 16

Discussion

Harari: Does each event in your plots fall into only one of your tubes?

Pless: To the same level of truth as you were using (namely 5-10%) the answer is yes. And the overlaps are especially interesting because, in order to have interference, there must be overlap in all four variables. So for the first time we can isolate the true interference region.

Flatté: What about proton polarization?

Pless: In this case we have an unpolarized target reaction.

Flatté: I don't agree. If the proton has flip in one case, and not in the other, they won't interfere.

Ballam: You're not saying every event in the region has to interfere, are you?

Pless: Certainly not. Just that if interference occurs it has to be there. I can determine the degree of coherence. The point is that I can put each event into one and only one bucket and explain them all. If I extrapolate the resonance events into the interference region, and remove them, if I find, e.g., events left over, then there was constructive interference. In our case we find no events left, so there was no interference.

Harari: You assume all events are either ρ or N* and you don't know which. But I think they can be both at the same time.

Pless: You write the separate amplitudes and add them.

Harari: No. This is not the duality reasoning. I am not quarreling with your analysis when you say there is no interference, but the general method is suspect. The uncertainty is just the percentage of the overlap region.

Pless: There is a discrepancy between you and the theory group at M.I.T.

Harari: I can only tell you what you can't do, not what you can do....

[The problem was not resolved. It was agreed that the method can reduce the apparent overlap region to manageable size.]

Discussion

Derrick: Does anybody believe these resonances exist?

Peaslee: We do.

Ballam: At SLAC such resonances have been looked for in $\pi^- p \rightarrow p\bar{p}p$ reactions.

Peaslee: That would be a good way to look for them, as our result indicates they are coupled strongly to $N\bar{N}$.

N - η RESONANCES

T. Kitagaki

Tohoku University Group*
Sendai, Japan

Investigation of the N - η system may be important for the study of non-strange baryon resonances, because of its pure $I=\frac{1}{2}$ isotopic spin state and the relatively low angular momenta involved. A study of the N - η system in the mass region of 1,500 - 2,000 MeV would be especially important, as it might give a base for further phase shift analysis of nonstrange baryon systems in the higher mass region.

We are studying the N - η system in the following two reactions:

$$\bar{p}p \rightarrow \bar{p}p\eta \quad , \text{ at } 6.95 \text{ GeV/c } (s = 14.9 \text{ GeV}^2) \tag{1}$$

$$\pi^- p \rightarrow \pi^- p\eta \quad , \text{ at } 7.85 \text{ GeV/c } (s = 15.6 \text{ GeV}^2) \tag{2}$$

In both reactions the eta events are obtained from two-prong events only (in the neutral decay modes) to avoid problems with I = 3/2 Δ backgrounds. We present the following preliminary results.

1. $\bar{p}p$ Reactions

8,700 two-prong events were measured in 17,806 frames of 6.95 GeV/c $\bar{p}$ film taken by the BNL 80" bubble chamber. The missing mass distribution, $\bar{p}p \rightarrow \bar{p}p(MM)$, is shown in Fig. 1a, where all two-prong events are included. That is, all two-prong events are treated as $\bar{p}p \rightarrow \bar{p}p(MM)$, even if they are $\bar{p}\pi^+(MM)$ or $\pi^- p(MM)$ events. The mass resolution in the figure is rather poor. However, a bump may be recognized in the eta region. Finally 154 events were selected as the $\bar{p}p\eta$ events, and the FAKE test showed that the final 154 events have a signal to noise ratio of 2.4/1. The hatched area of the 154 events in Fig. 1a is consistent with this signal to noise ratio.

This reaction is symmetric for both the $\bar{p}$ and p. However in our measurements the low momentum protons were deliberately cut out. The

---

* T. Kitagaki, K. Takahashi, S. Tanaka, K. Hasegawa, T. Sato, R. Sugahara, K. Tamai, H. Kichimi, T. Okusawa and S. Hoguchi

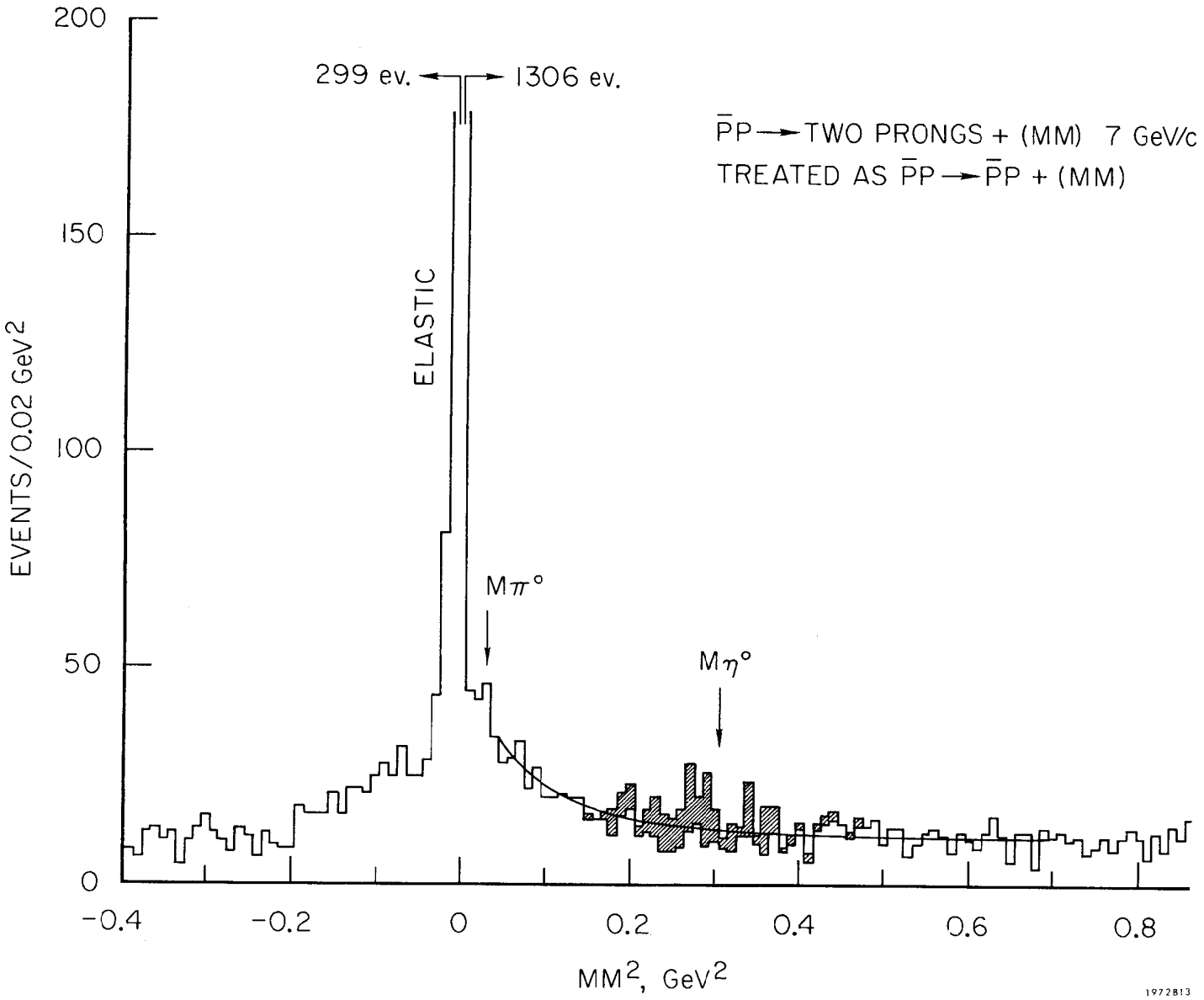

FIG. 1a--Missing mass distribution.

effect of the bias due to this selection criterion depresses the number of events in the low mass side of the $\bar{p}$ - η mass distribution significantly; therefore we will discuss only the p - η system.

The p - η mass plot is shown in Fig. 4a. The hatched area containing 62 events is with $|t| \leq 0.35$ GeV^2, and the purity of the eta is relatively good there. It shows two peaks in the mass regions of 1,500 - 1,700 MeV and 1,750 - 2,000 MeV. Further discussions will be made later in Section III.

2. π^-p Reactions

23,000 frames of 7.85 GeV/c π^- pictures taken by the BNL 80" BC were scanned, and 12,780 two-prong events were measured. Figure 1b shows the missing mass distribution for $\pi^-p \rightarrow \pi^-$p(MM), and the distribution includes all two-prong events even if they are $\pi^-\pi^+$(MM) events. Here again a low eta bump is seen, and about 90 eta production events are estimated to be in the bump.

In the case of $\pi^-p \rightarrow \pi^-p\eta$, there are two groups of eta. The fireworks of Fig. 2a is the directional plot of eta momenta (tail length ~p) and Fig. 2b is the P^*_η - cos θ^* plot. Events in the left-hand side of Figs. 2a and 2b are mainly p - η events, and the right-hand side events are π^- - η events which include A_2. Also the Dalitz plot, Fig. 3, shows two perpendicular bands of p - η and π^- - η. However, the selection of eta is still not good in this case and the signal to noise ratio of eta events/non-eta events is estimated to be about 1/1.5 in Fig. 2. Since we have not been very strict in selecting our events, we are currently investigating the effects of the $\pi^-\pi^+$ background as well as the Δ (π^-p) background.

Figure 4b is a p - η mass plot of η events, with the t cut, which rejects the major part of the π^- - η events.

3. Discussion

Figure 5a is a plot of B vs. M(pη) in the $\bar{p}p \rightarrow \bar{p}p\eta$ reaction, where B is the gradient of the t distribution:

$$B = \frac{d}{dt}\left(\log \frac{d}{dt}\right), \quad \text{for the interval } t_1 < |t| < t_1 + 0.30 \text{ GeV}^2.$$

B is averaged over the t interval of $|t| = t_1 \rightarrow t_1 + 0.30$ GeV^2 with the mass

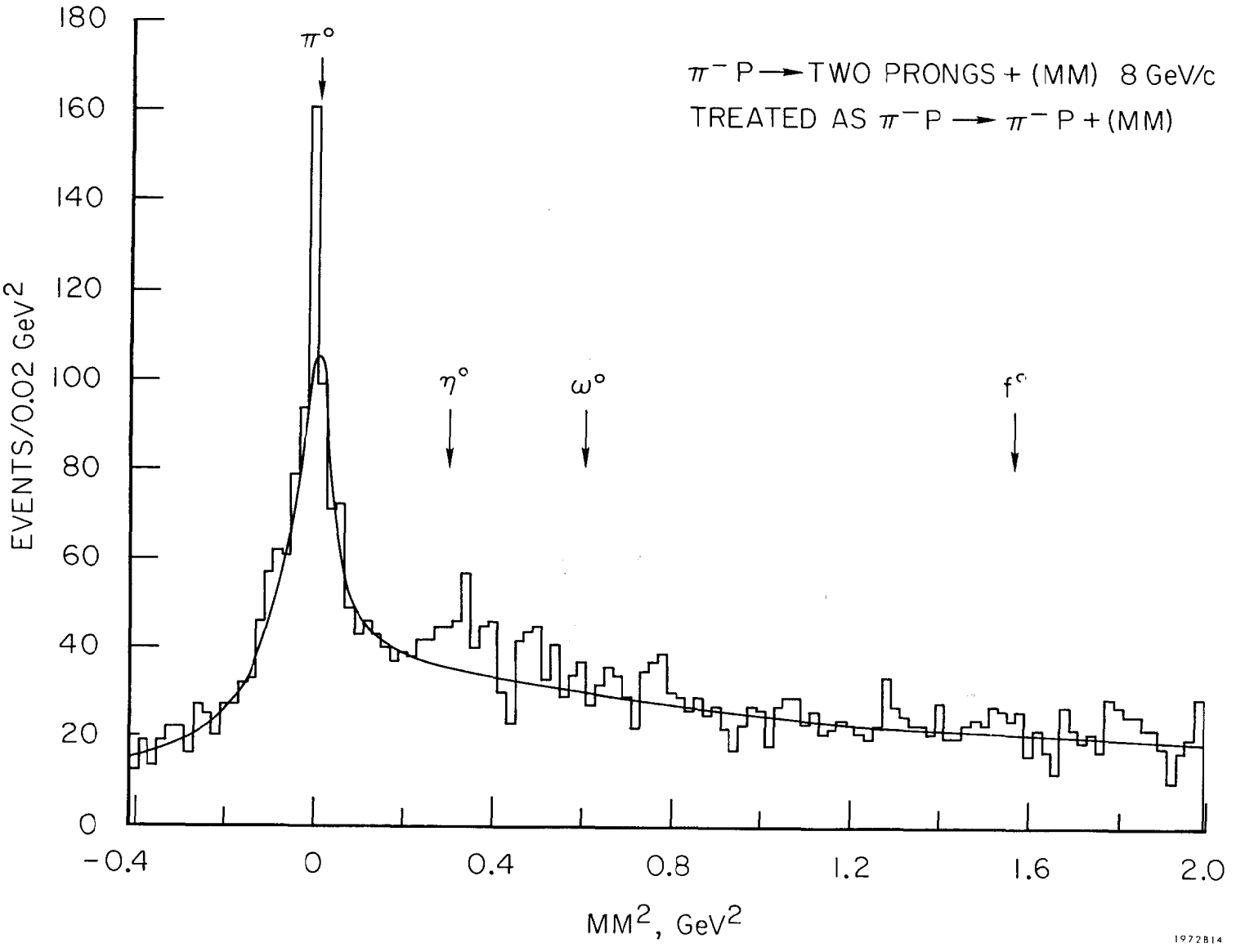

FIG. 1b--Missing mass distribution.

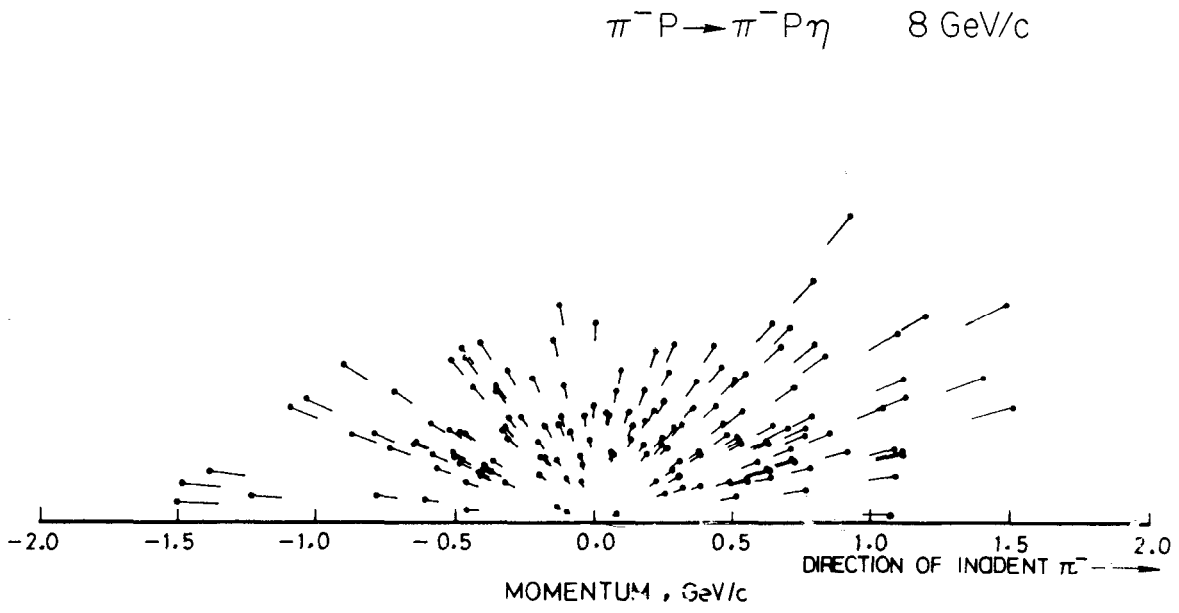

FIG. 2a--Momentum of η in CMS.

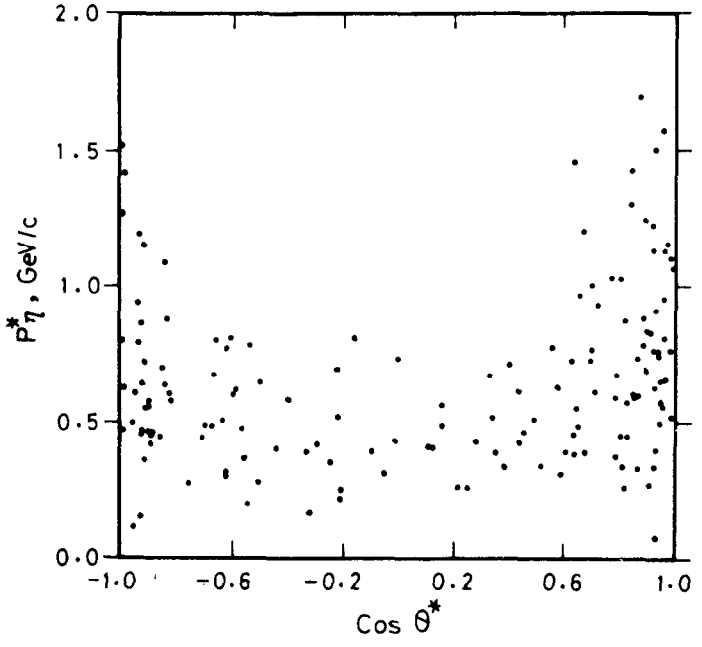

FIG. 2b--P^*_η versus cos θ^* plot.

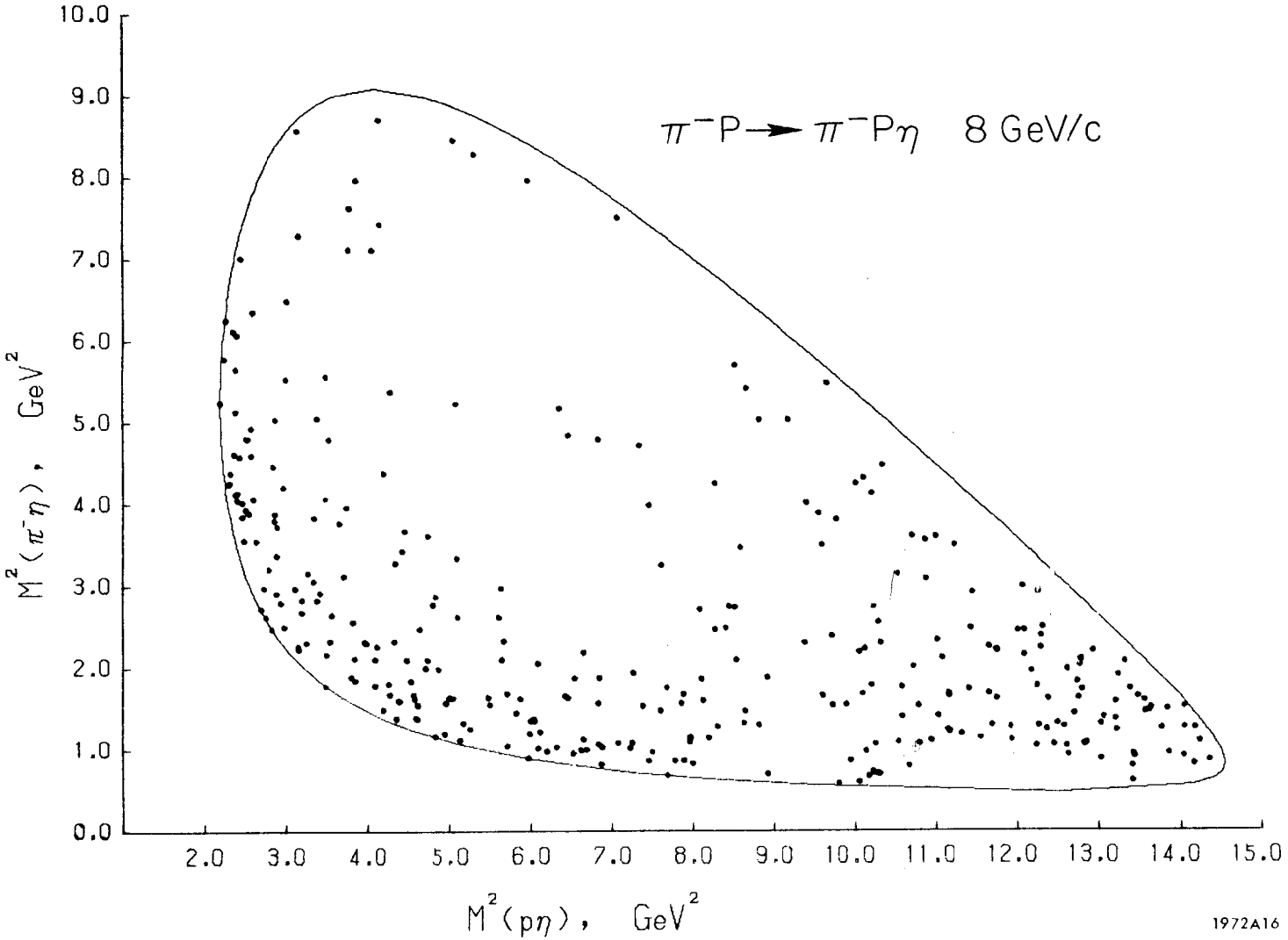

FIG. 3--Dalitz plot for 325 events.

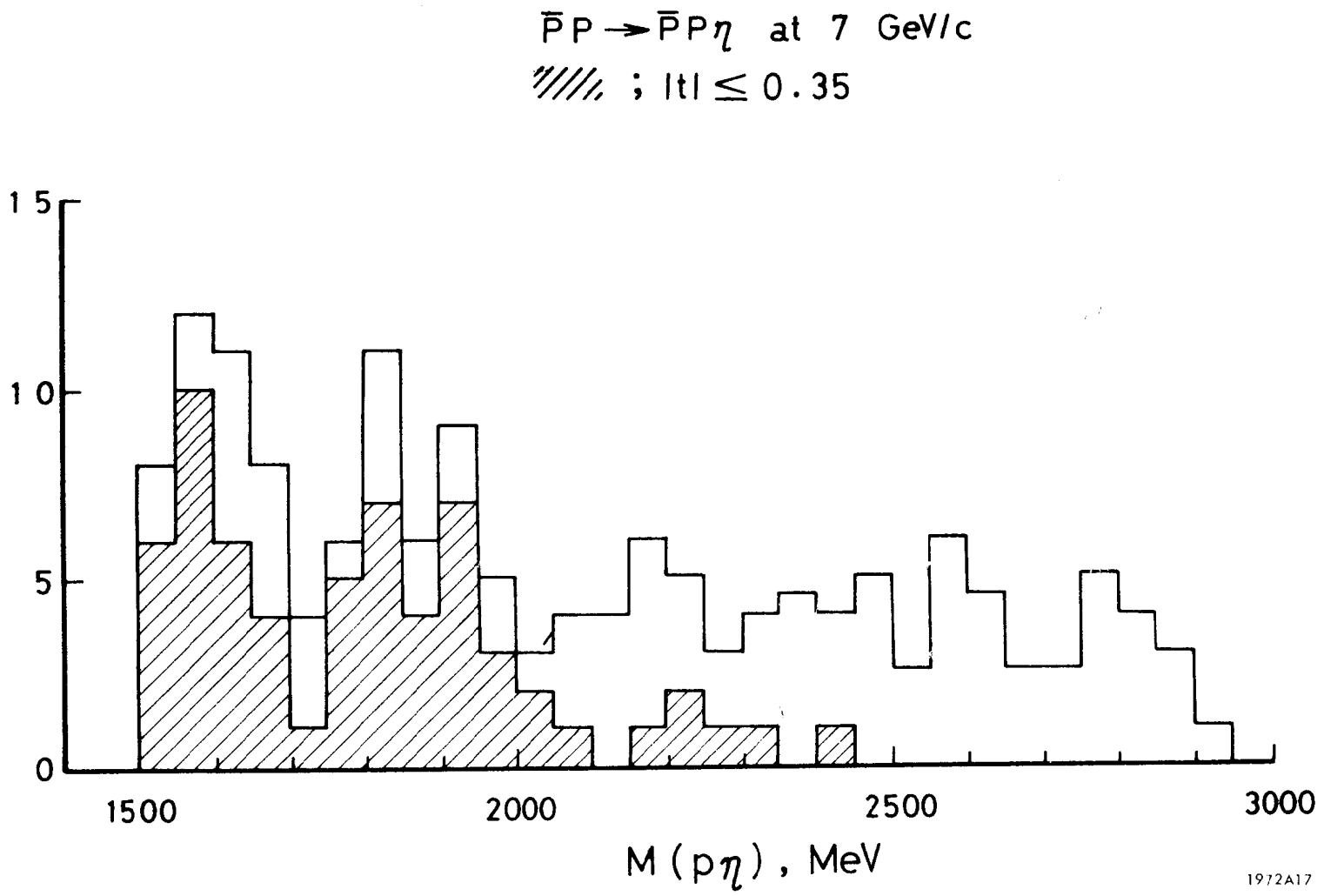

FIG. 4a--Mass plot of Nη.

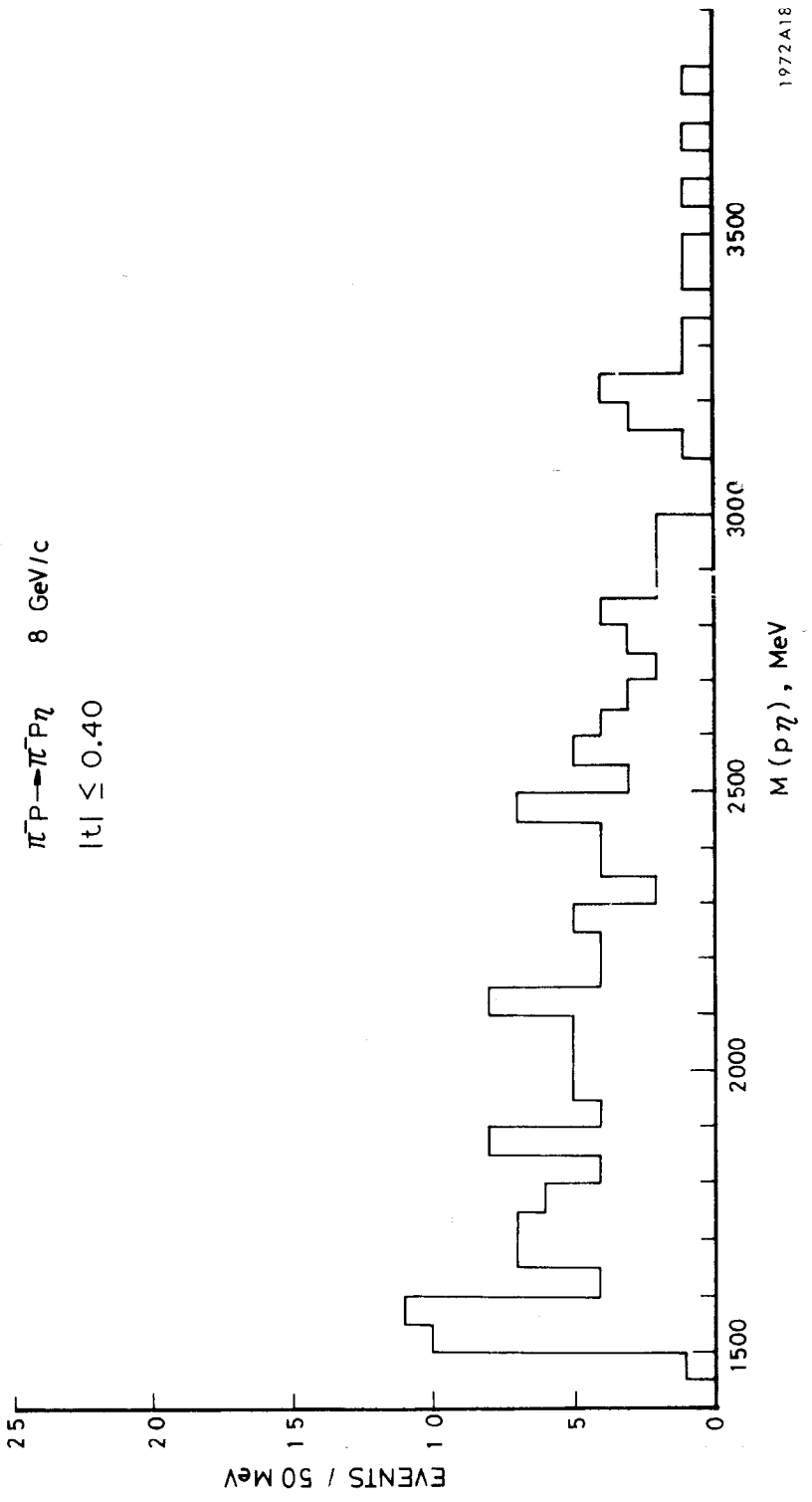

FIG. 4b--Mass plot of $N\eta$.

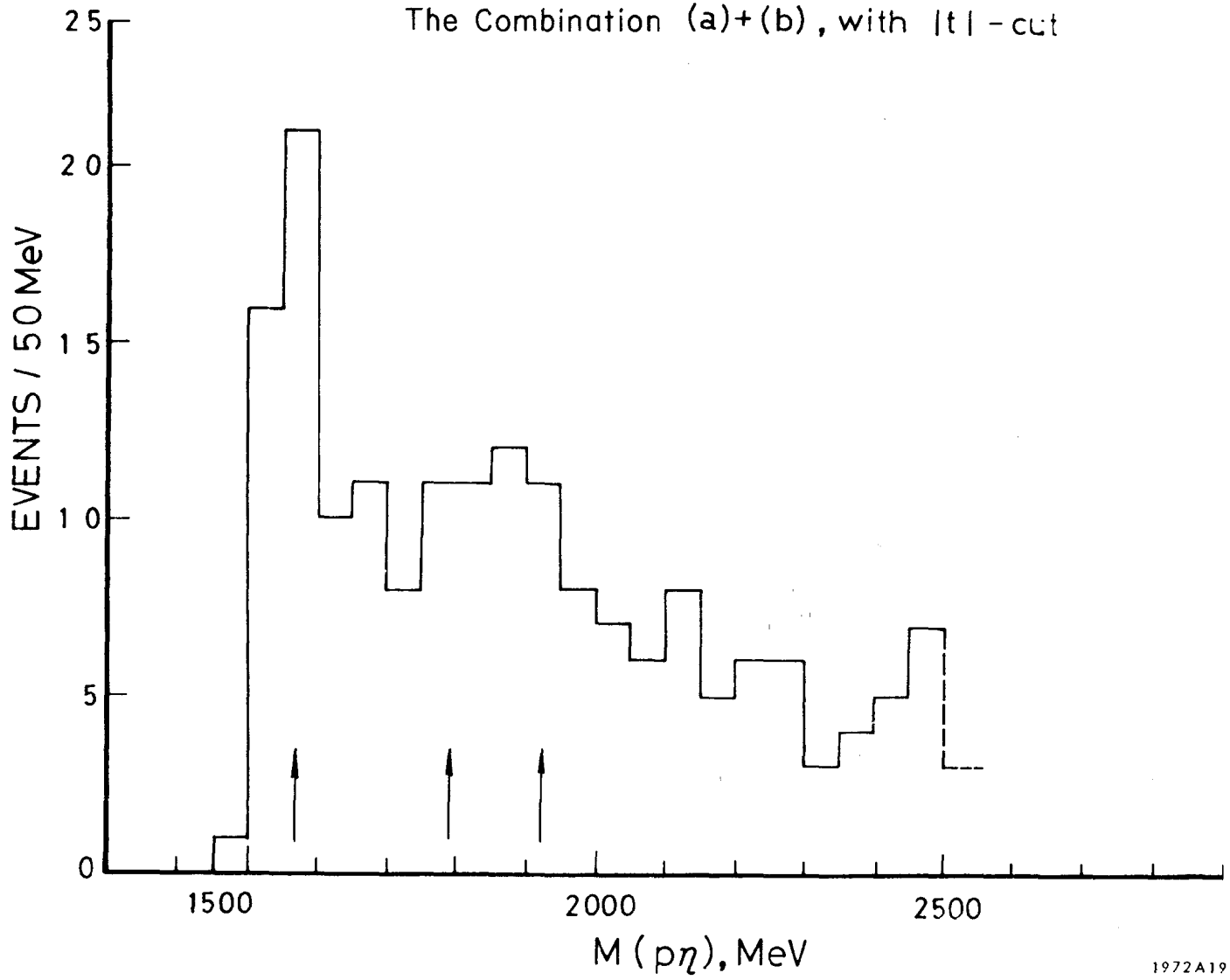

FIG. 4c--Mass plot of Nη.

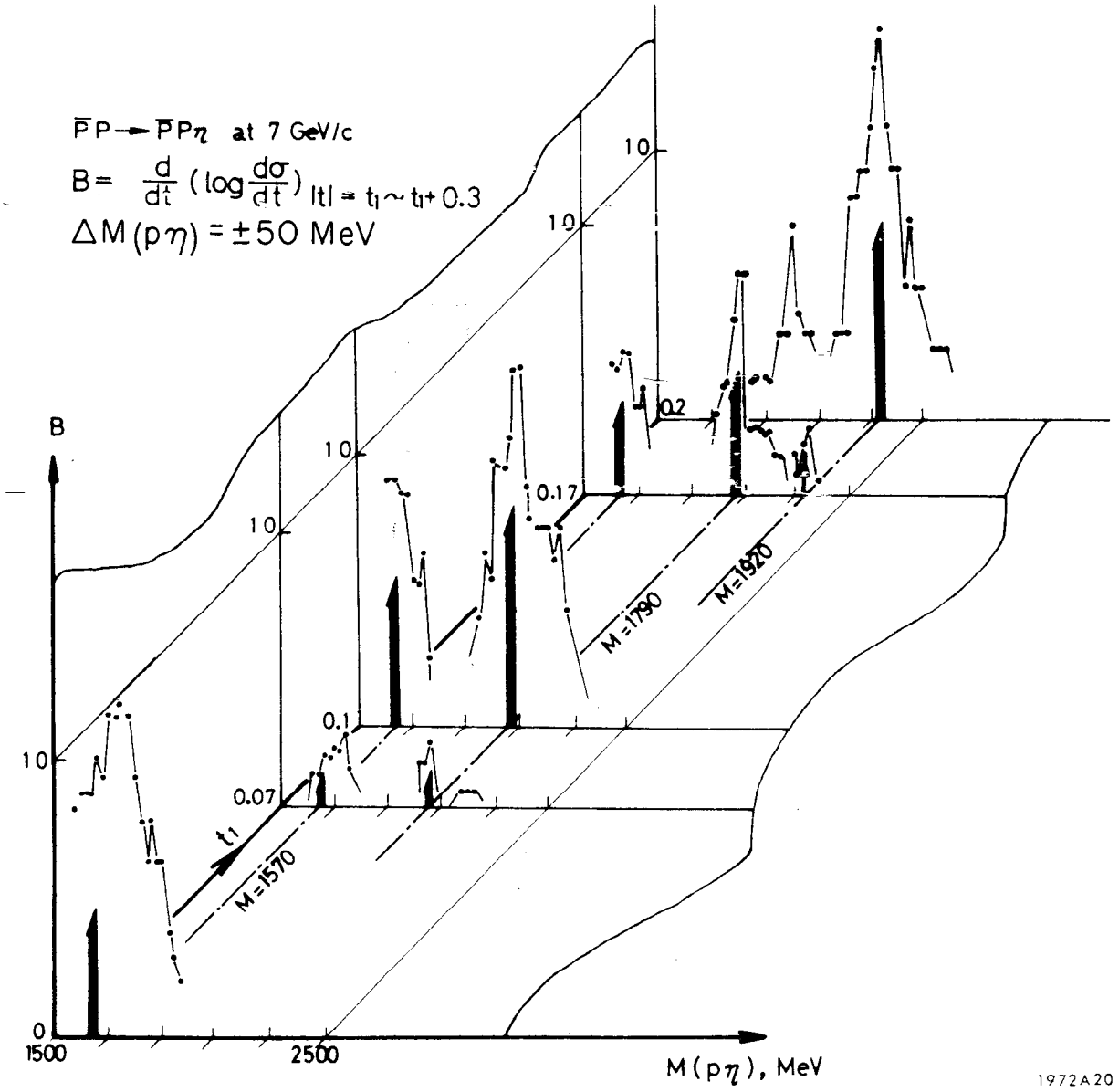

FIG. 5a--B versus M(pη).

width of $M(p\eta) \pm 50$ MeV. The change of B with respect to the mass value $M(p\eta)$ is examined for different t intervals. The figure shows that the B value rises up more than 10 at $M(p\eta) \approx 1,570$ MeV. This value, 1,570 MeV, exactly corresponds to the peak value of the first peak in the mass distribution of Fig. 4. In Fig. 5a there are other peaks in B along M = 1,790 and 1,920 MeV. These two peaks of B rise up at $t_1 \geq 0.1 \sim 0.2\,\mathrm{GeV}^2$. It suggests that the first peak, 1,570 MeV, is diffractive, but the other two are due to a single meson exchange mechanism.

Figure 5b is a similar B vs. $M(p\eta)$ plot for the $\pi^- p \to \pi^- p\eta$ reaction. The purity of eta events in this case is expected to be less than that of the $\bar{p}p$ reaction, and the larger noise due to background can be expected. However, similar peak structures are seen again in Fig. 5b. B peaks at several t intervals for the 1,570 MeV mass as well as for masses 1,790 and 1,920 MeV. For the 1,790 MeV mass B does not have structure until t_1 exceeds $0.1\,\mathrm{GeV}^2$ in a similar way as in the case shown in Fig. 5a. However B peaks at 1,920 MeV for $t_1 \approx 0$ as well as for higher values. In Fig. 5b we see some indication that B peaks at higher mass values. However, we will not discuss it here.

Figure 4c is the combination of the two mass plots of Fig. 4a and 4b. There the first peak in the mass plot seems to correspond to the first structure in B at 1,570 MeV. Also, the second broad enhancement around 1850 MeV may correspond to the structures in B at 1,790 and 1,920 MeV. This could mean the second enhancement may be a composite of at least two resonances.

Figure 6 is a plot of the decay angular distributions of the $N - \eta$ system, $\cos\theta$ in the Gottfried-Jackson frame, vs. $M(p\eta)$: Figure 6a for $\bar{p}p\eta$ and Fig. 6b for $\pi^- p\eta$. Figure 6 shows a heavy contamination due to background, especially for the high mass region. At present the $\pi^- - \eta$ events and background have not been separated well from the $p - \eta$ events. However, the $\cos\theta$ distribution at the first peak in the 1,570 MeV mass region, if interpreted as a resonance, favors the assignment of $J = \frac{1}{2}$, neglecting the background concentration on the left-hand side of the angular distribution.

The other considerations are as follows. Figure 7 shows the momenta in the center-of-mass system of $N - \pi$, $N - \eta$ and $N - \omega$ as a function of mass. It is seen that the momenta are low in the case of $N - \eta$ and $N - \omega$

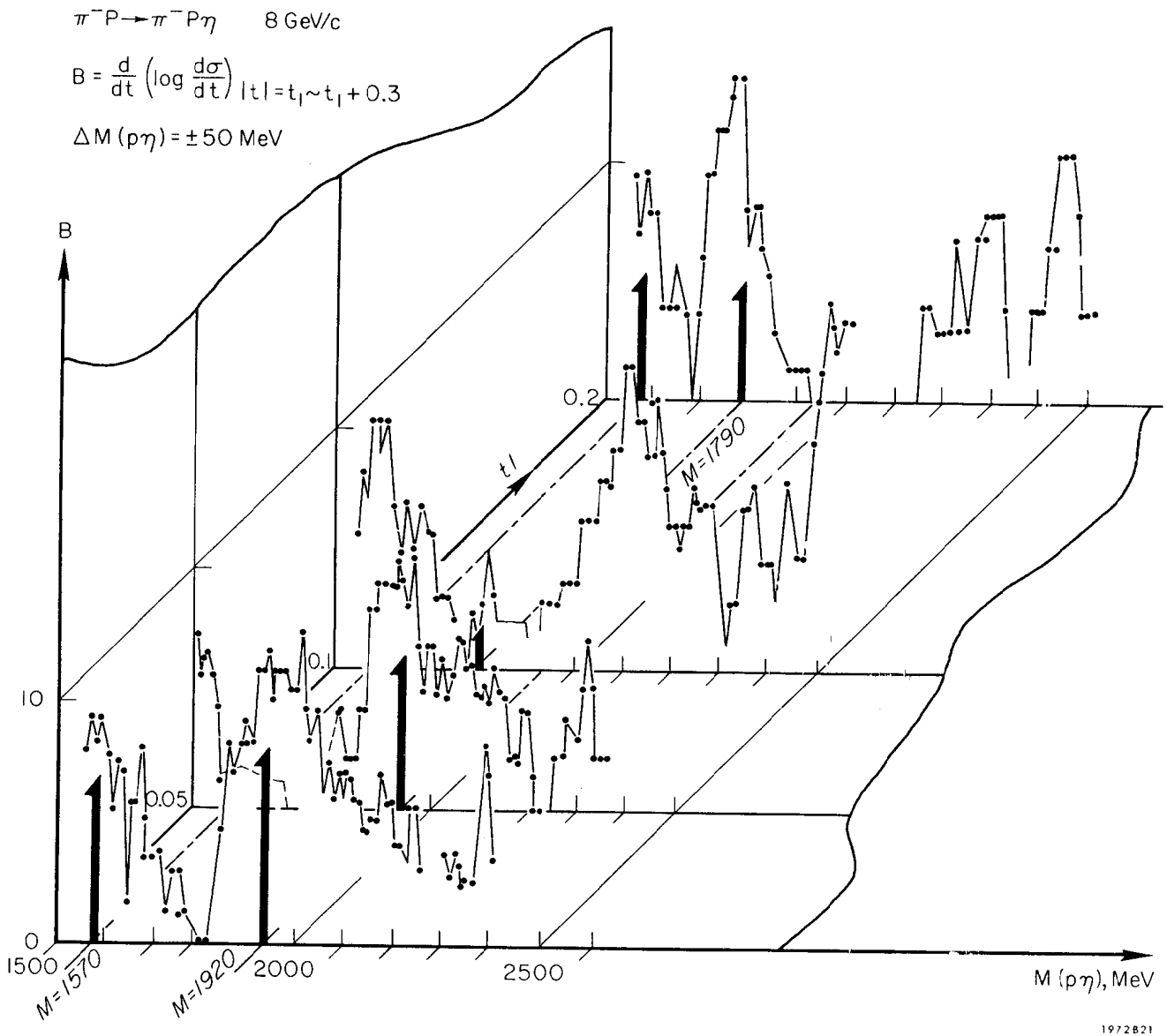

FIG. 5b--B versus M(pη).

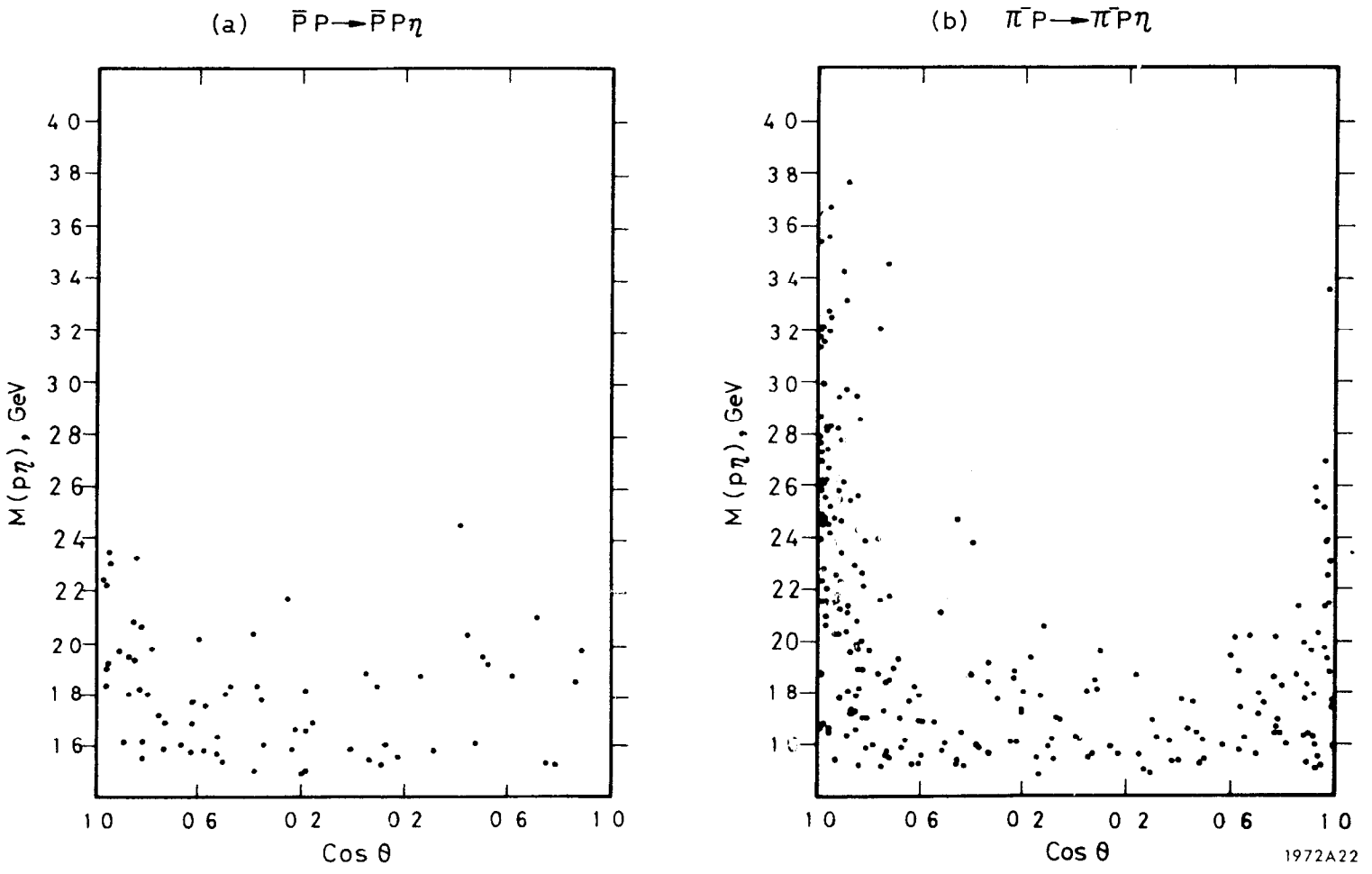

FIG. 6--Cos θ versus M(pη) plot (with t-cut).

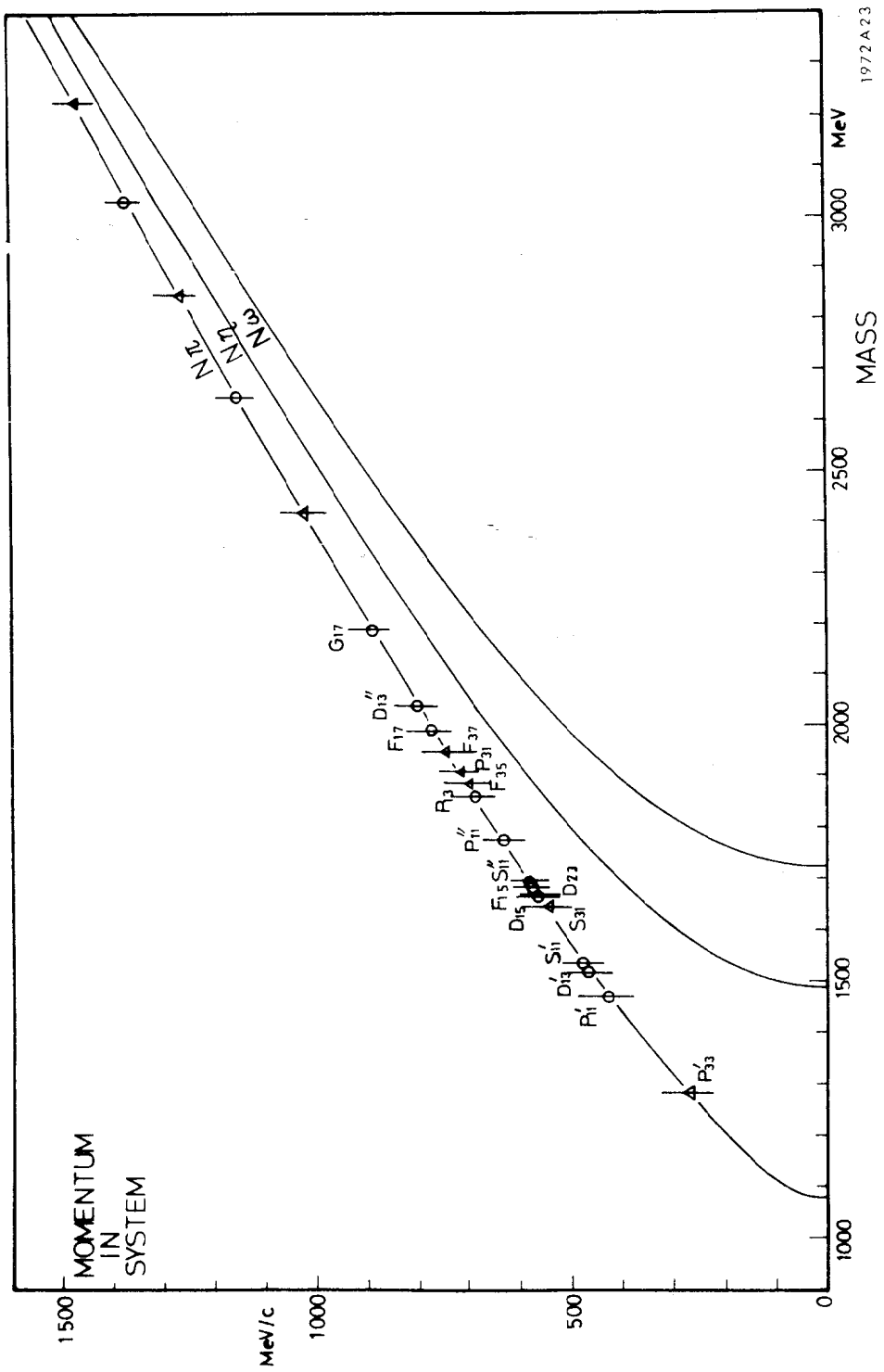
MOMENTUM IN SYSTEM
MeV/c
1500
1000
500
0
1000
1500
2000
2500
3000
MeV
MASS
1972A23
N1/2
N1/2
N3/2
G17
D13''
F17
F37
P31
F35
R3
P11''
F15
S11''
D15
D23
S31
D13'
S11'
P11'
P33'

FIG. 7

compared to the case of N - π, especially in the mass region below 2,000 MeV. Figure 8 is the "size" of N - π systems given by

$$r_\ell = (\ell \sim \ell + 1)\ \lambda \quad .$$

The radii of the N* and Δ resonances appearing in the Rosenfeld Table are plotted on Fig. 8; black bars are N* and white bars Δ. In this figure all the reported resonances are understood well, if we assume an interaction range of 1.05 fermi. Indeed, πN scattering data give the dotted line in Fig. 8; so the potential scattering and the size of the existing resonances are consistent.

We apply the same range directly to the N - η system (Fig. 9). Again, the N - η resonances appearing in the Rosenfeld Table are shown by white bars. Using the same arguments in analyzing the peaks observed in our p - η mass plot, we obtain the following results from Fig. 9.

(a) The first peak around 1,570 MeV may be the $S_{11}(1535)$.

(b) The second peak, with $I = \frac{1}{2}$ and $\ell \lesssim 2$, might correspond to the phase shift results.

(c) The second peak, if separated, may be

1,790 MeV	$P_{11}(1780)$
1,920 MeV	$P_{13}(1860)$

Studies on t distributions and a hexagonal plot suggest that the first and the second peaks are produced by different mechanisms; the first one diffractive, though it is in an unnatural parity state. Obviously further studies are desired and data are being collected for this purpose.

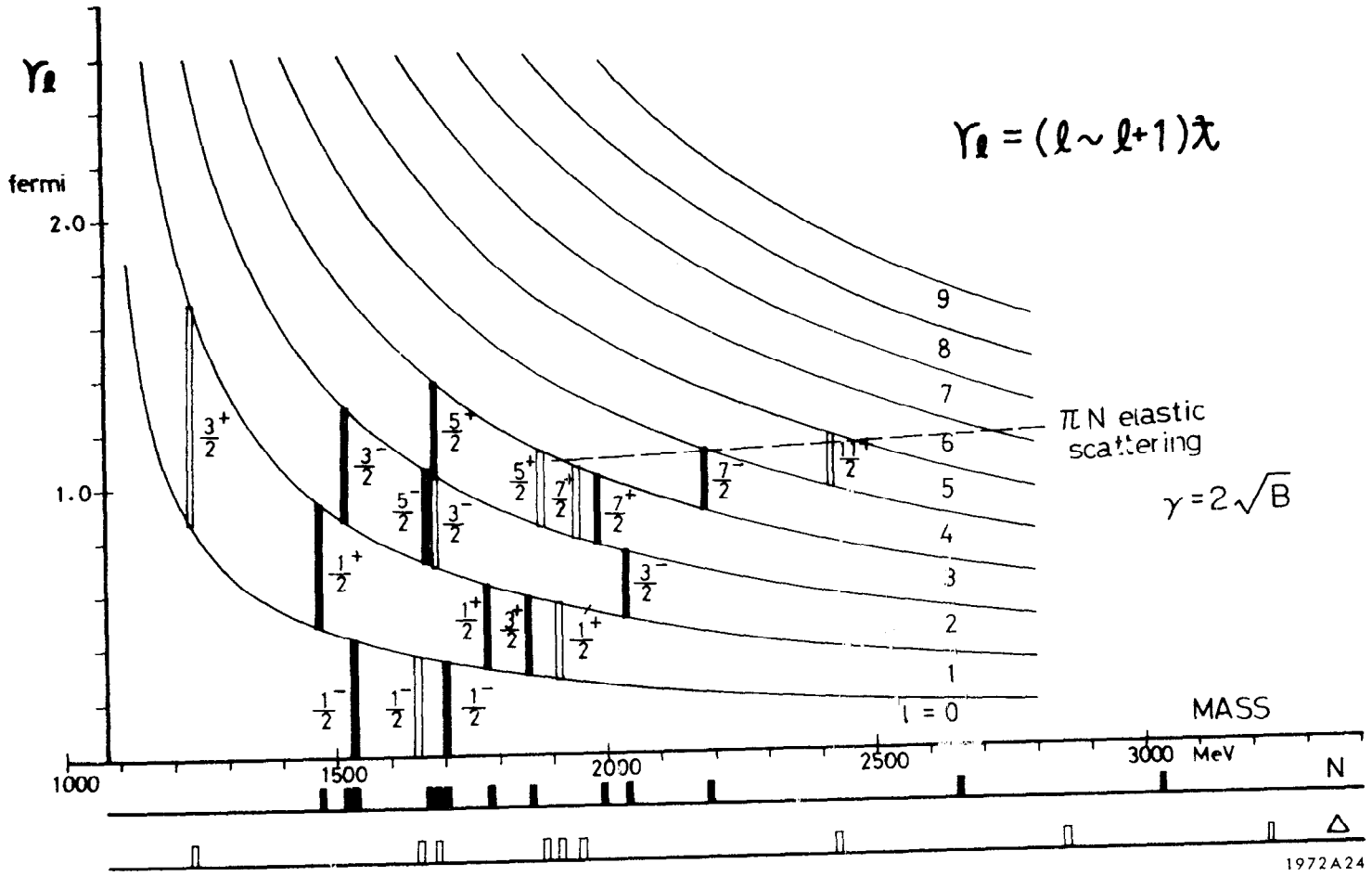

FIG. 8--N-π system.

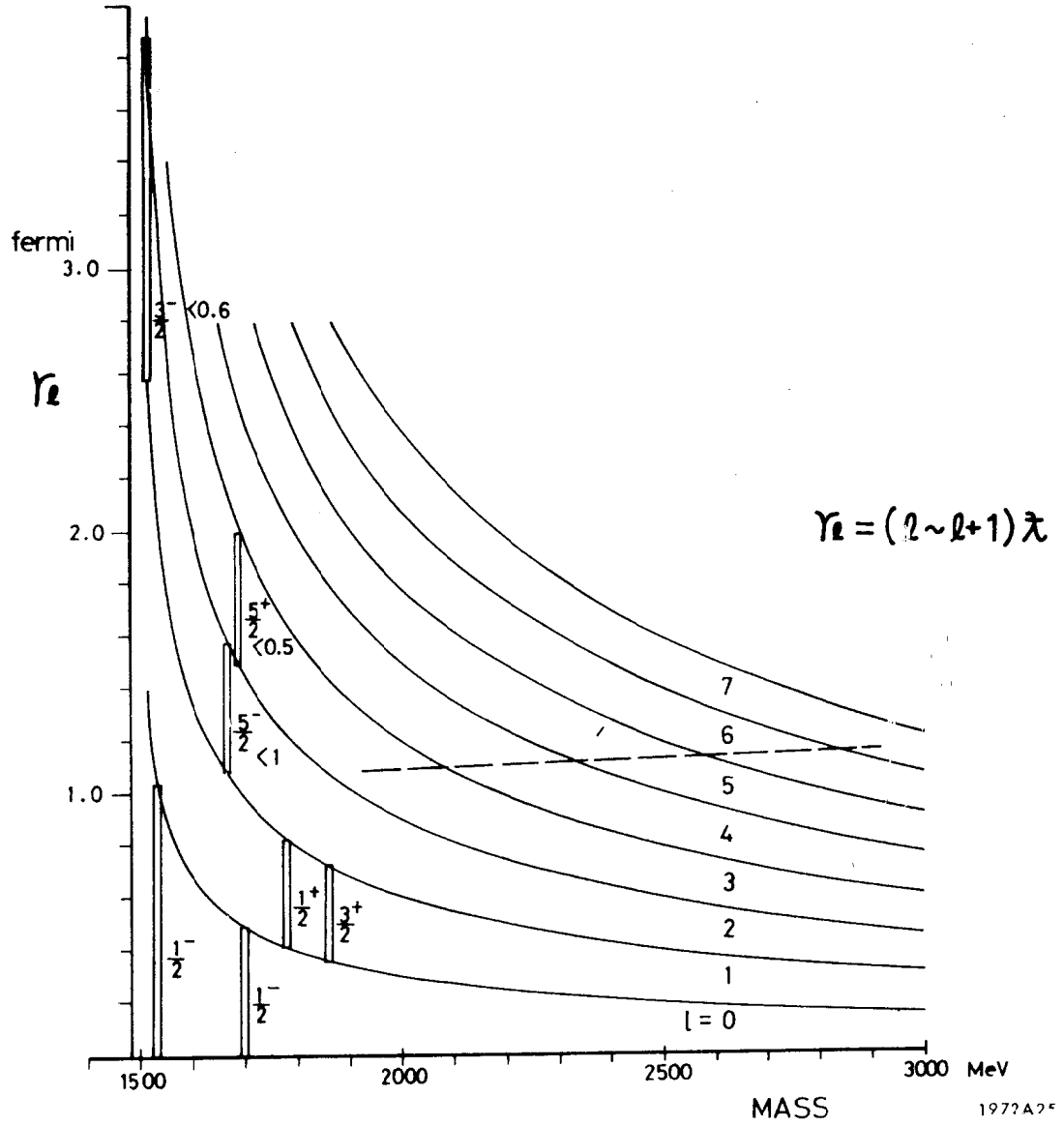

FIG. 9--N-η system.

Discussion

Flatté: Are you planning to measure more film of the same kind?

Kitagaki: We have more π film to measure. All of the $\bar{p}$ film has been measured.

Derrick: Notre Dame has film with 7 or 8 GeV π^- p in the same kind of reactions. How does your data compare with theirs?

Takahashi: It is the same kind of film, and exactly the same energy. It is a collaboration.

Derrick: What is the comparison?

Takahashi: The $\pi^- \eta$ mass system looks almost the same.

Derrick: So there is a big threshold peak at the A_2.

Takahashi: Right, and the angular distribution is as shown.

Flatté: Brookhaven has film of 6 GeV π^-. They measured all of their 2-prongs in order to publish the results on the A_2. They must have a tremendous number of events.

Skillicorn: 60,000, but there was too much background to make an analysis of η p.

Derrick: No sense of adventure!

$\pi^- p \rightarrow \pi\pi N$ REACTIONS AT 8 GeV/c

Kasuke Takahashi

Tohoku University Group*
Sendai, Japan

Abstract

A study of $\pi^- p \rightarrow \pi \pi N$ at 8 GeV/c was made by analyzing the combined data consisting of 3229 events of $\pi^- p \rightarrow \pi^- \pi^+ n$ and 1496 events of $\pi^- \pi^0 p$ final state. The data are based on separate measurements carried out at the University of Pennsylvania, University of Notre Dame, and Tohoku University.

Analysis of the $(\pi^- \pi^+)$ dipion system gives evidence of a possible new resonance of mass (2080 ± 20) MeV with a width $\Gamma = 160 \pm 20$ MeV. Possible isospin of the resonance is I = 1, and its angular momentum quantum number may be either 1^-, 3^-, or 5^-.

Extensive studies of production angular distributions at very small momentum transfer squared and decay angular distributions are made for ρ^0 and f^0 mesons. Comparison of the results for ρ^0 with the Vector Dominance Model (VDM) predictions have shown a reasonable agreement.

The study of single-pion production processes in pion-nucleon interactions has always been a central problem in the elementary particle reactions. It is a fairly old problem in terms of a simple one-pion-exchange process. At the same time, it is also quite new and even very controversial in the sense that no single theoretical model has been successful in explaining the process very well. It has also been emphasized strongly that extensive studies of the process are needed with much higher statistics in order to get better and further insight into this very fundamental process.[1]

---

*T. Kitagaki, K. Takahashi, S. Tanaka, K. Abe, M. Kondo, H. Hasegawa, T. Sato, R. Sugahara, K. Tamai, H. Kichimi, T. Okusawa, and S. Noguchi.

In this report I would like to give some preliminary results of our study of the $\pi^- p \to \pi\pi N$ reactions at 8 GeV/c. My talk is based on the combined data of the University of Pennsylvania, University of Notre Dame, and Tohoku University. We, at Tohoku University, have so far measured about 13,000 two-prong events and have identified 782 events of the reaction

$$\pi^- p \to n\pi^-\pi^+ \qquad (1)$$

and 351 events of the reaction

$$\pi^- p \to \pi^-\pi^0 p \qquad (2)$$

We have compared various features of our data with those of the previous data,[2] measured by the Pennsylvania and Notre Dame groups, by using the same series of exposures in the BNL 80" hydrogen bubble chamber. Having reached the conclusion that all the data are compatible for combined analysis, we then combined the data and obtained 3229 events of the reaction (1), and 1496 events of the reaction (2).

In this report, however, we shall confine ourselves mainly to reaction (1) and mention only briefly reaction (2) where it is necessary.

The discussions I will present may be summarized by three points; namely the results of our studies on production angular distributions of ρ^0 and f^0 at very small $|t|$ (invariant four momentum transfer squared), on decay angular distributions of these mesons, and on the possible existence of a new meson with a mass of 2080 MeV. Some comparisons of our results on ρ^0 meson with the Vector Dominance Model (VDM) predictions will also be made.

Figure 1a shows an invariant mass distribution of the $\pi^-\pi^+$ dipion system in the reaction (1). Figures 1b, 1c, and 1d are the distributions of the separate data for Notre Dame, for Pennsylvania and for Tohoku, respectively. As clearly seen, ρ^0 and f^0 mesons are prominent .

The g^0 meson with a peak mass value = 1660 MeV is also observed as a bump standing more than 7-standard deviations above the nonresonant background. There is also seen a new bump at $\pi\pi$ mass = 2080 MeV

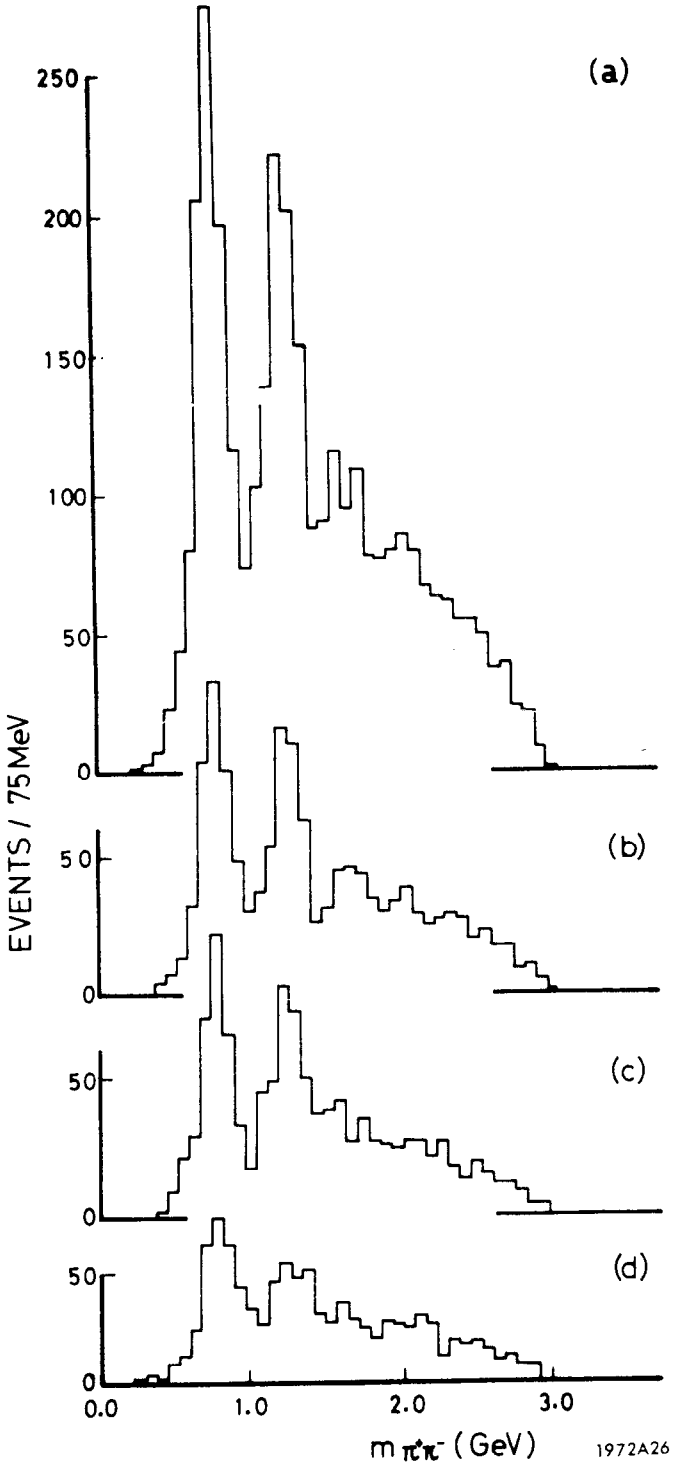

FIG. 1--Invariant mass distribution of the $(\pi^-\pi^+)$ system, (a) for the combined data, (b) for the Notre Dame data, 1,321 events, (c) for the Pennsylvania data, 1,127 events, and (d) for the Tohoku data, 782 events.

peaking at 3 or 4 standard deviations above the background. We have parameterized the distribution with a nonresonant phase space and four resonances of the Breit-Wigner type with parameters given in Table 1. I shall come back to the discussion of this possible new resonance later on.

1. The Reaction $\pi^- p \to \rho^o n$

In Fig. 2 we give production angular distributions of the ρ^o. The ρ^o mass interval was taken from 0.675 to 0.875 MeV. We estimate that about 20% of the events in this mass region are non-ρ^o events. The absolute scale has been normalized to our value of the total cross section for ρ^o production tabulated in Table 1. Figure 2a shows the detailed structure of the t-distribution in the very small $|t|$ region, and Fig. 2b shows the overall distribution. Our resolution in $|t|$ is estimated to be ± 0.003 $(\text{GeV/c})^2$ at $|t| = 0.01$ $(\text{GeV/c})^2$ $(= \frac{1}{2}\mu^2$, where μ is the pion mass). The distribution does not show any particular dip in the $|t|$ region below μ^2.

Theoretical curves shown in Fig. 2 are: the solid line for simple one-pion-exchange (OPE);[3] and the dashed line for one-pion-exchange (OPEA).[4] Apparently OPE does not reproduce any feature of the production angular distribution, whereas OPEA gives a good fit not only to the overall features but also to the prominent structure in the very forward direction.

Decay angular distributions of ρ^o events have also been analyzed. In our analysis we have utilized the decay anguiar variables ($\cos\theta$ and ϕ) in the helicity frame as well as in the usual Gottfried-Jackson frame. Figures 3a and 3b show decay angular distributions of ρ^o in the helicity frame. Figures 4a and 4b are those in the usual Gottfried-Jackson frame. The forward-backward asymmetry parameter in $\cos\theta$, $R = (F - B)/(F + B)$, is found to be 0.35 ± 0.04 in the helicity frame. This may indicate that in addition to the P-wave there is some contribution from S-wave in the ρ-mass region. It must also be mentioned that in the charged ρ^- decay there is no appreciable asymmetry observed.

If both S- and P-wave pion-pion interactions are considered, the general decay angular distribution can be expressed in terms of the density matrix

Table 1

Parameters for the Reaction $\pi^- p \rightarrow \pi^- \pi^+ n$ at 8 GeV/c

	Events	(mb)	M_0 (GeV)	Γ (GeV)
Notre Dame	1,321	0.89 ± 0.05		
Pennsylvania	1,127	1.08 ± 0.08		
Tohoku	781	1.12 ± 0.15		
Weighted Average	3,229	0.99 ± 0.07		
		Fitted Parameters		
$\rho^0 \rightarrow \pi^+ \pi^-$	Combined 0.244 ± 0.019 mb		0.79	0.18
$f^0 \rightarrow \pi^+ \pi^-$	Combined 0.184 ± 0.017 mb		1.27	0.19
$g^0 \rightarrow \pi^+ \pi^-$	Combined	~ 60 μb	1.68	0.30
$g^{0\prime} \rightarrow \pi^+ \pi^-$	Combined	~ 30 μb	2.08	0.16

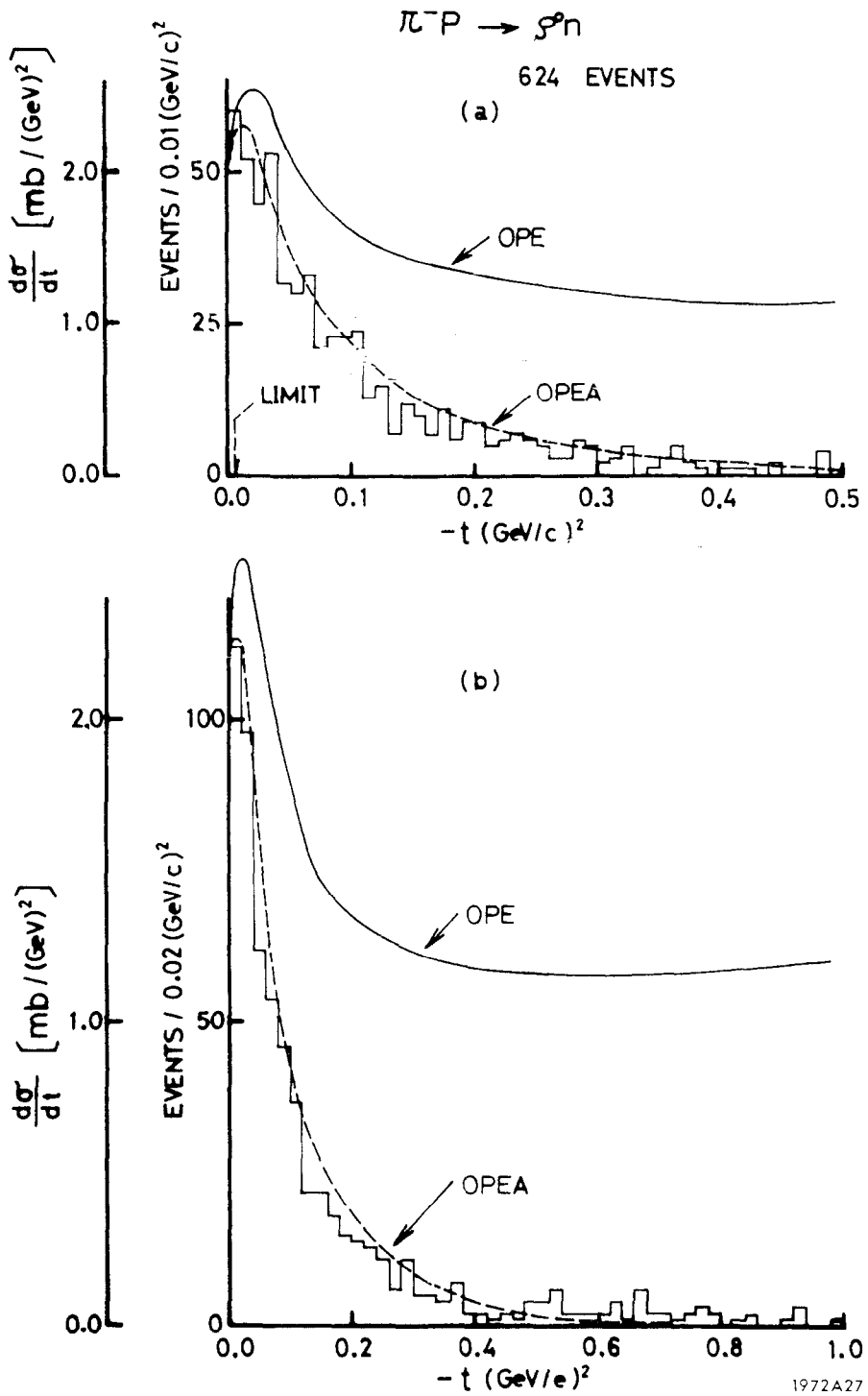

FIG. 2--Production angular distribution $d\sigma/dt$ for the ρ^0 region. Theoretical curves are: solid line, OPE; and dashed line, OPEA.

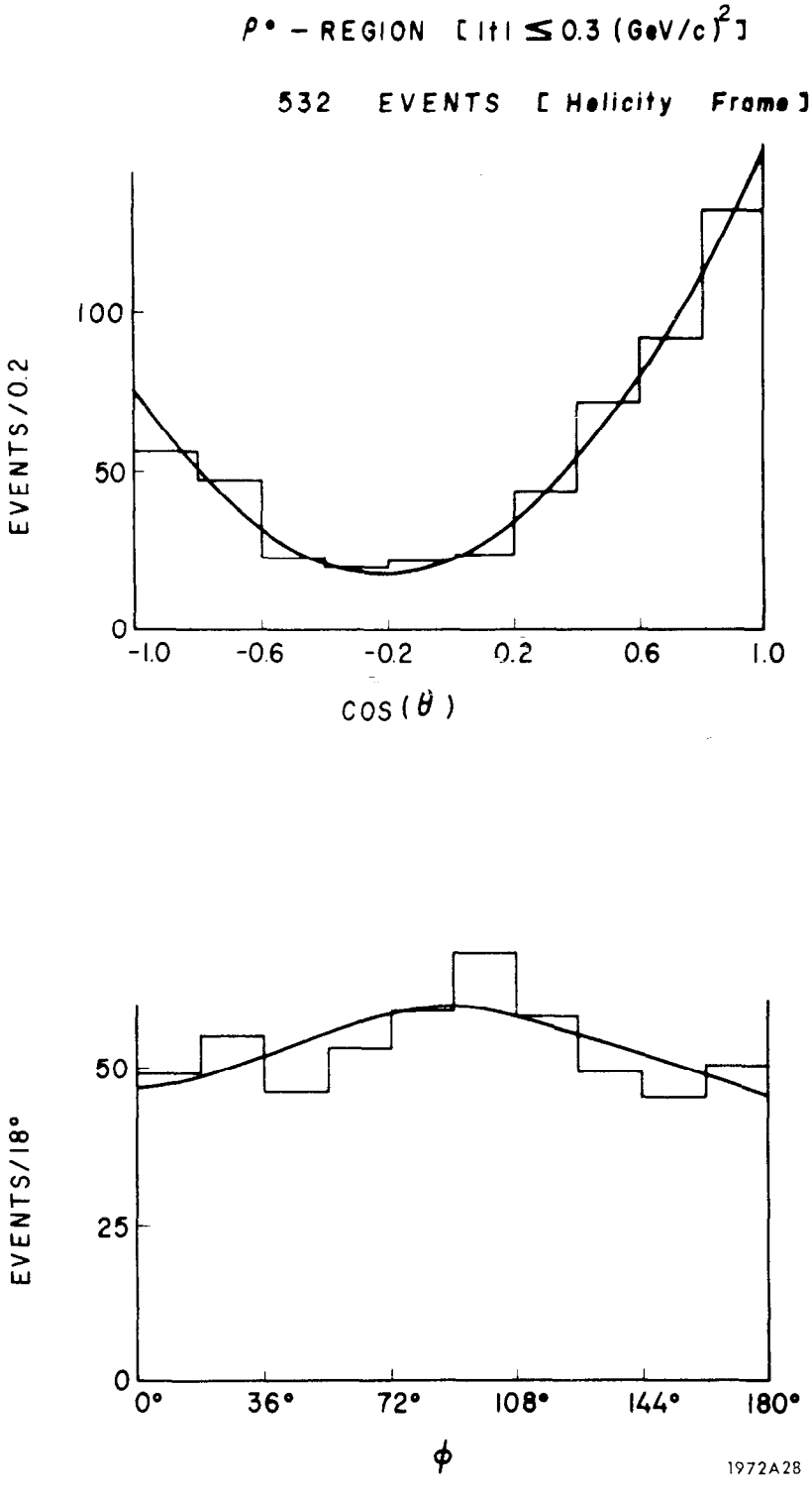

FIG. 3--Decay angular distribution for the ρ^{o} region in the helicity frame.

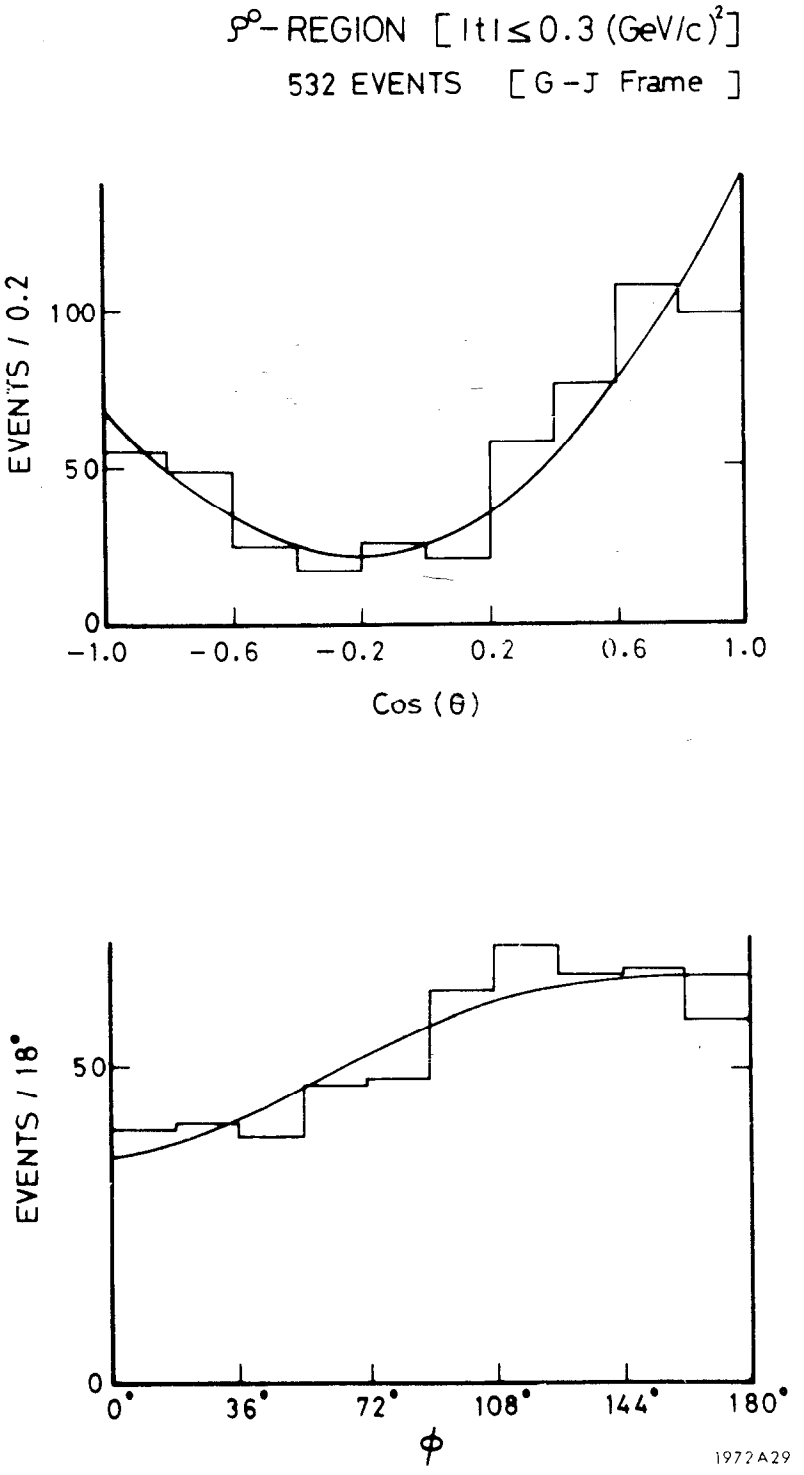

FIG. 4--Decay angular distribution for the ρ^0 region in the Gottfried-Jackson frame.

elements $\rho_{mm'}$ in an appropriate frame. It is expressed as follows:

$$W(\theta,\phi) = \left(\frac{3}{4\pi}\right)\Big[\rho^{p}_{00}\cos^2\theta + \rho^{p}_{11}\sin^2\theta - \sqrt{2}\,\mathrm{Re}\left(\rho^{p}_{10}\right) \times \sin 2\theta\cos\phi - \rho^{p}_{1-1}\sin^2\theta\cos 2\phi\Big] + \left(\frac{\sqrt{\varepsilon}}{4\pi}\right)\Big[-2\sqrt{2}\,\mathrm{Re}\left(\rho^{sp}_{10}\right)\sin\theta\cos\phi + 2\,\mathrm{Re}\left(\rho^{sp}_{00}\right)\cos\theta\Big] + \frac{1}{4\pi}\rho^{s}_{00} \qquad (3)$$

where ρ^{s}_{00} corresponds to pure S-wave, and ρ^{sp}_{00} and ρ^{sp}_{10} correspond to S-P interference effects. We have assumed an S-wave contribution of about 7%. Normalization was made according to the equation:

$$\rho^{p}_{00} + 2\rho^{p}_{11} + \rho^{s}_{00} = 1 \qquad (4)$$

The density matrices thus obtained in the helicity frame are shown in Fig. 5, and those in the G-J frame are shown in Fig. 6. The solid curves in Fig. 5 and in Fig. 6 are theoretical calculations based on the OPEA model.[4]

Here again OPEA gives reasonably good fits. The presence of non-zero values for $\mathrm{Re}\left(\rho^{sp}_{00}\right)$ is a strong indication of the S-wave effects.

Now discussions about the comparison of the results on ρ^{o} production with the predictions of the Vector Dominance Model (VDM) are in order. Figures 6 and 7 show some of these comparisons. Theoretical curves shown with the dashed lines in Fig. 6 and by the solid lines in Fig. 7 are taken from Cho and Sakurai.[5] The dashed curve in Fig. 7b is normalized to the 7% S-wave contribution, since the experimental points are obtained in the normalization of $\rho^{p}_{00} + 2\rho^{p}_{11} + \rho^{s}_{00} = 1$ with 7% S-wave admixture. Considering the fact that the theoretical curve has no variable parameter in the predictions, agreement with the data is quite good.

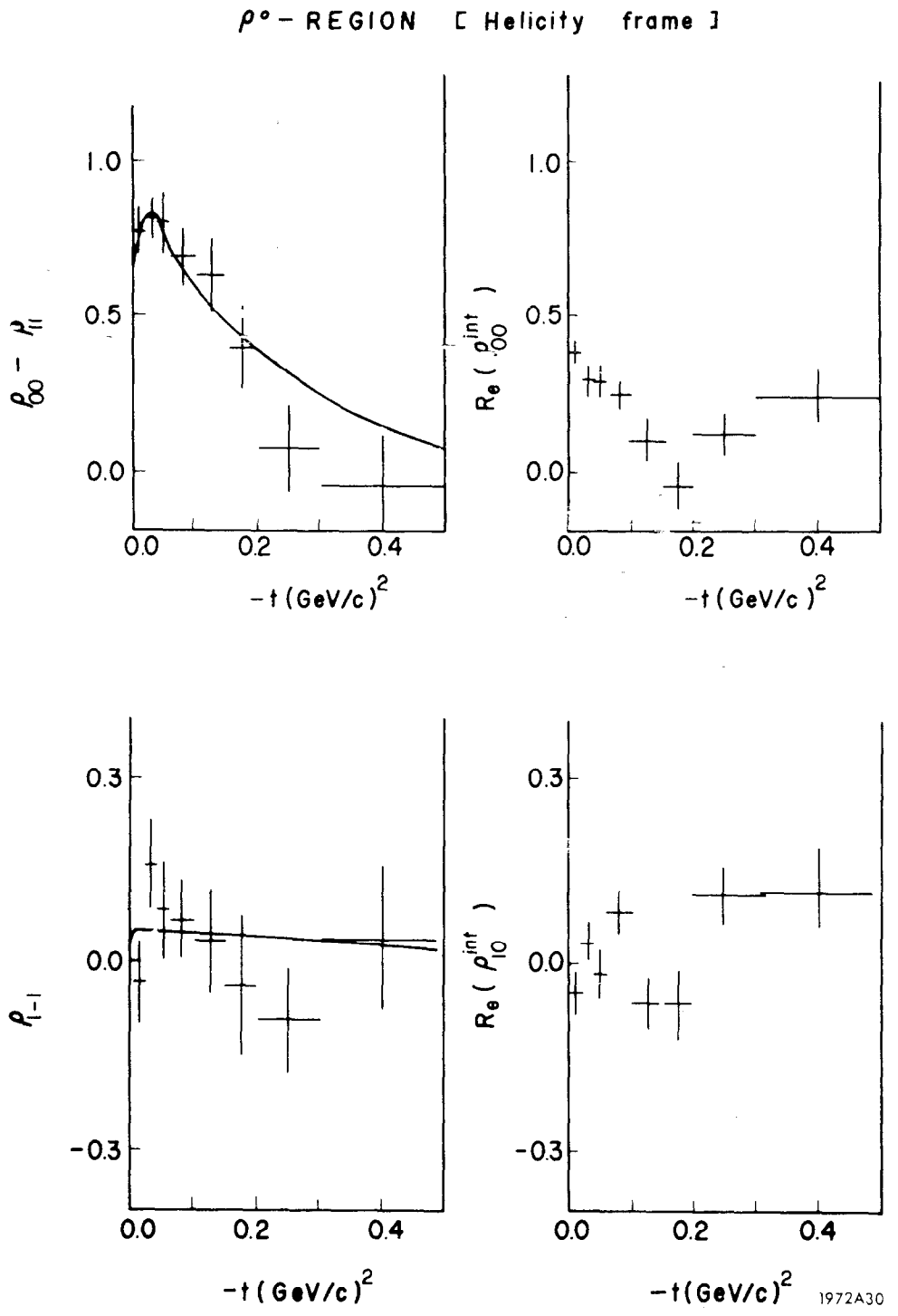

FIG. 5--Density matrix elements for the ρ^0 region in the helicity frame. Theoretical curves shown with solid lines are predictions of the OPEA model.

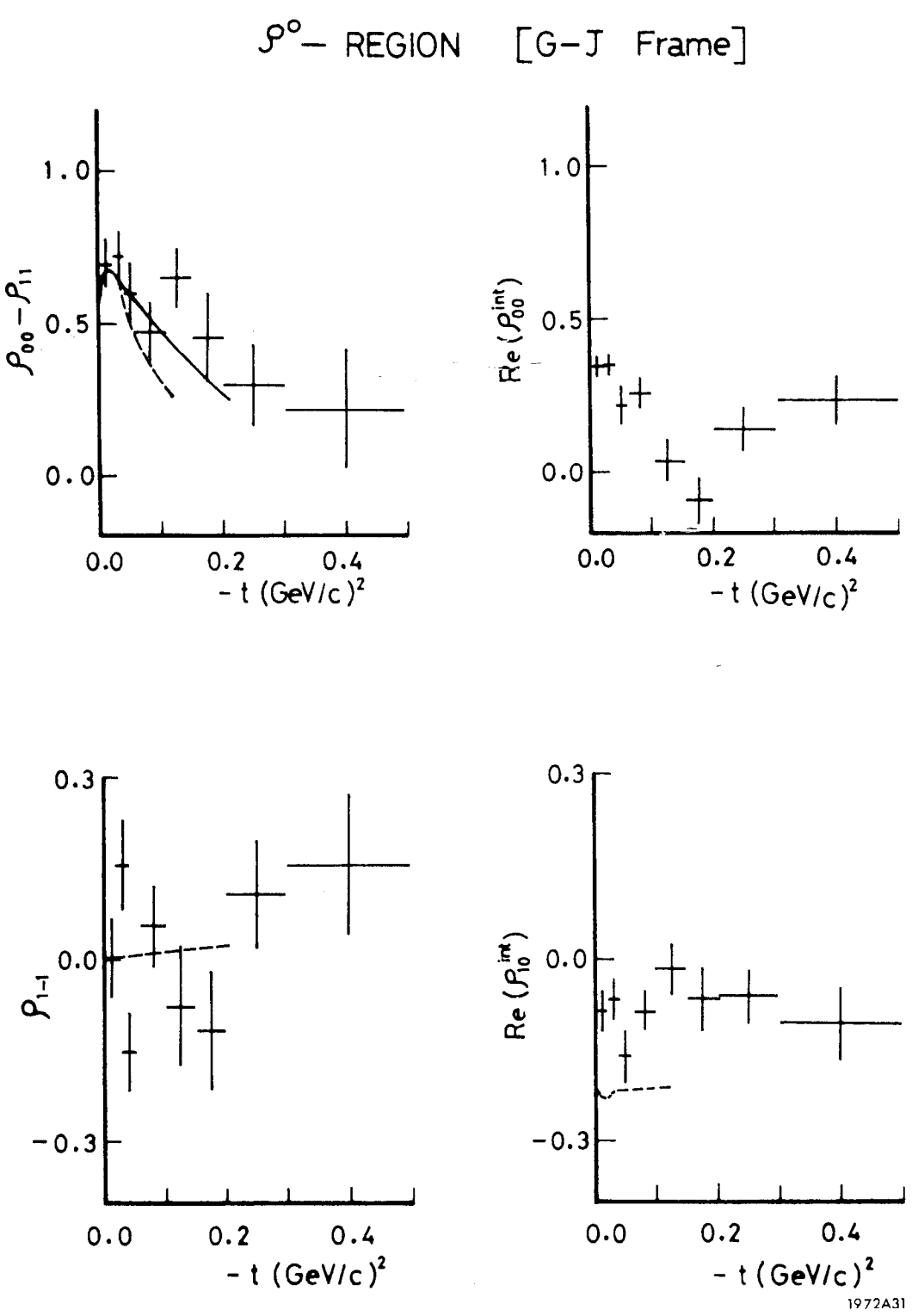

FIG. 6--Density matrix elements for the events in the ρ^0 region in the Gottfried-Jackson frame. The solid curve gives the prediction of OPEA. Theoretical curves shown by dashed lines are predictions from the Vector Dominance Model (VDM).

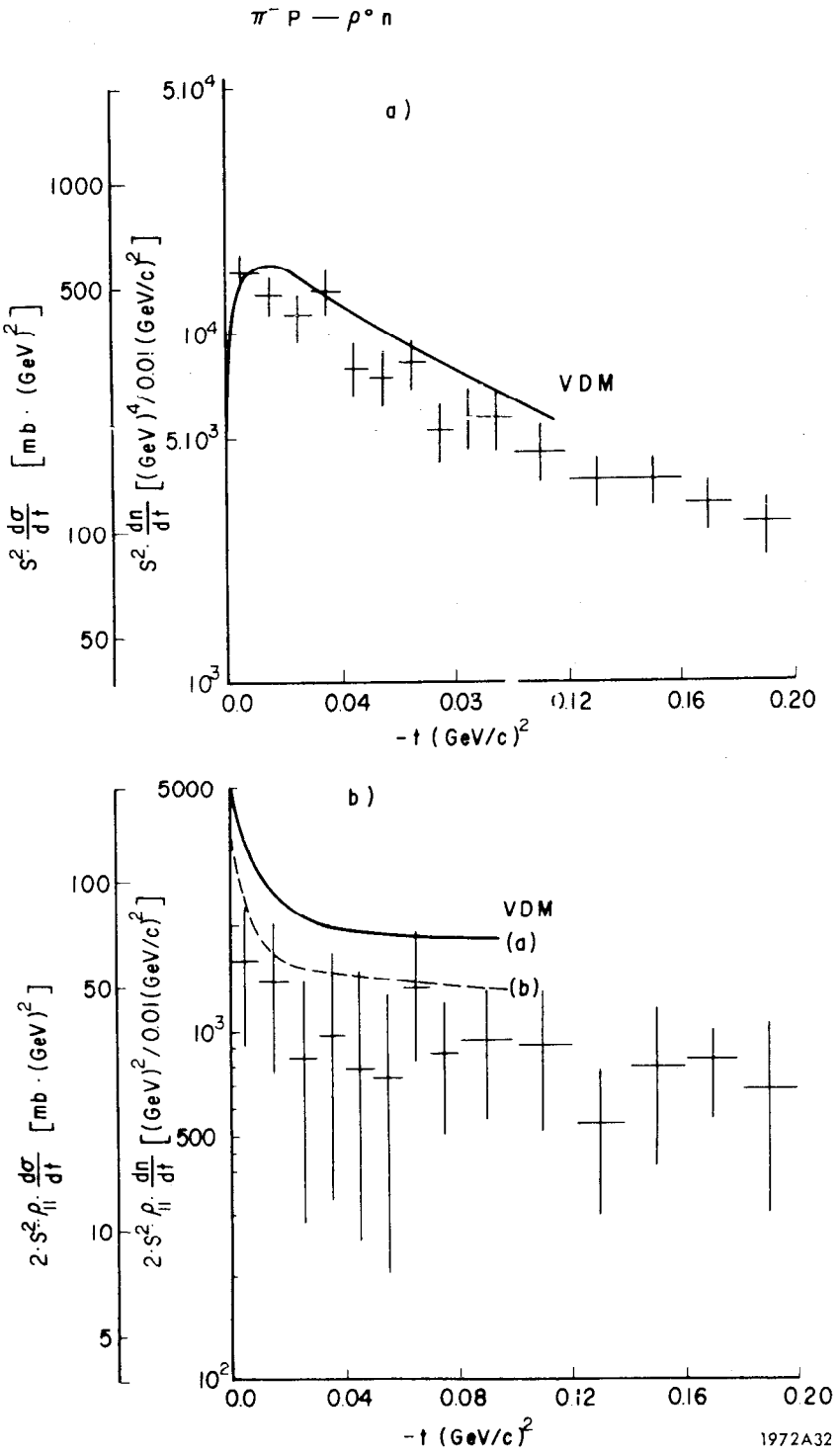

FIG. 7--Comparison of the ρ^0 production data with the VDM predictions. The dashed curve in (b) is the curve normalized to the 7% S-wave admixture.

2. Results in the f^o Mass Region

Figures 8a and 8b show the t-distributions of the f^o production cross section: 8a gives the detailed structure in the forward direction and 8b the overall features. The mass interval of the f^o events was taken from 1,170 to 1,370 MeV. Again the absolute scale of the cross section has been normalized to our estimate of the production cross section of the f^o given in Table 1.

The theoretical curve shown with the solid line is for pure OPE. As in the case of ρ^o production, OPE predicts too large a cross section. A calculation of the OPEA model has also been tried (but not shown in the figure). The prediction of the OPEA, though much better than OPE, is still rather larger than the experimental value. More statistics may be necessary before we can mention anything very definite on whether the observed dip in the cross section near t_{min} is real or not. It may be, however, appropriate to say that the f^o cross section at very small t looks a little different from that in the case of the ρ^o region. In order to see the reason, G. Takeda with his collaborators has tried some theoretical calculations from the gauge invariant point of view, in exact analogy with the VDM in the ρ^o case.[6]

The theoretical curve shown with the dashed line in Fig. 8 is a calculation based on the gauge invariance model for a tensor meson in which the f^o meson has the same behavior as a graviton. The curve has a peak near $|t| = \mu^2$ and has a nonzero value of $d\sigma/dt$ in the very forward direction (at $t \sim t_{min}$). The fitting to the experimental data seems rather good. The absolute cross section gives a value of $(g^2/4\pi)\, m_f^2 = 16$, which seems to be reasonable.[7]

Angular distributions were also studied. Figures 9a and 9b show the angular distributions (in the helicity-frame) of the f^o events in the mass interval from 1,170 to 1,370 MeV. It is interesting to note that the $\cos\theta$ distribution of f^o decay is more symmetric than that in the case of the ρ^o, but the ϕ distribution looks less symmetric. The dashed lines in the figures indicate the curves obtained in terms of the density matrix elements for the pure D-wave only. The solid curves are for an admixture of D- and P-wave.

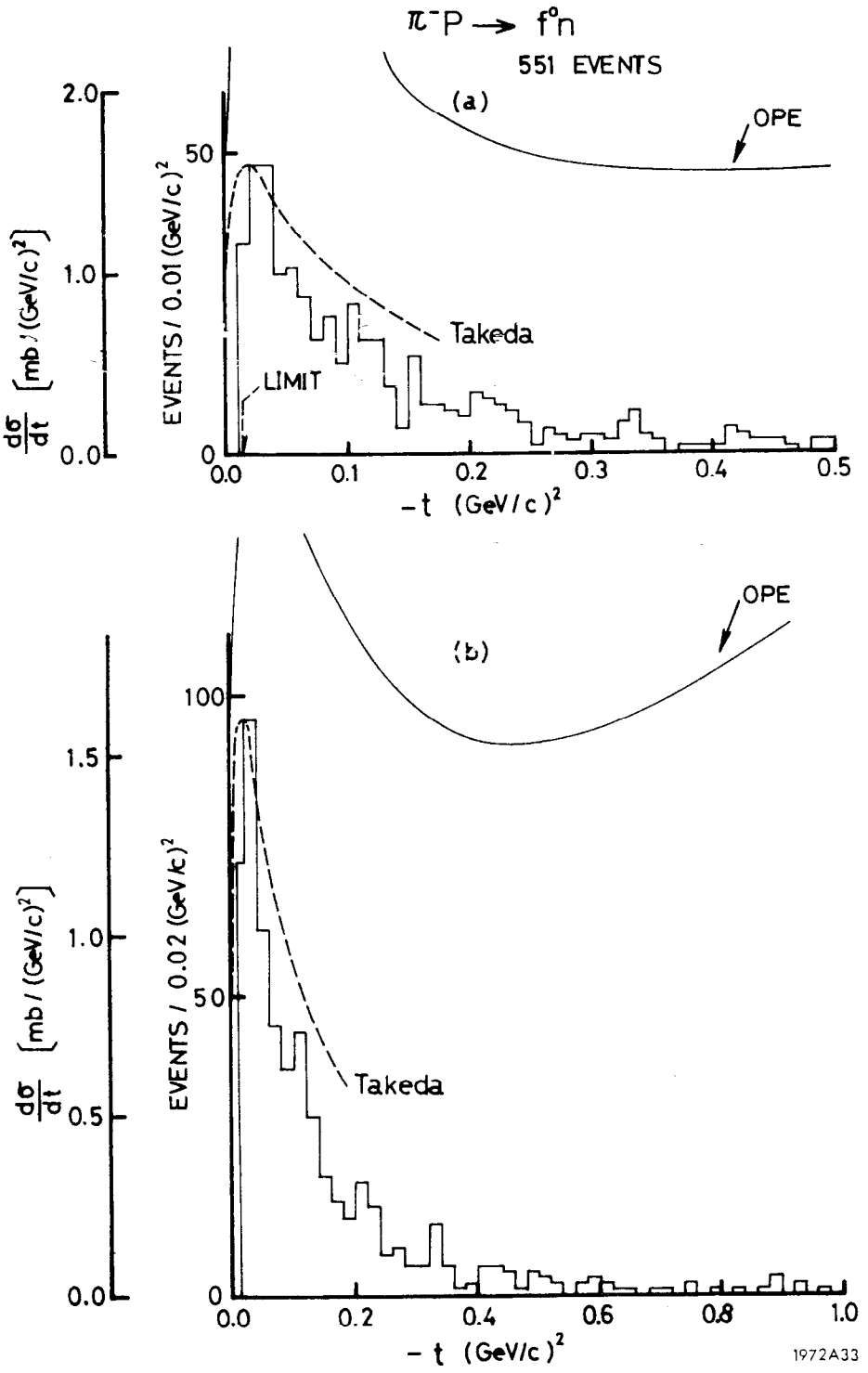

FIG. 8--Production angular distribution, $d\sigma/dt$, for the ρ^0 region.

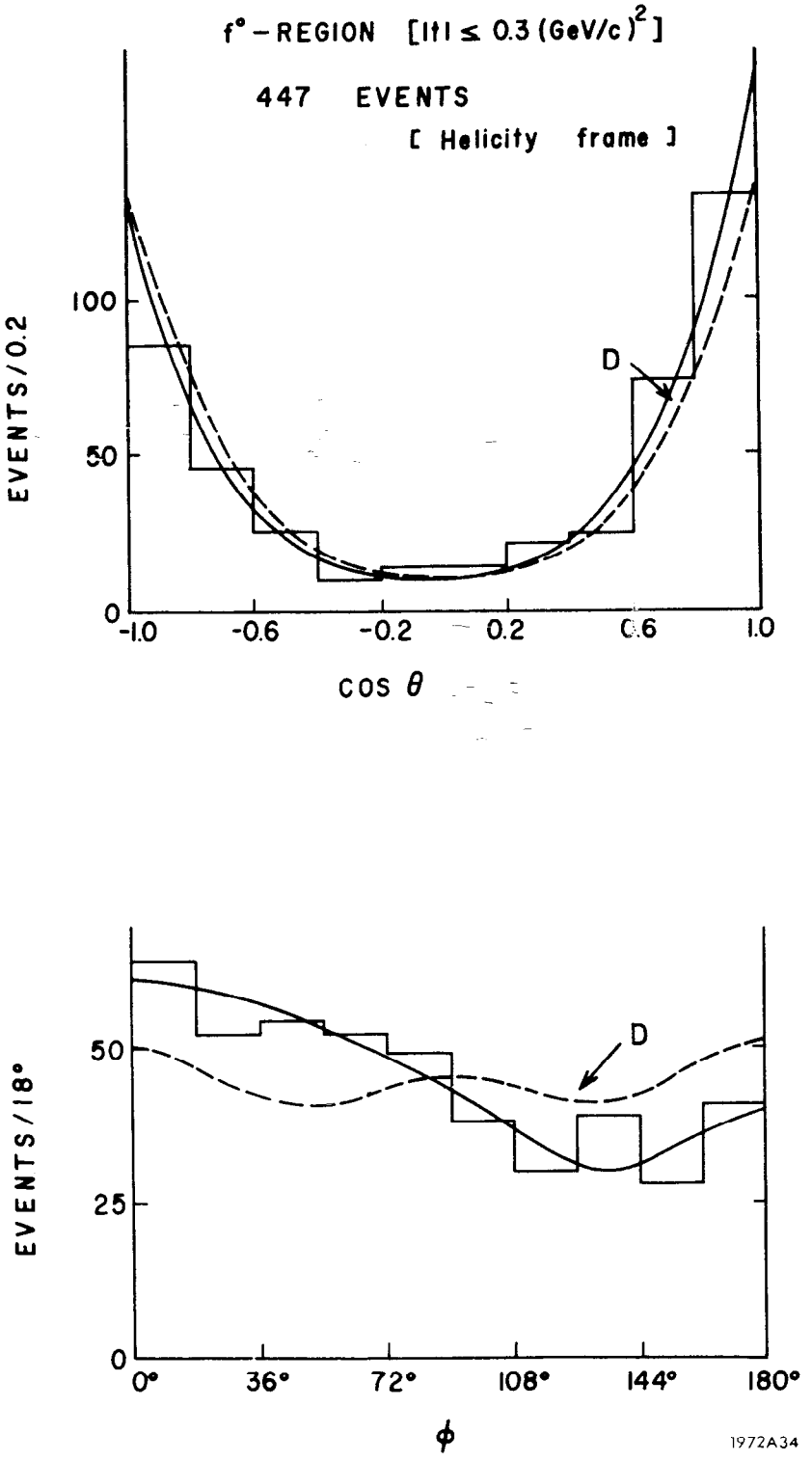

FIG. 9--Decay angular distribution for the f^{o} region in the helicity frame. Dashed lines are for pure D-wave, and solid curves are for the mixture of P-wave and D-wave.

Fitting with the D-wave, plus some P-wave admixture, gives a much better agreement with the experimental curve than the one with the pure D-wave only. This result together with the discrepancies from the expectation seen in some of the density matrix elements such as ρ_{11} and ρ_{22}, indicates that there is an appreciable non-D-wave component present. This conslusion is in accord with the recent analysis of 7 GeV $\pi^- p$ data by Oh et al. [8]

Some comparisons with theory were also tried to explain the density matrix elements of f^o in the helicity frame. The density matrices for the f^o events are given in Fig. 10, together with theoretical predictions obtained from the gauge invariance model[6] which are shown with solid lines. Density matrix elements such as ρ_{00}, ρ_{11} and ρ_{2-2} are in reasonable agreement. The values for ρ_{1-1} and ρ_{22}, however, are not. The ρ_{22} element, in particular, has a negative value, while the theory predicts zero.

3. Evidence for a New Dipion Resonance at $M_{\pi^+\pi^-} = 2,080$ MeV

Let us now turn our discussion to the possible evidence for a new meson at the dipion mass = 2,080 MeV. As shown in Fig. 1a, we see a new peak standing up with about 4 standard deviations significance from the background. We have described the mass distribution with nonresonant phase-space and with the four resonances of the Breit-Wigner type using the parameters given in Table 1. In order to see the effect more clearly we have also tried plotting dipion mass spectra for the events in the backward region of $\cos\theta$. Figures 11a and 11b are typical examples. Though the statistics are relatively poor, we can see the effect without any background, following the now-well-established g^o meson peaking at 1,660 MeV.

The effect was also investigated in its decay angular distributions. The asymmetry parameter in $\cos\theta$, namely the forward-backward ratio $R \equiv (F - B)/(F + B)$ was plotted as a function of the dipion mass. The slope of the ratio R as a function of the dipion mass, that is $R' \equiv dR/dm_{\pi\pi}$, was also checked and is depicted in Fig. 12 together with the value for R.

The decay angular distributions of the $\pi^+\pi^-$ system are analyzed as a function of dipion mass in the helicity frame, giving various moments for

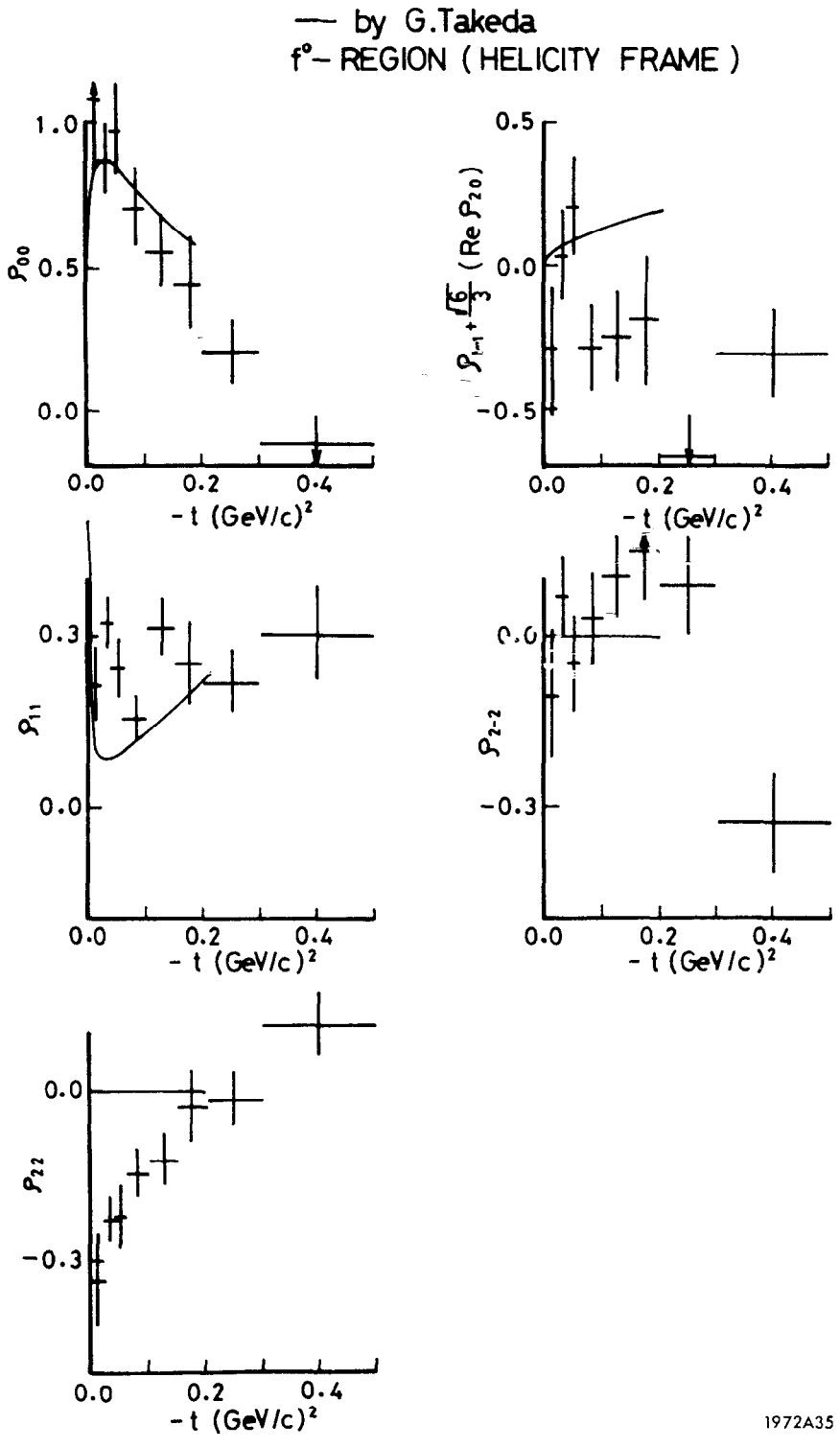

FIG. 10--Density matrix elements in the helicity frame for the events in the f^0 region. Solid lines are predictions of the gauge invariance model.

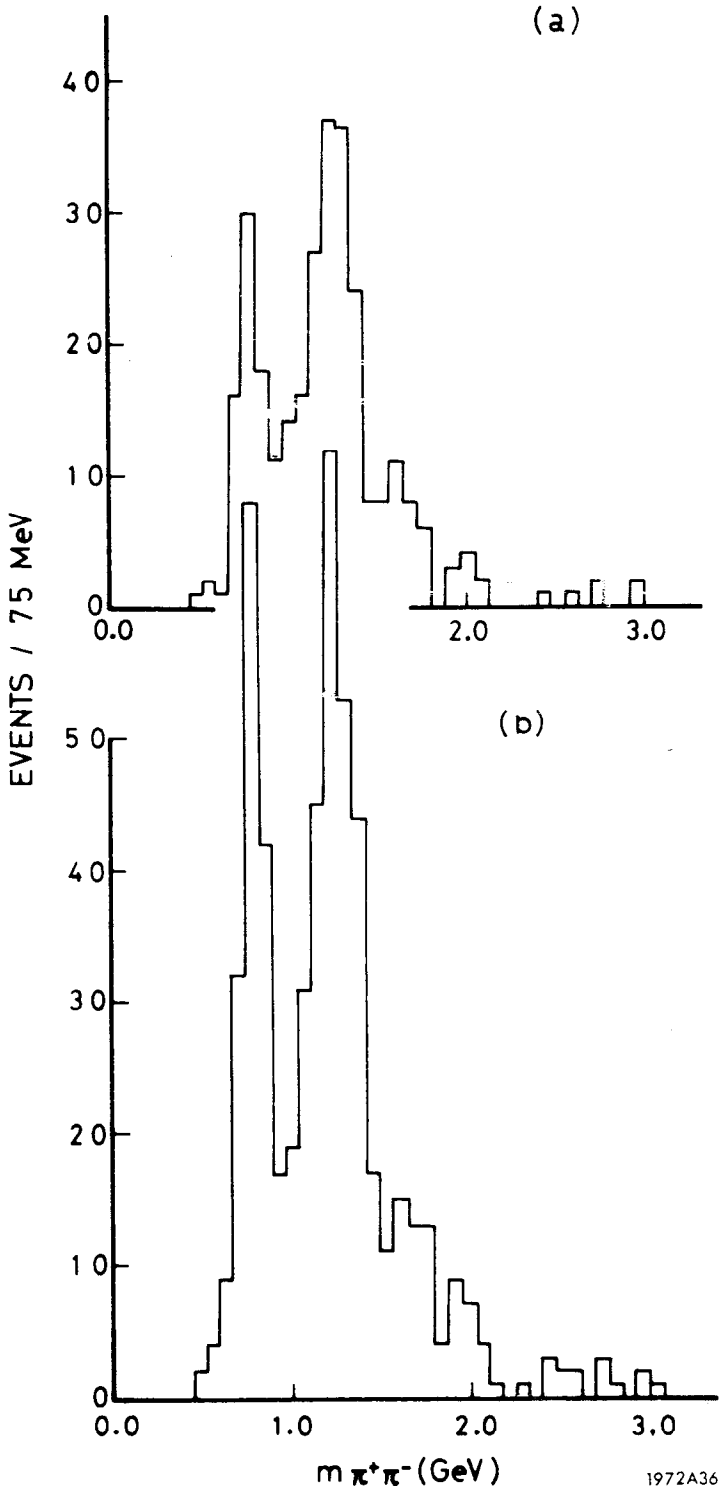

FIG. 11--$\pi^+\pi^-$ mass spectra for the events (a) in the region cos $\theta \leq -0.8$ and (b) in the region cos $\theta \leq -0.5$ in the helicity frame.

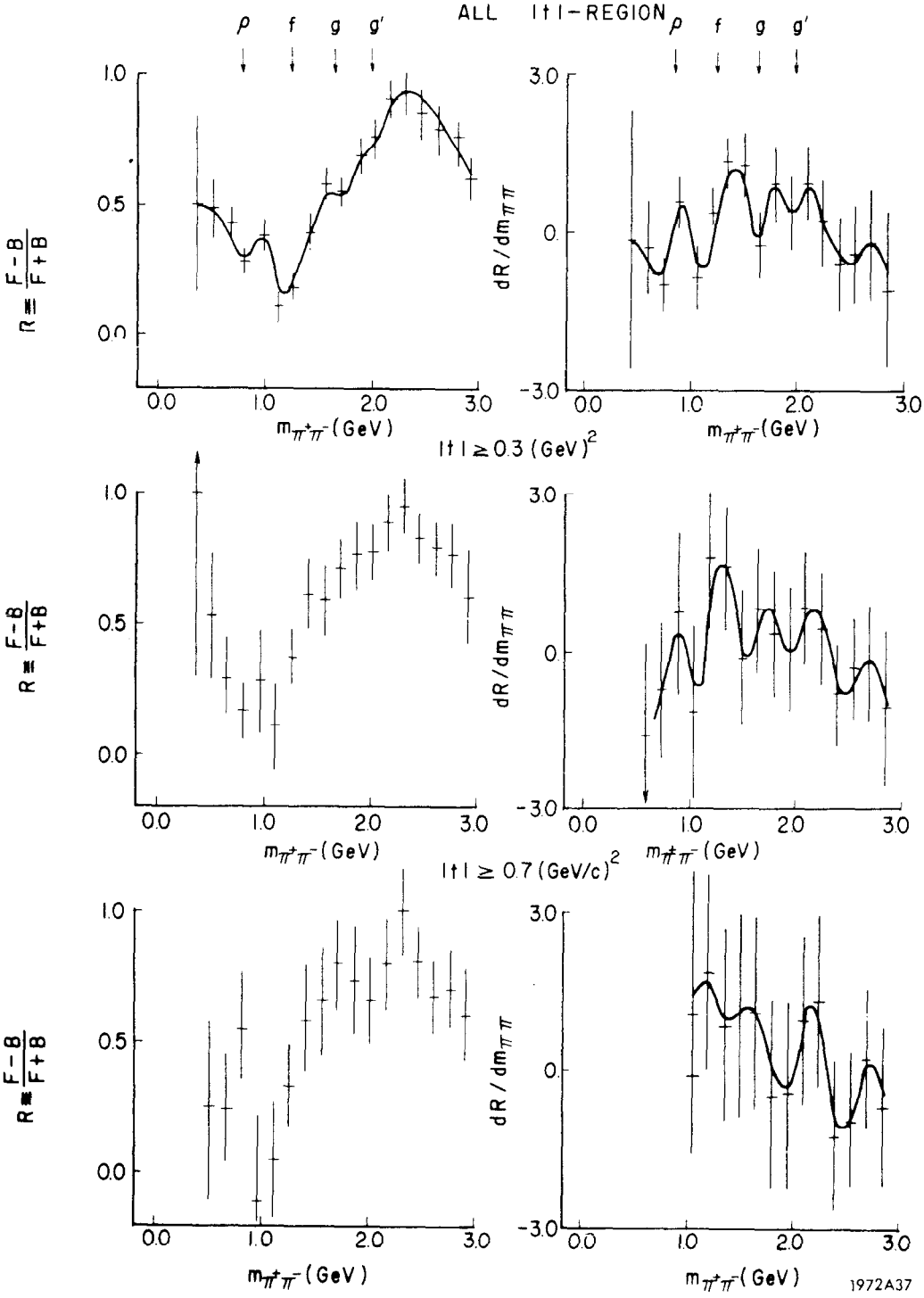

FIG. 12--Forward-backward asymmetry parameter in the cos θ distribution shown as a function of $m_{\pi^+\pi^-}$. Solid lines are hand-drawn. The arrows indicate the positions of resonances.

the Legendre polynomials. Some relevant moments are shown in Fig. 13. It would be plausible to say that the A_6 moment and possibly the A_8 moment have some small nonzero values at the dipion mass of $\sim$2,100 MeV. This fact may indicate that the angular momentum for this dipion system might be not bigger than three or four, but we cannot exclude the possibility that it might even be one or five. From the point of view of a possible spin-parity assignment, an isospin analysis of the system is very essential. We have thus analyzed the $\pi^-\pi^o$ events in the reaction (2). Preliminary results for this study give the $\pi^-\pi^o$ mass distribution shown in Fig. 14. A slight indication of a bump at $\sim$2,100 MeV can be seen in the spectrum, which gives the production cross section ratio $r = \sigma(\pi^-\pi^o)/\sigma(\pi^-\pi^+) \approx 1/2$. This ratio is very similar to the values for the cross section ratios for ρ^-/ρ^o and g^-/g^o. If we assume that the production process for the new meson is similar to those for ρ and g mesons, the ratio of charged to neutral components could indicate that a possible isospin of the system would be one as in the case of ρ and g. This results in the conclusion that a possible spin-parity could be $J^p = 1^-, 3^-, 5^-$. We need further investigation with better statistics to explore these possibilities.

A word should be given here about two previous reports relevant to this dipion enhancement. The reports came from a collaboration of the California Institute of Technology and the University of Rochester,[9] and also from the BNL-Carnegie collaboration.[10] The CIT-Rochester group has observed an indication of a resonating amplitude in the annihilation angular distributions of antiprotons into the dipion system with a possible angular momentum $\ell = 3$, which in turn gives a possible isospin I = 1 for the $\pi^+\pi^-$ system, since G-parity requires it. They assigned a mass value for system to be M_o=2.12 GeV. Another report came from the BNL-Carnegie collaboration in 1969. In their missing-mass experiment for the reaction $\pi^-p \rightarrow X^-p$ they observed a peak at $m(X^-)$ = 2,085 MeV. In reviewing this information, it seems to us very likely that our new dipion enhancement, which we call g' (2,100) tentatively, may well correspond to that reported by these people. It may, however, be too early to say whether this meson fits well onto the daughter trajectories of the ρ meson Regge Pole predicted from the dual resonance model.[11] (See Fig. 15.)

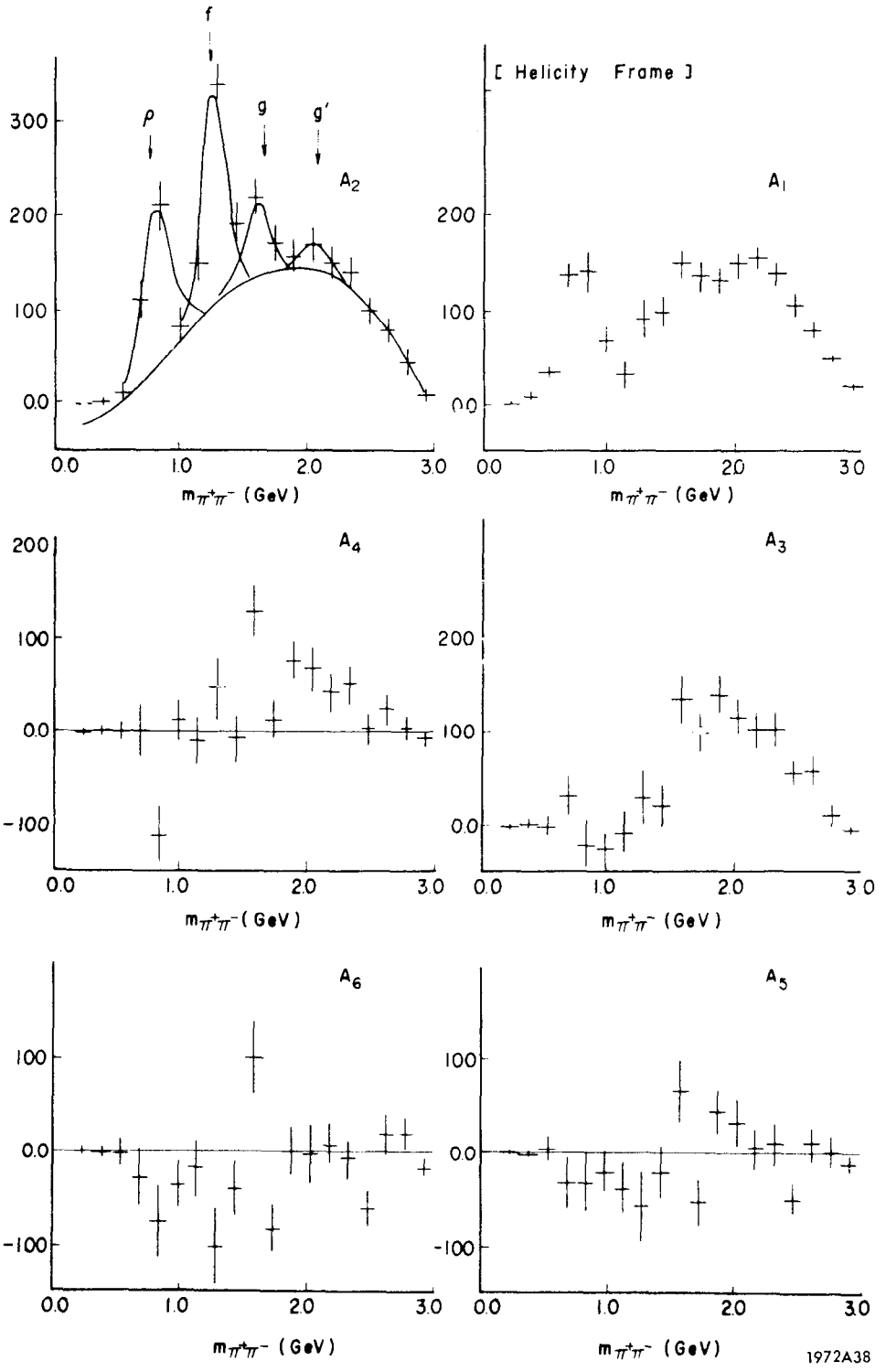

FIG. 13--Legendre moments of the cos θ distribution of the $\pi^+\pi^-$ dipion system in the helicity frame. Solid lines are hand-drawn.

FIG. 13--Cont'd.

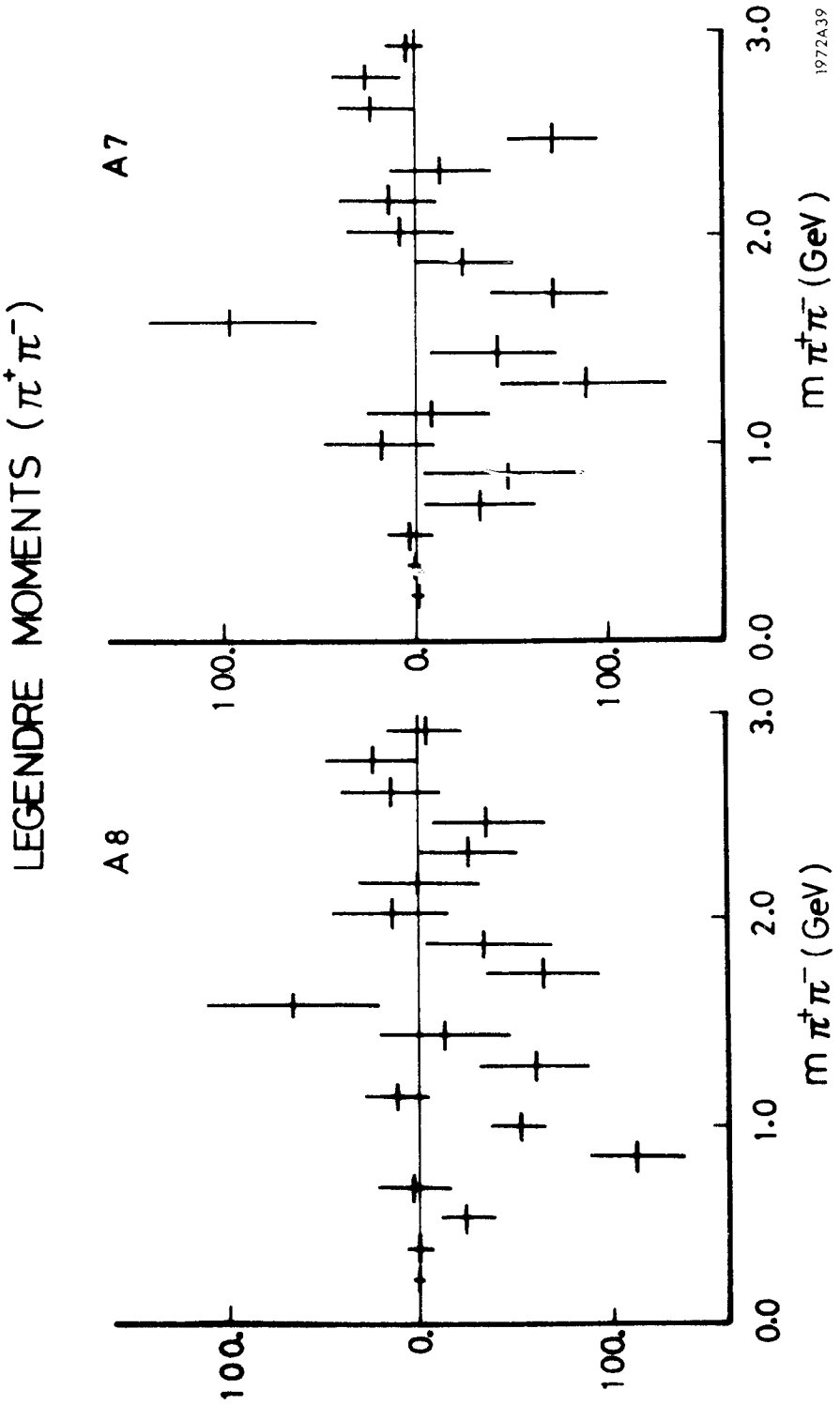
LEGENDRE MOMENTS ($\pi^+\pi^-$)
A7
A8
100.
0.
100.
0.0
1.0
2.0
3.0
m $\pi^+\pi^-$ (GeV)
1972A39

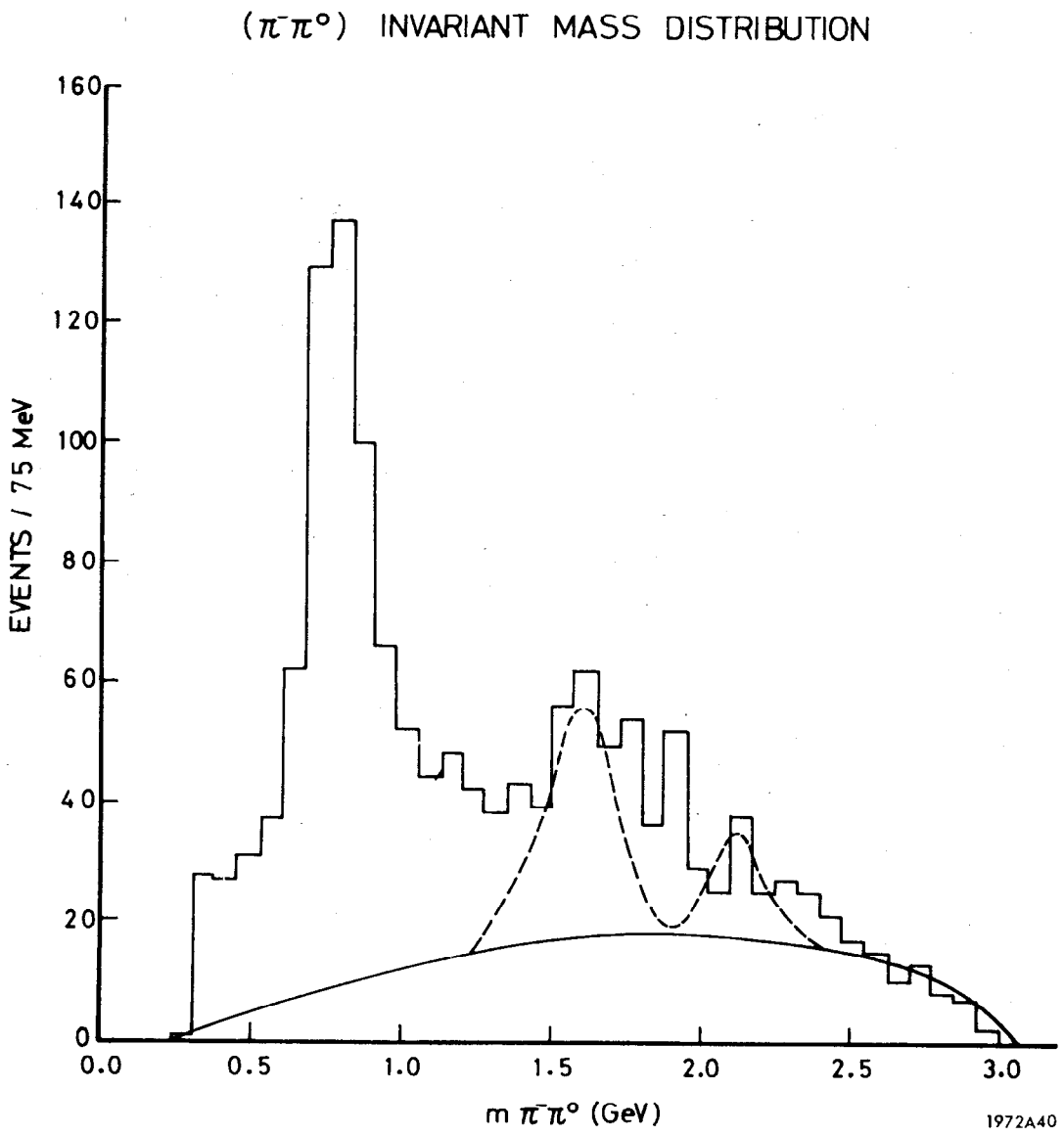

FIG. 14--Invariant mass distribution of the $\pi^-\pi^o$ system in reaction (2), 1,496 events. The solid curve indicates an approximate phase space distribution, and dashed curves are hand-drawn.

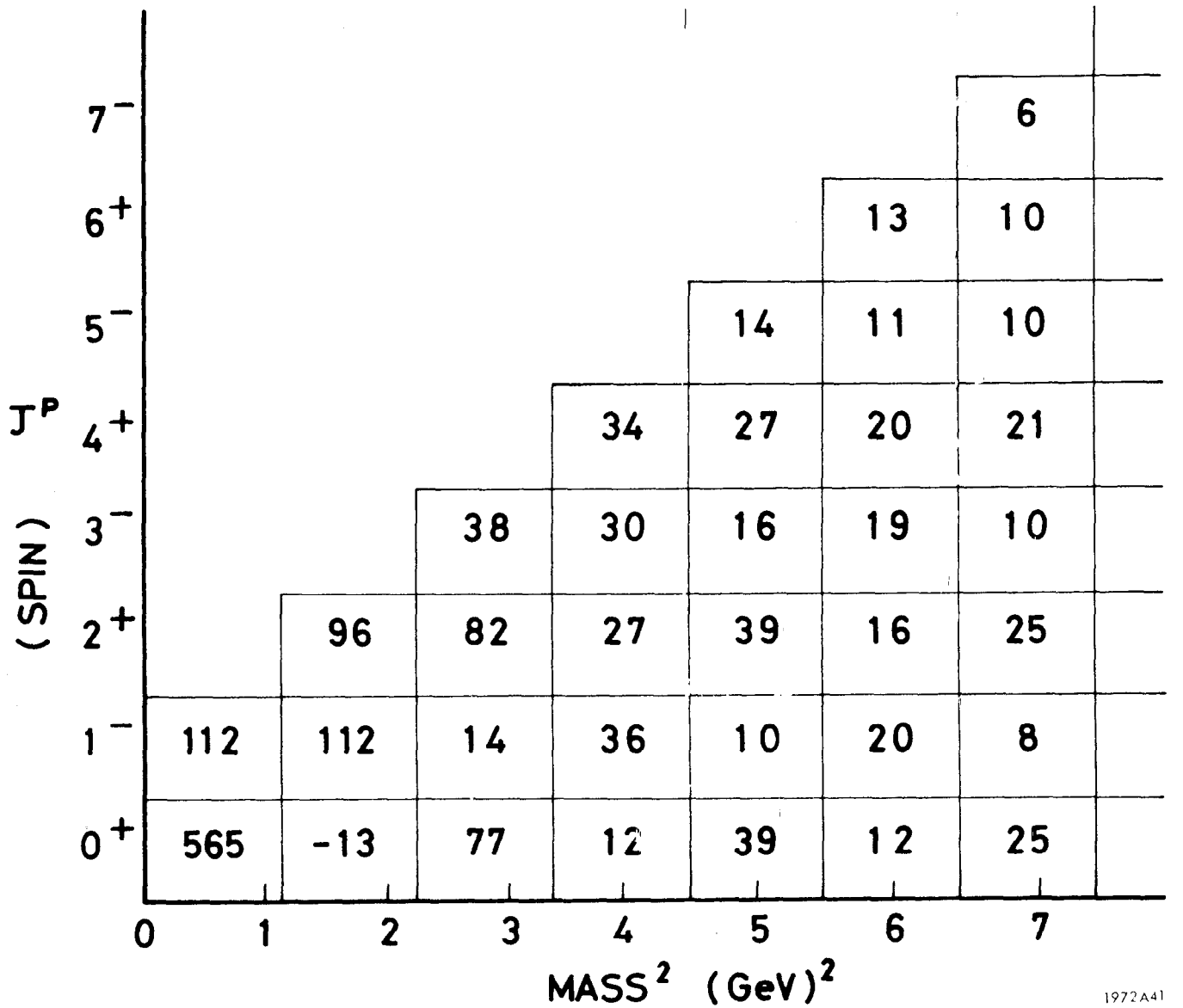

FIG. 15--Trajectories and particles in the Veneziano model for π-π scattering. Numbers are elastic partial widths in MeV. (See Ref. 11.)

We would like to express our sincere appreciation to Professor Walter Selove of the University of Pennsylvania for giving us the opportunity to use this $\pi^- p$ film. We wish also to thank our colleagues at the University of Notre Dame for their support.

References

1. G. Kane, Review talk at the Meeting on Experimental Meson Spectroscopy, Philadelphia, May 1970 (W. A. Benjamin, New York, 1970).
2. The previous work done under the collaboration of the University of Pennsylvania and the University of Notre Dame, has been published: J. A. Poirier et al., Phys. Rev. 163, 1462 (1967).
3. K. Gottfried and J. D. Jackson, Nuovo Cimento 34, 735 (1964).
4. P. K. Williams, Phys. Rev. D1, 1312 (1970). See also Ref. 1.
5. C. F. Cho and J. J. Sakurai, Phys. Rev. D2, 517 (1970).
6. G. Takeda, talk at this Seminar.
7. In this calculation we used Eq. (2) of the following paper by G. Takeda. If calculated from the 2π decay width Γ, using the world averaged experimental value $\Gamma_{ave} = 150$ MeV, then we expect $(g^2/4\pi)\, m_f^2 = 43$.
8. B. Y. Oh et al., Phys. Rev. D1, 2494 (1970).
9. H. Nicholson et al., Phys. Rev. Letters 23, 603 (1969).
10. E. W. Anderson et al., Phys. Rev. Letters 22, 1390 (1969).
11. J. Shapiro, Phys. Rev. 179, 1345 (1969); J. D. Jackson, Rev. Mod. Phys. 42, 12 (1970).

Discussion

Pless: What model did you use for the background? When you mention three-body phase spaces, are they Lorentz invariant phase space?

Takahashi: Yes, they are; and we used four Breit-Wigner type resonances and invariant phase space added incoherently.

Flatté: What does the neutron-π mass distribution look like?

Takahashi: The distributions for $n\pi^-$ and $n\pi^+$ do not seem to have any strong resonance signals. Further analysis on this point is under way.

Flatté: When you discuss angular distribution analysis, do you take just the region of $\pi\pi$ masses around the ρ^0 or f^0?

Takahashi: Yes.

Flatté: Have you tried to make any estimation of what the backgrounds do?

Takahashi: For the ρ^0 events we have a total of about 20% contamination from non-ρ^0 events. Because we only treat these data in the small $|t|$ region we neglect background effects, which would be most important in the large $|t|$ region.

Flatté: When you plot things as a function of t, and you get out to large values of t, you have much more of a problem.

Takahashi: That's right. So we don't say anything about the events for that region, because of the large contamination. Neither does the theory. Does that answer your question?

Ferbel: I am thinking in particular of the negative ρ_{22} you find. It would be interesting to see what the background has to say about that.

Takahashi: That is an interesting point. We haven't had enough time yet to check all these data in a more careful manner.

Pless: Without trying to appear to sell anything [laughter] ...

Takahashi: Yes, it will be interesting to discuss methods of purifying the data.

Pless: I thought that discussion was yesterday.

DOES THE f-MESON BEHAVE LIKE A MASSIVE GRAVITON?

Gyo Takeda

Tohoku University
Sendai, Japan

In this short note we shall study whether the f-meson behaves like a massive graviton and couples to the conserved energy momentum tensor.

Recent experimental results[1] on the differential cross sections for $\pi N \to fN$ at 8 GeV/c showed the existence of a sharp forward peak at $t \approx -\mu^2$, where t is the momentum transfer squared, and μ is the mass of pion. This indicates the dominance of the one-pion-exchange contribution, corresponding to Fig. 1a. Since the f-meson is assumed to couple to the conserved energy momentum tensor $T^{\mu\nu}$, the contributions due to the nucleon pole diagrams (Figs. 1b and 1c) should also be taken into account.

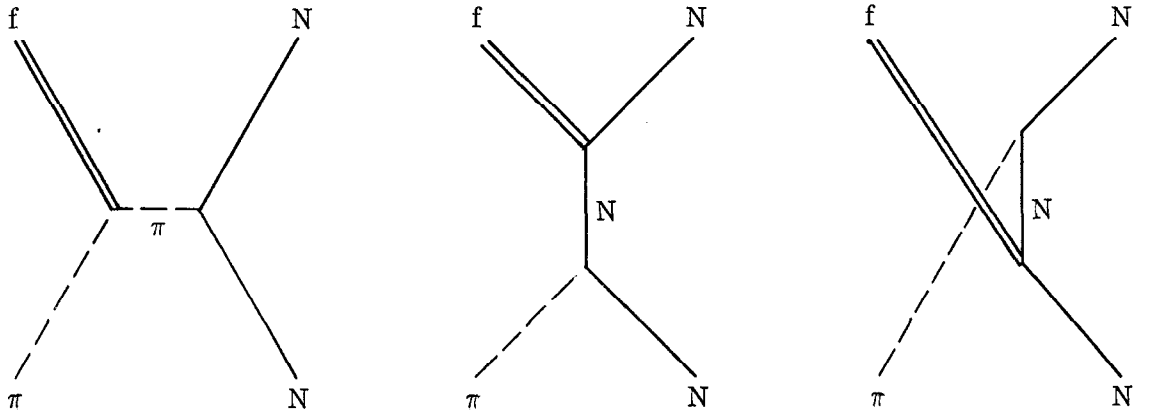

FIG. 1

We calculate the differential cross section for $\pi N \to fN$ at small $|t$ in the Born approximation, corresponding to Figs. 1a, 1b, and 1c. The coupling between the f-meson and $T^{\mu\nu}$ is taken as

$$H = g\, f_{\mu\nu}\, T^{\mu\nu} \quad , \tag{1}$$

where g is the coupling constant, and $f_{\mu\nu}$ is the field operator of the f-meson. The conserved energy momentum tensor $T^{\mu\nu}$ is the sum of the energy momentum tensors of pions and nucleons.

The calculated differential cross section is given by

$$\frac{d\sigma}{d|t|} = \frac{2\pi}{p^2 s} \frac{f^2}{4\pi} \frac{g^2}{4\pi} m_f^2 \left[- \frac{t m_f^2}{24 (t-\mu^2)^2} \left(1 - 4 \frac{\mu^2 + t}{m_f^2} \right) - \frac{t}{6 (t-\mu^2)^2} + \frac{1}{4} \right], \qquad (2)$$

where p and s are the incoming pion momentum and the total energy squared in the center-of-mass system, respectively, and m_f is the mass of the f-meson. The coupling constant $f^2/4\pi$ (=14.5) is the pion-nucleon coupling constant.

The first term in the bracket of Eq. (2) is the pion pole term, while the second and third terms are the interference and nucleon pole terms, respectively. The interference term is negative, and its magnitude relative to the magnitude of the pion pole term increases with increasing $|t|$. Thus the forward peak in $d\sigma/d|t|$ becomes sharper than the corresponding peak in the case of pure one-pion exchange. Furthermore, the third term gives a finite value of $d\sigma/d|t|$ at t=0.

We have neglected terms of order m_f^2/s (≈ 0.1) and $|t|/m_f^2$, which would appear in the bracket of Eq. (2). Therefore, the expression (2) for $d\sigma/d|t|$ should be applicable only for large s and small $|t|$ [$|t| \lesssim 0.1$ (GeV/c)^2]. The pion pole term is larger than the other terms by a factor of the order of $m_f^2/|t|$. Therefore, any correction to the pion pole term of the order of $|t|/m_f^2$ should be taken into account. We introduce the combined form factor G(t) for the $f\pi\pi$ and πNN vertices in the following simple form:

$$G(t) = \frac{M^2 - \mu^2}{M^2 - t} \qquad (3)$$

where M is an adjustable parameter of order m_f.

The calculated differential cross section and density matrices are compared with the experimental results. (See Figs. 8 and 10 of the preceding paper by K. Takahashi.) The t-dependence of $d\sigma/d|t|$ for small values of $|t|$ [0.1 (GeV/c)$^2 \geq |t| \geq |t_{min}|^2 \simeq 0.6\,\mu^2$] fits reasonably well with the experimental one. We have used a rather weak form factor G(t) with M=1 GeV. The calculated values of the density matrices are not in contradiction with the experimental values.

The magnitude of the coupling constant $g^2/4\pi$ was adjusted to give a good fit to the observed $d\sigma/d|t|$ at the forward peak. The value of the dimensionless

coupling constant thus determined is $m_f^2 g^2/4\pi = 16$, which is compared to the theoretical value $m_f^2 g^2/4\pi = 40$ obtained from the observed decay width of the f-meson into two pions ($\Gamma = 150$ MeV). The theoretical value is higher than the experimental one by a factor 2.5.

Let us consider various corrections which might reduce the discrepancy in the magnitude of the coupling constant:

(a) The experimental errors in the normalization of $d\sigma/d|t|$ are estimated to be about 15%.

(b) The uncertainty in the decay width of the f-meson into two pions is of the order of 30%. If we take $\Gamma(f \to 2\pi)$ as 100 MeV instead of 150 MeV, the theoretical value of the coupling constant is larger than the experimental one by a factor 1.7 instead of 2.5.

(c) Corrections of order m_f^2/s to the theoretical expression, Eq. (2), for $d\sigma/d|t|$ will amount to be about 10%.

(d) We have used the form factor G(t) with M = 1 GeV. The form factor may depend more sensitively on t, which corresponds to choosing a smaller value of M. Then we can reduce the theoretical value of $d\sigma/d|t|$ at the forward peak by 30% without changing our good fit in the t-dependence of $d\sigma/d|t|$.

(e) The absorption corrections are expected to reduce the theoretical value of $d\sigma/d|t|$ at the forward peak, thus reducing the discrepancy in the magnitude of the coupling constant. Since the corresponding correction is of the order of 10% for the case of ρ-production ($\pi N \to \rho N$), we also expect a similar correction in our case.

In conclusion, further studies are necessary in order to test the hypothesis of universal coupling of the f-meson to the conserved energy momentum tensor. In particular, experiments on $\pi N \to fN$ reactions at higher energies and very small $|t|$ ($|t_{min}|$ decreases with increasing s) are important, since most of the corrections mentioned above are expected to become smaller then.

Reference

1. Preceding talk by K. Takahashi.

PION-PION SCATTERING: APPLICATION OF THE THEORY OF INTERMEDIATE NUCLEAR STRUCTURE

Gyo Takeda

Tohoku University
Sendai, Japan

Experiments[1] by missing mass spectrometers and bubble chambers have revealed the existence of quite a large number of boson resonances. Most of these resonances are either real single resonances or overlapping resonances, but some might correspond to some kind of intermediate structures such as those found in nuclear reactions in the intermediate energy regions.[2] We shall take pion-pion scattering as an example and discuss the possible occurrence of such intermediate structure and its qualitative properties.

We shall base our discussion on the Veneziano model of pion-pion scattering. In this model the elastic scattering amplitude without Pomeron contributions can be written as the sum of infinitely narrow resonance terms:

$$A^I(s,t) = -\frac{\sqrt{s}}{q} \sum_{\ell=0}^{\infty} (2\ell+1)\left[1+(-1)^{\ell+I}\right] \sum_{n=\ell}^{\infty} \frac{\Gamma^I_{el}(n,\ell)\, M_n}{s - M_n^2} P_\ell(\cos\theta) \qquad (1)$$

where I (=0 or 1) denotes the isotopic spin of the s-channel, M_n the mass of the nth resonance on the leading Regge trajectory as well as its daughters, and $\Gamma^I_{el}(n,\ell)$ the elastic width of the ℓ-wave resonance with mass M_n.

Actually the state (I,n,ℓ) is degenerate in general, and its degeneracy is large for those resonances lying on lower daughter trajectories. Since no general prescription for writing down multipion amplitudes is known, we shall use the amplitudes given by Paton and Chan,[3] which are applicable only for the case of negative intercept of the leading trajectory ($\alpha(0) < 0$). Then the degree of the degeneracy for a given (I,n,ℓ) can be computed, if we require the factorization property of the multipion amplitudes. The multiplicity $m(I,n,\ell)$ of the degenerate state is given in Fig. 1. Since pion-pion collisions can excite only states with normal parity and normal charge conjugation parity, we give also the degree of degeneracy for such states (see numbers in the brackets in Fig. 1). These latter numbers should be regarded as lower limits, because the addition of satellite terms, the existence of more than one kind of leading trajectory,

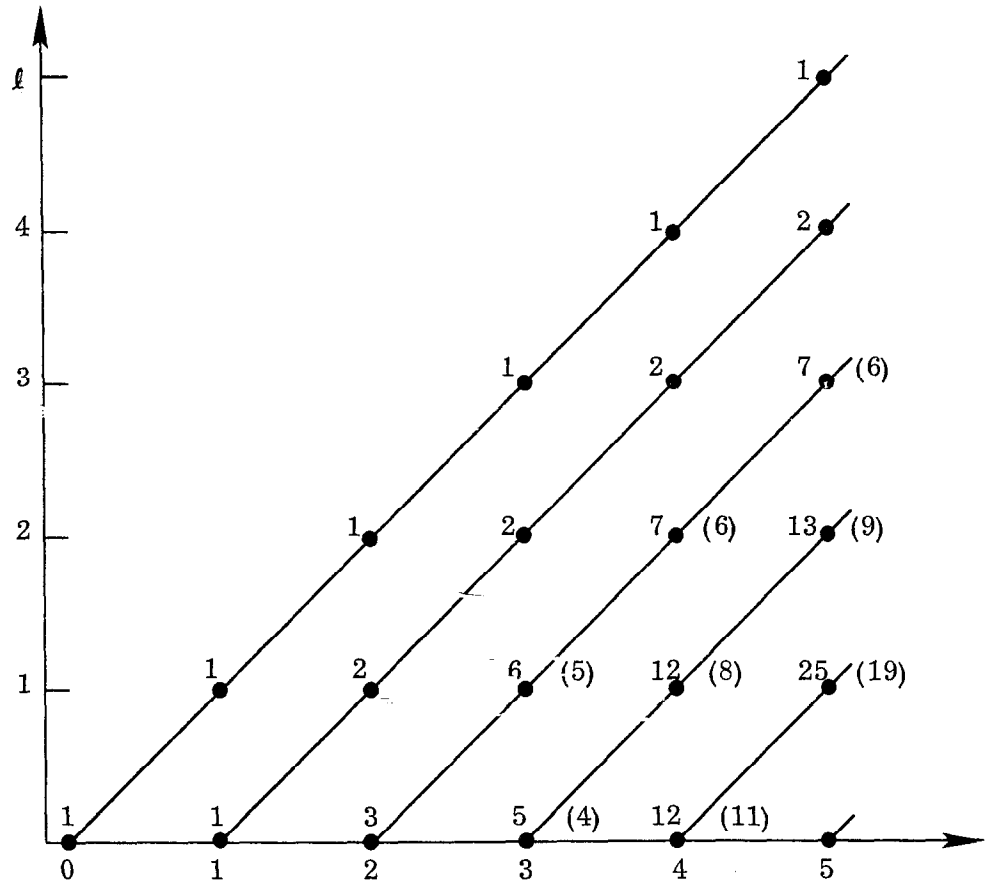

FIG. 1--The degree of degeneracy for given n and ℓ. (Numbers in the brackets refer to states with normal parity and normal charge conjugation parity.)

and adding trajectories with positive intercept are expected to increase the degree of degeneracy.

Now the Veneziano amplitude (1) has to be unitarized. This will introduce a finite width to each resonant state and furthermore remove the degeneracies. Then the amplitude becomes as follows:

$$A^I(s,t) = -\frac{\sqrt{s}}{q} \sum_\ell (2\ell+1) \left[1 + (-1)^{\ell+I}\right] A^I_\ell(s)\, P_\ell(\cos\theta) \quad , \tag{2}$$

where

$$A^I_\ell(s) = \sum_{n=\ell}^{\infty} \sum_{i=1}^{m} \frac{M_n(I,\ell,i)\, \Gamma_{el}(I,n,\ell,i)}{s - M_n^2(I,\ell,i) + i\, M_n(I,\ell,i)\, \Gamma(I,n,\ell,i)} \tag{3}$$

$M_n(I,\ell,i)$ and $\Gamma(I,n,\ell,i)$ $(i=1,2,\ldots,m)$ are the mass and total width of the ith resonance belonging to the nearly degenerate group of resonances.

Let us assume that corrections due to unitarization are small, which must be the case if the leading as well as daughter trajectories are almost linear in s. Then we expect that the mass splittings among the nearly degenerate states are small. The resonant state formed by pion-pion scattering in a collision time small compared with $h/\Delta M$ (ΔM = the average level distance among the m-fold states) is a certain linear combination of the m states $\psi_i(I,n,\ell)$. Furthermore, this linear combination can be approximately given by the nonunitarized Veneziano amplitude (1). We shall call this state the doorway state $\psi_d(I,n,\ell)$, and the formation of each resonant state $\psi_i(I,n,\ell)$ has to occur through the doorway state ψ_d. The elastic width $\Gamma_{el}(I,n,\ell)$ given by the nonunitarized amplitude is the elastic width of the doorway state and not the width of any single resonant state $\psi_i(I,n,\ell)$.

Next we shall use $\psi_d(I,n,\ell)$ and suitably chosen m-ℓ states $\phi_j(I,n,\ell)$ as the set of orthonormal states with given (I,n,ℓ). Each resonant state $\psi_i(I,n,\ell)$ is a linear combination of those basic states:

$$\psi_i = a_i \psi_d + \sum_{j=n}^{m-1} c_{ij}\phi_j \quad . \tag{4}$$

Assuming that the transition matrix element V between ψ_d and ϕ_j does not depend on j and equidistant distribution of M_i^2, we can calculate the distribution of $|a_i|^2$ over the m resonant states ψ_i:

$$|a_i|^2 \simeq \frac{\pi V^2/D}{(M_i^2 - M_\alpha^{2\,2} + (\pi|V|^2/D)^2} \cdot \frac{D}{\pi} \tag{5}$$

where D is the constant level spacing in M_i^2. If our simple assumptions are not exact, then V and D should be regarded as the average values of the matrix elements and level distances respectively.

The elastic width of the state ψ_i is given by $|a_i|^2 \Gamma_{el}$. When the degree of degeneracy m is very large, we can replace the sum over the states i in Eq. (3) by integration and obtain the following expression:

$$A_\ell^I(s) \simeq \sum_{n=\ell}^{\infty} \frac{M_d \Gamma_{el}}{s - M_d^2 + i\left(\Gamma_\downarrow + \Gamma^\uparrow\right)M_d} \tag{6}$$

where $\Gamma^{\uparrow}$ is the decay width of the doorway state ψ_d into any number of pion states and $\Gamma_{\downarrow}$ is given by

$$\Gamma_{\downarrow} M_d \simeq \pi |V|^2 / D \tag{7}$$

The width $\Gamma^{\uparrow}$ is called the escape width of the doorway state, and $\Gamma_{\downarrow}$ is called the compound width which is due to the decay of ψ_d into the compound states ψ_i. Both widths depend on I, n, and ℓ. M_d is the mass of the doorway state ψ_d and is approximately equal to M_n. Further modifications will be needed if experimental uncertainties in s exist. Assuming a Lorentzian distribution of s, $A_{\ell}^{I}(s)$ becomes as follows

$$A_{\ell}^{I}(s) = \sum_{n=\ell}^{\infty} \frac{M_d \Gamma_{el}}{s - M_d^2 + i(\Gamma_{\downarrow} + \Gamma^{\uparrow}) M_d + i\Delta s} \tag{8}$$

where Δs is the width of the distribution in s.

Now we shall discuss possible occurrences of the resonance-like intermediate structure with the width given by $\Gamma_{\downarrow} + \Gamma^{\uparrow}$.

1. Resonances on the leading Regge trajectory are expected to be non-degenerate. Most of them lying in low mass regions have been found experimentally and they are the most prominent resonances in that region. When we go to the higher mass region, the elastic width will decrease rapidly while the total width will increase slowly or remain almost constant. Therefore, it will become difficult to observe them in the high-mass region. On the other hand, it has been conjectured[4] that important resonances would lie on lower daughter trajectories when we go to higher energies and that their spins are given approximately by $\ell \sim s^{1/2} \sim n^{1/2}$. Thus there is a chance that we will observe an intermediate structure due to a large number of nearly degenerate states lying on a lower daughter trajectory.

As for resonances on the first daughter trajectory, there is some evidence for the existence of $\mathscr{E}(\simeq 700$ MeV) and ρ' under the ρ and f peaks respectively. They may constitute about 10% of the respective peak. When we go to higher mass regions ($\simeq$ 2100 MeV) there seems to exist a peak due to a mainly $\ell=3^-$ (I=1) state instead of a 4^+ (I=0) state.[5] This is another indication that the most important resonances will gradually change from those on higher trajectories to those on lower trajectories.

2. Suppose we find a resonance-like structure due to nearly degenerate m resonances lying on a daughter trajectory. We shall classify it into two cases.

(a) $\underline{M_d \Gamma^{\uparrow} > mD \gtrsim M_d \Gamma^{\downarrow}}$. In this case the collision time is rather short and there is not enough time to feel any detailed structure due to the existence of a large number of nearly degenerate compound states. The doorway state behaves like a real single resonant state. The total escape width $\Gamma^{\uparrow}$ is very hard to estimate, while its elastic width will be given approximately by the nonunitarized Veneziano amplitude. In Table 1 the calculated values of the elastic width are shown.

Table 1

The calculated values of the elastic width Γ_{el} for given n and ℓ. (The values are taken from the table of Shapiro,[6] 1969.)

6						13
5					14	11
4				34	27	20
3			38	30	16	19
2		96	88	27	39	16
1	112	112	14	36	10	20
0	565	-13	77	12	39	12
	1	2	3	4	5	6

(b) $\underline{M_d \Gamma_{\downarrow} \ll M_d \Gamma^{\uparrow}}$. In this case the observed peak will have a width given essentially by the compound width $\Gamma_{\downarrow}$. The magnitude of $\Gamma_{\downarrow}$ will depend on the degree of degeneracy m. Assuming that V does not depend on m, we obtain the following relations:

$$M\Gamma_{\downarrow} \propto m^{1/2}, \quad D \propto m^{-1/2} \quad \text{for } M\Gamma_{\downarrow} \simeq mD,$$
$$M\Gamma_{\downarrow} \propto m^{1/4}, \quad D \propto m^{-1/4} \quad \text{for } M\Gamma_{\downarrow} \simeq \sqrt{m}D.$$

The compound width has to satisfy $mD \gtrsim M\Gamma_{\downarrow} \gg D$. The level distance ΔM ($\simeq D/2M$) will decrease with increasing m and M, while $\Gamma_{\downarrow}$ will behave like either $m^{1/2}/M$ or $m^{1/4}/M$. When the relation $1 \sim \sqrt{s} \sim M$ does hold, m increases much faster than M with increasing mass, and $\Gamma_{\downarrow}$ will increase at least gradually for both cases.

The doorway state ψ_d is different for different entrance channels (2π, 4π, 6π, etc.). Therefore, the distribution of $|a_i|^2$ also differs for different channels. In Fig. 2 the typical distributions of $|a_i|^2$ for two channels α and β are

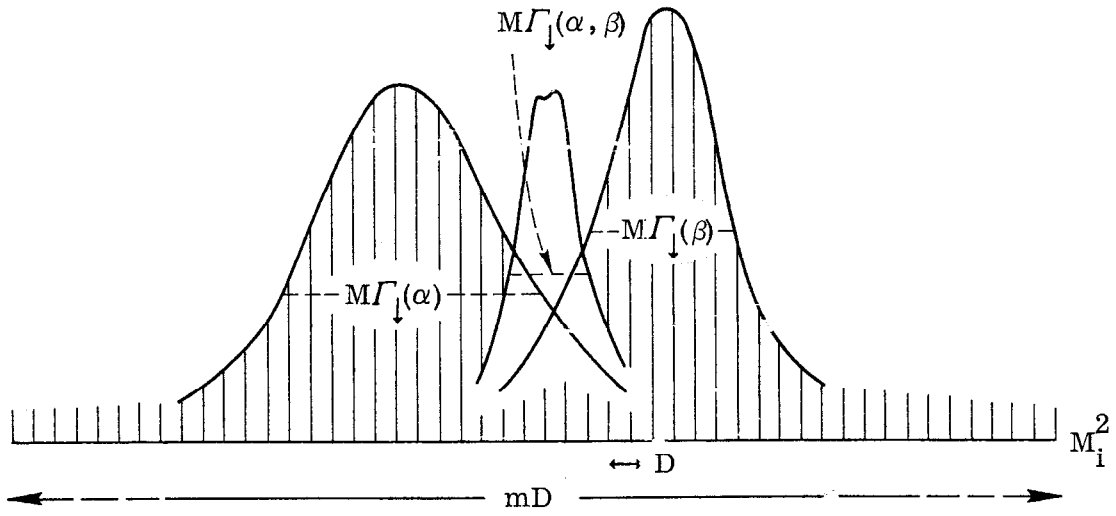

FIG. 2--Schematic illustration of the distributions of $|a_i(\alpha)|^2$, $|a_i(\beta)|^2$, and $a_i^*(\alpha)\, a_i(\beta)|$ over the compound states.

schematically shown. When $M\Gamma_\downarrow <$ mD, the compound widths $\Gamma_\downarrow(\alpha)$ and $\Gamma_\downarrow(\beta)$ will differ in general. When we measure the inelastic cross section for $\alpha \to \beta$, the observed width of a resonance-like structure is given by the width of the distribution of $|a_i^*(\alpha)\, a_i(\beta)|$ as shown in Fig. 2.

The magnitude of the peak in the cross section for the reaction $\alpha \to \beta$ is proportional to $\Gamma_\alpha \Gamma_\beta / \Gamma_\downarrow(\alpha,\beta)$, where Γ_α and Γ_β are the decay widths into entrance channels α and β, respectively, and $\Gamma_\downarrow(\alpha,\beta)$ is the width due to decays into the compound states. Since $\Gamma_\downarrow(\alpha,\beta)$ depends on α and β in a nonfactorizable way, the factorization property will be lost for this kind of intermediate structure. Furthermore, when the distributions of $a_i(\alpha)$ and $a_i(\beta)$ are peaked at different positions, a structure with a rather narrow width may appear in the inelastic reaction $\alpha \to \beta$. Some of the narrow resonances observed in high mass regions might be related to this effect. (Qualitatively we would not expect to see such narrow structure in elastic scattering, but this may be an empty statement for experimentalists.)

All the discussions presented here are very speculative and crude. However, the existence of similar phenomena in nuclear reactions at intermediate energies gives us strong support for this kind of study.

References

1. See, e.g., Experimental Meson Spectroscopy, edited by C. Baltay and A. Rosenfeld (Columbia University, New York, 1970).
2. Intermediate Structure in Nuclear Reactions, edited by H. P. Kennedy and R. Schrils (University Press of Kentucky, Lexington, 1968).
3. J. E. Paton and Chan Hong-Mo, Nucl. Phys. B10, 516 (1969).
4. See, e.g., H. Harari, Report No. SLAC-PUB-837 (1970).
5. K. Takahashi, "$\pi^- p \rightarrow \pi\pi N$ Reactions at 8 GeV/c," Paper No. 8 presented to this Seminar.
6. J. Shapiro, Phys. Rev. 179, 1345 (1969).

Discussion

Flatté: Why do you say that [the prediction of different behavior in elastic and inelastic channels] is an empty statement or prediction? We can observe inelastic and elastic channels.

Takeda: I do not mean exactly empty; but from my associations with experimentalists I think that without some prediction of numerical values it may effectively be an empty statement for them.

Plano: Do you expect all the resonances in the "intermediate structure" to have the same quantum numbers?

Takeda: Using a particular Veneziano model, we see that the degree of degeneracy increases with mass [see Fig. 1]. As I mentioned, any other model of this type would probably increase the degeneracy [but not change the mass much]. So we expect all the states in the enhancements to have the same quantum numbers.

Plano: How easy would it be to measure the individual levels? This relates to whether bubble chambers are accurate enough or not.

Takeda: I have used various experimental data and interpreted it according to my taste. There are some indications of high mass resonances given by the CERN missing mass spectrometer experiments, and also some of the bubble chamber experiments. These resonances seem to lie more or less on the linear trajectories, and the masses are spaced by roughly $(1\ \mathrm{GeV/c})^2$. Then the spacing for the structures in the range 3 to 4 GeV will be $1\ \mathrm{GeV}^2/2m \approx 200$ MeV. Since the multiplicity is ~ 10, we might guess the individual levels could be spaced by 10 - 20 MeV. But I have no real idea of the precise width of each individual state, as it depends on the transitions they may make.

Flatté: We can achieve 10 MeV resolution now.

Takeda: Yes. Some resonances in the Rosenfeld Tables, listed as uncertain, have very small widths, and may be this intermediate structure.

Harari: This is a question to experimentalists. Is there a simple rule to relate resolution to mass? The particles will become close together in mass, being spaced linearly in m^2.

Plano: It depends on the technique. I will explain a method for obtaining ~ 1 MeV resolution for 4 - 5 GeV resonances. [See Plano's paper.]

Flatté: No present bubble chamber experiment is limitted by the uncertainty in beam energy.

WHAT IS VECTOR-MESON DOMINANCE? COMPARISONS OF SINGLE-PION PHOTOPRODUCTION AND ρ PRODUCTION IN PION-NUCLEON COLLISIONS*

J. J. Sakurai

Department of Physics
University of California, Los Angeles
Los Angeles, California USA

About two years ago experimentalists (and also some theorists) working on applications of vector meson dominance to high energy photoproduction were confused. It started with the observation that the familiar relation alleged to be based on vector meson dominance

$$\mathcal{M}(\gamma_{\text{isovector}} + A \to B) = (e/f_\rho)\, \mathcal{M}(\rho^0_{\text{transverse}} + A \to B) \qquad (1)$$

is ambiguous because the notion of a transversely polarized ρ is frame-dependent. People started asking: In which frames does the ρ meson resemble the photon most closely? Even though the original suggestion due to Beder[1] was to test (1) in the center-of-mass s-channel helicity frame (hereafter referred to simply as the helicity frame), some people[2] advocated the use of the Donohue-Högaasen frame defined by the vanishing of Re (ρ_{10}), others said that vector meson dominance predictions are fulfilled if there exists a frame in which (1) is satisfied, which, of course, greatly reduces predictive power of (1).

Faced with such a deplorable state of affairs, I felt that I could no longer remain silent. My present talk is an outcome of a series of investigations started around that time in collaboration with a student of mine, C. F. Cho, who will be here at Stanford (Physics Department) starting this summer. I'll discuss, almost exclusively, comparisons of the hadronic reaction

$$\pi^- p \to \rho^0 n \qquad (2)$$

with the photoproduction reactions

$$\begin{aligned} \gamma p &\to \pi^+ n \\ \gamma n &\to \pi^- p \quad , \end{aligned} \qquad (3)$$

but I hope that my present talk will be of some interest to those who are not necessarily working in this field. In any case, having given a talk yesterday covering the whole of high energy physics,[3] I feel like restricting myself to a very narrow subject today.

It is now common knowledge that at very small values of -t, the photoproduction reactions (3) exhibit features reminiscent of the very old predictions of the electric Born model, a simple perturbation model in which the one-pion-exchange amplitude is supplemented by the nucleon pole contributions with $\bar{N}N\gamma$ vertices of the pure γ_μ type. In fact, one of the earliest achievements of this great laboratory (first announced in this auditorium by Richter[4] at the 1967 Electron-Photon Conference) was the famous forward peak in π^+ photoproduction, unexpected to some local theorists[5] at that time but completely reasonable on the basis of the electric Born model; furthermore, the model also gave correctly the absolute magnitude and the energy dependence of charged-pion photoproduction. Subsequently experimentalists at DESY[6] using polarized photons showed that the A parameter defined by

$$A = \frac{\sigma_\perp - \sigma_\parallel}{\sigma_\perp + \sigma_\parallel} \tag{4}$$

also agrees with the electric Born model for very small values of -t.

Even though the model does fail, in fact, quite badly for $-t \gtrsim 2m_\pi^2$, at least we can conceive of a world in which all the predictions of the model are exact. If the notion of vector meson dominance is unambiguous in such a hypothetical world, then we can use the electric Born model as a "theoretical laboratory" to test some of the conjectures theorists have been making.

In the electric Born model for photoproduction, we start with the minimal electromagnetic Lagrangian where the photon coupling is introduced via $\partial_\mu \to \partial_\mu \mp ieA_\mu$, and then just compute the lowest order graphs. If we are to compute the analogous hadronic amplitude in the spirit of vector meson dominance, the underlying interaction Lagrangian must satisfy the ρ-photon analogy substitution rule:

$$eA_\mu^{(\text{isovector})} \longleftrightarrow f_\rho \rho_\mu^0 \quad .$$

This simply amounts to saying that, as far as the ρ meson interaction is concerned, we should start with the 1960 Lagrangian[7] (or the 1954 Yang-Mills[8]

Lagrangian) in which the ρ was postulated to be coupled universally to the isospin, in much the same way as the isovector photon is coupled universally to the isovector charge. So the relevant part of the interaction Lagrangian is given by

$$\mathscr{L}_{\text{int.}} = ig_{\pi NN}\,\bar{N}\gamma_5 \underset{\sim}{\tau} N\cdot\pi + f_\rho \underset{\sim}{\rho}_\mu \cdot \left(i\bar{N}\gamma_\mu \frac{\underset{\sim}{\tau}}{2} N - \underset{\sim}{\pi}\times\partial_\mu \underset{\sim}{\pi} + \ldots\right)$$

$$+ eA_\mu^{(\text{isovector})}\left(i\bar{N}\gamma_\mu \frac{\tau_3}{2} N - (\underset{\sim}{\pi}\times\partial_\mu\underset{\sim}{\pi})_3 + \ldots\right) \tag{5}$$

If you are considering electroproduction ($k^2 > 0$ space-like)

$$\begin{aligned} e^- p &\to e^- \pi^+ n \\ e^- n &\to e^- \pi^- p \end{aligned} \tag{6}$$

or lepton-pair production ($k^2 < 0$ time-like

$$\pi^- p \to e^-(\mu^-) + e^+(\mu^+)\, n \tag{7}$$

it is necessary to add a gauge invariant γ-ρ interaction

$$\mathscr{L}_{\gamma-\rho} = -\frac{1}{2}(e/f_\rho)\, F_{\mu\nu}(\partial_\mu \rho^o_\nu - \partial_\nu \rho^o_\mu) \tag{8}$$

which, however, vanishes at $k^2=0$. It is now a familiar result (thanks to Kroll, Lee and Zumino[9]) that (5) and (8), <u>when taken together</u>, lead to the famous current-field identity

$$j_\mu^{(\text{isovector})} = \left(m_\rho^2/f_\rho\right)\rho_\mu^o \quad . \tag{9}$$

Now everything is well defined. We just compute the photoproduction and analogous hadronic amplitudes in tree approximation, which is an euphemism for doing low order perturbation theory nowadays. In this manner the usual vector meson dominance relations[1,10]

$$\frac{d\sigma}{dt}(\gamma_{\text{isovector}}\, p \to \pi^+ n) = (e/f_\rho)^2 \left(|\vec{q}_\pi|/|\vec{k}_\gamma|\right)^2_{\text{c.m.}} \rho_{11} \frac{d\sigma}{dt}(\pi^- p \to \rho^o n) \tag{10a}$$

$$A(\gamma_{\text{isovector}}\, p \to \pi^+ n) = \left(\rho_{1-1}/\rho_{11}\right)_{\pi^- p \to \rho^o n} \tag{10b}$$

can be subjected to "experimental tests" in our theoretical laboratory. In Fig. 1 we show the results of our experiment,[11] which, by the way, is less costly than a typical SLAC experiment by about four orders of magnitude. Clearly the right and left sides of (10a) and (10b) bear no resemblance whatsoever in the Donahue-Högaasen frame. In contrast, in the helicity frame (10a) and (10b) do become exact at high energies, $s-m_p^2 \gg m_\rho^2$. So if the real world is like the simple electric Born world, there is no ambiguity whatsoever as to which is the preferred frame. Notice also that at low energies there is a substantial correction to the naive vector meson dominance relation [especially (10b)] even in the helicity frame.

While my collaborator and I were carrying out this experiment in our theoretical laboratory, we saw an interesting preprint by LeBellac and Plaut[12,13] who also advocated the use of the helicity frame. They showed that if some of the invariant amplitudes defined by Ball[14] many years ago (B_1, B_3, B_5, B_8) are independent of the vector meson mass, then the vector meson dominance relations (10a) and (10b) must hold exactly as $s \to \infty$ with t fixed provided we use the helicity frame but not any other frame. In their paper it is understood that the off-shell Ball amplitudes are mass-continued to relate (2) and (3) in the usual manner, i.e.,

$$\begin{aligned} B_i^{(\text{isovector } \gamma)}(s,t) &= (e/f_\rho)\, B_i(s,t,k^2)\Big|_{k^2=0} \\ B_i^{(\rho,\ \text{mass shell})} &= B_i(s,t,k^2)\Big|_{k^2=-m_\rho^2} \end{aligned} \tag{11}$$

In our electric Born model all the Ball amplitudes can readily be shown to be completely independent of k^2 as $s \to \infty$ with t fixed; so our results are quite consistent with their findings. This, by the way, is not so trivial as it sounds; if the CGLNFNW[15] amplitudes were used in place of the Ball amplitudes, the k^2 dependence would be strong even in the electric Born model.[16] I'll come back to this point later.

Before I present discussion based on the invariant amplitudes in some detail, it is necessary for me to make a little digression on what I call the conserved ρ source hypothesis. Everybody agrees that the electromagnetic interactions must satisfy the following two properties. First, the source of the

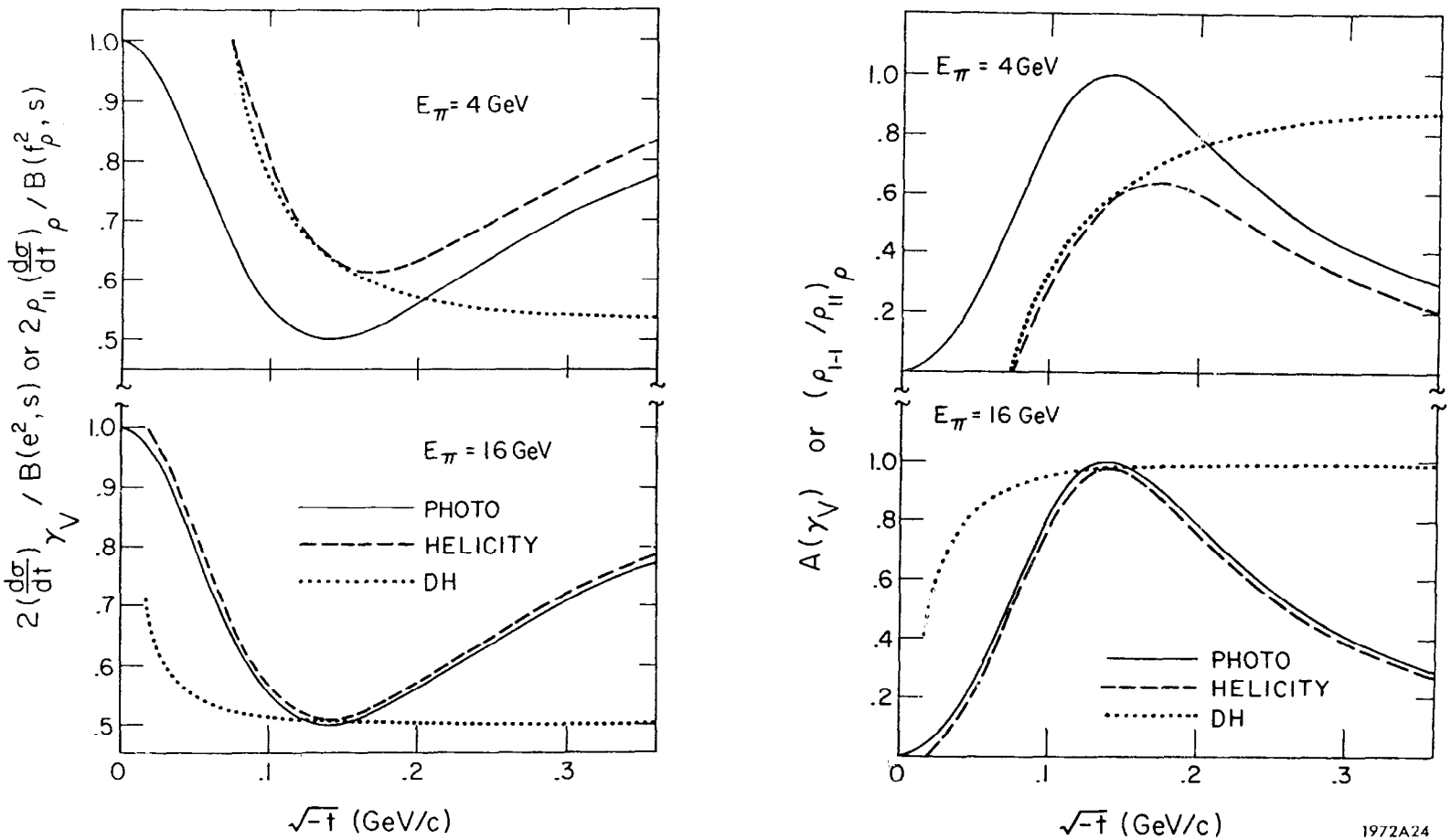

FIG. 1--Tests of (10a) and (10b) in the electric Born model. $B(f_\rho^2, s)$ and $B(e^2, s)$ are defined by $B(f_\rho^2, s) = (f_\rho^2/4\pi)(g_{\pi NN}^2/4\pi)\ \pi/(|q|_{c.m.}^2\ s)$; $B(e^2, s) = (e^2/4\pi)(g_{\pi NN}^2/4\pi)\ \pi/(|k|_{c.m.}^2\ s)$ so that $(d\sigma/dt)_\gamma/B(e^2, s)$ and $\rho_{11}(d\sigma/dt)_\rho/B(f_\rho^2, s)$ become equal when (10a) is satisfied. Photo, D-H and helicity stand for photoproduction, ρ production in the Donohue-Högaasen frame and ρ production in the helicity frame, respectively.

Maxwell field must be conserved. Second, the matrix element for a process in which a single photon is emitted or absorbed satisfies gauge invariance, i.e., if the amplitude is $\epsilon_\mu \mathcal{M}_\mu$ where ϵ is the photon polarization vector, then

$$k_\mu \mathcal{M}_\mu = 0 \tag{12}$$

Now in plain terms the vector meson dominance hypothesis says that the ρ meson is like the photon. It is then natural to ask whether the special features of the photon interactions mentioned above are shared also by the ρ meson interactions.

Most people have little trouble in understanding what is meant by a conserved ρ source within the context of Lagrangian models. The 1960 Lagrangian of Eq. (5) is considered to satisfy the conserved ρ source hypothesis because the $\rho\pi\pi$ and $\rho\bar{N}N$ coupling constants are related in a definite manner by the universality relation[7]

$$f(\pi^+ \leftrightarrow \rho^0\pi^+) : f(p \leftrightarrow \rho^0 p) : f(n \leftrightarrow \rho^0 n) = 1 : \frac{1}{2} : \frac{1}{2} \tag{13}$$

etc. In contrast a Lagrangian in which this universality relation does not hold is considered to be a bad Lagrangian which violates the conserved ρ source hypothesis.

Much less transparent is the meaning of the gauge condition, or better the conservation equation (12), when the vector meson is massive. To see this let us assume that (12) is not satisfied. We can, however, always add to $\mathcal{M}_\mu$ a term proportional to k_μ such that a new $\mathcal{M}_\mu$ satisfies (12). Specifically let

$$\mathcal{M}_\mu^{(\text{new})} = \mathcal{M}_\mu^{(\text{old})} - \left(k \cdot \mathcal{M}^{(\text{old})}\right) k_\mu / k^2 \tag{14}$$

Evidently

$$k_\mu \mathcal{M}_\mu^{(\text{new})} = 0 \quad . \tag{15}$$

Now the physical amplitude with ρ meson helicity λ is given by $\epsilon_\mu^{(\lambda)} \mathcal{M}_\mu$ where $k \cdot \epsilon^{(\lambda)} = 0$.[17] It is therefore clear that $\mathcal{M}_\mu^{(\text{old})}$ and $\mathcal{M}_\mu^{(\text{new})}$ lead to exactly the same physical consequences. So the requirement (12) does not provide us with any physically observable consequence, at least for the on-shell S matrix.

It is instructive to work out, for later purposes, the full implications of this observation using a simple but specific example. We consider

$$\rho^0(k) + p(p) \rightarrow \pi^+(\pi) + n(p') \tag{16}$$

in a hypothetical world where both the pion and nucleon are scalar, i.e., 0^+. The symbols in parentheses stand for the four-momenta of the respective particles. Because of energy momentum conservation there are only there independent four-vectors which we take to be k, q, and P defined by

$$P = (p+p')/2 \tag{17}$$

We can write

$$\mathcal{M}_\mu = B_1 P_\mu + B_2 q_\mu + B_3 k_\mu \tag{18}$$

There is no $\epsilon_{\mu\nu\lambda} P_\nu q_\lambda k$ term because of parity conservation. The conservation equation (12) leads to

$$B_1(u-s)/4 + B_2 \left(-m_\pi^2+k^2+t\right)/2 + B_3 k^2 = 0 \tag{19}$$

Notice that this equation merely fixes the amplitude B_3, a purely off-shell amplitude which makes no contribution to the observable $\epsilon_\mu^{(\lambda)} \mathcal{M}_\mu$. In particular no relation is obtained between B_1 and B_2.

This situation should be contrasted with the case where the ρ meson mass vanishes. If $k^2=0$, the conservation equation becomes the usual gauge-invariance relation

$$B_1(u-s)/4 + B_2\left(-m_\pi^2+t\right)/2 = 0 \ , \tag{20}$$

hence we do obtain a nontrivial restriction between B_1 and B_2. As a result, there is only one independent amplitude. In summary, the gauge condition or the conservation equation requires that B_1 and B_2 in the photon case be related by (20), but the identically-looking conservation equation in the massive ρ case leads to no relation between B_1 and B_2 whatsoever.[18]

From a purely kinematical point of view this difference between the $m_\rho \neq 0$ case and the $m_\rho = 0$ case is not at all surprising. In the massless case the $\lambda=0$ (longitudinal) state must be absent, and, since the $\lambda=\pm 1$ (transverse) amplitudes are related to each other by parity, there should be only one independent amplitude. In fact, the gauge condition is nothing more than a kinematical constraint arising from the fact that the massless particle has only two helicity states. In contrast, in the massive case there is the $\lambda=0$ state also, and it is not surprising that we have one more independent invariant amplitude. Yet our inability to obtain a nontrivial relation between B_1 and B_2 in the $m_\rho \neq 0$ case is disturbing

to vector meson dominance enthusiasts who want to believe that ρ mesons must somehow behave like photons.

When in doubt, it is often profitable to go back to our theoretical laboratory. We still consider the reaction (16) where the nucleon and pion are both 0^+ particles, and compute the invariant amplitudes in Born approximation. We obtain apart from $\sqrt{2}g_{\pi NN}f_{\rho\pi\pi}$,

$$\begin{aligned} B_1 &= r\left(\frac{1}{s-m_N^2} - \frac{1}{u-m_N^2}\right) \\ B_2 &= \frac{2}{t-m_\pi^2} + \frac{r}{2}\left(\frac{1}{s-m_N^2} + \frac{1}{u-m_N^2}\right) \end{aligned} \tag{21}$$

where

$$r \equiv f_{\rho NN}/f_{\rho\pi\pi} \ , \tag{22}$$

and our normalization convention for the ρ meson coupling constants is such that

$$r \to 1$$

in the universality limit, i.e., as (13) becomes exact. The purely off-shell amplitude B_3 is not given unambiguously by the usual Feynman rule, which is, of course, just for computing $\epsilon_\mu \mathcal{M}_\mu$. We take the point of view that B_3 is to be determined by the conservation equation (19). We then obtain, as $s \to \infty$ with t finite,

$$B_3 = -\frac{1}{k^2}(1-r) - \frac{1}{t-m_\pi^2} \tag{23}$$

The most remarkable feature of these Born amplitudes is their k^2 dependence. First, as far as B_1 and B_2 go, we have no difficulty since as $s \to \infty$ with t fixed, the k^2 dependence implicitly contained in the kinematical constraint equation

$$s+t+u = 2m_N^2 + m_\pi^2 - k^2 \tag{24}$$

becomes unimportant, and as a result both B_1 and B_2 become independent of k^2. The k^2 dependence of B_3 is much more interesting. For arbitrary values of $r = f_{\rho NN}/f_{\rho\pi\pi}$, the amplitude depends violently on k^2. However, with the universality relation r=1, B_3 becomes completely independent of k^2. Since the universality relation is a consequence of the requirement that the ρ couplings be

analogous to the photon couplings, it is suggestive to formulate vector meson dominance by postulating that the k^2 dependence of the off-shell amplitudes be as smooth as possible. After all, if the dynamics of photon processes is to resemble that of ρ meson processes, the invariant amplitudes should better not depend too violently on the vector meson mass.

At this point it is instructive to write down the equations that relate the invariant amplitudes B_i and the helicity amplitudes f_λ where λ stands for the ρ meson helicity. With s large and -t small, we have

$$\begin{aligned} f_0 &= \sqrt{-k^2}\,(B_2+B_3) \\ f^{(-)} &\equiv f_1-f_{-1} = -\sqrt{-2t}\left[B_2-(B_1/2)\right] \\ f^{(+)} &\equiv f_1+f_{-1} = 0 \end{aligned} \quad , \tag{25}$$

where, in writing down f_0, we have eliminated B_1 using (19) in favor of B_2 and B_3. There are a few important points to be noted here. First, if B_1 and B_2 are independent of k^2, then the transverse amplitudes are independent of k^2 in the helicity frame. Now the rotation matrix that connects the helicity frame to some other frame necessarily mixes $f_{\pm1}$ and f_0, the latter being strongly dependent on the ρ meson mass. It therefore follows that the naive vector meson dominance relation (1) must be tested in the helicity frame.

As $k^2 \to 0$, i.e., as the ρ meson mass is switched off, the $\lambda=0$ (longitudinal) amplitude goes smoothly to zero provided that the invariant amplitudes including B_3 are smoothly varying as $k^2 \to 0$. Notice, however, that this nice property of the longitudinal amplitude is not automatically satisfied in an arbitrary model. We merely recall that when the underlying Lagrangian violates the conserved ρ source hypothesis, B_3 has a pole at $k^2=0$ see Eq. (23) ; in such a case the longitudinal amplitude not only remains nonvanishing but actually becomes singular as $k^2 \to 0$. Thus, when Born amplitudes are computed with a Lagrangian violating the conserved ρ source hypothesis, the $k^2 \to 0$ transition to the massless case is far from smooth.[19]

So far we have been working with the invariant amplitudes defined by (18). Our choice of invariant amplitudes is analogous to Ball's choice for photoproduction amplitudes with the realistic spins. The characteristic feature of this set is that the three amplitudes are not independent of each other but are related by the conservation equation (19). There is another set of invariant amplitudes

analogous to the set chosen by Chew, Goldberger, Low and Nambu[15] for single-pion photoproduction (with the realistic spin) and by Fubini, Nambu and Wataghin[15] for single-pion photoproduction:

$$\mathcal{M}_\mu = A_1\left[P_\mu(q\cdot k) - q_\mu(P\cdot k)\right] + A_2\left[k^2 q_\mu - (q\cdot k)k_\mu\right] \tag{26}$$

Here the quantities in the brackets already satisfy the conservation equation. Because there is no redundant amplitude, it may appear superior to use the CGLNFNW-like set rather than the Ball-like set in applications of vector meson dominance. However, the amplitudes in the CGLNFNW-like set can be seen to be far from smooth in k^2 even in the ultrasimple Born model. We simply note that the two sets are related by

$$\begin{aligned} A_1 &= \frac{B_1}{q\cdot k} = \frac{2B_1}{t-m_\pi^2-k^2} \\ A_2 &= \frac{B_3}{q\cdot k} = \frac{2B_3}{t-m_\pi^2-k^2} \end{aligned} \tag{27}$$

Obviously A_1 and A_2 cannot be smooth when B_1 and B_3 are, as in the Born model with universality. Put in another way, A_1 and A_2 have kinematical singularities at $k^2 = t-m_\pi^2$, and it therefore is not appropriate to apply the smoothness hypothesis to them.

Before we leave the hypothetical world of scalar pions and scalar nucleons, let us note one more very important point. In the Born model with universality, all three invariant amplitudes, $B_{1,2,3}$, are completely independent of k^2 as $s\to\infty$ with t fixed. Suppose this is true quite generally. Then the conservation equation (19) actually becomes two separate equations

$$\begin{aligned} B_2\left(-m_\pi^2+t\right) - sB_1 &= 0 \\ B_2 + 2B_3 &= 0 \end{aligned} \tag{28}$$

where we have assumed that s is very large. This means that even in the massive ρ case, there is only one independent amplitude. As a result, we can relate the longitudinal ($\lambda=0$) to the transverse amplitudes ($\lambda=\pm1$) as follows:

$$f_0 = -\left(m_\rho/2\sqrt{-2t}\right) f^{(-)} \qquad (s\to\infty, \text{ fixed } t) \tag{29}$$

In other words, the independence of k^2 hypothesis for all three Ball-type amplitudes leads to a completely nontrivial result: The longitudinal amplitude can be computed once the transverse amplitudes are given.[20]

Let us now return to the real world where the nucleon and pion are $1/2^+$ and 0^-, respectively. Everything we have done in the hypothetical world can be carried out with the realistic spins. The only difference is that there are more amplitudes to worry about. We have altogether eight invariant amplitudes defined by Ball,[14] which are free of kinematical singularities, and two conservation constraints analogous to (19). As a result, the number of independent amplitudes is six; this agrees with the counting method based on helicity amplitudes

$$(2s_\rho+1)(2s_N+1)^2/2 = 6 \tag{30}$$

where the factor 1/2 is due to parity conservation.

The transverse helicity amplitudes can be expressed in terms of B_1, B_3, B_5, and B_8 in Ball's notation, and if all four turn out to be independent of k^2, the usual vector meson dominance relations (10a) and (10b) hold in the helicity frame at high s with fixed t but not in any other frame. This is essentially the results of LeBellac and Plaut.[12]

So far everything is straightforward. Let us now assume that not only $B_{1,3,5,8}$ but also the remaining Ball amplitudes are independent of k^2, which can be shown to be the case in the electric Born model. The two conservation equations then yield four relations, just as we obtained two relations [cf. (28)] from the single conservation equation (19). As a result, there are 8-4=4 independent amplitudes, the same number of invariant amplitudes as in the photoproduction case. This means that we can predict the longitudinal amplitudes once the transverse amplitudes are given[20]:

$$\begin{aligned} f_{+;0+} &= \left(m_\rho/2\sqrt{-2t}\right) f_{+;1+} - f_{+;-1+} \\ f_{-;0+} &= -\left(m_\rho/\sqrt{-2t}\right) f_{-;1+} \end{aligned} \tag{31}$$

where the subscripts are defined by $f_{\lambda'_N;\lambda_\rho,\lambda_N}$ for the reaction inverse to (2).

How are we going to test our predictions? We first look at the "old" predictions according to which $\rho_{11}^{(H)}\, d\sigma/dt$ for the hadronic reaction (2) is compared to the average of the cross sections for $\gamma p \to \pi^+ p$ and $\gamma n \to \pi^- p$ (Ref. 21) multiplied by $(f_\rho/e)^2$ where $e^2/4\pi \simeq 1/137$ and $f_\rho^2/4\pi \simeq 2$ from the Orsay Storage Ring results.

This is shown in the lower part of Fig. 2 where the experimental points are obtained from the high statistics 15 GeV/c wire-spark-chamber experiment of the SLAC Diboson Spectrometer Group[22] here. The smooth curve which lies somewhat above the experimental points representing $2\left(s-m_p^2\right)^2 \rho_{11}^{(H)}\, d\sigma/dt$ is a Jackson-Quigg[23] type fit to the photoproduction cross section which will be mentioned later. Both the shape and absolute magnitude are in fair agreement with vector meson dominance, especially if we consider the fact that the quoted experimental values for $\rho_{11}^{(H)} d\sigma/dt$ are somewhat sensitive to the manner in which the s-wave pion-pair contribution is subtracted out. In particular note that the observed $\rho_{11}^{(H)} d\sigma/dt$ does exhibit a dramatic peak analogous to the famous photoproduction peak.[24] This shows that no matter what your favorite explanation for the photoproduction peak may be based on — the electric Born model, pure Regge poles with conspiracy, Regge poles with absorptive cuts, or Veneziano-type models — the same dynamical mechanism is also at work in the analogous hadronic reaction.

Even more striking is our prediction on $d\sigma/dt$ itself which, as you can see from Fig. 2, is due predominantly to the longitudinal ($\lambda_\rho=0$) contribution. The curve which almost goes through the data points for $\left(s-m_p^2\right)^2 d\sigma/dt$ was obtained as follows:

(i) Start with the helicity amplitudes for photoproduction obtained using the method of Jackson and Quigg,[23] which takes into account the finite-energy-sum-rule integrals evaluated by Fox.[25] Modify them slightly so that we obtain a reasonable fit to the high energy photoproduction data. (For details see Cho's thesis.[26])

(ii) Use vector meson dominance to get the transverse ($\lambda_\rho=\pm1$) amplitudes for the hadronic reaction (2).

(iii) Use Eq. (31) to obtain the longitudinal ($\lambda_\rho=0$) amplitudes.

Notice that once photoproduction fits are made, there is no adjustable parameter in the model. It is in this manner that we predicted the curve for $d\sigma/dt$ (total, including the longitudinal contribution) shown in Fig. 2. Considering the crudeness of the model, the data points appear to be in remarkable agreement with out theoretical curve. So starting with the purely transverse photoproduction amplitudes, we have successfully predicted $d\sigma/dt$ for $\pi^- p \to \rho^0 n$, which, as is evident from Fig. 2, is made up mostly of the longitudinal contribution.

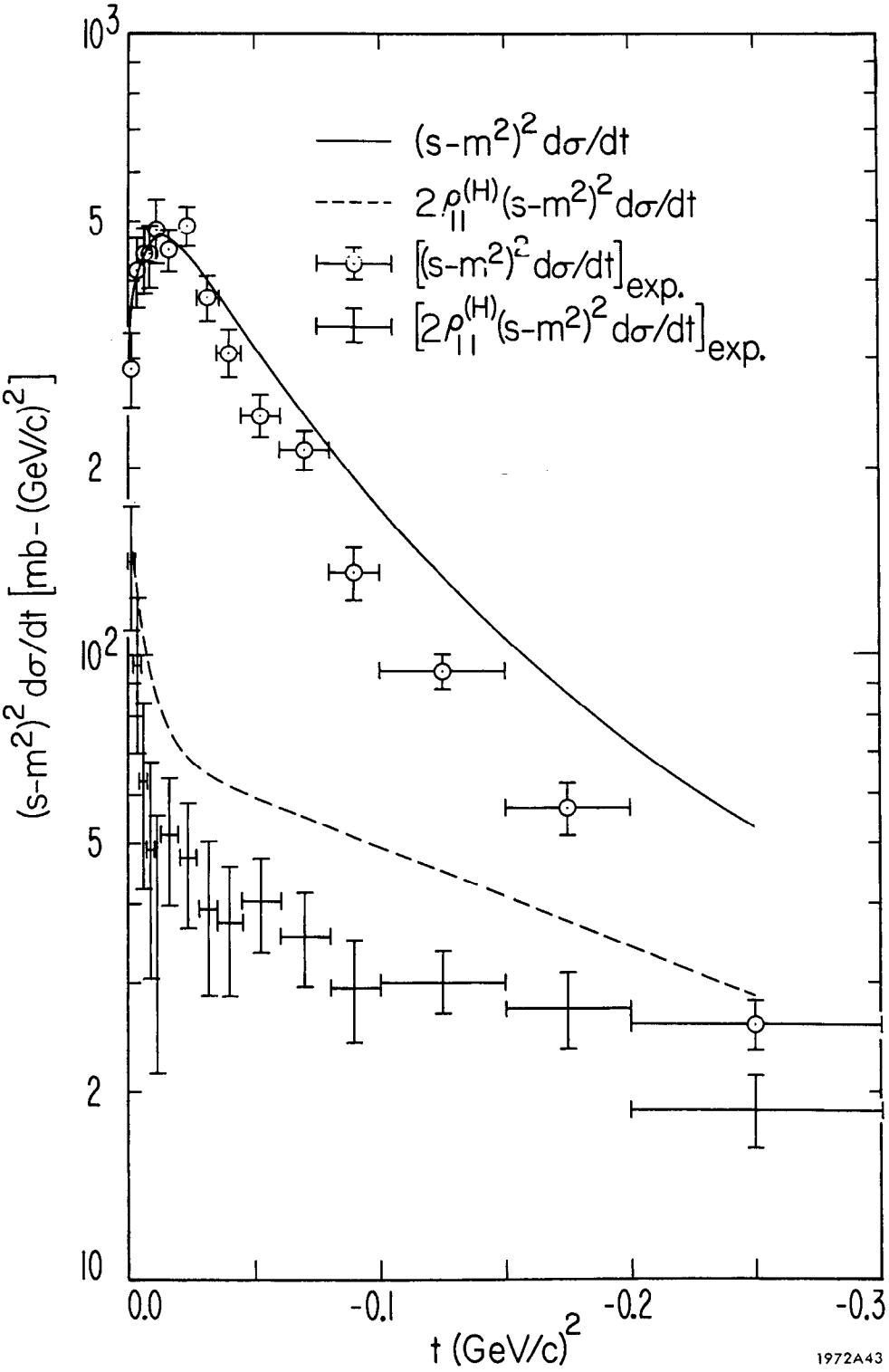

FIG. 2--The hadronic cross sections for $\pi^- p \to \rho^0 n$. The data points obtained by the SLAC Diboson Spectrometer Group (Ref. 22) represent $(s-m_p^2)^2\, 2\rho_{11}^{(H)}\, d\sigma/dt$ and $(s-m_p^2)^2\, d\sigma/dt$. The theoretical curves are our no-adjustable-parameter predictions described in the main text.

We can also predict the density matrix, as shown in Fig. 3 where the data points in the Jackson frame are taken from a CERN-Munich collaboration experiment[27] of a few years ago. (This incidentally is a poor statistics experiment by present-day standards.) Our predictions, which contain no adjustable parameter, appear to be at least as good as the predictions of OPEA (one-pion exchange with absorption) with two adjustable parameters.[28]

[Note added: The day after this talk was given the density matrix from the high statistics experiment of the SLAC-Diboson Spectrometer Group[22] became available to me. The observed helicity frame density matrix elements are compared to our predictions in Fig. 4. Even though the degree of agreement is not perfect, it is, in my opinion, as good as we have a right to expect. (We should not be too greedy!) Finally, in Fig. 5 we test the polarization relation (10b) in the helicity frame; the curve is again based on Cho's photoproduction amplitudes.[26] The predicted sharp peak in ρ_{1-1}/ρ_{11} at $-t \simeq m_\pi^2$ is nicely reproduced by the experimental data. The fact that ρ_{1-1} is everywhere positive indicates the dominance of natural-parity (t-channel) exchange[29] in transverse ρ production, just as in photoproduction. At large -t, there is some discrepancy, which, however, appears to be much less serious than in the earlier bubble chamber data[30] at lower energies.]

Having stated our main results, let me briefly mention a few remaining problems. Since the notion of off-shell amplitudes plays a central role in our formulation of vector meson dominance, we may naturally ask whether we can follow the k^2 dependence of the invariant amplitudes B_i. It is important to realize that in a theory with the current field identity the off-shell amplitudes are in principle measurable at every value of k^2, not just at $k^2=0$ (photoproduction) and $k^2=-m_\rho^2$ (the analogous ρ meson reaction). The fundamental relation is

$$B_i^{(\text{e.m. isov.})}(s,t,k^2) = (e/f_\rho)\left(m_\rho^2/m_\rho^2+k^2\right) B_i(s,t,k^2) \qquad (32)$$

where the left-hand side can be studied in the lepton pair production process (7) for $k^2 < 0$ (time-like) and in single-pion electroproduction (6) for $k^2 > 0$ (space-like). In Cho's thesis[26] predictions for the electroproduction process are discussed in some detail. Unfortunately the model is supposed to be applicable only for[31]

$$s-m_N^2 \gg m_\rho^2 + k^2 \quad . \qquad (33)$$

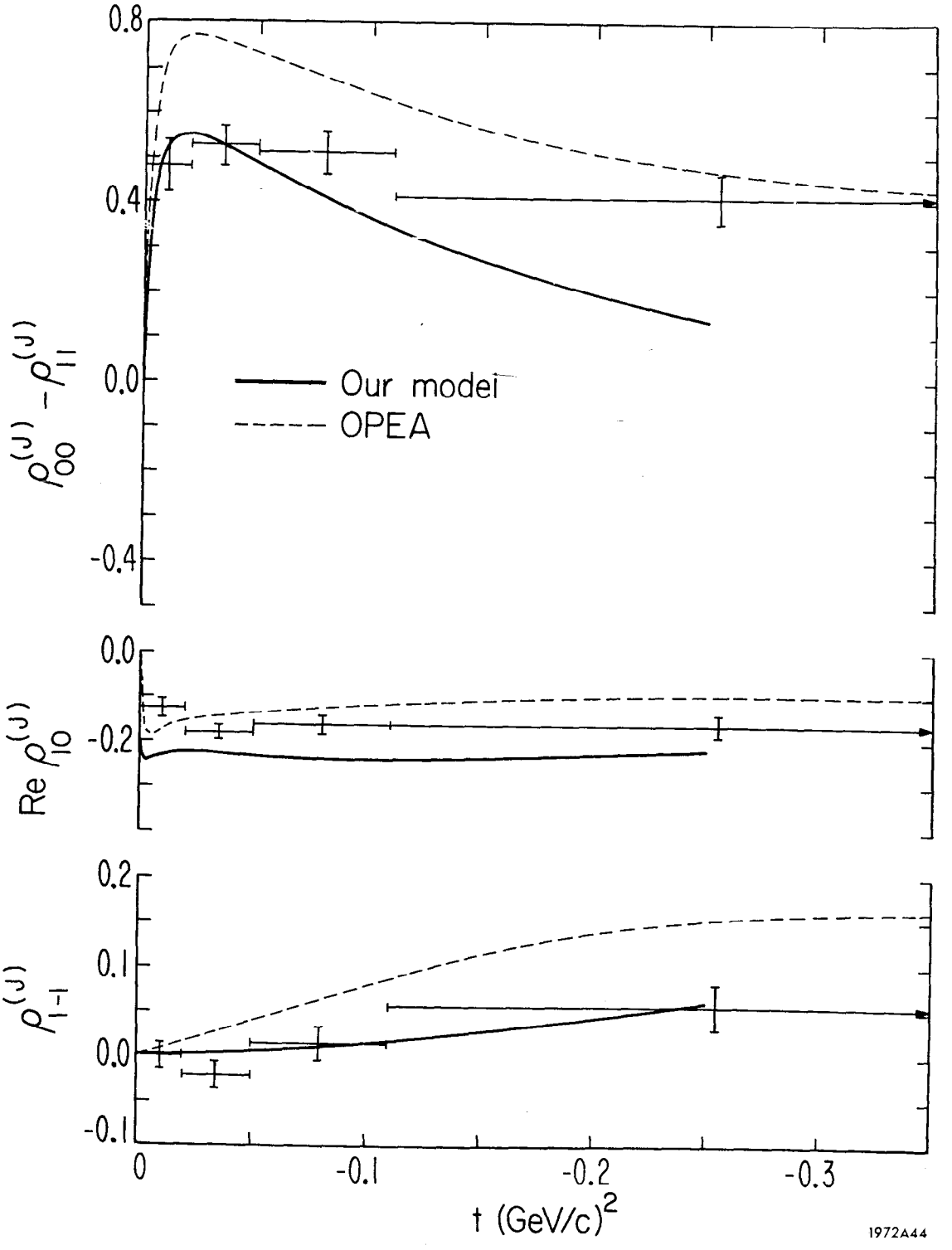

FIG. 3--The density matrix elements in the Jackson frame obtained in the CERN-Munich collaboration of Ref. 27. The solid curves are our no-adjustable-parameter predictions described in the main text. The dashed curves are based on the absorptive one-pion-exchange model with two adjustable parameters.

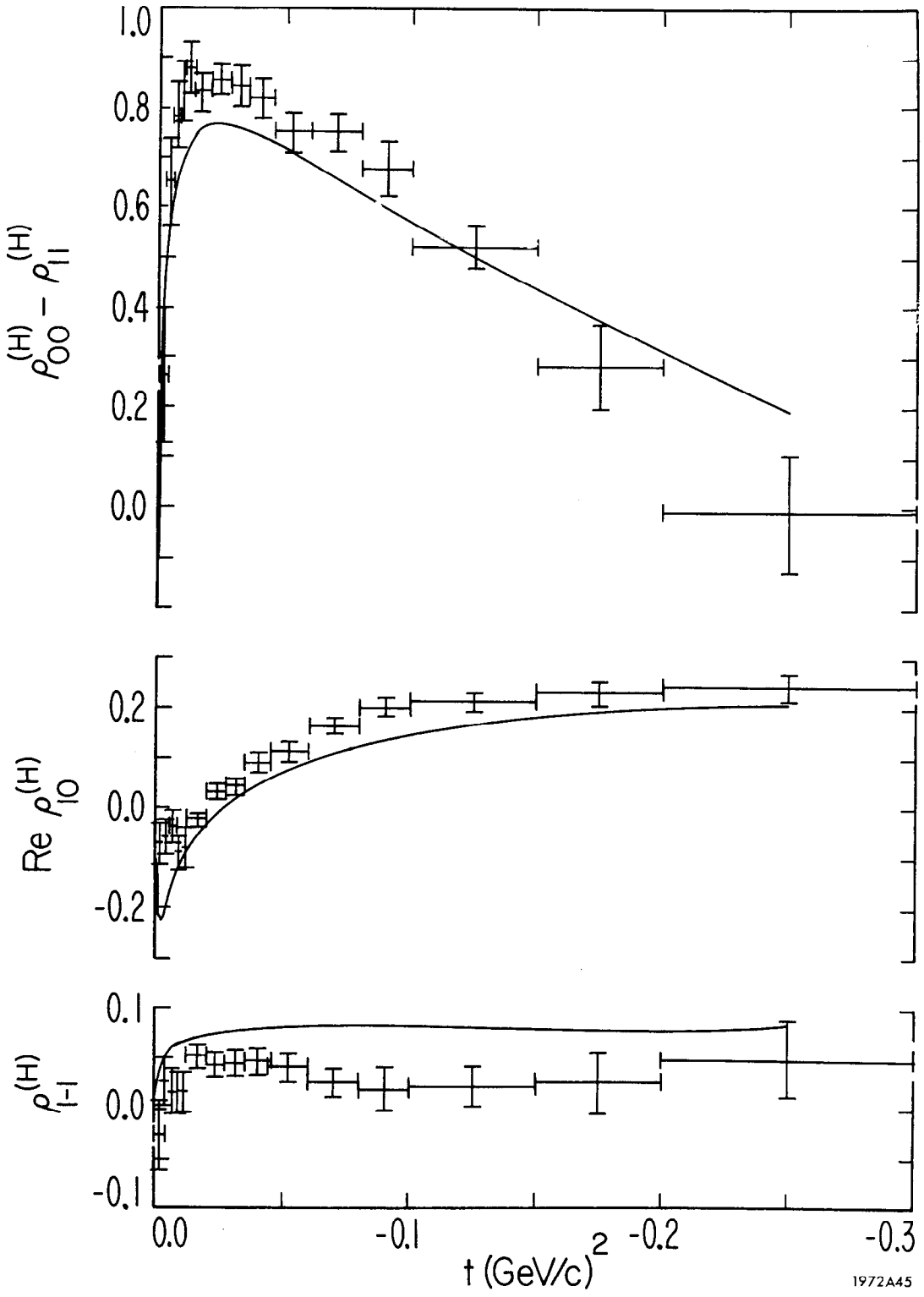

FIG. 4--The density matrix elements in the helicity frame measured by the SLAC Diboson Spectrometer Group. The solid curves are our no adjustable-parameter predictions described in the main text.

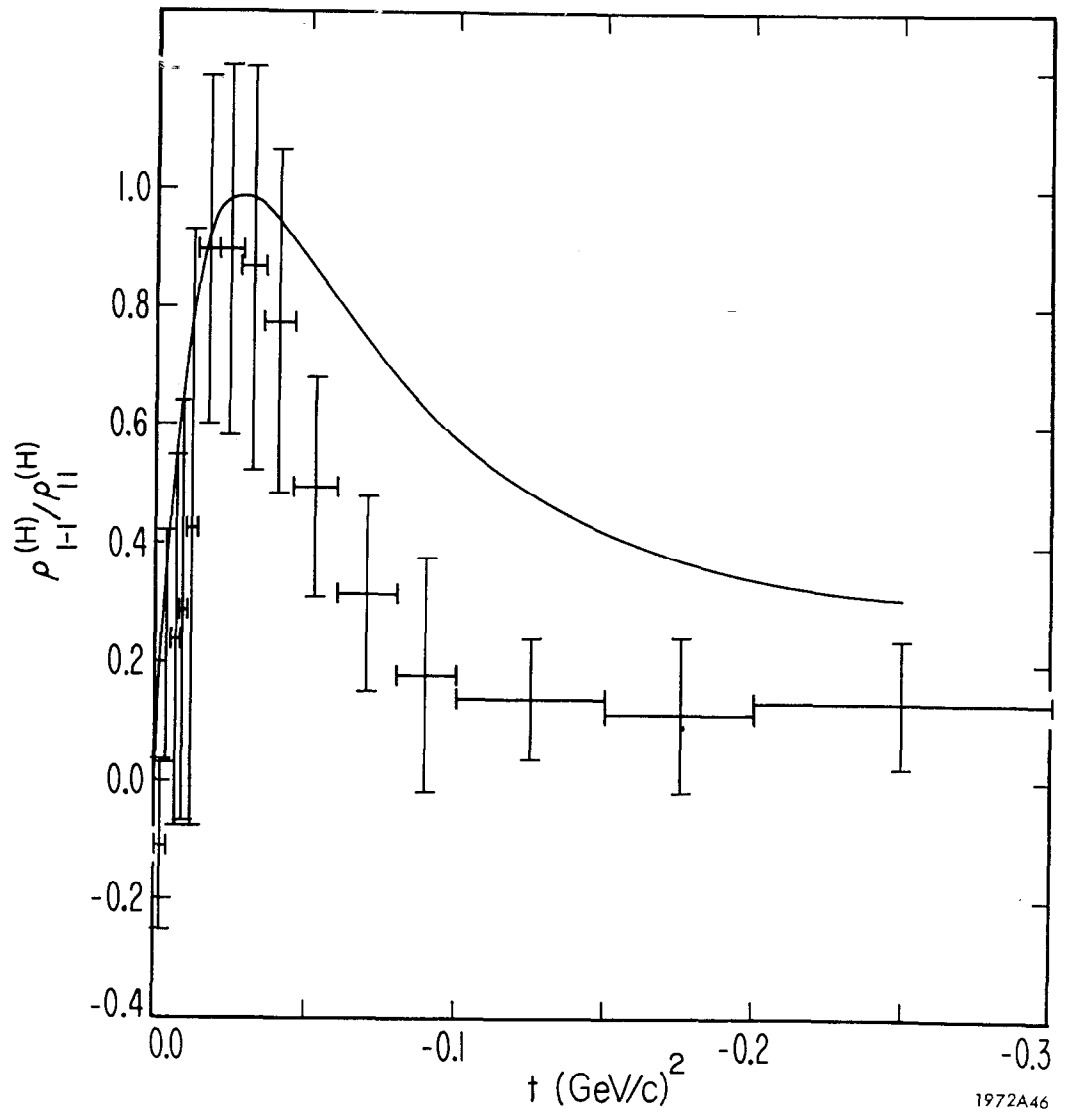

FIG. 5--ρ_{1-1}/ρ_{11} in the helicity frame determined by the SLAC Diboson Spectrometer Group. The solid curve is our no-adjustable-parameter prediction described in the main text.

and the available data from CEA (Pipkin's group[32]) do not cover this region. Even so, the manner in which the longitudinal contribution grows with k^2 in the CEA data seems to be in qualitative agreement with Cho's predictions.

From a more theoretical point of view there is still plenty of work to be done. In particular we should examine the k^2 dependence of the invariant amplitudes in various model calculations. As already pointed out by LeBellac and Plaut[12] and discussed further in Cho's thesis,[26] in single-particle exchange models (elementary or Reggeized), some of the Ball amplitudes do depend on k^2; this is true particularly when high spin objects are exchanged. It is not known, however, whether this disease could be cured by considering many single-particle exchange amplitudes simultaneously. In this connection the k^2 dependence of Veneziano-type amplitudes[33] may be worth studying.

Another general problem concerns the choice of invariant amplitudes. We all agree that the invariant amplitudes to which we apply the smoothness hypothesis should be free of kinematical zeros and kinematical singularities. In practice, if our investigations on the reactions (2) and (3) teach us anything, it appears that we should choose a set of amplitudes in such a way that the smoothness hypothesis applied to them automatically leads to smooth $f_{\lambda_\rho=\pm1}$ and smooth $f_{\lambda_\rho=0}/\sqrt{-k^2}$ at high energies. It is amusing that the smoothness of $f_{\lambda_\rho=\pm1}$ and $f_{\lambda_\rho=0}/\sqrt{-k^2}$ is just what we expect when we dominate the space components of the current matrix element by the ρ meson propagator.[34]

In conclusion, let me summarize the main points. The starting point of vector meson dominance should <u>not</u> be Eq. (1). Rather we should take the point of view that Eq. (1) is derivable at high s in the helicity frame from the requirement that the kinematical-singularity-free invariant amplitudes vary little with k^2. And this smoothness hypothesis, in turn, can be justified in some simple-minded models such as the electric Born model with a conserved ρ source. Our guiding philosophy is that the smoothness hypothesis abstracted from simple models actually holds in the real world. In this sense it may be likened to the attitude of Gell-Mann who boldly asserted that the commutation relations among electromagnetic and weak currents in the real world are identical to those in the ultrasimple free-quark-field model even though the real world is probably not made up of quarks.

From a practical point of view our approach selects the helicity frame as the only preferred frame as $s \to \infty$ with t finite. Furthermore, the independence

of k^2 hypothesis for the Ball amplitudes leads to completely nontrivial relations between the longitudinal and transverse amplitudes, and comparisons with the recent high statistics data appear encouraging.

About a year and a half ago one of the review speakers[35] in an international conference summarized the status of vector meson dominance in single-pion photoproduction by the following remarks.

> "Although it was originally found to work well for single-pion photoproduction, more recent data from experiments using polarized photon beams indicate that there are serious discrepancies. Theoretical attempts to explain these discrepancies have largely destroyed the original simplicity of the model ... it appears that the simple model will never recover from the theoretical attacks made while trying to explain the apparent discrepancy."

Well, it appears that the simple model <u>has</u> recovered together with additional nontrivial results.

References

1. D. S. Beder, Phys. Rev. 149, 1203 (1966). See also C. Iso and H. Yoshii, Ann. Phys. 47, 424 (1968); H. Joos, Acta Phys. Austriaca, Suppl. 4 (1967).
2. A. Białas and K. Zalewski, Phys. Letters 28B, 436 (1969).
3. J. J. Sakurai, "High energy physics in the seventies," the Proceedings of this Joint Seminar.
4. B. Richter in the Proceedings of the 1967 International Symposium on Electron and Photon Interactions at High Energies (Stanford Linear Accelerator Center, Stanford, 1967). A. M. Boyarski et al., Phys. Rev. Letters 20, 300 (1968); 21, 1767 (1968).
5. S. D. Drell and J. D. Sullivan, Phys. Rev. Letters 19, 268 (1967).
6. C. Geweniger et al., Phys. Letters 29B, 41 (1969); H. Burfeindt et al., Phys. Letters 33B, 509 (1971).
7. J. J. Sakurai, Ann. Phys. 11, 1 (1960).
8. C. N. Yang and R. L. Mills, Phys. Rev. 96, 191 (1954).
9. N. M. Kroll, T. D. Lee and B. Zumino, Phys. Rev. 157, 1376 (1967).
10. M. Krammer and D. Schildknecht, Nucl. Phys. B7, 583 (1968).
11. C. F. Cho and J. J. Sakurai, Phys. Letters 30B, 119 (1969). See also N. N. Achasov, V. I. Belinicher and L. M. Samkov, JETP Letters 6, 103 (1967); C. D. Froggatt and D. Morgan, Phys. Letters 33B, 582 (1970).
12. M. LeBellac and G. Plaut, Nuovo Cimento 64A, 95 (1969).
13. Besides LeBellac and Plaut and us, a number of authors have argued that the only natural frame is the helicity frame: H. Frass and D. Schildknecht Nuclear Physics B6, 395 (1968); W. T. Potter and J. D. Sullivan, Nuovo Cimento 68A, 623 (1970); W. Schmidt, Phys. Rev. 188, 2458 (1969); S. G. Brown, Phys. Rev. D1, 207 (1970); A. Dar, Nucl. Phys. B19, 259 (1970); J. T. Donohue, Phys. Rev. D1, 1972 (1970); P. D. Mannheim (to be published).
14. J. S. Ball, Phys. Rev. 124, 2014 (1961).
15. G. F. Chew, M. L. Goldberger, F. E. Low and Y. Nambu, Phys. Rev. 106, 1345 (1957); S. Fubini, Y. Nambu and V. Wataghin, Phys. Rev. 111, 329 (1958).
16. F. T. Meiere, Phys. Letters 30B, 44 (1969); W. T. Potter and J. D. Sullivan (Ref. 13); S. G. Brown (Ref. 13).

17. Explicitly, $\epsilon_\mu^{(\pm 1)} = (1/\sqrt{2})\ (\pm 1,\ -i,\ 0;\ 0)$, $\epsilon_\mu^{(0)} = (1/m_\rho)(0,\ 0,\ k_0;\ i|\vec{k}|)$ where the z axis is taken to be in the direction of the ρ meson and our metric is such that $\epsilon_\mu = (\vec{\epsilon};\ i\epsilon_0)$.

18. For a related discussion, see D. Horn and M. Jacob, Nuovo Cimento 56A, 83 (1968).

19. For an interesting discussion of a "catastrophe" arising from a vector meson with mass nearly equal to zero coupled to a nonconserved source, see S. Weinberg, Phys. Rev. Letters 13, 495 (1964).

20. C. F. Cho and J. J. Sakurai, Phys. Rev. D2, 517 (1970).

21. As is well known, by forming this average we can isolate the isovector photon contribution to a very good approximation.

22. Private communication from D.W.G.S. Leith and E. E. Kluge.

23. J. D. Jackson and C. Quigg, Phys. Letters 29B, 236 (1969).

24. For earlier (somewhat indirect) evidence for the forward peak in $\rho_{11}^{(H)}$ $\rho_{11}^{(H)}(d\sigma/dt)_{\pi^- p \to \rho^0 n}$, see J. H. Scharenguivel et al., Phys. Rev. Letters 24, 332 (1970).

25. G. C. Fox (unpublished).

26. C. F. Cho (to be published).

27. H. D. Hyams et al., Nucl. Phys. B7, 1 (1968).

28. See e.g., J. D. Jackson, Rev. Mod. Phys. 37, 484 (1965).

29. The connection between the sign of $\rho_{1-1}^{(H)}$ (or A) and natural vs. unnatural parity exchange (in the t-channel) is discussed by P. Stichel, Zeit f. Phys. 180, 170 (1964); J. Ader et al., Nuovo Cimento 56A, 952 (1968).

30. L. J. Gutay et al., Phys. Rev. Letters 22, 22 (1969); R. Diebold and J. A. Poirier, Phys. Rev. Letters 22, 255, 906 (1969).

31. I now feel that the condition (33) is quite essential if simple-minded vector meson dominance relations are to work at all in electroproduction. In the usual language of inelastic electron scattering this condition implies that Bjorken's variable $\omega = 2m_\rho \nu/q^2$ must be large. See C. F. Cho and J. J. Sakurai, Phys. Letters 31B, 22 (1970); H. T. Nieh, Phys. Rev. D1, 3161 (1970); J. D. Sullivan, Nucl. Phys. B22, 358 (1970).

32. Private communication from F. M. Pipkin, A. M. Eisner and G. J. Feldman.

33. A. P. Contogouris, G. Gaskell and M. Svec, Nucl. Phys. B24, 237 (1970); B. Humpert (to be published).

34. J. J. Sakurai, Phys. Rev. Letters 22, 981 (1969).

35. R. E. Diebold, Comments on Nuclear and Particle Physics 3, 170 (1969).

PHYSICS WITH THE 12' BUBBLE CHAMBER*

M. Derrick

Argonne National Laboratory
Argonne, Illinois USA

In this talk I would like to give the present status and future plans for doing physics with the 12' hydrogen bubble chamber. The situation is rapidly changing as we get more experience, so the present account is very much a transient snapshot. The chamber was described last summer by Tom Fields[1] in a paper he gave at the Dubna Conference on Instrumentation for High Energy Physics. Since the basic parameters are covered there, I have copied the next three sections from Fields' paper.

Team

I shall begin with the names of the people who have been responsible for this project. The entire team is led by E. Gale Pewitt, and consists of about 15 Argonne staff members and perhaps 30 Argonne support personnel, plus outside consultants and, of course, construction and industrial workers. Some of the key Argonne staff personnel were A. Tamosaitis, J. Purcell, J. Simpson, S. Stoy, D. Hillis, L. Genens, M. Bougon, H. Myers, R. Marema, O. Testard, R. Pubentz, J. Sheppard, K. Martin, and D. VanGundy. The project has also received valuable help from M. Derrick, L. Hyman, W. Welford, P. VanderArend, P. Marston, C. Laverick, and J. Fetkovich.

Now that the construction phase of the project is completed, about half of the original team is involved in the chamber shakedown phase. The operations crew which is carrying the responsibility for bringing the chamber into smooth operation numbers about 35 people, including staff members.

Design Features

Let me now turn to the design features of the chamber system. Decisions concerning these features were made in 1965 and 1966, and therefore reflect the main questions on large chamber design as they appeared at that time.

Figure 1 is a cross-sectional drawing of the chamber on which the principal systems can be seen. The chamber itself is a stainless steel vessel of 27,000 liters volume. Its wall thickness in most parts is 7.5 cm, with a thin (6 mm)

*Work supported by the U. S. Atomic Energy Commission.

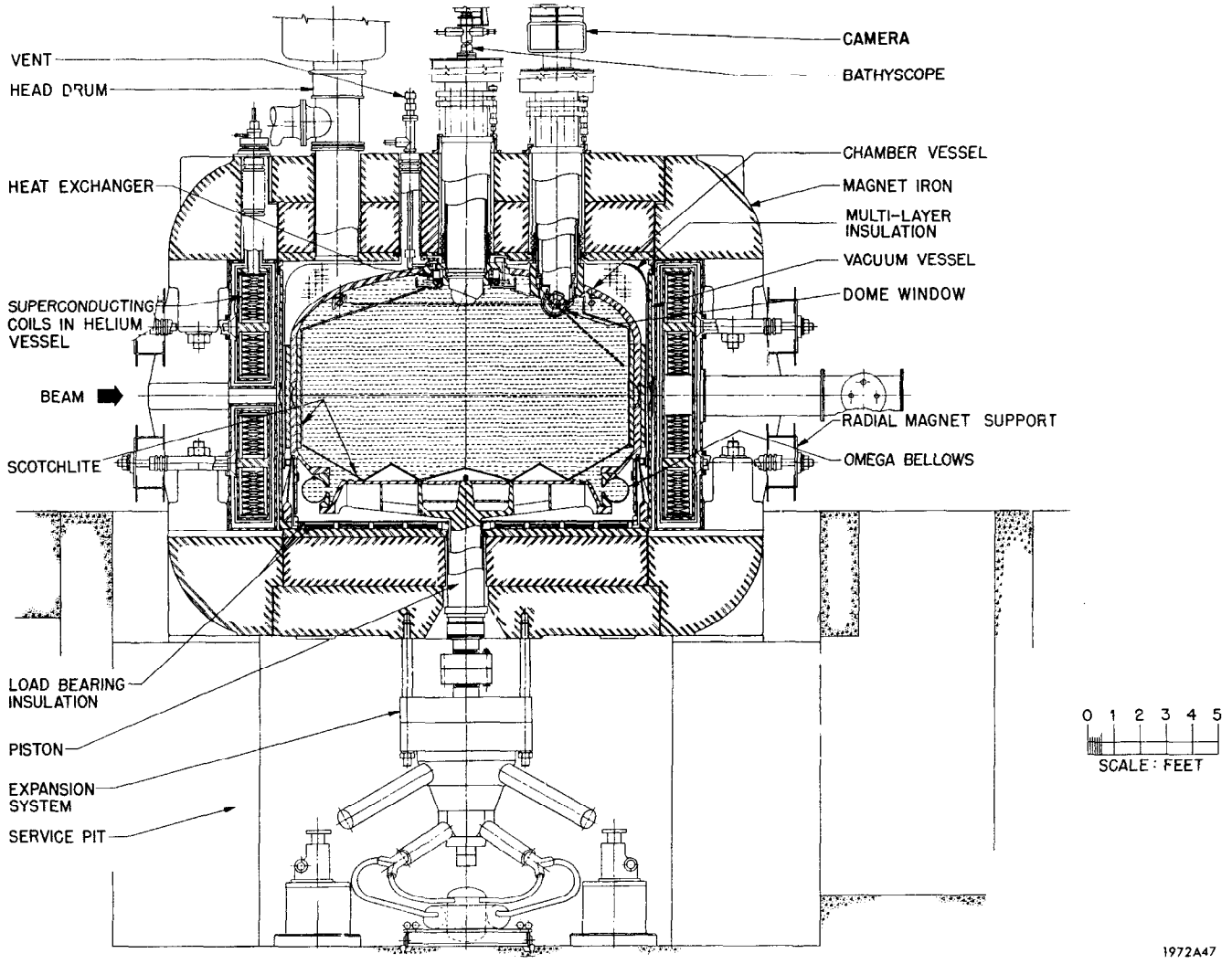

FIG. 1--Cross section of chamber and magnet.

beam window running around the entire mid-plane. The axial loads on the chamber wall are carried across the thin section by means of strengthening ribs on both the outside and the inside of the vessel. Figure 2 shows the chamber vessel ready for installation. Convection within the chamber is effected by the cooling coils (heat exchangers), as well as by the shroud which is located near the chamber walls. The visible interior of the chamber is covered with Scotchlite No. 1024 which is glued with epoxy to the 1.5 mm fiberglass shroud.

Illumination and photography of the chamber are achieved through four optical cartridges at the top of the chamber. Figure 3 shows part of an optical cartridge, with its three concentric "fisheye" windows. The cameras are located on corners of a 1.5 m square. There is a fifth optical cartridge centered at the top of the chamber for direct periscope viewing and Land photography of the chamber interior.

The low temperature part of the expansion mechanism consists of a moveable piston of 3 m diameter, which forms the floor of the chamber and is sealed to the main chamber body vessel by means of a stainless steel omega bellows of toroidal shape. The piston is actuated by means of a hydraulic system which is mounted below the chamber.

The remaining basic component of the bubble chamber system is the magnet. This consists of stabilized superconducting coils (niobium-titanium) mounted in a liquid helium cryostat and surrounded by an iron yoke. The particular design of this magnet was decisively influenced by the possibility that large superconducting coils might be unworkable, in which case this same magnet yoke could be operated with room temperature copper coils. In addition, a very convenient freedom from stray magnetic fields is achieved by the use of the iron yoke. The mass of iron also serves another purpose which is useful for a large mechanically pulsed system, and that is to provide a more or less inertial system to which the other parts can be attached.

Of course a very large number of auxiliary devices such as refrigerators, power supplies, instrumentation, storage dewars, etc., are required to make such a system complete. These however are usually fairly conventional in their design, and most are available through standard industrial sources. The key features needed in this auxiliary equipment are reliability, safety, and economy.

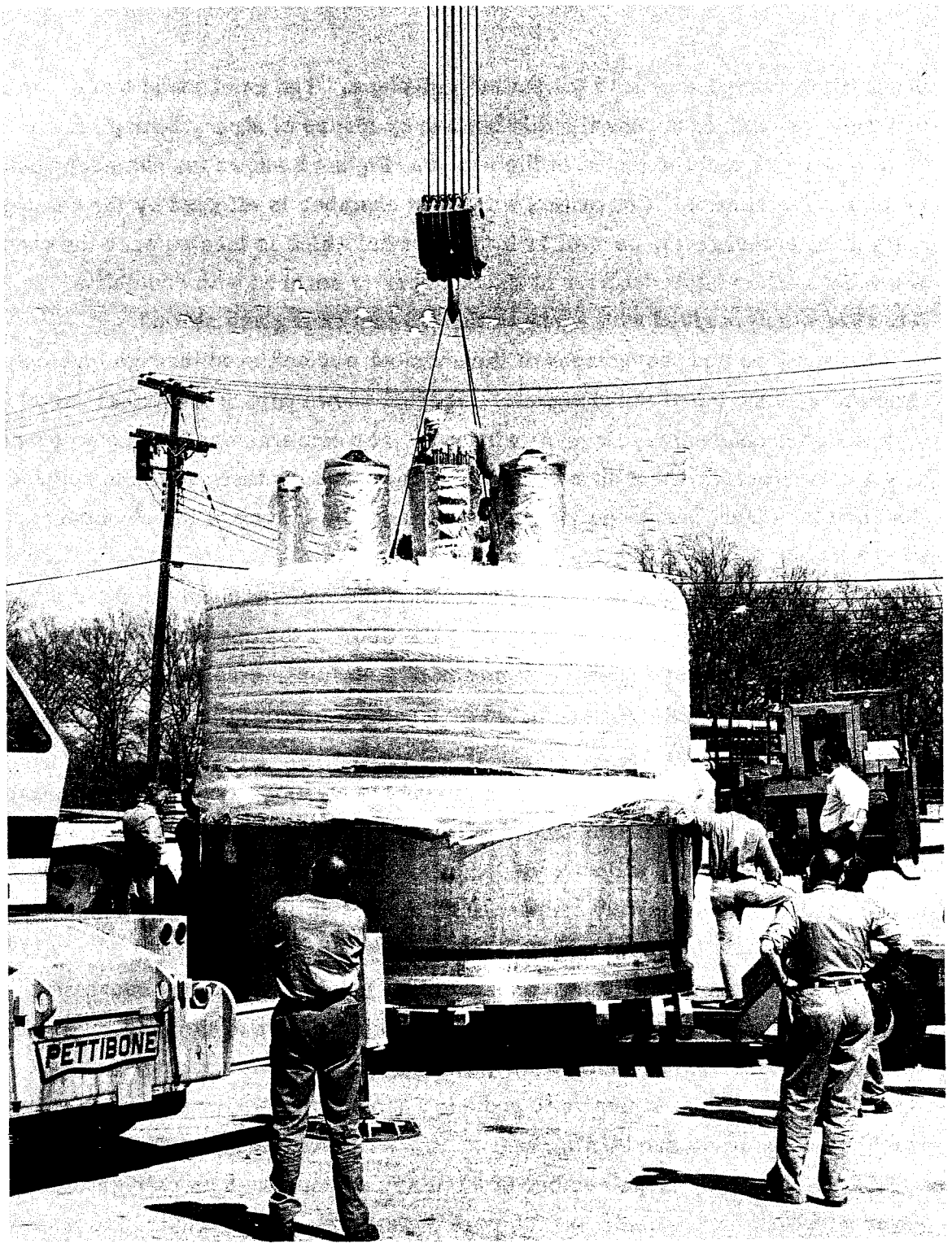

1972A48

FIG. 2--Chamber vessel ready for installation.

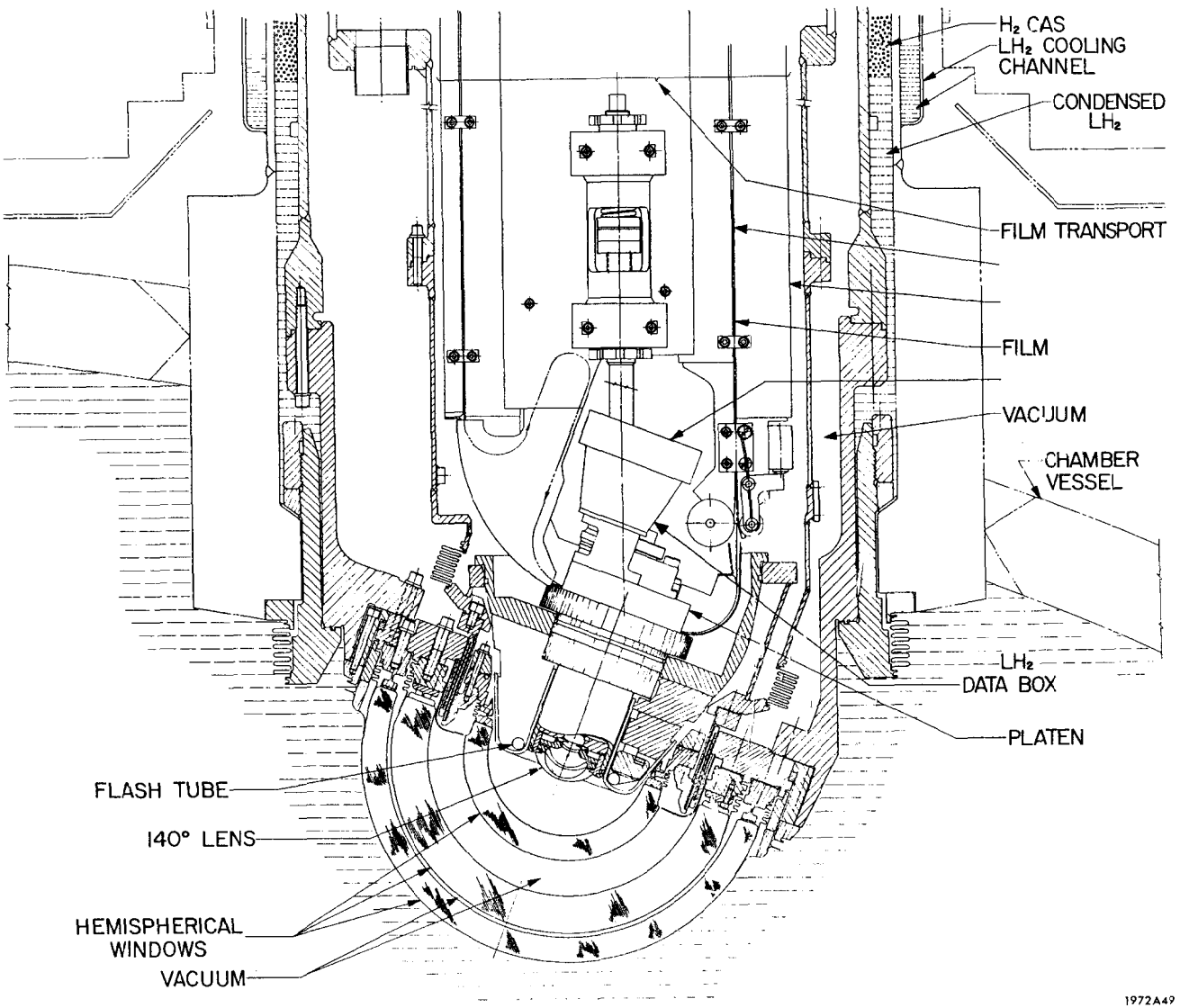

FIG. 3--Lower end of optical cartridge showing lens, flash tubes and domed windows.

Thermodynamic Considerations

Returning to the design criteria for the bubble chamber itself, the thermodynamic performance of the chamber was considered to be crucial. A primary aim was to minimize optical turbulence within the chamber. It was therefore decided to exert considerable care to minimize the amount of the parasitic boiling within the chamber during the expansion pulse. This was a primary motivation for using the bellows as the seal, rather than a piston with a sliding seal. (An additional advantage of the bellows is its freedom from mechanical erosion, thus eliminating one potential source of unwanted dirt particles within the chamber.) Other ways in which parasitic boiling was minimized included the use of low boiling valve designs, avoiding sharp corners and cavities, welding all flanges to eliminate all bolts within the chamber, etc. These features were developed and checked in a series of tests using a 2-foot diameter model chamber.

Aspect Ratio

In choosing the volume and aspect ratio of the chamber, the main physics criterion was the size of the ν beam which is typically a few meters. In addition with a depth in the beam direction of 3 m, about one neutrino interaction per 10^3 pictures could be expected for a cross section of 10^{-38} cm^2 and a flux of 10^{10} ν's. Such a flux comes from $\sim 10^{12}$ protons hitting a target. Another important parameter is the density of liquid hydrogen -- 0.06 tons m^{-1} or 16 m^3/ton. These factors together with considerations coming from the velocity of sound (1 m msec^{-1}) and the use of wide angle lenses led to the design shown in Fig. 1.

Another most important consideration was the desire to see all the chamber volume by all the cameras which helps minimize the scanning and data reduction problems.

For hadron physics the fractional momentum error on tracks is an important parameter. It is given by[2]

$$\left(\frac{\Delta p}{p}\right)^2 = \frac{2.66}{H^2 \ell} + \frac{1.44\ 10^{-4}\ p^2\ \epsilon^2}{H^2 \ell^5}$$

H = kg
p = MeV/c
ϵ = microns in space
ℓ = cms

The quantity ϵ is the space reconstruction accuracy and increases approximately proportionally to chamber size ($\epsilon \sim \ell$). Therefore for a large chamber one can gain in measuring accuracy as $\sim H\ell^{3/2}$. In practice the scattering term dominates the momentum precision for low energy long tracks. For $\epsilon = 250\ \mu$ (500 μ)

the scattering dominates below ~ 20 GeV (10 GeV). In that case one gains in accuracy over smaller chambers as $H\ell^{1/2}$. One concludes that for physics at 10 GeV or less, which is the ZGS energy region, the 12' chamber will have better momentum accuracy than the 2 m sized chambers now in use. So the design of Fig. 1 is also good for hadron physics.

This can be seen rather clearly in Fig. 4 which is a specific example taken from the 1968 NAL summer study.[2] For the track lengths assumed and energies < 12 GeV, scattering dominates and the 12' chamber is better than the smaller chambers by the square root of the ratio of the track lengths involved. For a 1 m interaction region this will be a factor of ~ 1.7. For the same relative momentum accuracy the 12' chamber will have three times the counting rate of the 2 m chamber.

Trapping

Another advantage of the circular shape is that low momentum particles will be trapped. For a particle starting out horizontally at the center of trapping momentum is ~ 540 MeV/c and can be up to twice this for a most favorable case of a particle starting near the wall. For example we have observed one event of the reaction $\nu p \rightarrow \mu^- p \pi^+$ in which all three final state particles come to rest in the hydrogen and the two mesons decay.

Secondary Interactions

Since in bubble chamber hydrogen 1 b = 1 ft, a typical mean free path for a high energy particle is 30 ft which is comparable to the size of the chamber. In some cases, such as low energy particles or antinucleons, the mean free path can be much smaller. The conversion length for high energy γ rays in liquid hydrogen is 43 ft. Considering that each π^o gives two γ rays in decay, the probability of one of these converting is a useful fraction (~ 35% for a potential flight path of 8 ft) similar to the K^o detection probability in existing chambers. Figure 5 shows a two-prong pp interaction with 3 electron pairs pointing at the vertex.

The secondary interactions results in two advantages:

1. Qualitative information is obtained on the nature of the particle or interaction, e.g., if an associated electron pair or neutron star is visible then the event clearly is not one vertex 4c. This can be used in selecting the type of events one wants to measure.

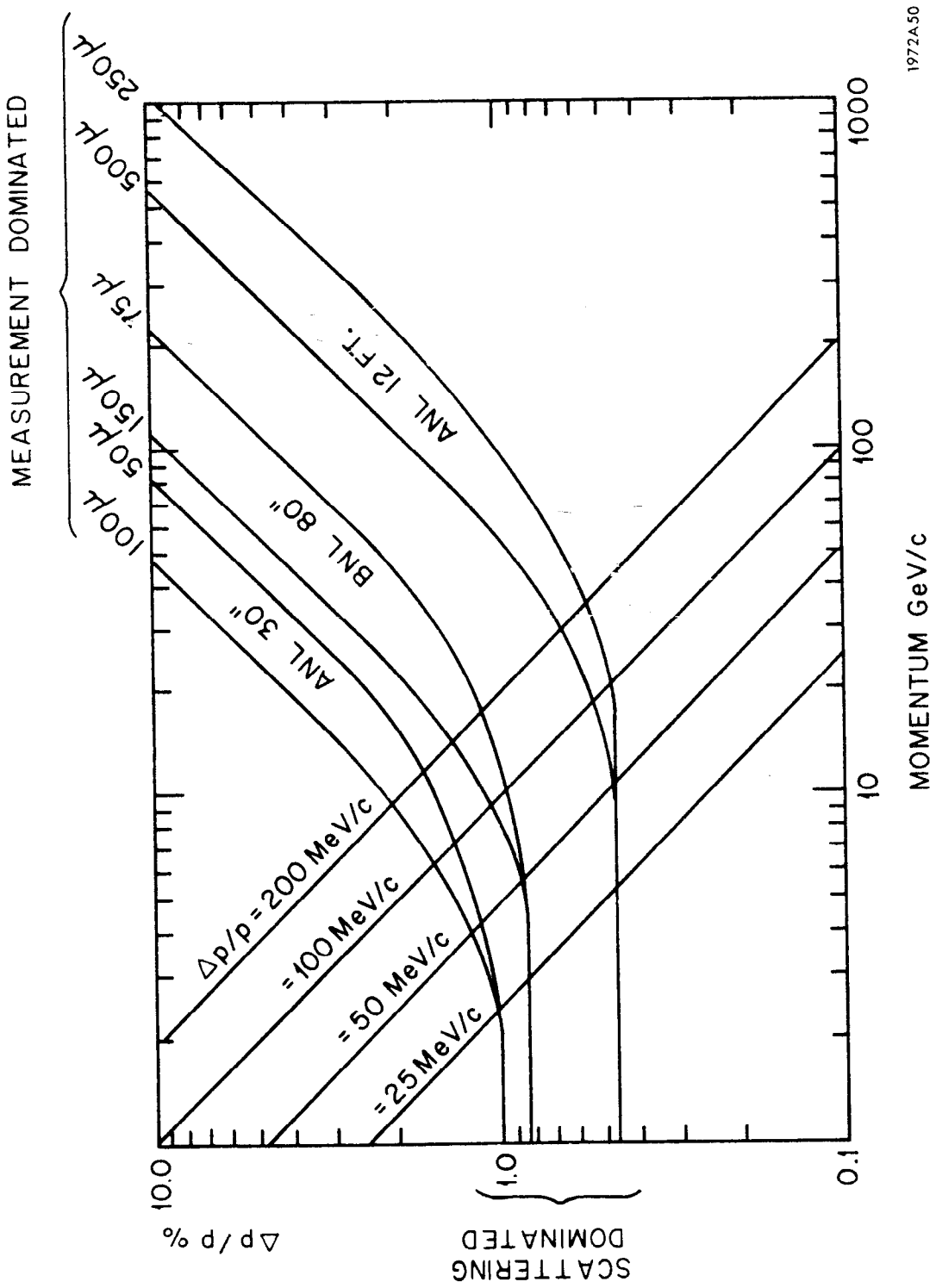

FIG. 4--Total momentum error ($\Delta p/p$) in percent for three different bubble chambers as calculated from equation given in the text. The parameters assumed are: ANL 30" 50 cm track 32 kg, BNL 80" 100 cm track 20 kg, ANL 12' 300 cm track 20 kg. The setting error (ϵ) values assumed are shown on the figure.

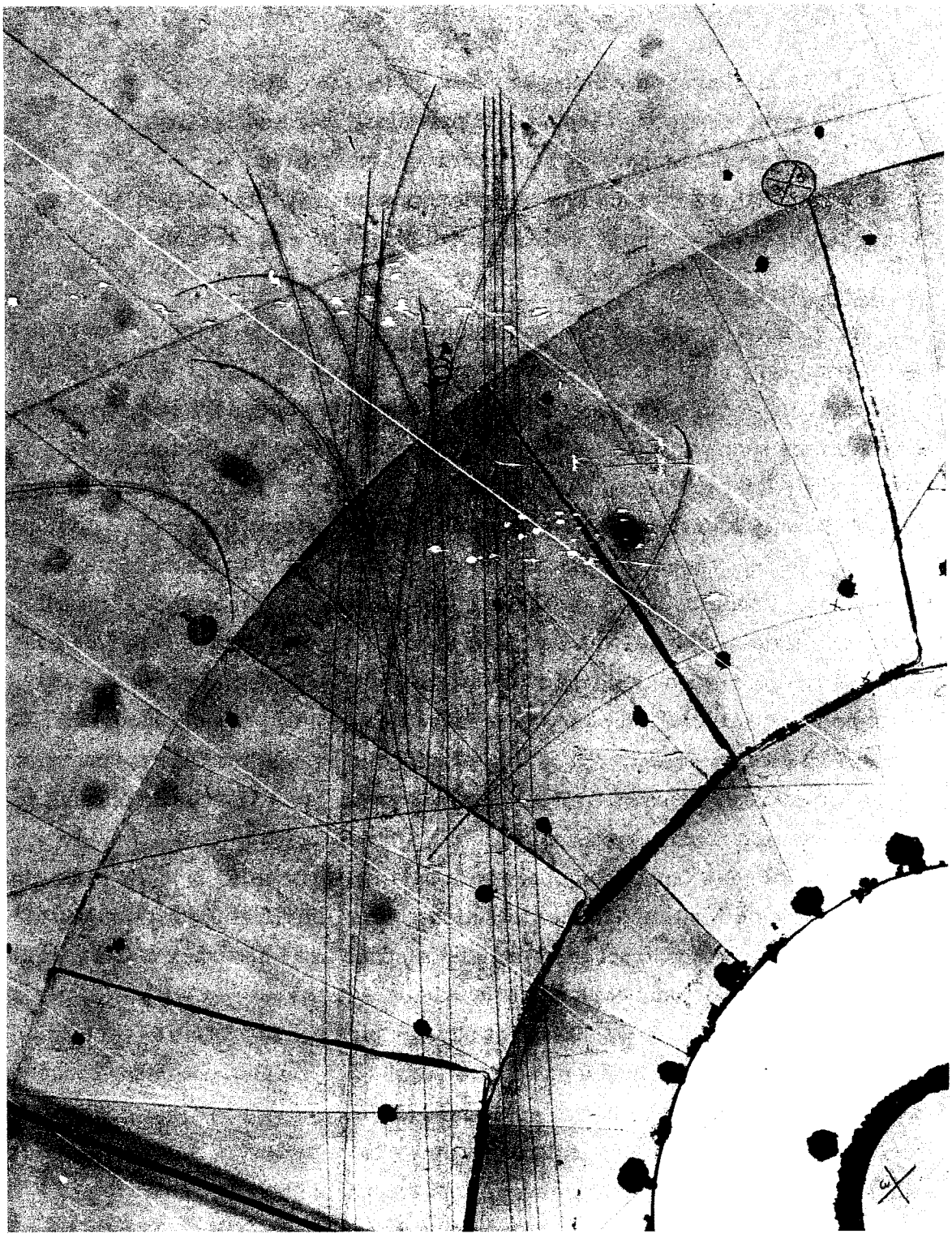

FIG. 5--Two-prong pp interaction at 12 GeV/c with three γ rays converting to electron pairs.

2. By measuring the directions and, in the case of electron pairs, energies of the neutral particles, extra constraints are available that will reduce fitting ambiguities.

A hydrogen chamber of this size is partaking of some of the properties of a heavy liquid chamber whilst still keeping the pure primary target.

Setting Accuracies

As we have discussed, the momentum accuracy for normal long tracks does not depend very much on the accuracy of space reconstruction. Even so ϵ is important and we are currently trying to understand the factors that control it. Short tracks such as provided by charged hyperon decays or particles that give a secondary interaction will have a momentum accuracy limited by ϵ. It also enters directly into the angle errors of neutral particles.

The optical constants of the chamber are determined by a straightforward but complex procedure.[3] Each camera lens is carefully mapped in a special distortion fixture so that from points on the film one can get the direction cosines of the corresponding light ray in space. In the bubble chamber the ray must be tracked through the three hemispheral windows that surround each camera as seen in Fig. 3. To do this exactly requires a previous measurement of the optical properties of each window plus an accurate knowledge of their positions when the photograph was taken.

As we all know from experience with smaller chambers, it takes some time to converge on a final satisfactory solution. From the first pictures in the 12' chamber we can reconstruct the fiducials in space to an accuracy of 200 μ in the beam plane. When some obvious difficulties are taken care of we expect to reduce this figure to 100 μ. The first physics pictures of 12 GeV/c protons were taken using only 3 of the possible 4 views, and various problems connected with film motion in the cameras were encountered.

With the preliminary optical constants we have measured and reconstructed some 12 GeV/c proton tracks going across the whole chamber, and so of 3.7 m length. The tracks are reconstructed using a modified TVGP.[4] The FRMS is shown in Fig. 6a and peaks at 12.5 μ corresponding to an ϵ of 750 μ in space. Figure 6b shows the same distribution for a selection of beam tracks that give interactions, and so are roughly of half the length of those in a. The FRMS now peaks at 8-9 μ corresponding to 500 μ in space. These two distributions

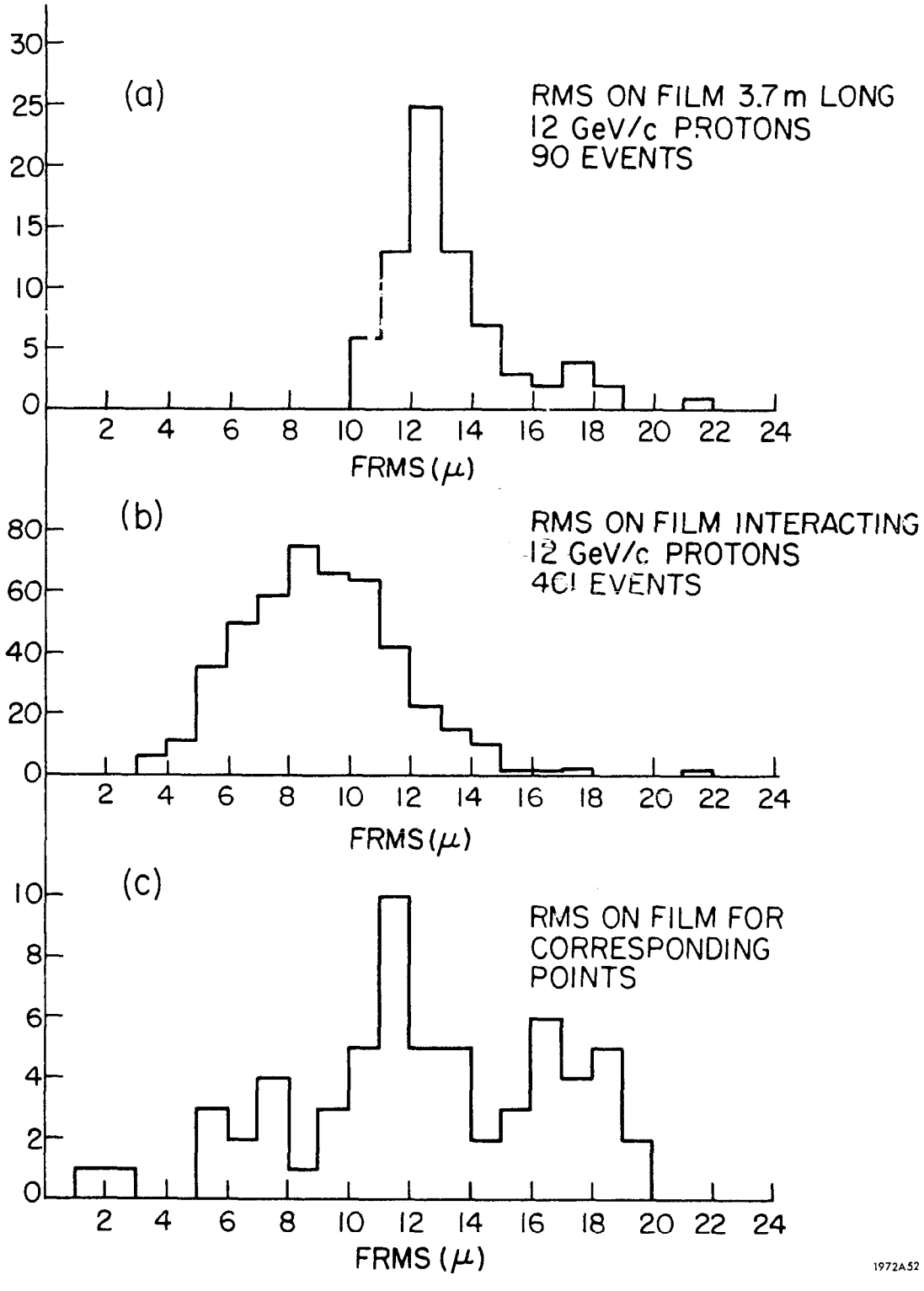

FIG. 6--Film RMS error of measured points as given by geometry program for (a) full length beam tracks, (b) beam tracks of interactions and (c) corresponding points.

show that there is some long-range systematic problem, which is not unexpected. Also shown in Fig. 6c is the distribution for event vertices and end points. The distribution is broader probably because vertices are more difficult to measure than tracks.

These results are all very preliminary and a few more months of work are needed to obtain a fuller understanding of the systematic problems.

Events can still be reconstructed and fitted, however, and Fig. 7 shows the t distribution of pp scattering at 12 GeV/c based on 139 events that give a 4c fit. The more interesting physics of course is in the 1c events giving final states like $pp\pi^o$ and $pn\pi^+$, especially because of the γ ray conversion, and neutron interactions will help separate a clean sample. Results are not yet available for the lower constraint classes.

Experimental Program

I will conclude by briefly discussing the experimental program that is presently foreseen for the chamber and use the different experiments as illustrations of the use of the special properties of this device.

The chamber was built to do neutrino physics[5] and the large volume chosen for that reason. We are still working on the first short ν exposure and have so far collected 12 events of the reaction $\nu p \rightarrow \mu^- p \pi^+$. With a long run in deuterium we hope to accumulate about 1000 examples of the reaction $\nu n \rightarrow \mu^- p$ as well as several hundred single pion production events.

The other weak interaction experiment approved is a study of K_L^o decays[6] in which the trapping property is used to identify the different decay modes of the K^o meson. A 1 GeV/c π^- beam will be built in the decay space now used for the ν experiment. K^o's (600 MeV/c Γ = 90 MeV/c) made by associated production will decay in the chamber. About 1 decay per picture can be obtained and so 300 K pictures will lead to 200 K leptonic decays. Essentially all the particles can be identified by a combination of trapping, energy loss and interactions, leading to a very clean separation between the different decay modes.

The parameter $\xi = f_-/f_+$ can be measured by three methods simultaneously

1. $K_{e3}/K_{\mu 3}$ ratio
2. Dalitz plot distribution
3. muon polarization

and will give an uncertainty on ξ of ~ 0.03.

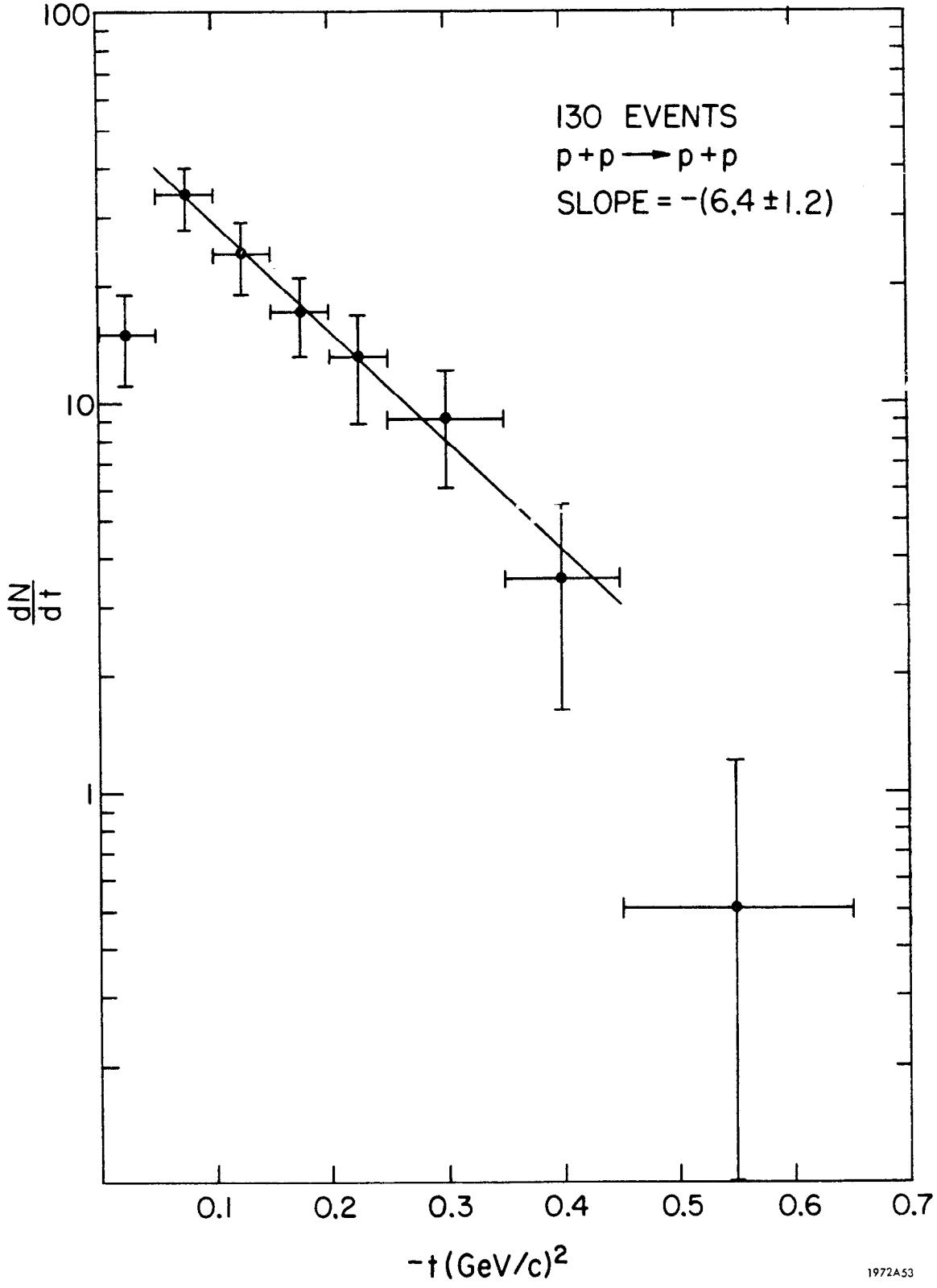

FIG. 7--Angular distribution of pp elastic scattering at 12 GeV/c as measured from 130 4c events in the 12' chamber. The loss at small t comes from the usual scanning bias.